NASA
Technical
Paper
1971

June 1982

In-Flight Transition Measurement on a 10° Cone at Mach Numbers From 0.5 to 2.0

David F. Fisher and
N. Sam Dougherty, Jr

NASA

NASA Technical Paper 1971

1982

In-Flight Transition Measurement on a 10° Cone at Mach Numbers From 0.5 to 2.0

David F. Fisher
Ames Research Center
Dryden Flight Research Facility
Edwards, California

N. Sam Dougherty, Jr.
Arnold Research Organization, Inc.
Arnold Air Force Station, Tennessee

NASA

National Aeronautics and Space Administration

Scientific and Technical Information Branch

IN-FLIGHT TRANSITION MEASUREMENT ON A 10° CONE AT MACH NUMBERS FROM 0.5 TO 2.0

David F. Fisher
NASA Ames Research Center
Dryden Flight Research Facility

and

N. Sam Dougherty, Jr.
Arnold Research Organization, Inc.

INTRODUCTION

Flow disturbances in a wind tunnel can create an environment much different from the flight environment. In addition, the flow environment in one wind tunnel may be significantly different from that in another, each wind tunnel having certain errors in the simulation of desired flight conditions. The differences can appear as premature and unpredictable laminar-to-turbulent boundary layer transition and as changes in turbulent skin friction and flow separation characteristics. The cumulative effect of differences in the boundary layer characteristics on the wind tunnel model can degrade the accuracy of the prediction of the full-scale vehicle's performance in flight.

With today's needs for improved accuracy in the use of wind tunnels to make even better predictions about flight, there has been a focused effort to study flow quality in wind tunnels to assess inaccuracies in simulation and to develop corrections to wind tunnel data. One means of study that has been attempted is to test a standard simple body shape in several wind tunnels and in flight at matched test conditions and then to correlate the wind tunnel and flight data; the data acquired in flight would be the basis of comparison for the wind tunnels. For a valid comparison, the same body would have to be tested in flight and in the wind tunnel at as nearly the same test conditions as possible: Mach number, Reynolds number, incidence angle, and heat transfer.

To produce this type of comparison, the free-stream disturbance levels of 23 wind tunnels in the United States and Europe were measured during tests on a sharp, slender smooth cone known as the Arnold Engineering Development Center (AEDC) 10° transition cone. The results of these tests have already been documented (refs. 1 to 7). This same cone and its related instrumentation was mounted on the nose of an F-15 aircraft and flown at the NASA Dryden Flight Research Facility at Mach numbers from 0.5 to 2.0 and at altitudes from 1500 meters (5000 feet) to 15,000 meters (50,000 feet). As in the previous wind tunnel studies, the laminar-to-turbulent transition location of the cone boundary layer was used as the Reynolds number parameter sensitive to free-stream disturbances.

This report presents the results of the flight tests. The data presented are transition Reynolds numbers based on length measured from the cone apex and flight flow disturbance measurements. The data act as reference data for the previously acquired wind tunnel data and assisted in the identification of the probable mechanism of instability leading to transition.

The wind-tunnel-to-flight correlations are presented in references 8 and 9.

SYMBOLS AND ABBREVIATIONS

Physical quantities in this report are given in the International System of Units (SI) and parenthetically in U.S. Customary Units. Quantities were nondimensionalized whenever possible to show functional relationships.

a	acceleration, g
C_p	pressure coefficient
C_{y_β}	side force coefficient due to sideslip
$C_{y_{\delta_r}}$	side force coefficient due to rudder deflection
D	dewpoint, °C (°F)
d	probe diameter (fig. 6)
F	nondimensional peak center frequency, $\frac{2\pi f \nu_e}{U_e^2}$

F_{min}	nondimensional lower bound frequency of peak
F_{max}	nondimensional upper bound frequency of peak
f	frequency, Hz
$G_x(f)$	power spectral density function
g	gravitational constant, m/sec^2 (ft/sec^2)
H	1962 standard atmosphere pressure altitude, m (ft)
L	length of cone, 113.0 cm (44.5 in.)
M	Mach number
Pr	Prandtl number
p	pressure, N/m^2 (lb/ft^2); barometric pressure, mb (lb/ft^2)
p'	fluctuating pressure, N/m^2 (lb/ft^2)
$\sqrt{\bar{p}_s'^2}$	average static root-mean-square fluctuating pressure, N/m^2 (lb/ft^2)
$\sqrt{\bar{p}_{t_2}'^2}$	average impact root-mean-square fluctuating pressure, N/m^2 (lb/ft^2)
Q_w	heat transfer rate, W/m^2 (Btu/ft^2-sec)
q	dynamic pressure, N/m^2 (lb/ft^2)
Re_T	end of transition Reynolds number
Re_t	onset of transition Reynolds number
Re_x	Reynolds number based on length from cone apex
RH	relative humidity over liquid water, percent

RHO atmospheric density, gm/m^3 (lb/ft^3)

r temperature recovery factor (0.88 for turbulent flow, 0.84 for laminar flow)

S aircraft wing area m^2, ft^2

T temperature, K (°R), atmospheric temperature, °C (°F)

THETA wind direction (table 4), deg from North

t time, sec

U velocity, m/sec (ft/sec)

U/ν unit Reynolds number, per m (per ft)

V windspeed, m/sec, knots

W aircraft weight, N (lb)

X_T end of transition location, cm (in.)

X_t onset of transition location, cm (in.)

x distance along a cone ray from the cone apex, cm (in.)

Z geometric altitude, m (ft)

α cone angle of attack with respect to airstream, deg

α' angle-of-attack offset angle (eq. (6)), deg

β cone yaw angle with respect to airstream, deg

β' angle-of-sideslip offset angle (eq. (7)), deg

Γ total incidence angle with respect to airstream (eq. (11)), deg

γ ratio of specific heats for air, 1.4

Δ differential or increment

δ_r rudder deflection, deg

θ_c cone half angle, deg

ν kinematic viscosity, m^2/sec (ft^2/sec)

ϕ	cone azimuthal angle relative to cone top center ray (fig. 1(b)), deg

Subscripts:

ac	aircraft
aw	adiabatic wall
b	radiosonde balloon
e	boundary layer edge
i	impact
ind	indicated
min	minimum
max	maximum
p	traversing pitot
t	total
w	at wall
x	longitudinal axis through aircraft center of gravity
y	yaw axis through aircraft center of gravity
α	in pitch plane
β	in yaw plane
0	zero incidence and zero heat transfer
1	at forward microphone on cone surface (x = 45.7 cm (18 in.))
2	at aft microphone on cone surface (x = 66.0 cm (26 in.))
∞	free stream

TEST APPARATUS

Cone Description

Two cones were used in this flight experiment. The 10° transition cone (fig. 1) was used for all in-flight transition measurements. This was the same cone and instrumentation that was used in the wind tunnel tests of references 1 to 7; it is described in references 1 and 7. A second 10° cone, the facsimile cone (which was used earlier in the wind tunnel tests of ref. 10), was instrumented for the flight tests with static pressure orifices, thermocouples, and heat flux gages. This cone was used for cone/aircraft envelope expansion flights and in-flight static pressure distribution and heat transfer measurements.

Both cones had a semivertex angle of 5° and an apex bluntness less than 0.10 millimeter (0.004 inch) in equivalent diameter. The surface finish for both was 0.25 micron (10 μin.) or better. Each cone was 91.44 centimeters (36.00 inches) in length, with the cone extension increasing that length to 113.0 centimeters (44.50 inches).

Instrumentation

Transition cone. - The principal instrumentation used for the 10° transition cone consisted of a traversing pitot probe, microphones, and temperature measurement instrumentation.

Traversing pitot probe: The traversing pitot probe shown in figure 1 is shown close up in figure 2. The probe was a 0.051-centimeter- (0.020-inch-) inner-diameter hypodermic needle flattened at the tip to an opening height of 0.015 centimeter (0.006 inch). A close-coupled 0.238-centimeter- (0.094-inch-) diameter differential semiconductor strain gage pressure transducer was located inside the probe head. The probe traversed fore and aft along the surface of the cone on the top-center ray over a distance from the cone apex of 41.4 centimeters (16.3 inches) to 87.3 centimeters (35.3 inches) (x/L = 0.37 to 0.79).

Microphones: On the knee of the traversing probe mechanism (figs. 1 and 3), a 0.238-centimeter- (0.094-inch-) diameter temperature-compensated semiconductor strain gage microphone was flush mounted in a tube to measure free-stream impact pressure fluctuations. The microphone was added for the flight experiment; it was not used during the wind tunnel tests.

Two microphones were mounted in the cone surface (figs. 1 and 4), one at $x/L = 0.404$ and $\phi = 225°$ and the other at $x/L = 0.584$ and $\phi = 180°$, to measure the cone's boundary layer pressure fluctuations. Because of the cone's curvature, the microphones were slightly depressed at the leading and trailing edges to be flush at the lateral edges. Two different sets of microphones were used. Condenser microphones 6.35 millimeters (0.25 inch) in diameter with preamplifiers close coupled inside the cone were limited to microphone temperatures of 325 K (585° R). These microphones were used for five flights (flights 349 to 353); they were the same as those used in most of the wind tunnel tests. Semiconductor strain gage sensors with temperature compensation from 222 K (400° R) to 367 K (660° R) were used for most of the flights (flights 327 to 348). The frequency response of all the microphones was limited by the frequency response of the recording electronics to 20 kilohertz.

Cone temperature measurement instrumentation: An iron-constantan thermocouple was mounted at $x/L = 0.80$ on the bottom center ray of the transition cone ($\phi = 180°$) to measure the cone's wall temperature. The thermocouple junction was flush mounted in a small hole and epoxied in place.

Facsimile cone. - An array of 0.51-millimeter- (0.020-inch-) diameter static pressure orifices and an array of thermal sensors were installed in the facsimile cone. The thermal sensors were heat flux gages and thermocouples. The heat flux gages were 0.2 millimeter (0.008 inch) thick and 6.35 millimeters (0.25 inch) in diameter. The thermal sensors were interchangeable with the static pressure orifices in the facsimile cone. A drawing of the facsimile cone showing the locations of the static pressure orifices is given in figure 5. A normal and a transverse accelerometer were mounted approximately 5 centimeters (2 inches) behind the cone extension on the sting. These accelerometers were ac coupled and monitored during the envelope expansion flights.

Instrumentation common to both cones. -

Fixed flow-sensing probe: The fixed flow-sensing probe (figs. 1 and 6) contained an impact pressure orifice and a ring of static pressure orifices 4.7 diameters back on the cylindrical portion of the probe for the measurement of airspeed and altitude. The probe required an in-flight calibration to correct for the influence of the aircraft's forward flow field. The data used for the position error curve (fig. 7) were obtained from the following two methods: (1) Pacer flights (for subsonic Mach numbers) (ref. 11) and (2) radar tracking (for subsonic and supersonic Mach numbers) (refs. 12 and 13). True free-stream Mach number, and indirectly pressure altitude and ambient, total, and dynamic pressures, were determined by using this position error curve.

Two pairs of orifices located 40° from the stagnation point of the hemispherical probe head in the pitch and yaw planes were used to measure angle of attack and angle of sideslip. Calibrations were determined in the NASA Ames 11- by 11-Foot Transonic and 9- by 7-Foot Supersonic Wind Tunnels and are given in appendix A.

Reference pressure instrumentation: Four mutually perpendicular orifices on the cone extension at $x/L = 0.940$ were manifolded to a precision 13-bit altitude transducer to provide a reference static pressure for the traversing pitot probe, the semiconductor strain gage microphones, and the facsimile cone static pressure array.

Total temperature probes: Two probes mounted on the aircraft nose were used to determine total temperature. (They are not visible in the figures.) The use of these probes is described in appendix B.

Flight Test Configuration

The flight test configuration was identical for the transition and the facsimile cones; both were mounted on the nose of the testbed aircraft as shown in figure 8. The nose boom could be pivoted vertically between flights to allow changes in incidence angle relative to the aircraft centerline. This was necessary to keep the cone near zero angle of attack for different combinations of aircraft speed, altitude, and weight. The distance from the apex of the cone to the apex of the aircraft nose was 2.13 meters (7.0 feet).

DATA ACQUISITION AND REDUCTION PROCEDURES

Flight Test Procedures

Each flight test point required that the cone be at a zero angle of attack, zero angle of sideslip, and zero heat transfer (adiabatic wall) condition simultaneously for approximately 2 minutes. With the cone inclination angle fixed before flight, the pilot centered the angle-of-attack and angle-of-sideslip needles by adjusting velocity and trimming the aircraft at the predetermined altitude for zero cone incidence. On several flights, intentional sideslip angles were flown to check the fixed flow-sensing probe calibration.

To achieve zero heat transfer on the cone at the designated test points, the target cone temperatures were computed for the test conditions using ambient air temperature data from a morning radiosonde balloon. For Mach numbers above approximately 1.2, this required that the cone be heat soaked on the ground at the end of the runway to a temperature between 104° C and 116° C (220° F and 240° F) before takeoff (fig. 9). After takeoff the cone's temperature was monitored and the flight schedule was adjusted so the cone would reach the target temperature at the test point. For test points for which the cone needed to be cooled, the pilot took the airplane to a higher altitude than the test point and cold soaked the cone until it reached the target temperature. The pilot then flew the airplane to the target altitude and Mach number.

For monitoring test conditions during flight, data from the airplane were transmitted to the ground station, processed in real time, and displayed on cathode ray tubes (CRT's) and strip charts.

A time history of Mach number, altitude, Reynolds number, angle of attack, and angle of sideslip for a typical pitot probe traverse is shown in figure 10. The figure shows that flight conditions changed very little during the traverse.

The test points at which measurements were made in flight are shown in the Mach number/altitude envelope in figure 11. The various symbol shapes distinguish between data acquired at different nominal dynamic pressures and nominal aircraft trim angles of attack. For each preset nose boom angle of the cone relative to the aircraft, the aircraft was trimmed to give zero indicated cone angle of attack at a particular M_∞ for a given altitude, thus defining a trace of nearly constant unit Reynolds number across the envelope. The same symbol shapes are used later in the data presentation for the same test conditions. As figure 11 shows, many of the test points in this program were repeated to investigate the degree of repeatability of the measurements in the flight environment.

Data Recording

Data were recorded on a 14-track tape recorder at 30 inches per second (IPS) using the standard Inter-Range Instrumentation Group (IRIG) wide band I technique. Data from the cone microphones, free-stream impact probe microphone, and cone accelerometers were analog signals each recorded on a separate track of the recorder. The remaining data were digitized at 200 samples per second and recorded on a single data track. The digitized data were also telemetered to a ground station, formatted in real time, and recorded on magnetic tape.

Data Reduction

Free-stream Mach number and altitude were obtained by applying the airspeed corrections shown in figure 7 to the values measured at the fixed flow-sensing probe. Values for total pressure, static pressure, dynamic pressure, and unit Reynolds number were determined by using the information in references 14 and 15.

The boundary layer edge conditions, M_e and U_e/ν_e, were calculated by using the surface static pressures measured during the facsimile cone flights (app. C). Onset and end of transition Reynolds numbers were computed at zero incidence as follows:

$$Re_{t_0} = \left(U_e/\nu_e\right)X_{t_0} \tag{1}$$

$$Re_{T_0} = \left(U_e/\nu_e\right)X_{T_0} \tag{2}$$

where X_t and X_T were onset and end of transition locations defined from measured values of x by the traversing pitot probe. Onset and end of transition locations, which are apparent in figure 12 (a typical pitot probe pressure trace), were defined in exactly the same way as was described in reference 7 for the wind tunnel tests.

Some of the flight data had to be corrected for small incidence angles, and most of the data had to be corrected for slight variations of the wall temperature from the adiabatic wall temperature. Corrections for nonzero incidence were based upon the wind tunnel data and the procedures of appendix D.

To correct the data for nonadiabatic wall temperatures, a turbulent cone recovery factor, r, equal to 0.88 (ref. 16), was used to determine the adiabatic wall temperature using the following relation:

$$T_{aw} = T_e \left[1 + r \frac{(\gamma - 1)}{2} M_e^2\right] \tag{3}$$

The placement of the T_w sensor at the aft limit of the pitot probe survey range ($x/L = 0.80$) assured a turbulent recovery temperature for cases when complete transition could be detected. The fairing of the flight temperature data discussed in RESULTS AND DISCUSSION was used to determine Re_{t_0} and Re_{T_0}.

The influence of atmospheric turbulence on the flight data could be isolated only when the pilot considered the level of turbulence to be moderate. Such encounters with turbulence were rare. The atmosphere over the flight test range appeared remarkably stable for most of the flights. The weather data recorded by the radiosonde balloons for each day of flight are presented in appendix E to document the atmospheric disturbance environment. When the pitot probe made a traverse during moderate atmospheric turbulence, the transition location became difficult to define and, as indicated in figure 13, flight conditions became unsteady, invalidating the test data.

Measurements by the cone surface and free-stream impact microphones of the flight disturbance environment were recorded on magnetic tape and processed to obtain power spectral density. Data at frequencies up to the upper recording frequency limit of 20 kilohertz were analyzed using a Fourier analyzer. The data were ensemble averaged for the 36-second interval preceding pitot probe traverse from the full-retract stow position ($x/L = 0.79$) and had a frequency resolution of 24.4 hertz.

The in-flight vibration measurements from the cone accelerometer package revealed the only significant vibration to lie below approximately 200 hertz. In addition, the cone/aircraft fuselage bending natural frequencies were found to be 5.6 hertz in the lateral direction and 7.0 hertz in the vertical direction during ground vibration test. Accordingly, the cone microphone data were high pass filtered during the data reduction process at 200 hertz, giving an overall bandwidth from 200 hertz to 20 kilohertz. The free-stream impact probe microphone data were analyzed without filtering from 0 hertz to 20 kilohertz.

RESULTS AND DISCUSSION

Effects of Cone Temperature

During the flight tests it was possible to control the transition cone's temperature within ±6 percent of the adiabatic wall temperature, T_{aw}, for about 90 percent of the test points by using the method described in Flight Test Procedures. Even this small deviation in temperature had a large influence on transition location, however, as shown in figure 14. The data have been grouped by Mach number and nondimensionalized by the adiabatic wall temperature transition Reynolds number. The adiabatic wall temperature transition Reynolds number was determined from fairings of the flight data for each nominal Mach number. The sensitivity of transition Reynolds number to heat transfer appears to have been essentially independent of Mach number and proportional to the temperature ratio T_w/T_{aw}. The trend of the data in figure 14 shows a strong heat transfer influence on transition, delayed transition occurring when the boundary layer was cooled ($T_w/T_{aw} < 1.0$), earlier transition occurring when the boundary layer was heated ($T_w/T_{aw} > 1.0$). Also shown in figure 14 are data obtained during a rapid excursion of total temperature at $M = 1.2$ in the AEDC 4-Foot Transonic (4T) Wind Tunnel. These data show the same trend as the flight data. According to the theoretical flat plate e^9 method from reference 17, transition onset for a Mach number of 0.85 also follows the trend of the flight data. A curve was fit through the flight data and used for correcting nonadiabatic data to adiabatic conditions.

Transition Reynolds Number

The transition Reynolds numbers measured in flight corrected to adiabatic wall temperatures are shown as a function of local Mach number in figure 15. This figure includes 82 test points (39 of which were acquired at supersonic speeds) gathered from 27 flights over a 2.5 month time period. The data form a nearly linear band. Transition Reynolds number was a function of Mach number and ranged from about 3.5×10^6 at a Mach number of 0.5 to above 9.0×10^6 at Mach numbers above 1.6. Actual measurements of X_t, X_T, and the corresponding flight conditions are tabulated in table 1 together with the corrected values of end of transition Reynolds number, Re_{T_0}, and onset of transition Reynolds number, Re_{t_0}. Figure 16 shows that the ratio of onset of transition Reynolds number to end of transition Reynolds number is independent of Mach number and dynamic pressure and has a mean value of 0.86. Most of the data are within ±5 percent of this mean value.

Transition Reynolds number was plotted as a function of unit Reynolds number in figure 17 for nominal Mach numbers to determine whether the present data had the unit Reynolds number effect shown for higher Mach numbers in references 7, 18, and 19. Even at Mach numbers where there were a substantial number of data over a wide range of unit Reynolds numbers at adiabatic conditions, the data are inconclusive.

Flight Disturbance Environment

Indications of laminar instability were found in the microphone spectra. For purposes of illustration, the spectra obtained during two flight test points from all three microphone signals (free-stream impact, forward cone, and aft cone) are shown in figures 18(a) and 18(b). In figure 18(a), the forward cone microphone was under transitional flow, and the aft cone microphone was under fully developed turbulent flow. In figure 18(b), the forward cone microphone was under laminar flow and the aft cone microphone was under transitional flow. In all cases when the boundary layer was laminar or transitional, there was a broad peak in the pressure fluctuation spectra similar to those shown in figures 18(a) and 18(b). The nondimensional frequency at which the peak occurs is denoted in figure 18 by F; the subscripts 1 and 2 refer to the forward and aft cone microphones, respectively. The nondimensional frequencies for these peaks are documented in table 2, where F denotes the peak center frequency and F_{min} and F_{max} denote the lower and upper bounds of the peak. When the boundary layer was turbulent, the spectra were characteristically smooth, with higher power over most of the recorded bandwidth than for the laminar spectra except at the peaks.

Spectra recorded in several flights at the same nominal Mach numbers are shown in figures 19(a) and 19(b). The variable between spectra in both figures 19(a) and 19(b) is the Reynolds number based on the cone microphone location. The dominant feature in these cone boundary layer spectra is the peak, which decreases in frequency and increases in power as Re_x increases at a given M_e. Finally, at the location near the end of transition, X_T, the peak disappears into the smooth, broadband spectrum characteristic of a turbulent boundary layer.

The spectral peaks appeared to exhibit a prescribed behavior in terms of the variation of absolute frequency, f, with M_e, as shown in figures 20(a) to 20(d). The center frequencies increase as M_e increases. A ratio of the frequencies f_1/f_2, when peaks occurred in the spectra from both microphones at a given flight condition, was approximately the inverse of the ratio of the distance from the cone apex, $(X_2/L)/(X_1/L)$, and therefore the microphone Reynolds numbers, Re_{x_2}/Re_{x_1}. Hence, the peak frequencies are functions of both Re_x and M_e. This relationship was not as well defined at the highest dynamic pressures (fig. 20(d)).

The nondimensional center peak frequencies are shown in figure 21 and show a clear dependence upon Reynolds number and Mach number. The data agree well with recent calculations by Mack since his publication of reference 20 adjusted by the usual cone-planar similarity rule (where the Reynolds number on a cone is three times that on a flat plate). The calculations by Mack are for the first mode laminar instability, that is, Tollmien-Schlichting waves, and the calculations agree with the characteristics of the spectra; thus, Tollmien-Schlichting waves are probably the cause of transition.

Naturally growing Tollmien-Schlichting waves can be detected only in a low disturbance free-stream environment. As shown by the free-stream impact microphone overall pressure fluctuations (figs. 22(a) and 22(b)), the level of disturbance in the flight environment was very low compared with that in most wind tunnels. The flight disturbance level varied from about 0.005 percent to about 0.03 percent (fig. 22(a)) when normalized by the free-stream total pressure. When the free-stream impact overall pressure fluctuations are normalized by free-stream dynamic pressure, q_∞ (fig. 22(b)), the data collapse better and the values range from 0.16 percent at the lower Mach numbers to 0.017 percent near Mach 2. The different flags on the symbols, which denote flights made on different days, indicate the day-to-day variations in the atmosphere. The disturbances did not seem to be dominated by engine noise, although some discrete tones appeared randomly in the spectra, and some of these may have come from the engine inlets, fans, or compressors.

The amplitudes recorded by the cone microphones only under laminar flow conditions are shown in figure 23. When the cone boundary layer was turbulent, the cone surface microphone recorded pressure fluctuations in the near-field turbulent boundary layer. When the boundary layer was transitional, the amplification of the low end of the frequency spectrum during transition produced large overall values of indicated pressure fluctuation. Only under laminar conditions could the cone surface microphones measure disturbances imposed from the free stream, and this measurement was altered by the laminar boundary layer receptivity. As the spectral data in figure 19 show, the laminar boundary layer selectively amplifies certain frequencies in the spectrum, increasing some of the values sensed by the microphone.

The cone surface static pressure fluctuations, $\sqrt{\overline{p_s'^2}}$, are shown normalized by p_∞ and q_∞ in figures 23(a) and 23(b) as a function of M_e. As a percentage of p_∞, the laminar pressure fluctuations seem to increase with increasing M_e; as a percentage of q_∞ (fig. 23(b)), they decrease with increasing M_e. A comparison of figures 22(b) and 23(b) shows that at the highest M_e the cone surface pressure fluctuation is essentially the same as the free-stream impact pressure fluctuation. The differences between the cone surface and free-stream impact pressure fluctuation amplitudes increase as M_e decreases.

As before, the different flags on the symbols (fig. 23) denote flights on different days to indicate day-to-day variations. The open symbols denote data acquired with the semiconductor strain gage microphones used at the higher Mach numbers and higher temperatures. The solid symbols denote data acquired with condenser microphones like those used in the wind tunnels. The data from both types of microphones agree well. The laminar and transitional spectra measured by both sets of microphones had the same characteristics, verifying that the peaks were associated with the boundary layer and not anomalies introduced by the sensors.

Data Comparison

The corrected end of transition Reynolds number at zero angles of incidence and adiabatic wall temperature conditions is plotted against the normalized cone surface pressure fluctuations, $\sqrt{\overline{p_s'^2}}/q_\infty$, in figure 24(a). It should be noted that $\sqrt{\overline{p_s'^2}}$ is the overall level (200 Hz to 20 kHz) of disturbance measured by the cone microphone under a laminar boundary layer. The flight data show good agreement with the wind tunnel data from reference 7.

A similar plot of end of transition Reynolds number with the normalized impact pressure fluctuations, $\sqrt{\overline{p_{t_2}'^2}}/q_\infty$, is shown in figure 24(b). The data scatter about a fairing was within ±20 percent, as in figure 24(a). The fluctuating impact pressure probe was not installed on the traversing probe during the wind tunnel tests, so no comparable wind tunnel data are available.

CONCLUDING REMARKS

A flight test program was performed during which in-flight measurements of boundary layer transition and atmospheric disturbance measurements were made on a 10° transition cone tested previously in 23 wind tunnels. The data were acquired in flight at Mach numbers from 0.5 to 2.0 and at altitudes from 1500 meters (5000 feet) to 15,000 meters (50,000 feet) to provide a set of reference data for wind-tunnel-to-flight correlation.

Transition Reynolds number was a function of Mach number and ranged from about 3.5×10^6 at a Mach number of 0.5 to above 9.0×10^6 at Mach numbers above 1.6.

The wall temperature ratio, T_w/T_{aw}, had a strong effect on transition Reynolds number. Transition was delayed when the boundary layer was cooled, and early transition occurred when the boundary layer was heated.

In a laminar or transitional boundary layer on the cone, the microphones detected a broad peak in the spectrum. The nondimensional center peak frequency agreed well with calculations by Mack for first mode laminar instability, that is, Tollmien-Schlichting waves, identifying Tollmien-Schlichting waves as the probable cause of transition.

The disturbance level was low in flight as determined by the free-stream impact and cone microphones.

The comparison of flight transition Reynolds number to cone surface pressure fluctuations was in good agreement with the same comparison using the data from the wind tunnels.

Ames Research Center
Dryden Flight Research Facility
National Aeronautics and Space Administration
Edwards, California 93523
May 28, 1981

APPENDIX A

FLOW ANGLE MEASUREMENT

Cone incidence angle was derived from the measurements of flow angle using the orifices in the fixed flow-sensing probe. Before the flight tests, the probe was calibrated in two wind tunnels at the NASA Ames Research Center; during these wind tunnel calibrations the probe was mounted on the sting in the flight test configuration. The differential pressures in the probe were calibrated for sensitivity during the transition asymmetry calibrations. The resulting differential pressure coefficients, ΔC_{p_α} and ΔC_{p_β}, were calculated as follows:

$$\Delta C_{p_\alpha} = \frac{\Delta p_\alpha}{q_\infty} \tag{4}$$

and

$$\Delta C_{p_\beta} = \frac{\Delta p_\beta}{q_\infty} \tag{5}$$

The sign conventions were positive ΔC_{p_α} for positive cone angle of attack and positive ΔC_{p_β} for flow from the right (looking forward). Linear approximations of the sensitivities were defined in terms of $\frac{d\left(\Delta C_{p_\alpha}\right)}{d\alpha}$ and $\frac{d\left(\Delta C_{p_\beta}\right)}{d\beta}$.

The data defining $\frac{d\left(\Delta C_{p_\alpha}\right)}{d\alpha}$ and $\frac{d\left(\Delta C_{p_\beta}\right)}{d\beta}$ are shown in figure 25, the wind tunnel flow angle being measured by the tunnel sting support system. The theoretical curve shown in figure 25 was obtained using the method of Hsieh (ref. 21). The deviations of the measurements from the theory are believed to be due to the combined effects of the cone's flow field, the misalinement of the probe relative to the cone, and probe manufacturing tolerances. The equations used to reduce the flight data were

$$\alpha_{ind} = \frac{d\alpha}{d\left(\Delta C_{p_\alpha}\right)} \Delta C_{p_\alpha} + \alpha' \tag{6}$$

$$\beta_{ind} = \frac{d\beta}{d\left(\Delta C_{p_\beta}\right)} \Delta C_{p_\beta} + \beta' \tag{7}$$

where $\frac{d\alpha}{d\left(\Delta C_{p_\alpha}\right)}$, $\frac{d\beta}{d\left(\Delta C_{p_\beta}\right)}$, α', and β' were functions of M_∞ as defined by the calibrations.

An appreciable misalinement of the probe in the sideslip plane was indicated by the cone measurement of sideslip when ΔC_{p_β} equaled 0. The data showing the offset angle, β', are given in figure 26. Data are included from tests made in two other tunnels as well -- the Langley 4- by 4-Foot Supersonic Pressure Tunnel and the AEDC 4-Foot Transonic Wind Tunnel. The β' data scatter was about ±0.15°. A constant value of 0.57° was selected as a mean misalinement value.

When the cone was carefully positioned at zero angle of attack, the angle indicated by the fixed flow-sensing probe in the four wind tunnels was as shown in figure 27. The data scatter was about ±0.2° from a theoretical inviscid solution for the velocity vector at that location given by the method of reference 22 for subsonic flow and by conical flow theory for supersonic flow. The theoretical solution seems to provide a good fairing for the data, indicating no appreciable misalinement of the probe in the angle-of-attack plane. In-flight checks of cone angle of attack and angle of sideslip were made as a check on the wind tunnel calibrations. The accelerometer method of reference 23 was used to check angle of attack. According to this method, if the aircraft is held stable at a constant altitude and velocity, the aircraft longitudinal acceleration can be expressed as a function of aircraft angle of attack, where

$$\sin \alpha_{ac} = a_{x_{ac}} \tag{8}$$

Correcting for small constant rates of change in altitude and velocity, the equation becomes, after solving for angle of attack,

$$\alpha_{ac} = \arcsin\left(a_{x_{ac}} - \frac{\Delta U_\infty}{g\Delta t}\right) + \arcsin\left(\frac{\Delta H}{U_\infty \Delta t}\right) \tag{9}$$

The cone angle of attack was determined using the preset inclination angle of the cone relative to the aircraft longitudinal axis (which was known); the results are shown in figure 28. The subsonic data agree well with the wind tunnel calibration. The supersonic data are inconclusive because of the limited number of suitable data points.

Two methods were used to check the cone angle of sideslip. The first method used the equations of motion simplified for steady state test conditions where

$$a_{y_{ac}} = \frac{q_\infty S}{W}\left(C_{y_{\delta_r}} \delta_r + C_{y_\beta} \beta_{ac}\right) \tag{10}$$

Aircraft angle of sideslip was calculated from this equation, and the cone sideslip was determined by correcting for the misalinement between the cone and aircraft axes. The results are shown by the square symbols in figure 29. The data for the open symbols are for flights 327 to 344; the data for the solid symbols are for flights 345 to 353. A shift of about 0.5° in angle of sideslip occurred between flights 344 and 345 and was sensed by the pilot.

Facsimile cone data from a sensitive differential pressure transducer across diametrically opposed static orifices in the yaw plane at $x/L = 0.40$ during flights 358 and 359 confirmed the shift in sideslip angle, as shown in figure 29. The data for differential pressure and indicated angle of sideslip were faired, and the intercept of $\Delta C_{p_\beta} = 0$ was chosen as the true zero angle of sideslip. The data from flights 345 to 353, 358, and 359 were corrected accordingly.

APPENDIX B

TOTAL TEMPERATURE MEASUREMENT

It was necessary to know the free-stream static temperature of the atmosphere, T_∞, at all flight conditions in order to compute airspeed, U_∞, unit Reynolds number, $U_\infty/{}_\infty$, and the adiabatic wall recovery temperature on the cone, T_{aw}. The direct measurement of T_∞ during flight is not practical. Hence, total temperature, T_t, was measured by using two independent temperature probes installed on the aircraft fuselage.

The readings from these two probes differed by an average of 1.5 percent -- a significant amount for experimental research in transition. Two methods were used to ascertain which probe gave the better reading. The first was to compare the value of T_∞ computed from the measured T_t with the radiosonde weather data discussed in appendix E. The second method was to measure the rate of heat transfer, Q_w, on the surface of the facsimile cone together with surface temperature, T_w. A check showed that Q_w approached zero as T_w/T_{aw} approached 1.0, which verified the accuracy of the measurements of T_w, Q_w, and T_t, since T_t was used to compute T_{aw}. This check also verified the accuracy of the computation of boundary layer edge flow conditions M_e and T_e and the accuracy of the laminar and turbulent recovery factors, r, used in computing T_{aw}.

The first total temperature probe (probe 1) was installed on the side of the aircraft nose. The second probe (probe 2) was installed beneath the nose. Both probes were sufficiently large to place the temperature-sensing element outside the aircraft boundary layer. Probe 2 was installed about halfway through the flight test program (for flight 339), after readings from probe 1 were suspected of being in error (the readings were suspiciously low compared with ground weather data on the runway before takeoff). Typical comparisons of the in-flight temperature data with the radiosonde data from appendix E are shown in figure 30. The second probe (probe 2) showed better agreement with the radiosonde data at all airspeeds and altitudes. The apparent error in the probe 1 readings was not a simple alteration in recovery factor, r.

Because of the error, a correction to the probe 1 readings for all flights prior to flight 339 was devised. The method of doing so was to continue to record the probe 1 readings after flight 339 to establish a basis for estimating the error before flight 339. The corrected value of T_t was cross-checked against a theoretical T_t for the radiosonde measurements each day. The accuracy of the T_t measurements from probe 2 is estimated to have been within ±0.3 percent. With corrections, the accuracy of the T_t measurements before flight 339 is estimated to have been approximately ±0.4 percent.

The facsimile cone with thermal instrumentation was flown before the first flight test of the 10° transition cone (flight 327). The thermal instrumentation in the facsimile cone was a second source of temperature measurements and actually verified the accuracy of the T_t corrections applied. Shown in figure 31 are Q_w versus T_w/T_{aw} at $\phi = 135°$ for two of the heat flux gages (those at $x/L = 0.40$ and 0.67) at different times of a selected period of transient flight conditions. In figure 31, the fairing of T_w/T_{aw} approaches unity as Q_w approaches 0.

APPENDIX C

CONE STATIC PRESSURE MEASUREMENTS

Cone static pressure distributions were measured on the facsimile cone at Mach numbers from 0.55 to 1.68 during two flights. The static pressure orifices were connected to a single transducer using a Scanivalve. The static pressure orifice locations are shown in figure 5.

Typical data showing the axial surface pressure distribution are presented in figures 32(a) to 32(e). The data were recorded at near zero cone incidence. At subsonic Mach numbers, the flight data are compared with the theoretical pressure distribution for zero incidence from small perturbation theory (ref. 24). The axial surface pressure gradients were all essentially zero, favorable gradients having been expected by theory for the cone alone. At supersonic Mach numbers, the cone surface pressure distribution agreed reasonably well with the conical theory of reference 15.

In figure 33, for M = 0.6, when a portion of the forward fuselage was included in a theory using the Euler equations, the theory agreed well with the flight data.

The nearly constant cone surface pressure at each free-stream Mach number was used to derive the relationships for local Mach numbers, unit Reynolds numbers, and dynamic pressures used in this report and shown in figures 34(a) to 34(c).

APPENDIX D

TRANSITION ASYMMETRY AT NONZERO INCIDENCE

The data that were acquired to define transition asymmetry (transition at nonzero incidence) are compiled in table 3. It was considered important to perform transition asymmetry calibrations on the actual transition cone because of the possibility of body-peculiar geometric imperfections (the two surface-mounted microphones, for example). No other such data are available for the Mach number range of this flight test program. There are data for Mach numbers of 2 and higher, however, so data were acquired on the cone at free-stream Mach numbers up to 4.5 to permit the results of this investigation to be compared with the results of other investigations. This appendix represents the only complete compilation of asymmetry data for this cone. Some of the data were presented in references 6 and 7 to illustrate the importance of controlling incidence angle in wind tunnels and to show that the sensitivity of transition to small incidence angle varies with Mach number.

The calibrations for asymmetry were obtained in several NASA Ames and Langley Research Center wind tunnels. When possible, data at the same test conditions were acquired in more than one wind tunnel, since it was recognized that wind-tunnel-dependent characteristics might affect the observed sensitivities. The data presented in table 3 were all acquired using the traversing pitot probe. The most complete set of data, which also appeared to be the most self-consistent, was acquired in the NASA Ames 11- by 11-Foot Transonic Wind Tunnel and 9- by 7-Foot Supersonic Wind Tunnel.

The transition asymmetry data were acquired by pitching the cone in increments through a range of angles of attack; the pitot probe trace was along the top center ray, as it was in the flight test program. The yaw angle was held at zero while angle of attack was changed so that at positive angles of attack the pitot probe trace was along the leeward ray ($\phi = 0°$). At negative angles of attack, the pitot probe traced the windward stagnation ray ($\phi = 180°$). The cone was then yawed in increments through a range of angles of sideslip at zero angle of attack, placing the pitot probe at $\phi = 90°$ for positive angles of sideslip and at 270° for negative angles of sideslip. Transition asymmetry was thereby defined on four rays circumferentially about the cone.

The procedure used in correcting the flight data for nonzero incidence was essentially the same as that used in references 25 and 26 for cones in free flight in an aeroballistic range, except that references 25 and 26 used four measurement points at the cone edge rays as viewed in the silhouette by two shadowgraph cameras oriented 90° to one another. The total incidence angle, Γ, is given by

$$\Gamma = \left(\alpha^2 + \beta^2\right)^{1/2} \tag{11}$$

In the present experiment, the location of the pitot probe trace relative to the windward stagnation ray could be defined by the expression

$$\phi = \tan^{-1} \frac{\beta}{\alpha} - 180° \tag{12}$$

Since ϕ and Γ can occur in any random combination in flight, a rationale was developed for interpolating between the four ϕ data points of the present calibrations. In reference 26, data from several supersonic and hypersonic sources were collected, some detailing variations in ϕ as fine as 10°. The family of curves shown in figure 35 was derived for transition onset, X_t. Reference 27 showed generally good agreement with these curves for free-launched cones in another aeroballistic range for $\alpha/\theta_c \geq 0.3$ and $M_\infty \cong 4.5$.

The present calibration data, which were acquired after the data in references 25 and 26, are shown in figure 36. The present data are in reasonably good agreement on the leeward (0°) and windward (180°) rays with other published data (refs. 26 and 28 to 30) at Mach numbers at the boundary layer edge, M_e, of approximately 2.0 and from 4.36 to 5.15 (figs. 36(a) and 36(b), respectively). The sensitivity of transition to angle of attack seems to be about the same for values of M_e from 2.0 to 5.5, but, as will be shown in figure 37, changes dramatically as M_e decreases from 2.0 to about 0.4, and is approximately constant for M_e = 0.4 to 0.9.

The curves in reference 26 were used to create a rationale for interpolation, and the data from table 3 were used to develop the curves shown in figure 37. The method for correcting X_t and X_T to zero incidence values was, therefore, to find the curve for the value of M_e closest to that of the flight data point, to obtain the ratio of X_T/X_{T_0} from this curve for the known values of Γ and ϕ, and to divide the measured value of X_t or X_T by that ratio. The ratios $(X_t)/(X_{t_0})$ and $(X_T)/(X_{T_0})$ were assumed to be identical.

APPENDIX E

WEATHER DATA

Radiosonde data for the atmospheric conditions of each day of flight were provided by the USAF Flight Test Center Ground Weather Monitoring Station at Edwards Air Force Base. Data were acquired at regular intervals from the surface to an altitude of 15,000 meters (50,000 feet). The data included barometric pressure, atmospheric density, temperature, relative humidity, windspeed, and wind direction, and are tabulated in table 4. The sources of measurement uncertainty are discussed in reference 31.

The significance of the radiosonde temperature data to the present investigation was mentioned in appendix B. The windspeed and wind direction data are important because these disturbance environment data may be correlated with the turbulence encountered at various test altitudes on particular days.

Week-to-week or season-to-season changes in the atmosphere could have affected the results presented herein. However, the data in this appendix show that the atmosphere was remarkably stable during the particular days when flight tests were made.

REFERENCES

1. Credle, O. P.; and Carleton, W. E.: Determination of Transition Reynolds Number in the Transonic Mach Number Range. AEDC-TR-70-218, Arnold Eng. Dev. Ctr., Oct. 1970. (Available from DTIC as AD 875995.)

2. Dougherty, N. S., Jr.; and Steinle, Frank W., Jr.: Transition Reynolds Number Comparisons in Several Major Transonic Tunnels. AIAA Paper No. 74-627, July 1974.

3. Vaucheret, Xavier: Acoustic Fluctuations Generated by the Ventilated Walls of a Transonic Wind Tunnel. Windtunnel Design and Testing Techniques, AGARD-CP-174, Mar. 1976, pp. 25-1–25-10.

4. Ross, R.; and Rohne, P. B.: The Character of Flow Unsteadiness and Its Influence on Steady State Transonic Wind Tunnel Measurements. Windtunnel Design and Testing Techniques, AGARD-CP-174, Mar. 1976, pp. 45-1–45A-2.

5. Mabey, D. G.: Boundary Layer Transition Measurements on the AEDC 10° Cone in Three RAE Wind Tunnels and Their Implications. R & M No. 3821, British A.R.C., June 1976.

6. Whitfield, Jack D.; and Dougherty, N. Sam, Jr.: A Survey of Transition Research at AEDC. Laminar-Turbulent Transition, AGARD-CP-224, Oct. 1977, pp. 25-1–25-20.

7. Dougherty, N. Sam, Jr.: Influence of Wind Tunnel Noise on the Location of Boundary-Layer Transition on a Slender Cone at Mach Numbers from 0.2 to 5.5. AEDC-TR-78-44, Arnold Eng. Dev. Ctr., Mar. 1980.

8. Dougherty, N. S., Jr.; and Fisher, D. F.: Boundary Layer Transition on a 10-Degree Cone: Wind Tunnel/Flight Data Correlation. AIAA Paper No. 80-0154, Jan. 1980.

9. Dougherty, N. Sam, Jr.; and Fisher, David F.: Boundary-Layer Transition Correlation on a Slender Cone in Wind Tunnels and Flight for Indications of Flow Quality. AEDC-TR-81-26, Feb. 1982.

10. Pate, S. R.: Measurements and Correlations of Transition Reynolds Numbers on Sharp Slender Cones at High Speeds. AIAA J., vol. 9, no. 6, June 1971, pp. 1082-1090.

11. Herrington, Russel M.; Shoemacher, Paul E.; Bartlett, Eugene P.; and Dunlap, Everett W.: Flight Test Engineering Handbook. AF Tech. Rept. No. 6273, Air Force Flight Test Ctr., Edwards AFB. Rev. June 1964.

12. Larson, Terry J.; and Ehernberger, L. J.: Techniques Used for Determination of Static Source Position Error of a High Altitude Supersonic Airplane. NASA TM X-3152, 1975.

13. Webb, Lannie D.: Characteristics and Use of X-15 Air-Data Sensors. NASA TN D-4597, 1968.

14. U.S. Standard Atmosphere, 1962. NASA, U.S. Air Force, U.S. Weather Bur., Dec. 1962.

15. Ames Research Staff: Equations, Tables, and Charts for Compressible Flow. NACA Rept. 1135, 1953. (Supersedes NACA TN 1428.)

16. Evvard, John C.; Tucker, Maurice; and Burgess, Warren C., Jr.: Transition-Point Fluctuations in Supersonic Flow. J. Aeronaut. Sci., vol. 21, no. 11, Nov. 1954, pp. 731-738, 748.

17. Reshotko, E.: Drag Reduction by Cooling in Hydrogen Fueled Aircraft. J. Aircraft, vol. 16, Sept. 1979, pp. 584-590.

18. Beckwith, Ivan E.; Bertram, Mitchel H.: A Survey of NASA Langley Studies on High-Speed Transition and the Quiet Tunnel. NASA TM X-2566, 1972.

19. Potter, J. Leith; and Whitfield, Jack D.: Effect of Unit Reynolds Number, Nose Bluntness, and Roughness on Boundary Layer Transition. AEDC TR-60-5, Arnold Eng. Dev. Ctr., Mar. 1960.

20. Mack, Leslie M.: Boundary-Layer Stability Theory. NASA CR-131501, 1969.

21. Hsieh, T.: Flow-Field Study About a Hemisphere-Cylinder in the Transonic and Low Supersonic Mach Number Range. AEDC-TR-75-114, Arnold Eng. Dev. Ctr., Nov. 1975.

22. Hess, J. L.; and Smith, A. M. O.: Calculation of Potential Flow About Arbitrary Bodies. Progress in Aeronautical Sciences, Vol. 8, D. Küchemann, ed., c.1967, Pergamon Press Ltd., pp. 1-138.

23. Beeler, De E.; Bellman, Donald R.; and Saltzman, Edwin J.: Flight Techniques for Determining Airplane Drag at High Mach Numbers. NACA TN 3821, 1956.

24. Wu, Jain-Ming; and Lock, Robert C.: A Theory for Subsonic and Transonic Flow Over a Cone - With and Without Small Yaw Angle. Tech. Rept. RD-74-2, U.S. Army Missile Command, Dec. 1973.

25. Potter, J. Leith: Studies of Boundary-Layer Transition on Aeroballistic Range Models. AEDC-TR-73-194, Arnold Eng. Dev. Ctr., May 1974.

26. Potter, J. Leith: Boundary-Layer Transition on Cones Near Mach One in an Aeroballistic Range. AEDC-TR-74-115, Arnold Eng. Dev. Ctr., Jan. 1975.

27. Reda, Daniel C.: Boundary-Layer Transition Experiments on Sharp, Slender Cones in Supersonic Freeflight. NSWC/WOL TR 77-59, Naval Surface Weapons Ctr., Sept. 1977.

28. Krogmann, P.: An Experimental Study of Boundary Layer Transition on a Slender Cone at Mach 5. Laminar-Turbulent Transition, AGARD-CP-224, Oct. 1977, pp. 26-1–26-12.

29. Stetson, K. F.: Effect of Bluntness and Angle of Attack on Boundary Layer Transition on Cones and Biconic Configurations. AIAA Paper No. 79-0269, Jan. 1979.

30. Stetson, Kenneth F.; and Rushton, George H.: Shock Tunnel Investigation of Boundary-Layer Transition at M = 5.5. AIAA J., vol. 5, no. 5, May 1967, pp. 899-906.

31. Meteorological Data Error Estimates. Document 110-77, Range Commanders Council, White Sands Missile Range. Second rev., Jan. 1977.

TABLE 1.–10° TRANSITION CONE FLIGHT DATA

(a) SI Units

H, m; U_∞/ν_∞, per m × 10^6; q_∞, kN/m^2; X_t and X_T, cm; Re_{t_0} and Re_{T_0}, × 10^6; T_t, T_w, T_∞, and T_{∞_b}, K;

α and β, deg; $\left(\sqrt{\overline{p'_{t_2}}^2}/q_\infty\right)100$, $\left(\sqrt{\overline{p'_{t_2}}^2}/p_{t_\infty}\right)100$, $\left(\sqrt{\overline{p'_{s_1}}^2}/q_\infty\right)100$, and $\left(\sqrt{\overline{p'_{s_2}}^2}/q_\infty\right)100$, percent

Time of day	M_∞	H	$\frac{U_\infty}{\nu_\infty}$	q_∞	X_t	X_T	T_w/T_{aw}	Re_{t_0}	Re_{T_0}	T_t	T_w	T_∞	T_{∞_b}	α	β	$\frac{\sqrt{\overline{p'_{t_2}}^2}}{q_\infty}$ × 100	$\frac{\sqrt{\overline{p'_{t_2}}^2}}{p_{t_\infty}}$ × 100	$\frac{\sqrt{\overline{p'_{s_1}}^2}}{q_\infty}$ × 100	$\frac{\sqrt{\overline{p'_{s_2}}^2}}{q_\infty}$ × 100
FLT 327 8-14-78 AIRCRAFT TRIM ANGLE - 2.50 DEG																			
8:54	1.20	12245	7.4	18.67	52.8	62.5	1.035	4.96	5.90	279.4	281.4	216.9	215.9	-.24	-.04	******	******	******	******
9: 0	1.08	11324	7.4	17.72	53.1	62.0	1.012	4.17	4.94	277.6	274.4	225.1	221.4	-.22	-.03	.0670	.0278	.0990	.1090
9: 7	.86	9596	7.3	14.56	50.5	56.4	1.014	3.94	4.40	269.7	269.2	234.9	233.9	-.02	-.04	.0970	.0306	.2240	.4350
9:18	.66	6035	8.0	14.51	52.3	70.6	.969	3.27	4.41	287.2	275.6	264.2	265.3	.01	-.01	.1070	.0243	.1460	******
9:24	.55	3135	9.2	14.75	*****	*****	.973	****	****	296.2	286.1	279.3	282.8	-.07	.20	.1590	.0275	2.5220	1.3780
9:30	.74	8171	7.2	13.26	*****	*****	1.036	****	****	273.8	280.2	246.8	246.4	.03	.16	.0980	.0261	1.1220	.5580
9:35	.54	3008	9.0	14.17	*****	50.8	.976	****	3.74	296.2	287.2	279.8	283.8	.05	-.03	.1520	.0253	1.9410	1.7150
FLT 328 8-16-78 AIRCRAFT TRIM ANGLE - 2.50 DEG																			
10:13	1.52	14889	6.8	19.92	61.2	71.1	1.071	8.28	9.07	296.9	305.9	203.1	204.5	-.44	.27	.0397	.0170	.0930	.0630
10:20	1.36	14265	5.5	17.33	60.7	71.1	1.068	6.30	7.38	283.3	292.9	206.8	205.7	-.19	-.05	.0413	.0177	.0800	.0818
10:23	1.17	12171	7.3	18.05	50.5	57.7	1.046	4.88	5.74	279.5	284.9	219.4	216.5	-.39	-.09	.0517	.0213	.0980	.1170
FLT 329 8-18-78 AIRCRAFT TRIM ANGLE - 2.50 DEG																			
10:11	1.39	13996	7.1	18.90	67.8	78.2	1.036	5.14	7.08	284.0	284.3	204.8	209.6	-.16	0.00	.0306	.0132	.0481	.0493
10:18	1.20	12212	7.5	18.91	66.5	75.7	.999	4.91	5.62	280.4	272.7	217.7	217.1	-.16	-.09	.0487	.0204	.0498	.0478
10:22	1.12	11671	7.4	17.81	53.3	64.8	1.001	3.91	4.87	276.7	270.4	221.2	220.2	-.31	.15	.0613	.0245	.0708	.0613
10:28	.86	9777	7.1	14.08	52.8	58.9	1.005	3.76	4.26	269.6	266.8	234.9	235.4	-.02	.03	.0934	.0296	.1224	.0275
10:31	.85	9787	7.0	13.79	54.6	61.7	1.005	3.79	4.33	269.1	266.3	235.1	235.3	-.11	-.01	.0953	.0300	.1098	.2250
10:36	.75	8199	7.3	13.60	55.4	64.3	.988	3.68	4.20	274.1	267.4	246.3	247.3	.08	.08	.1005	.0272	.0969	.6110
10:42	.68	6090	8.1	14.32	55.9	57.6	.967	3.46	4.19	294.8	272.7	260.7	262.4	-.10	-.01	.1057	.0244	.0954	.3500
10:48	.54	2946	9.3	14.60	*****	*****	.970	****	****	294.6	283.7	278.3	279.9	0.00	.11	.1060	.0179	1.6900	1.6070

***** NOT MEASURED DURING FLIGHT

TABLE 1.–Continued

(a) Continued

H, m; U_∞/ν_∞, per m × 10^6; q_∞, kN/m^2; X_t and X_T, cm; Re_{t_0} and Re_{T_0}, × 10^6; T_t, T_w, T_∞, and T_{∞_b}, K;

α and β, deg; $\left(\sqrt{\bar{p}'^{\,2}_{t_2}}/q_\infty\right)100$, $\left(\sqrt{\bar{p}'^{\,2}_{t_2}}/p_{t_\infty}\right)100$, $\left(\sqrt{\bar{p}'^{\,2}_{s_1}}/q_\infty\right)100$, and $\left(\sqrt{\bar{p}'^{\,2}_{s_2}}/q_\infty\right)100$, percent

Time of day	M_∞	H	$\frac{U_\infty}{\nu_\infty}$	q_∞	X_t	X_T	T_w/T_{aw}	Re_{t_0}	Re_{T_0}	T_t	T_w	T_∞	T_{∞_b}	α	β	$\frac{\sqrt{\bar{p}'^{\,2}_{t_2}}}{q_\infty}$ × 100	$\frac{\sqrt{\bar{p}'^{\,2}_{t_2}}}{p_{t_\infty}}$ × 100	$\frac{\sqrt{\bar{p}'^{\,2}_{s_1}}}{q_\infty}$ × 100	$\frac{\sqrt{\bar{p}'^{\,2}_{s_2}}}{q_\infty}$ × 100
FLT 330 8-23-78 AIRCRAFT TRIM ANGLE - 1.50 DEG																			
9:35	1.44	12140	9.2	27.48	70.1	82.0	.987	5.96	6.97	305.1	290.6	215.6	214.8	.04	.11	.0670	.0262	.0440	.0440
9:39	1.35	11522	9.4	26.57	57.2	67.1	1.005	5.59	6.55	296.5	288.3	217.3	218.7	.06	.10	.0621	.0267	.0820	.1870
9:43	1.23	10651	9.4	25.38	52.6	52.2	1.008	5.21	6.16	292.0	286.1	224.2	224.9	.07	.05	.0417	.0175	.1430	1.2530
9:47	1.17	9609	9.8	26.05	48.0	56.6	.999	4.68	5.53	292.1	284.3	229.3	231.3	.03	.07	.0355	.0145	.3660	.2560
9:52	.89	7378	9.5	21.50	43.7	50.0	.995	3.92	4.48	290.6	284.3	250.8	250.3	.01	.05	.0905	.0300	.7010	.6320
FLT 331 8-24-78 AIRCRAFT TRIM ANGLE - 1.50 DEG																			
9:34	1.57	13004	8.8	28.49	*****	*****	.943	****	****	320.2	290.1	214.5	214.8	-.20	-.03	.0195	.0083	.0354	.0317
9:41	1.27	10682	9.5	26.91	54.6	52.2	.996	5.13	5.84	296.5	286.6	224.2	223.5	-.02	.01	.0612	.0262	.1039	.7650
9:47	.84	5662	10.7	24.18	*****	48.5	.978	****	4.40	299.3	288.3	252.3	262.2	-.13	.10	.0972	.0302	.5820	.5610
9:51	.72	3648	11.4	23.70	*****	46.2	.971	****	4.15	305.7	293.5	276.9	278.5	-.09	0.00	.1026	.0266	1.4690	.4440
9:53	.72	3619	11.3	23.41	*****	*****	.979	****	****	305.5	295.8	276.8	278.6	-.16	-.03	.1102	.0282	2.2610	.5060
FLT 332 8-25-78 AIRCRAFT TRIM ANGLE - 1.50 DEG																			
10: 6	1.71	14193	8.1	27.96	*****	*****	1.002	****	****	334.7	320.6	211.2	211.7	-.13	.01	.0218	.0089	.0468	.0351
10:12	1.49	13007	8.3	25.66	63.2	72.4	1.042	7.07	8.15	310.1	311.1	214.7	214.9	-.16	.04	.0375	.0161	.0472	.0452
10:20	.93	7995	9.4	21.79	48.3	57.2	1.008	4.57	5.53	269.6	286.6	246.9	245.2	-.07	0.00	.0822	.0287	.1950	1.2450
FLT 333 8-25-78 AIRCRAFT TRIM ANGLE - 1.50 DEG																			
13:34	1.54	12811	8.9	26.39	67.3	85.3	1.018	6.90	8.81	315.4	308.8	213.9	214.9	-.13	.04	.0439	.0187	.0435	.0344
13:43	1.20	10649	9.1	24.13	74.7	84.8	1.001	6.99	7.68	290.7	283.2	225.7	223.9	.38	-.07	.0488	.0203	.0408	.0876
13:46	1.29	10635	9.6	26.06	73.2	82.3	.976	6.08	6.84	300.8	284.9	225.7	224.0	.01	-.05	.0424	.0181	.0389	.0324
13:51	.93	8041	9.3	21.55	52.6	61.0	.996	4.64	5.38	289.4	283.2	246.8	244.8	-.04	-.06	.0784	.0272	.0713	.2092
13:54	.89	7462	9.4	22.45	50.0	56.9	.993	4.41	5.01	291.0	284.3	251.2	249.9	.01	-.10	.0873	.0289	.1049	.9580
13:58	.79	5554	10.1	21.74	47.2	54.9	.980	4.04	4.69	297.7	287.8	264.6	264.5	-.09	-.07	.0982	.0283	.1455	2.2440
13:59	.79	5583	10.1	21.63	41.1	50.3	.984	3.63	4.43	297.7	288.9	264.6	264.3	-.05	-.09	.1013	.0292	.2229	.8910

***** NOT MEASURED DURING FLIGHT

TABLE 1.-Continued

(a) Continued

H, m; U_∞/ν_∞, per m × 10^6; q_∞, kN/m^2; X_t and X_T, cm; Re_{t_0} and Re_{T_0}, × 10^6; T_t, T_w, T_∞, and T_{∞_b}, K;

α and β, deg; $\left(\sqrt{\overline{p'_{t_2}}^2}/q_\infty\right)100$, $\left(\sqrt{\overline{p'_{t_2}}^2}/p_{t_\infty}\right)100$, $\left(\sqrt{\overline{p'_{s_1}}^2}/q_\infty\right)100$, and $\left(\sqrt{\overline{p'_{s_2}}^2}/q_\infty\right)100$, percent

Time of day	M_∞	H	$\frac{U_\infty}{\nu_\infty}$	q_∞	X_t	X_T	T_w/T_{aw}	Re_{t_0}	Re_{T_0}	T_t	T_w	T_∞	T_{∞_b}	α	β	$\frac{\sqrt{\overline{p'_{t_2}}^2}}{q_\infty}$ × 100	$\frac{\sqrt{\overline{p'_{t_2}}^2}}{p_{t_\infty}}$ × 100	$\frac{\sqrt{\overline{p'_{s_1}}^2}}{q_\infty}$ × 100	$\frac{\sqrt{\overline{p'_{s_2}}^2}}{q_\infty}$ × 100
FLT 334 9- 1-78 AIRCRAFT TRIM ANGLE - 1.00 DEG																			
10:35	1.56	10876	11.5	39.12	66.0	76.5	1.005	7.94	9.19	332.1	320.6	223.4	224.7	.03	-.07	.0393	.0167	.0439	.0279
10:39	1.41	9265	12.7	40.94	53.1	61.0	1.004	6.98	8.02	324.1	314.4	231.8	234.1	-.04	-.08	.0299	.0129	.1221	.0178
10:43	1.33	7929	13.5	44.24	*****	*****	.976	****	****	330.8	312.7	244.4	245.6	-.03	-.06	.0371	.0159	.4260	.6040
FLT 335 9- 1-78 AIRCRAFT TRIM ANGLE - 1.00 DEG																			
13:49	1.71	11647	11.4	42.04	61.3	68.6	.984	8.45	9.22	350.3	329.4	221.0	221.3	-.05	-.04	.0251	.0102	.0487	.0267
13:53	1.50	11039	10.9	35.58	52.1	63.2	1.041	7.57	9.23	324.3	325.0	223.7	224.0	-.10	-.07	.0249	.0107	.0573	.1777
13:56	1.19	7733	12.4	36.87	*****	*****	1.015	****	****	319.1	314.4	247.9	247.2	-.82	-.11	.0477	.0198	.4820	.6670
FLT 336 9- 6-78 AIRCRAFT TRIM ANGLE - 1.00 DEG																			
14:49	1.76	11712	11.8	44.00	*****	*****	1.004	****	****	353.8	338.8	218.4	221.3	-.15	-.03	.0543	.0218	.0430	.1021
FLT 337 9- 8-78 AIRCRAFT TRIM ANGLE - 1.00 DEG																			
11:33	1.57	11051	11.3	38.59	66.0	78.5	1.012	8.25	9.61	328.0	318.9	219.7	221.6	-.07	.02	.0330	.0140	.0403	.0926
11:39	1.49	10577	11.3	37.35	65.8	76.7	.990	7.33	8.38	322.1	307.1	223.1	222.2	-.08	0.00	.0323	.0139	.0345	.0264
11:42	1.33	9882	10.9	33.32	58.2	66.6	1.012	6.88	7.81	310.4	304.3	229.3	224.9	.11	-.06	.0366	.0156	.0426	.0885
FLT 338 9-13-78 AIRCRAFT TRIM ANGLE - 1.00 DEG																			
10:10	1.76	11959	11.2	41.85	*****	*****	1.010	****	****	353.8	341.0	218.4	218.8	-.09	.01	.0512	.0207	.0551	.1984
10:18	1.39	9766	11.5	30.62	56.1	67.6	.987	5.93	7.13	323.6	306.8	233.4	231.1	-.14	.01	.0308	.0133	.0389	.5210
FLT 339 9-25-78 AIRCRAFT TRIM ANGLE - 1.00 DEG																			
13: 8	1.66	11346	11.3	38.40	59.7	69.1	1.020	7.86	9.10	331.4	324.4	219.2	*****	-.07	-.07	.0313	.0132	.0654	.1434
13:13	1.48	11139	10.6	34.14	57.7	64.5	1.023	7.20	8.06	317.3	312.7	223.2	*****	-.07	-.08	.0230	.0099	.0404	.0968
13:16	1.38	9514	11.6	37.73	*****	*****	.995	****	****	322.3	310.5	233.9	*****	-.16	-.12	.0295	.0127	.3620	.5460

***** NOT MEASURED DURING FLIGHT

TABLE 1.–Continued

(a) Continued

H, m; U_∞/ν_∞, per m × 10^6; q_∞, kN/m^2; X_t and X_T, cm; Re_{t_0} and Re_{T_0}, × 10^6; T_t, T_w, T_∞, and T_{∞_b}, K;

α and β, deg; $\left(\sqrt{\overline{p'_{t_2}}^2}/q_\infty\right)100$, $\left(\sqrt{\overline{p'_{t_2}}^2}/p_{t_\infty}\right)100$, $\left(\sqrt{\overline{p'_{s_1}}^2}/q_\infty\right)100$, and $\left(\sqrt{\overline{p'_{s_2}}^2}/q_\infty\right)100$, percent

Time of day	M_∞	H	$\frac{U_\infty}{\nu_\infty}$	q_∞	X_t	X_T	T_w/T_{aw}	Re_{t_0}	Re_{T_0}	T_t	T_w	T_∞	T_{∞_b}	α	β	$\frac{\sqrt{\overline{p'_{t_2}}^2}}{q_\infty}$ × 100	$\frac{\sqrt{\overline{p'_{t_2}}^2}}{p_{t_\infty}}$ × 100	$\frac{\sqrt{\overline{p'_{s_1}}^2}}{q_\infty}$ × 100	$\frac{\sqrt{\overline{p'_{s_2}}^2}}{q_\infty}$ × 100
FLT 340 9-28-78 AIRCRAFT TRIM ANGLE - .75 DEG																			
14: 5	2.03	11837	13.5	57.17	*****	*****	.955	****	****	394.6	356.3	216.4	214.7	.08	.02	.0162	.0057	.0328	.0236
FLT 341 10- 2-78 AIRCRAFT TRIM ANGLE - .75 DEG																			
12:26	1.83	10677	14.2	55.64	53.3	62.0	1.003	7.92	9.28	367.9	351.4	220.6	220.4	-.15	0.00	.0429	.0167	.0890	1.4180
FLT 342 10- 2-78 AIRCRAFT TRIM ANGLE - .75 DEG																			
14:49	1.57	9604	13.3	47.02	46.0	55.4	1.023	7.26	8.86	342.0	336.1	229.1	227.8	-.26	-.05	.0277	.0118	1.0040	1.5650
FLT 343 10- 4-78 AIRCRAFT TRIM ANGLE - .75 DEG																			
12:32	1.92	11276	13.8	55.59	59.7	69.9	.984	7.54	8.82	375.6	350.8	216.7	216.4	-.02	.03	******	******	******	******
12:36	1.54	10667	11.9	39.64	42.2	51.8	1.045	6.93	8.56	327.2	328.9	221.9	220.6	-.19	.06	******	******	******	******
FLT 344 10- 4-78 AIRCRAFT TRIM ANGLE - .75 DEG																			
14:50	1.81	10724	13.9	54.06	51.3	58.2	1.001	7.37	8.43	364.4	347.6	220.3	220.1	-.18	-.01	.0308	.0121	1.0290	1.5270
14:54	1.61	10873	12.1	41.85	48.5	55.9	1.026	7.14	8.33	334.3	328.9	220.2	219.1	-.31	.04	.0289	.0122	.9480	.7540
FLT 345 10- 5-78 AIRCRAFT TRIM ANGLE - .75 DEG																			
14:20	1.47	9357	13.1	44.00	44.7	53.1	1.021	6.82	8.14	331.4	326.1	231.6	230.6	-.10	-.04	.0290	.0125	.7580	.4990
14:24	1.61	10473	12.7	44.66	48.5	54.6	.999	6.30	7.15	339.9	325.6	223.4	222.7	-.38	-.10	.0252	.0106	1.3150	.5770
FLT 346 10-11-78 AIRCRAFT TRIM ANGLE - .75 DEG																			
13:40	2.06	11570	14.0	51.24	*****	*****	.932	****	****	403.8	355.7	219.1	218.2	-.06	.63	.0575	.0199	.0586	1.4310

***** NOT MEASURED DURING FLIGHT

TABLE 1.–Continued

(a) Continued

H, m; U_∞/ν_∞, per m × 10^6; q_∞, kN/m^2; X_t and X_T, cm; Re_{t_0} and Re_{T_0}, × 10^6; T_t, T_w, T_∞, and T_{∞_b}, K;

α and β, deg; $\left(\sqrt{\overline{p'_{t_2}}^2}/q_\infty\right)100$, $\left(\sqrt{\overline{p'_{t_2}}^2}/p_{t_\infty}\right)100$, $\left(\sqrt{\overline{p'_{s_1}}^2}/q_\infty\right)100$, and $\left(\sqrt{\overline{p'_{s_2}}^2}/q_\infty\right)100$, percent

Time of day	M_∞	H	$\frac{U_\infty}{\nu_\infty}$	q_∞	X_t	X_T	T_w/T_{aw}	Re_{t_0}	Re_{T_0}	T_t	T_w	T_∞	T_{∞_b}	α	β	$\frac{\sqrt{\overline{p'_{t_2}}^2}}{q_\infty}$ × 100	$\frac{\sqrt{\overline{p'_{t_2}}^2}}{p_{t_\infty}}$ × 100	$\frac{\sqrt{\overline{p'_{s_1}}^2}}{q_\infty}$ × 100	$\frac{\sqrt{\overline{p'_{s_2}}^2}}{q_\infty}$ × 100
FLT 347 10-12-78 AIRCRAFT TRIM ANGLE - .75 DEG																			
14:33	1.79	10728	13.5	52.91	45.7	53.6	.999	7.87	8.52	368.6	350.8	224.7	223.9	-.27	.49	.0470	.0186	.9130	.4250
FLT 348 10-13-78 AIRCRAFT TRIM ANGLE - .75 DEG																			
14:46	1.55	9731	13.0	46.59	43.2	49.8	.990	5.69	6.50	345.5	328.9	232.9	230.7	-.39	.40	******	******	******	******
FLT 349 10-24-78 AIRCRAFT TRIM ANGLE - 2.50 DEG																			
13: 6	.56	3110	9.6	16.18	*****	*****	.995	****	****	296.6	292.8	278.1	273.7	.05	.48	******	******	******	******
13:17	1.16	12102	7.3	18.00	57.2	64.5	1.002	4.59	5.26	279.8	273.2	220.2	221.1	-.20	.65	******	******	******	******
13:32	.87	10201	7.0	13.65	51.6	56.9	1.009	3.95	4.34	263.3	261.4	228.6	226.4	-.06	.48	******	******	******	******
13:33	.88	10152	7.1	14.03	49.3	56.4	1.003	3.65	4.15	264.8	261.4	229.3	226.8	-.05	.45	******	******	******	******
13:39	.65	9589	7.2	14.17	49.5	57.4	.994	3.56	4.17	267.1	261.4	233.6	230.8	-.08	.57	******	******	******	******
13:47	.75	8135	7.4	13.74	50.3	58.4	.985	3.49	4.08	272.4	264.9	244.3	240.2	-.09	.56	******	******	******	******
13:54	.75	8260	7.3	13.50	51.8	61.2	.990	3.54	4.17	270.9	264.9	243.5	239.9	-.07	.24	******	******	******	******
13:57	.75	8230	7.4	13.50	*****	47.2	.990	****	3.66	270.9	264.9	243.6	240.0	-.01	.68	******	******	******	******
14: 0	.75	8213	7.4	13.74	52.6	58.4	.992	3.60	4.05	270.9	265.6	243.3	240.0	-.11	.01	******	******	******	******
14: 9	.62	5673	7.9	13.12	50.5	57.2	.972	3.30	3.73	282.8	272.6	262.8	259.1	.05	.49	******	******	******	******
14:11	.63	5690	8.0	13.69	45.8	55.9	.978	3.31	3.79	283.5	274.9	262.7	258.9	-.13	.26	******	******	******	******
14:13	.63	5702	8.0	13.65	*****	46.0	.976	****	3.29	284.2	275.5	263.4	258.9	-.17	.73	******	******	******	******

***** NOT MEASURED DURING FLIGHT

TABLE 1.–Continued

(a) Continued

H, m; U_∞/ν_∞, per m × 10^6; q_∞, kN/m^2; X_t and X_T, cm; Re_{t_0} and Re_{T_0}, × 10^6; T_t, T_w, T_∞, and T_{∞_b}, K;

α and β, deg; $\left(\sqrt{\bar{p}_{t_2}'^2}/q_\infty\right)100$, $\left(\sqrt{\bar{p}_{t_2}'^2}/p_{t_\infty}\right)100$, $\left(\sqrt{\bar{p}_{s_1}'^2}/q_\infty\right)100$, and $\left(\sqrt{\bar{p}_{s_2}'^2}/q_\infty\right)100$, percent

Time of day	M_∞	H	$\frac{U_\infty}{\nu_\infty}$	q_∞	X_t	X_T	T_w/T_{aw}	Re_{t_0}	Re_{T_0}	T_t	T_w	T_∞	T_{∞_b}	α	β	$\frac{\sqrt{\bar{p}_{t_2}'^2}}{q_\infty}$ × 100	$\frac{\sqrt{\bar{p}_{t_2}'^2}}{p_{t_\infty}}$ × 100	$\frac{\sqrt{\bar{p}_{s_1}'^2}}{q_\infty}$ × 100	$\frac{\sqrt{\bar{p}_{s_2}'^2}}{q_\infty}$ × 100
FLT 350 10-25-78 AIRCRAFT TRIM ANGLE - 3.50 DEG																			
13: 7	.52	2309	9.3	14.75	*****	*****	.999	****	****	302.4	300.2	286.6	285.9	-.42	.60	******	******	******	******
13:13	.56	2502	6.7	13.02	*****	*****	1.000	****	****	299.5	297.9	285.3	285.7	-.06	.54	******	******	******	******
13:22	.57	5291	7.6	11.97	*****	49.0	1.006	****	3.90	283.5	283.0	266.0	264.2	-.05	.49	******	******	******	******
13:37	1.09	14207	5.2	11.44	57.9	68.1	1.043	4.10	4.98	261.1	266.1	210.6	268.3	-.39	.49	******	******	******	******
13:44	.66	8453	6.5	10.34	49.8	58.2	1.014	3.62	4.19	260.3	261.4	239.7	236.2	.19	.50	******	******	******	******
13:57	.86	12591	5.6	9.46	67.6	75.7	1.024	4.02	4.50	251.8	253.7	218.3	217.1	-.04	.13	******	******	******	******
13:59	.87	12453	5.2	9.62	63.0	74.9	1.022	3.78	4.47	250.9	252.5	217.7	217.4	-.11	.16	******	******	******	******
14: 3	.90	12422	5.3	10.34	62.2	76.2	1.004	3.24	4.13	256.4	253.1	220.4	217.4	-.55	-.02	******	******	******	******
14:11	.77	10607	5.8	9.91	55.9	64.0	.999	3.25	3.79	254.1	250.7	227.3	221.8	-.26	.48	******	******	******	******
FLT 351 10-31-78 AIRCRAFT TRIM ANGLE - 3.50 DEG																			
9:14	.57	5417	7.8	11.68	*****	*****	1.021	****	****	272.4	276.1	255.7	257.0	.28	.89	.1093	.0200	.4440	.2140
9:17	.60	5573	8.1	12.99	*****	*****	1.015	****	****	272.4	274.3	254.1	256.1	-.14	.49	.1054	.0208	.3270	.2100
9:25	1.16	14442	5.0	12.40	*****	*****	.998	****	****	278.5	270.8	219.3	217.1	-.53	.56	.0643	.0263	.0528	.0632
9:29	1.17	14851	4.9	11.87	*****	*****	1.002	****	****	276.1	269.6	216.4	216.2	-.57	.29	******	******	******	******
9:31	1.18	14570	5.1	12.59	*****	*****	1.002	****	****	273.0	270.2	216.4	216.9	-.79	.08	******	******	******	******
9:44	1.08	14363	4.8	10.82	84.3	*****	1.000	****	****	269.4	263.2	218.6	217.3	-.30	.48	.0746	.0292	.0615	.0762
9:54	.92	13499	4.6	9.05	68.6	78.7	1.021	3.76	4.40	256.4	257.2	219.2	219.3	-.28	.52	.0903	.0309	.0838	.1057
FLT 352 10-31-78 AIRCRAFT TRIM ANGLE - 3.50 DEG																			
13:39	.50	4266	7.7	10.63	*****	48.8	.995	****	3.72	279.1	276.1	245.2	263.9	-.01	.57	******	******	******	******
13:51	.60	7211	6.6	10.01	47.2	56.4	1.001	3.20	3.82	266.3	264.3	248.6	246.8	-.01	.57	******	******	******	******
14:46	.71	10693	5.4	8.43	56.4	64.5	1.005	3.21	3.68	246.2	244.7	223.6	223.6	-.17	.52	******	******	******	******
14:54	.71	10691	5.4	8.47	62.5	69.9	.997	3.30	3.71	246.2	242.8	223.5	223.6	-.16	.27	******	******	******	******
14:56	.71	10736	5.3	8.38	55.1	62.0	.991	2.70	3.06	247.8	242.8	225.0	223.6	-.22	.12	******	******	******	******

***** NOT MEASURED DURING FLIGHT

TABLE 1.–Continued

(a) Concluded

H, m; U_∞/ν_∞, per m × 10^6; q_∞, kN/m^2; X_t and X_T, cm; Re_{t_0} and Re_{T_0}, × 10^6; T_t, T_w, T_∞, and T_{∞_b}, K;

α and β, deg; $\left(\sqrt{\overline{p'_{t_2}}^2}/q_\infty\right)100$, $\left(\sqrt{\overline{p'_{t_2}}^2}/p_{t_\infty}\right)100$, $\left(\sqrt{\overline{p'_{s_1}}^2}/q_\infty\right)100$, and $\left(\sqrt{\overline{p'_{s_2}}^2}/q_\infty\right)100$, percent

FLT 353 11- 1-78 AIRCRAFT TRIM ANGLE - 4.50 DEG

Time of day	M_∞	H	$\frac{U_\infty}{\nu_\infty}$	q_∞	X_t	X_T	T_w/T_{aw}	Re_{t_0}	Re_{T_0}	T_t	T_w	T_∞	T_{∞_b}	α	β	$\frac{\sqrt{\overline{p'_{t_2}}^2}}{100q_\infty}$	$\frac{\sqrt{\overline{p'_{t_2}}^2}}{100p_{t_\infty}}$	$\frac{\sqrt{\overline{p'_{s_1}}^2}}{100q_\infty}$	$\frac{\sqrt{\overline{p'_{s_2}}^2}}{100q_\infty}$
13: 8	.44	2047	6.3	10.73	*****	*****	.989	****	****	290.1	285.9	279.3	272.7	-.31	.58	.1136	.0135	.3670	.2450
13:16	.62	7934	6.3	9.67	*****	*****	1.053	****	****	263.3	274.9	244.6	233.4	-.04	.54	******	******	******	******
13:22	.50	4327	7.5	10.25	*****	46.0	.992	****	3.40	279.8	276.1	266.6	265.7	-.16	.65	.1211	.0178	.4750	.1630
13:25	.50	4326	7.5	10.15	*****	47.0	.995	****	3.33	279.1	276.1	266.0	265.7	-.09	.22	******	******	******	******
13:27	.49	4169	7.5	10.15	44.2	51.1	.992	3.04	3.49	279.8	276.1	266.9	266.8	-.15	.05	.1181	.0169	.2650	.2590
13:42	1.10	15615	4.1	9.19	*****	*****	1.012	****	****	265.6	262.6	214.1	214.2	-.43	.59	.0753	.0298	.0735	.0891
13:55	.57	7203	6.4	9.19	53.3	59.4	.983	3.09	3.51	264.8	258.4	248.5	241.7	-.21	.62	.1067	.0195	.1149	.4720
14:17	.82	12727	4.5	9.14	74.2	84.1	.986	3.15	3.81	254.1	247.1	223.8	219.2	-.39	.62	******	******	******	******
14:27	.70	10751	7.5	8.09	52.1	61.7	1.008	4.21	5.02	244.7	244.1	222.8	221.1	-.22	.51	.1099	.0271	.1074	.4060

***** NOT MEASURED DURING FLIGHT

TABLE 1.-Continued

(b) U.S. Customary Units

H, ft; U_∞/ν_∞, per ft × 10^6; q_∞, lb/ft^2; X_t and X_T, in.; Re_{t_0} and Re_{T_0}, × 10^6; T_t, T_w, T_∞, and T_{∞_b}, °R;

α and β, deg; $\left(\sqrt{\overline{p'_{t_2}}^2}/q_\infty\right)100$, $\left(\sqrt{\overline{p'_{t_2}}^2}/p_{t_\infty}\right)100$, $\left(\sqrt{\overline{p'_{s_1}}^2}/q_\infty\right)100$, and $\left(\sqrt{\overline{p'_{s_2}}^2}/q_\infty\right)100$, percent

Time of day	M_∞	H	$\frac{U_\infty}{\nu_\infty}$	q_∞	X_t	X_T	T_w/T_{aw}	Re_{t_0}	Re_{T_0}	T_t	T_w	T_∞	T_{∞_b}	α	β	$\frac{\sqrt{\overline{p'_{t_2}}^2}}{q_\infty}$ × 100	$\frac{\sqrt{\overline{p'_{t_2}}^2}}{p_{t_\infty}}$ × 100	$\frac{\sqrt{\overline{p'_{s_1}}^2}}{q_\infty}$ × 100	$\frac{\sqrt{\overline{p'_{s_2}}^2}}{q_\infty}$ × 100
FLT 327 8-14-78 AIRCRAFT TRIM ANGLE - 2.50 DEG																			
8:54	1.20	40176	2.27	390	20.8	24.6	1.035	4.96	5.90	503.0	506.5	390.5	388.6	-.24	-.04	******	******	******	******
9: 0	1.08	37155	2.26	370	20.9	24.4	1.012	4.17	4.94	499.6	494.0	405.1	398.5	-.22	-.03	.0670	.0278	.0990	.1090
9: 7	.86	31490	2.21	304	19.9	22.2	1.014	3.94	4.40	485.5	484.5	422.9	421.0	-.02	-.04	.0970	.0306	.2240	.4350
9:19	.66	19802	2.45	303	20.6	27.8	.969	3.27	4.41	517.0	496.1	475.6	477.5	.01	-.01	.1070	.0243	.1460	******
9:24	.55	10288	2.79	308	*****	*****	.973	****	****	533.1	514.9	502.7	509.0	-.07	.20	.1590	.0275	2.5220	1.3780
9:30	.74	26810	2.20	277	*****	*****	1.036	****	****	492.8	504.4	444.2	443.6	.03	.16	.0980	.0261	1.1220	.5580
9:36	.54	9869	2.74	296	*****	20.0	.976	****	3.74	533.1	516.9	503.7	510.9	.05	-.03	.1520	.0253	1.9410	1.7150
FLT 328 8-16-78 AIRCRAFT TRIM ANGLE - 2.50 DEG																			
10:13	1.52	48949	2.08	416	24.1	28.0	1.071	8.28	9.07	534.5	550.7	365.6	368.1	-.44	.27	.0397	.0170	.0930	.0630
10:20	1.36	46870	1.98	362	23.9	28.0	1.068	6.30	7.38	510.0	527.2	372.3	370.3	-.19	-.05	.0413	.0177	.0800	.0818
10:23	1.17	39934	2.21	377	19.9	22.7	1.046	4.88	5.74	503.1	512.6	395.0	389.7	-.39	-.09	.0517	.0213	.0980	.1170
FLT 329 8-18-78 AIRCRAFT TRIM ANGLE - 2.50 DEG																			
10:11	1.39	45921	2.15	396	26.7	30.8	1.036	6.14	7.08	511.2	511.7	368.7	377.3	-.16	0.00	.0306	.0132	.0481	.0493
10:18	1.21	40067	2.28	395	26.2	29.8	.999	4.91	5.62	504.8	490.9	391.9	390.7	-.16	-.09	.0487	.0204	.0498	.0478
10:22	1.12	38292	2.25	372	21.0	25.5	1.001	3.91	4.87	498.0	466.7	398.1	396.4	-.31	.15	.0613	.0245	.0708	.0613
10:28	.96	32077	2.15	294	20.8	23.2	1.005	3.76	4.20	485.3	480.3	422.8	423.8	-.02	.03	.0934	.0296	.1224	.0275
10:31	.85	32110	2.12	288	21.5	24.3	1.005	3.79	4.33	484.3	479.3	423.2	423.6	-.11	-.01	.0953	.0300	.1098	.2250
10:36	.75	26900	2.23	284	22.2	25.3	.986	3.68	4.20	493.3	481.4	443.4	445.2	.08	.08	.1005	.0272	.0969	.6110
10:42	.68	19983	2.46	299	22.0	26.6	.967	3.46	4.19	512.7	490.9	469.3	472.4	-.10	-.01	.1057	.0244	.0954	.3500
10:48	.54	9667	2.82	305	*****	*****	.970	****	****	530.2	510.7	501.0	503.9	0.00	.11	.1080	.0179	1.6900	1.6070

***** NOT MEASURED DURING FLIGHT

TABLE 1.–Continued

(b) Continued

H, ft; U_∞/ν_∞, per ft × 10^6; q_∞, lb/ft^2; X_t and X_T, in.; Re_{t_0} and Re_{T_0}, × 10^6; T_t, T_w, T_∞, and T_{∞_b}, °R;

α and β, deg; $\left(\sqrt{\overline{p'_{t_2}}^2}/q_\infty\right)100$, $\left(\sqrt{\overline{p'_{t_2}}^2}/p_{t_\infty}\right)100$, $\left(\sqrt{\overline{p'_{s_1}}^2}/q_\infty\right)100$, and $\left(\sqrt{\overline{p'_{s_2}}^2}/q_\infty\right)100$, percent

Time of day	M_∞	H	$\frac{U_\infty}{\nu_\infty}$	q_∞	X_t	X_T	T_w/T_{aw}	Re_{t_0}	Re_{T_0}	T_t	T_w	T_∞	T_{∞_b}	α	β	$\frac{\sqrt{\overline{p'_{t_2}}^2}}{q_\infty}$ × 100	$\frac{\sqrt{\overline{p'_{t_2}}^2}}{p_{t_\infty}}$ × 100	$\frac{\sqrt{\overline{p'_{s_1}}^2}}{q_\infty}$ × 100	$\frac{\sqrt{\overline{p'_{s_2}}^2}}{q_\infty}$ × 100
FLT 330 8-23-78 AIRCRAFT TRIM ANGLE - 1.50 DEG																			
9:35	1.44	39832	2.79	574	27.6	32.3	.987	5.96	6.97	549.1	523.1	388.1	386.6	.04	.11	.0670	.0262	.0440	.0440
9:39	1.35	37805	2.85	555	22.5	26.4	1.005	5.59	6.55	533.7	519.0	391.1	393.6	.06	.10	.0621	.0267	.0820	.1870
9:43	1.23	34946	2.86	530	20.7	24.5	1.008	5.21	6.16	525.6	514.9	403.5	404.8	.07	.05	.0417	.0175	.1430	1.2530
9:47	1.17	32185	3.00	544	18.9	22.3	.999	4.68	5.53	520.7	511.7	412.7	416.4	.03	.07	.0355	.0145	.3660	.2560
9:52	.89	24203	2.90	449	17.2	19.7	.995	3.92	4.46	523.0	511.7	451.4	450.5	.01	.05	.0905	.0300	.7010	.6320
FLT 331 8-24-78 AIRCRAFT TRIM ANGLE - 1.50 DEG																			
9:34	1.57	42065	2.67	595	*****	*****	.943	****	****	576.4	522.1	386.1	386.6	-.20	-.03	.0195	.0083	.0354	.0317
9:41	1.27	35046	2.94	562	21.5	24.5	.996	5.13	5.84	533.7	515.9	403.5	402.3	-.02	.01	.0612	.0262	.1039	.7650
9:47	.84	18578	3.27	505	*****	19.0	.978	****	4.40	538.8	519.0	472.2	472.0	-.13	.10	.0972	.0302	.5820	.5610
9:51	.77	11971	3.46	495	*****	18.2	.971	****	4.15	550.2	528.3	498.5	501.3	-.09	0.00	.1026	.0266	1.4690	.4440
9:53	.72	11874	3.44	489	*****	*****	.979	****	****	549.9	532.4	498.3	501.4	-.16	-.03	.1102	.0282	2.2610	.5060
FLT 332 8-25-78 AIRCRAFT TRIM ANGLE - 1.50 DEG																			
10: 5	1.71	46566	2.46	584	*****	*****	1.002	****	****	602.5	577.0	380.2	381.1	-.13	.01	.0218	.0089	.0468	.0351
10:12	1.49	42674	2.54	536	24.9	28.5	1.042	7.07	8.15	558.2	559.9	386.5	386.8	-.16	.04	.0375	.0161	.0472	.0452
10:20	.93	26233	2.86	455	19.0	22.5	1.008	4.67	5.53	521.3	515.9	444.4	441.4	-.07	0.00	.0822	.0287	.1950	1.2450
FLT 333 8-25-78 AIRCRAFT TRIM ANGLE - 1.50 DEG																			
13:34	1.54	42033	2.72	593	26.5	33.6	1.018	6.90	8.81	567.7	555.8	385.1	386.8	-.13	.04	.0439	.0187	.0435	.0344
13:43	1.20	34939	2.77	504	29.4	33.4	1.001	6.99	7.68	523.3	509.7	406.3	403.0	.38	-.07	.0488	.0203	.0408	.0876
13:46	1.29	34893	2.99	586	28.8	32.4	.976	6.08	6.84	541.5	512.8	406.3	403.2	.01	-.05	.0424	.0181	.0389	.0324
13:51	.93	26382	2.83	450	20.7	24.0	.996	4.64	5.38	521.0	509.7	444.2	440.7	-.04	-.06	.0784	.0272	.0713	.2092
13:54	.89	24287	2.88	449	19.7	22.4	.993	4.41	5.01	523.8	511.7	452.1	449.9	.01	-.10	.0873	.0289	.1049	.9590
13:58	.79	18224	3.08	454	18.6	21.6	.980	4.04	4.69	535.8	518.0	476.3	476.2	-.09	-.07	.0982	.0283	.1455	2.2440
13:59	.79	18318	3.09	456	16.2	19.8	.984	3.63	4.43	535.8	520.0	476.3	475.6	-.05	-.09	.1013	.0292	.2229	.6910

***** NOT MEASURED DURING FLIGHT

TABLE 1.–Continued

(b) Continued

H, ft; U_∞/ν_∞, per ft × 10^6; q_∞, lb/ft^2; X_t and X_T, in.; Re_{t_0} and Re_{T_0}, × 10^6; T_t, T_w, T_∞, and T_{∞_b}, °R;

α and β, deg; $\left(\sqrt{\bar{p}'^{\,2}_{t_2}}/q_\infty\right)100$, $\left(\sqrt{\bar{p}'^{\,2}_{t_2}}/p_{t_\infty}\right)100$, $\left(\sqrt{\bar{p}'^{\,2}_{s_1}}/q_\infty\right)100$, and $\left(\sqrt{\bar{p}'^{\,2}_{s_2}}/q_\infty\right)100$, percent

Time of day	M_∞	H	$\frac{U_\infty}{\nu_\infty}$	q_∞	X_t	X_T	T_w/T_{aw}	Re_{t_0}	Re_{T_0}	T_t	T_w	T_∞	T_{∞_b}	α	β	$\frac{\sqrt{\bar{p}'^{\,2}_{t_2}}}{q_\infty} \times 100$	$\frac{\sqrt{\bar{p}'^{\,2}_{t_2}}}{p_{t_\infty}} \times 100$	$\frac{\sqrt{\bar{p}'^{\,2}_{s_1}}}{q_\infty} \times 100$	$\frac{\sqrt{\bar{p}'^{\,2}_{s_2}}}{q_\infty} \times 100$
FLT 334 9- 1-78 AIRCRAFT TRIM ANGLE - 1.00 DEG																			
10:35	1.56	35683	3.51	817	26.0	30.1	1.005	7.94	9.19	597.8	577.0	402.1	404.5	.03	-.07	.0393	.0167	.0439	.0279
10:39	1.41	30398	3.86	855	20.9	24.0	1.004	6.98	8.02	583.3	565.9	417.3	421.3	-.04	-.08	.0299	.0129	.1221	.0178
10:43	1.33	26017	4.13	924	*****	*****	.976	****	****	595.5	562.9	439.9	442.0	-.03	-.06	.0371	.0159	.4260	.6040
FLT 335 9- 1-78 AIRCRAFT TRIM ANGLE - 1.00 DEG																			
13:49	1.71	38214	3.48	878	32.0	34.9	.984	8.45	9.22	630.5	593.0	397.8	398.4	-.05	-.04	.0251	.0102	.0487	.0267
13:53	1.50	36218	3.31	743	20.5	24.9	1.041	7.57	9.23	583.7	585.0	402.6	403.2	-.10	-.07	.0249	.0107	.0573	.1777
13:58	1.19	25372	3.77	770	*****	*****	1.015	****	****	572.6	565.9	446.2	445.0	-.82	-.11	.0477	.0198	.4820	.6670
FLT 336 9- 6-78 AIRCRAFT TRIM ANGLE - 1.00 DEG																			
14:49	1.76	38428	3.60	919	*****	*****	1.004	****	****	636.9	609.8	393.2	398.4	-.15	-.03	.0543	.0218	.0430	.1021
FLT 337 9- 8-78 AIRCRAFT TRIM ANGLE - 1.00 DEG																			
11:33	1.57	36259	3.45	806	26.0	30.9	1.012	8.25	9.81	590.4	574.0	395.5	398.8	-.07	.02	.0330	.0140	.0403	.0926
11:39	1.49	34704	3.45	780	27.1	31.0	.990	7.33	6.36	579.8	552.8	401.5	399.9	-.06	0.00	.0323	.0139	.0345	.0264
11:42	1.33	32424	3.31	696	22.9	26.0	1.012	6.88	7.81	558.8	547.7	412.8	404.9	.11	-.06	.0366	.0156	.0426	.0885
FLT 338 9-13-78 AIRCRAFT TRIM ANGLE - 1.00 DEG																			
10:10	1.76	39336	3.41	874	*****	*****	1.010	****	****	636.9	613.8	393.2	393.9	-.09	.01	.0512	.0207	.0551	.1984
10:18	1.39	32042	3.50	769	22.1	26.6	.987	5.93	7.13	582.5	555.8	420.1	415.9	-.14	.01	.0308	.0133	.0389	.5210
FLT 339 9-25-78 AIRCRAFT TRIM ANGLE - 1.00 DEG																			
13: 8	1.59	37233	3.44	802	23.5	27.2	1.020	7.86	9.10	596.6	584.0	394.6	*****	-.07	-.07	.0313	.0132	.0654	.1434
13:13	1.49	36547	3.22	713	22.7	25.4	1.023	7.20	8.06	571.2	562.9	401.8	*****	-.07	-.08	.0230	.0099	.0404	.0968
13:16	1.38	31215	3.61	788	*****	*****	.995	****	****	580.1	558.9	420.8	*****	-.16	-.12	.0295	.0127	.3820	.5460

***** NOT MEASURED DURING FLIGHT

TABLE 1.–Continued

(b) Continued

H, ft; U_∞/ν_∞, per ft × 10^6; q_∞, lb/ft^2; X_t and X_T, in.; Re_{t_0} and Re_{T_0}, × 10^6; T_t, T_w, T_∞, and T_{∞_b}, °R;

α and β, deg; $\left(\sqrt{\bar{p}_{t_2}'^2}/q_\infty\right)100$, $\left(\sqrt{\bar{p}_{t_2}'^2}/p_{t_\infty}\right)100$, $\left(\sqrt{\bar{p}_{s_1}'^2}/q_\infty\right)100$, and $\left(\sqrt{\bar{p}_{s_2}'^2}/q_\infty\right)100$, percent

Time of day	M_∞	H	$\frac{U_\infty}{\nu_\infty}$	q_∞	X_t	X_T	T_w/T_{aw}	Re_{t_0}	Re_{T_0}	T_t	T_w	T_∞	T_{∞_b}	α	β	$\frac{\sqrt{\bar{p}_{t_2}'^2}}{q_\infty}$ × 100	$\frac{\sqrt{\bar{p}_{t_2}'^2}}{p_{t_\infty}}$ × 100	$\frac{\sqrt{\bar{p}_{s_1}'^2}}{q_\infty}$ × 100	$\frac{\sqrt{\bar{p}_{s_2}'^2}}{q_\infty}$ × 100
FLT 340 9-28-78 AIRCRAFT TRIM ANGLE - .75 DEG																			
14: 5	2.03	38836	4.10	1194	*****	*****	.955	****	****	710.3	641.3	389.6	386.5	.08	.02	.0162	.0057	.0328	.0236
FLT 341 10- 2-78 AIRCRAFT TRIM ANGLE - .75 DEG																			
12:26	1.83	35031	4.33	1162	21.0	24.4	1.003	7.92	9.28	662.2	632.5	397.1	396.8	-.15	0.00	.0429	.0167	.0890	1.4180
FLT 342 10- 2-78 AIRCRAFT TRIM ANGLE - .75 DEG																			
14:49	1.57	32167	4.05	982	16.1	21.8	1.023	7.26	8.86	615.6	604.9	412.3	410.0	-.26	-.05	.0277	.0118	1.0040	1.5650
FLT 343 10- 4-78 AIRCRAFT TRIM ANGLE - .75 DEG																			
12:32	1.92	36997	4.22	1161	23.5	27.5	.984	7.54	8.82	676.1	631.5	390.1	389.5	-.02	.03	******	******	******	******
12:36	1.54	34998	3.63	828	16.6	20.4	1.045	6.93	8.56	589.0	592.0	399.4	397.0	-.19	.06	******	******	******	******
FLT 344 10- 4-78 AIRCRAFT TRIM ANGLE - .75 DEG																			
14:50	1.81	35185	4.25	1129	20.2	22.9	1.001	7.37	8.43	655.9	625.6	396.6	396.2	-.18	-.01	.0308	.0121	1.0290	1.5270
14:54	1.61	35673	3.70	674	19.1	22.0	1.026	7.14	8.33	601.7	592.0	396.4	394.4	-.31	.04	.0289	.0122	.9480	.7540
FLT 345 10- 5-78 AIRCRAFT TRIM ANGLE - .75 DEG																			
14:20	1.47	30699	3.99	919	17.6	20.9	1.021	6.82	8.14	596.6	587.0	416.8	415.1	-.10	-.04	.0290	.0125	.7580	.4990
14:24	1.51	34363	3.88	937	19.1	21.5	.999	6.30	7.15	611.8	586.0	402.1	400.8	-.38	-.10	.0252	.0106	1.3150	.5770
FLT 346 10-11-78 AIRCRAFT TRIM ANGLE - .75 DEG																			
13:40	2.06	37960	4.27	1279	*****	*****	.932	****	****	726.9	640.3	394.4	392.7	-.06	.63	.0575	.0199	.0586	1.4310

***** NOT MEASURED DURING FLIGHT

TABLE 1.—Continued

(b) Continued

H, ft; U_∞/ν_∞, per ft × 10^6; q_∞, lb/ft^2; X_t and X_T, in.; Re_{t_0} and Re_{T_0}, × 10^6; T_t, T_w, T_∞, and T_{∞_b}, °R;

α and β, deg; $\left(\sqrt{\overline{p'_{t_2}}^2}/q_\infty\right)100$, $\left(\sqrt{\overline{p'_{t_2}}^2}/p_{t_\infty}\right)100$, $\left(\sqrt{\overline{p'_{s_1}}^2}/q_\infty\right)100$, and $\left(\sqrt{\overline{p'_{s_2}}^2}/q_\infty\right)100$, percent

Time of day	M_∞	H	$\frac{U_\infty}{\nu_\infty}$	q_∞	X_t	X_T	T_w/T_{aw}	Re_{t_0}	Re_{T_0}	T_t	T_w	T_∞	T_{∞_b}	α	β	$\frac{\sqrt{\overline{p'_{t_2}}^2}}{q_\infty} \times 100$	$\frac{\sqrt{\overline{p'_{t_2}}^2}}{p_{t_\infty}} \times 100$	$\frac{\sqrt{\overline{p'_{s_1}}^2}}{q_\infty} \times 100$	$\frac{\sqrt{\overline{p'_{s_2}}^2}}{q_\infty} \times 100$
FLT 347 10-12-78 AIRCRAFT TRIM ANGLE - .75 DEG																			
14:33	1.79	35198	4.10	1105	16.0	21.1	.999	7.87	8.52	663.5	631.5	404.5	403.1	-.27	.49	.0470	.0186	.9130	.4250
FLT 348 10-13-78 AIRCRAFT TRIM ANGLE - .75 DEG																			
14:46	1.55	31928	3.96	973	17.0	19.6	.990	5.69	6.50	621.9	592.0	419.3	415.2	-.39	.40	******	******	******	******
FLT 349 10-24-78 AIRCRAFT TRIM ANGLE - 2.50 DEG																			
13: 6	.58	10205	2.94	338	*****	*****	.995	****	****	533.9	527.0	500.5	492.6	.05	.46	******	******	******	******
13:17	1.16	39708	2.21	376	22.5	25.4	1.002	4.59	5.26	503.7	491.7	396.4	398.0	-.20	.65	******	******	******	******
13:32	.87	33470	2.12	285	20.3	22.4	1.009	3.95	4.34	474.0	470.5	411.5	407.5	-.06	.48	******	******	******	******
13:33	.88	33309	2.15	293	19.4	22.2	1.003	3.65	4.15	476.7	470.5	412.7	408.2	-.05	.45	******	******	******	******
13:39	.85	31463	2.20	296	19.5	22.6	.994	3.56	4.17	480.8	470.5	420.4	415.5	-.06	.57	******	******	******	******
13:47	.75	26690	2.27	287	19.8	23.0	.985	3.49	4.08	490.3	476.9	439.8	432.3	-.09	.56	******	******	******	******
13:54	.75	27102	2.24	282	20.4	24.1	.990	3.54	4.17	487.6	476.9	438.3	431.9	-.07	.24	******	******	******	******
13:57	.75	27002	2.25	282	*****	18.6	.990	****	3.66	487.6	476.9	438.5	432.0	-.01	.88	******	******	******	******
14: 0	.75	26947	2.27	287	20.8	23.0	.992	3.60	4.05	487.6	478.0	437.9	432.0	-.11	.01	******	******	******	******
14: 9	.62	18614	2.40	274	19.9	22.5	.972	3.30	3.73	509.0	490.6	473.0	466.4	.05	.49	******	******	******	******
14:11	.63	18670	2.45	286	19.2	22.0	.978	3.31	3.79	510.3	494.8	472.8	466.1	-.13	.26	******	******	******	******
14:13	.63	18709	2.44	285	*****	18.1	.978	****	3.29	511.6	495.9	474.1	466.0	-.17	.73	******	******	******	******

***** NOT MEASURED DURING FLIGHT

TABLE 1.–Continued

(b) Continued

H, ft; U_∞/ν_∞, per ft × 10^6; q_∞, lb/ft^2; X_t and X_T, in.; Re_{t_0} and Re_{T_0}, × 10^6; T_t, T_w, T_∞, and T_{∞_b}, °R; α and β, deg; $\left(\sqrt{\overline{p'_{t_2}}^2}/q_\infty\right)100$, $\left(\sqrt{\overline{p'_{t_2}}^2}/p_{t_\infty}\right)100$, $\left(\sqrt{\overline{p'_{s_1}}^2}/q_\infty\right)100$, and $\left(\sqrt{\overline{p'_{s_2}}^2}/q_\infty\right)100$, percent

Time of day	M_∞	H	$\frac{U_\infty}{\nu_\infty}$	q_∞	X_t	X_T	T_w/T_{aw}	Re_{t_0}	Re_{T_0}	T_t	T_w	T_∞	T_{∞_b}	α	β	$\frac{\sqrt{\overline{p'_{t_2}}^2}}{q_\infty}$ × 100	$\frac{\sqrt{\overline{p'_{t_2}}^2}}{p_{t_\infty}}$ × 100	$\frac{\sqrt{\overline{p'_{s_1}}^2}}{q_\infty}$ × 100	$\frac{\sqrt{\overline{p'_{s_2}}^2}}{q_\infty}$ × 100
FLT 350 10-25-78 AIRCRAFT TRIM ANGLE - 3.50 DEG																			
13: 7	.52	7577	2.84	308	*****	*****	.999	****	****	544.3	540.3	515.9	514.7	-.42	.60	******	******	******	******
13:13	.59	8209	2.65	272	*****	*****	1.000	****	****	539.1	536.2	513.5	514.2	-.06	.54	******	******	******	******
13:22	.57	17360	2.32	250	*****	19.3	1.006	****	3.90	510.3	509.4	478.8	475.5	-.05	.49	******	******	******	******
13:37	1.09	46612	1.58	239	22.8	26.8	1.043	4.10	4.98	469.9	479.0	379.0	483.0	-.39	.49	******	******	******	******
13:44	.65	27736	1.99	216	19.6	22.9	1.014	3.62	4.19	468.5	470.5	431.4	428.8	.19	.50	******	******	******	******
13:57	.88	41310	1.56	198	26.6	29.8	1.024	4.02	4.50	453.2	456.6	392.9	390.7	-.04	.13	******	******	******	******
13:59	.97	40858	1.59	201	24.6	29.5	1.022	3.78	4.47	451.7	454.5	391.9	391.3	-.11	.16	******	******	******	******
14: 3	.90	40755	1.63	216	24.5	30.0	1.004	3.24	4.13	461.5	455.5	396.6	391.4	-.55	-.02	******	******	******	******
14:11	.77	34800	1.76	207	22.0	25.2	.999	3.25	3.79	457.4	451.2	409.2	399.3	-.26	.48	******	******	******	******
FLT 351 10-31-78 AIRCRAFT TRIM ANGLE - 3.50 DEG																			
9:14	.57	17757	2.39	244	*****	*****	1.021	****	****	490.3	496.9	460.3	462.6	.28	.89	.1093	.0200	.4440	.2140
9:17	.69	18286	2.47	263	*****	*****	1.015	****	****	490.3	493.7	457.4	460.9	-.14	.49	.1054	.0208	.3270	.2100
9:25	1.16	47384	1.53	259	*****	*****	.998	****	****	501.3	487.4	394.7	390.8	-.53	.56	.0643	.0263	.0528	.0632
9:29	1.17	48725	1.48	248	*****	*****	1.002	****	****	497.0	485.3	389.5	389.2	-.57	.29	******	******	******	******
9:31	1.18	47805	1.56	263	*****	*****	1.002	****	****	491.4	486.4	389.5	390.4	-.79	.08	******	******	******	******
9:44	1.09	47125	1.45	226	33.2	*****	1.000	****	****	464.9	473.7	393.4	391.1	-.30	.48	.0746	.0292	.0615	.0762
9:54	.92	44290	1.41	189	27.0	31.0	1.021	3.76	4.40	461.5	463.0	394.8	394.7	-.28	.52	.0903	.0309	.0838	.1057
FLT 352 10-31-78 AIRCRAFT TRIM ANGLE - 3.50 DEG																			
13:39	.59	13997	2.34	222	*****	19.2	.995	****	3.72	502.3	496.9	441.3	475.0	-.01	.57	******	******	******	******
13:51	.69	23659	2.02	209	18.6	22.2	1.001	3.20	3.82	479.4	475.8	447.5	444.2	-.01	.57	******	******	******	******
14:46	.71	35093	1.65	176	22.2	25.4	1.005	3.21	3.68	443.2	440.4	402.5	402.4	-.17	.52	******	******	******	******
14:54	.71	35073	1.66	177	24.6	27.5	.997	3.30	3.71	443.2	437.1	402.3	402.4	-.16	.27	******	******	******	******
14:56	.71	35232	1.63	175	21.7	24.4	.991	2.70	3.06	446.1	437.1	405.0	402.4	-.22	.12	******	******	******	******

***** NOT MEASURED DURING FLIGHT

TABLE 1.–Concluded

(b) Concluded

H, ft; U_∞/ν_∞, per ft × 10^6; q_∞, lb/ft^2; X_t and X_T, in.; Re_{t_0} and Re_{T_0}, × 10^6; T_t, T_w, T_∞, and T_{∞_b}, °R;

α and β, deg; $\left(\sqrt{\overline{p_{t_2}'^2}}/q_\infty\right)100$, $\left(\sqrt{\overline{p_{t_2}'^2}}/p_{t_\infty}\right)100$, $\left(\sqrt{\overline{p_{s_1}'^2}}/q_\infty\right)100$, and $\left(\sqrt{\overline{p_{s_2}'^2}}/q_\infty\right)100$, percent

FLT 353 11- 1-78 AIRCRAFT TRIM ANGLE - 4.50 DEG

Time of day	M_∞	H	$\frac{U_\infty}{\nu_\infty}$	q_∞	X_t	X_T	T_w/T_{aw}	Re_{t_0}	Re_{T_0}	T_t	T_w	T_∞	T_{∞_b}	α	β	$\frac{\sqrt{\overline{p_{t_2}'^2}}}{q_\infty}$ × 100	$\frac{\sqrt{\overline{p_{t_2}'^2}}}{p_{t_\infty}}$ × 100	$\frac{\sqrt{\overline{p_{s_1}'^2}}}{q_\infty}$ × 100	$\frac{\sqrt{\overline{p_{s_2}'^2}}}{q_\infty}$ × 100
13: 8	.44	6715	2.54	224	*****	*****	.989	****	****	522.2	514.6	502.7	490.8	-.31	.58	.1136	.0135	.3670	.2450
13:16	.62	26031	1.93	202	*****	*****	1.053	****	****	474.0	494.8	440.2	420.1	-.04	.54	******	******	******	******
13:22	.50	14197	2.28	214	*****	18.1	.992	****	3.40	503.7	496.9	479.9	478.2	-.18	.65	.1211	.0178	.4750	.1630
13:25	.50	14196	2.28	212	*****	18.5	.995	****	3.33	502.4	496.9	478.8	478.2	-.09	.22	******	******	******	******
13:27	.49	13744	2.29	212	17.4	20.1	.992	3.04	3.49	503.7	496.9	460.5	460.2	-.15	.05	.1181	.0169	.2650	.2590
13:42	1.10	51232	1.24	192	*****	*****	1.012	****	****	478.1	472.6	385.3	385.6	-.43	.59	.0753	.0298	.0735	.0891
13:55	.67	23632	1.94	192	21.0	23.4	.983	3.09	3.51	476.7	465.2	447.3	435.0	-.21	.62	.1067	.0195	.1149	.4720
14:17	.92	41758	1.38	170	29.2	33.1	.986	3.15	3.81	457.4	444.7	402.9	394.6	-.39	.62	******	******	******	******
14:27	.70	35273	2.30	169	20.5	24.3	1.008	4.21	5.02	440.4	439.3	401.1	396.0	-.22	.51	.1099	.0271	.1074	.4060

***** NOT MEASURED DURING FLIGHT

TABLE 2.–LAMINAR INSTABILITY

Units for U_e are m/sec and ft/sec; for U_e/ν_e, per m × 10^6 and per ft × 10^6;
for $\sqrt{Re_{x_1}}$ and $\sqrt{Re_{x_2}}$, × 10^2; for $F_{1_{min}}$, F_1, $F_{1_{max}}$, $F_{2_{min}}$, F_2, and $F_{2_{max}}$, × 10^4

Time of day	M_∞	M_e	U_e	U_e	U_e/ν_e	U_e/ν_e	$\sqrt{Re_{x_1}}$	$F_{1_{min}}$	F_1	$F_{1_{max}}$	$\sqrt{Re_{x_2}}$	$F_{2_{min}}$	F_2	$F_{2_{max}}$
FLT 327 8-14-78														
9: 0	1.10	1.05	308	1011	7.96	2.43	19.1	.192	.364	.461	22.9	.103	.256	.351
9: 7	.86	.82	244	801	7.14	2.18	18.1	.269	.454	.595	21.7	.180	.310	.433
9:18	.66	.64	201	660	7.74	2.36	18.8	.322	.447	.544	22.6	.181	.326	.443
9:24	.55	.53	173	569	8.72	2.66	20.0	.333	.457	.540	24.0	*****	*****	*****
9:36	.54	.52	169	553	8.55	2.61	19.8	.305	.466	.567	23.8	*****	*****	*****
FLT 328 8-16-78														
10:13	1.52	1.47	421	1382	7.10	2.16	18.0	.158	.353	.483	21.7	.168	.246	.273
10:20	1.36	1.32	382	1252	6.71	2.04	17.5	.196	.376	.467	21.1	.197	.273	.393
10:23	1.18	1.14	335	1100	7.38	2.25	18.4	.203	.370	.532	22.1	.165	.276	.355
FLT 329 8-18-78														
10:11	1.39	1.34	335	1270	7.04	2.15	17.9	.267	.376	.426	21.6	*****	*****	*****
10:22	1.12	1.07	318	1042	7.22	2.20	18.2	.205	.392	.493	21.8	.137	.260	.356
10:26	.96	.81	245	802	6.84	2.08	17.7	.282	.470	.613	21.3	.124	.338	.489
10:31	.95	.81	242	794	6.77	2.07	17.6	.287	.468	.613	21.2	.123	.337	.445
10:36	.75	.72	220	722	7.03	2.14	17.9	.305	.496	.630	21.5	.163	.358	.524
10:42	.67	.64	202	661	7.79	2.37	18.9	.216	.440	.548	22.7	.220	.320	.400
10:48	.54	.52	166	544	9.05	2.76	20.3	.272	.448	.545	24.4	*****	*****	*****

***** NOT MEASURED DURING FLIGHT

TABLE 2.–Continued

Units for U_e are m/sec and ft/sec; for U_e/ν_e, per m × 10^6 and per ft × 10^6; for $\sqrt{Re_{x_1}}$ and $\sqrt{Re_{x_2}}$, × 10^2; for $F_{1_{min}}$, F_1, $F_{1_{max}}$, $F_{2_{min}}$, F_2, and $F_{2_{max}}$, × 10^4

Time of day	M_∞	M_e	U_e	U_e	U_e/ν_e	U_e/ν_e	$\sqrt{Re_{x_1}}$	$F_{1_{min}}$	F_1	$F_{1_{max}}$	$\sqrt{Re_{x_2}}$	$F_{2_{min}}$	F_2	$F_{2_{max}}$
FLT 330 8-23-78														
9:35	1.44	1.39	410	1347	9.32	2.84	20.6	.209	.304	.378	24.8	*****	.209	*****
9:39	1.34	1.30	388	1272	9.28	2.83	20.6	.134	.311	.402	24.8	.122	.225	.309
9:43	1.25	1.21	365	1199	9.31	2.84	20.6	.148	.329	.425	24.8	.139	.231	.314
9:47	1.16	1.12	338	1110	9.74	2.97	21.0	.221	.326	.419	25.4	*****	*****	*****
9:52	.89	.84	276	906	9.27	2.83	20.6	.160	.361	.479	24.7	*****	*****	*****
FLT 331 8-24-78														
9:41	1.27	1.23	367	1205	9.73	2.97	21.1	.132	.308	.405	25.4	*****	.220	*****
9:47	.84	.80	252	826	10.43	3.18	21.8	.144	.347	.459	26.2	*****	*****	*****
9:51	.73	.69	223	731	10.98	3.35	22.4	.154	.339	.467	26.9	*****	*****	*****
FLT 332 8-25-78														
10:12	1.49	1.45	429	1409	8.37	2.55	19.6	.108	.313	.397	23.5	.129	.224	.306
10:20	.94	.88	270	887	9.19	2.80	20.5	.187	.354	.460	24.6	*****	.263	*****
FLT 333 8-25-78														
13:34	1.55	1.50	447	1468	8.97	2.74	20.3	*****	.324	*****	24.3	*****	*****	*****
13:43	1.20	1.16	347	1140	9.16	2.79	20.5	*****	.365	*****	24.6	.162	.273	.365
13:51	.93	.88	270	885	9.14	2.79	20.4	.199	.370	.464	24.6	.153	.275	.339
13:54	.89	.84	260	854	9.32	2.84	20.6	.205	.371	.474	24.8	.161	.277	.345
13:58	.78	.75	237	780	9.91	3.02	21.3	.213	.349	.480	25.6	*****	*****	*****
13:59	.79	.75	239	783	9.87	3.01	21.3	.173	.352	.485	25.5	*****	*****	*****

***** NOT MEASURED DURING FLIGHT

TABLE 2.–Continued

Units for U_e are m/sec and ft/sec; for U_e/ν_e, per m × 10^6 and per ft × 10^6; for $\sqrt{Re_{x_1}}$ and $\sqrt{Re_{x_2}}$, × 10^2; for $F_{1_{min}}$, F_1, $F_{1_{max}}$, $F_{2_{min}}$, F_2, and $F_{2_{max}}$, × 10^4

Time of day	M_∞	M_e	U_e	U_e	U_e/ν_e	U_e/ν_e	$\sqrt{Re_{x_1}}$	$F_{1_{min}}$	F_1	$F_{1_{max}}$	$\sqrt{Re_{x_2}}$	$F_{2_{min}}$	F_2	$F_{2_{max}}$
FLT 334 9- 1-78														
10:39	1.41	1.36	421	1380	12.56	3.83	24.0	.151	.222	*****	28.8	*****	.155	*****
FLT 335 9- 1-78														
13:53	1.50	1.46	441	1447	10.94	3.34	22.4	.171	.245	*****	26.9	*****	*****	*****
FLT 336 9- 6-78														
14:49	1.76	1.71	516	1694	12.35	3.76	23.8	.148	.202	*****	28.6	*****	*****	*****
FLT 337 9- 8-78														
11:33	1.57	1.52	462	1515	11.38	3.47	22.8	*****	*****	*****	27.4	.120	.182	*****
11:42	1.33	1.29	394	1291	10.94	3.34	22.4	*****	.261	*****	27.0	.122	.200	.254
FLT 338 9-13-78														
10:10	1.75	1.70	509	1669	11.73	3.58	23.2	.134	.213	*****	27.8	.133	.163	.219
10:18	1.39	1.34	412	1352	11.72	3.57	23.2	*****	.229	*****	27.8	*****	*****	*****
FLT 339 9-25-78														
13: 8	1.60	1.55	466	1528	11.55	3.52	23.1	.153	.219	*****	27.8	.115	.167	.213
13:13	1.49	1.44	433	1420	11.04	3.36	22.5	.168	.240	.299	27.0	.108	.175	.236

***** NOT MEASURED DURING FLIGHT

TABLE 2.–Concluded

Units for U_e are m/sec and ft/sec; for U_e/ν_e, per m × 10^6 and per ft × 10^6; for $\sqrt{Re_{x_1}}$ and $\sqrt{Re_{x_2}}$, × 10^2; for $F_{1_{min}}$, F_1, $F_{1_{max}}$, $F_{2_{min}}$, F_2, and $F_{2_{max}}$, × 10^4

Time of day	M_∞	M_e	U_e	U_e	U_e/ν_e	U_e/ν_e	$\sqrt{Re_{x_1}}$	$F_{1_{min}}$	F_1	$F_{1_{max}}$	$\sqrt{Re_{x_2}}$	$F_{2_{min}}$	F_2	$F_{2_{max}}$
FLT 345 10- 5-78														
14:20	1.47	1.42	438	1436	13.21	4.03	24.5	.148	.223	*****	29.5	*****	*****	*****
FLT 351 10-31-78														
9:17	.60	.57	178	583	7.87	2.40	19.0	*****	.409	*****	22.8	*****	*****	*****
FLT 353 11- 1-78														
13:22	.50	.48	152	499	7.25	2.21	18.2	.205	.507	.758	21.9	*****	*****	*****
13:27	.49	.47	150	492	7.24	2.21	18.2	*****	.481	.660	22.2	*****	*****	*****
13:55	.57	.55	176	577	6.19	1.89	16.8	.312	.526	.710	20.2	*****	.375	*****
14:27	.70	.67	194	637	5.15	1.57	15.3	.427	.628	.798	18.4	*****	.440	*****

***** NOT MEASURED DURING FLIGHT

TABLE 3.—SENSITIVITY OF BOUNDARY LAYER TRANSITION TO CONE INCIDENCE ANGLE

(a) $M_\infty = 0.40$; $U_\infty/\nu_\infty \cong 9.8 \times 10^6$ per m (3.0×10^6 per ft); source, NASA Langley 16-Foot Transonic Dynamics Tunnel; test medium, freon

α, deg	β, deg	ϕ, deg	X_T/L	X_t/L
2.0	0	0	0.449	0.283
1.0	0	0	0.463	0.292
0	0	0	0.454	0.301
-1.0	0	180	0.407	0.328
-2.0	0	180	0.404	0.335

(b) $M_\infty = 0.60$; $U_\infty/\nu_\infty \cong 10.8 \times 10^6$ per m (3.3×10^6 per ft); source, NASA Ames 14-Foot Transonic Wind Tunnel

α, deg	β, deg	ϕ, deg	X_T/L	X_t/L
2.0	0	0	0.335	0.238
1.0	0	0	0.324	0.240
0.5	0	0	0.315	0.243
0	0	0	0.308	0.243
-0.5	0	180	0.299	0.267
-1.0	0	180	0.267	0.236
-2.0	0	180	0.272	0.247
0	2.0	90	0.202	0.178
0	1.0	90	0.288	0.229
0	0.5	90	0.310	0.254
0	0	90	0.308	0.243
0	-0.5	270	0.281	0.240
0	-1.0	270	0.252	0.202
0	-2.0	270	0.195	0.171

TABLE 3.-Continued

(c) $M_\infty = 0.80$; $U_\infty/\nu_\infty \cong 9.8 \times 10^6$ per m (3.0×10^6 per ft); source, AEDC 16-Foot Transonic Dynamics Tunnel

α, deg	β, deg	ϕ, deg	X_T/L	X_t/L
1.0	0	0	0.279	0.189
0.5	0	0	0.283	0.198
0	0	0	0.283	0.213
-0.5	0	180	0.267	0.218
-1.0	0	180	0.258	0.216

(d) $M_\infty = 0.90$; $U_\infty/\nu_\infty \cong 9.8 \times 10^6$ per m (3.0×10^6 per ft); source, NASA Ames 11- by 11-Foot Transonic Wind Tunnel

α, deg	β, deg	ϕ, deg	X_T/L	X_t/L
1.0	0	0	0.427	0.294
0.5	0	0	0.425	0.308
0	0	0	0.413	0.324
-0.5	0	180	0.411	0.328
-1.0	0	180	0.402	0.333
0	1.0	90	0.328	0.270
0	0.5	90	0.387	0.315
0	0	90	0.402	0.319
0	-0.5	270	0.378	0.303
0	-1.0	270	0.328	0.261

TABLE 3.—Continued

(e) $M_\infty = 0.90$; $U_\infty/\nu_\infty \cong 12.5 \times 10^6$ per m (3.8×10^6 per ft); source, NASA Ames 14-Foot Transonic Wind Tunnel

α, deg	β, deg	ϕ, deg	X_T/L	X_t/L
2.0	0	0	0.283	0.171
1.0	0	0	0.276	0.202
0.5	0	0	0.274	0.220
0	0	0	0.279	0.227
-0.5	0	180	0.263	0.222
-1.0	0	180	0.263	0.231
-2.0	0	180	0.274	0.247
0	2.0	90	0.187	0.164
0	1.0	90	0.283	0.213
0	0.5	90	0.288	0.236
0	0	90	0.308	0.249
0	-0.5	270	0.301	0.236
0	-1.0	270	0.222	0.189
0	-2.0	270	0.182	0.155

TABLE 3.–Continued

(f) $M_\infty = 0.95$; $U_\infty/\nu_\infty = 9.8 \times 10^6$ per m (3.0×10^6 per ft); source, NASA Ames 11- by 11-Foot Transonic Wind Tunnel

α, deg	β, deg	ϕ, deg	X_T/L	X_t/L
2.2	0	0	0.373	0.211
1.7	0	0	0.387	0.267
1.2	0	0	0.391	0.274
0.9	0	0	0.391	0.279
0.7	0	0	0.393	0.290
0.4	0	0	0.389	0.297
0.2	0	0	0.384	0.297
0	0	0	0.387	0.303
-0.3	0	180	0.384	0.315
-0.5	0	180	0.384	0.317
-0.8	0	180	0.382	0.317
-1.3	0	180	0.387	0.326
-1.8	0	180	0.396	0.346
0	2.2	90	0.261	0.218
0	1.6	90	0.265	0.220
0	1.1	90	0.308	0.243
0	0.8	90	0.333	0.261
0	0.6	90	0.360	0.288
0	0.3	90	0.382	0.301
0	0	90	0.389	0.303
0	-0.2	270	0.387	0.301
0	-0.4	270	0.373	0.292
0	-0.7	270	0.364	0.281
0	-0.9	270	0.339	0.265
0	-1.4	270	0.288	0.225
0	-1.9	270	0.272	0.222

TABLE 3.–Continued

(g) $M_\infty = 1.10$; $U_\infty/\nu_\infty = 9.8 \times 10^6$ per m (3.0×10^6 per ft); source, NASA Ames 11- by 11-Foot Transonic Wind Tunnel

α, deg	β, deg	ϕ, deg	X_T/L	X_t/L
2.2	0	0	0.344	0.198
1.7	0	0	0.382	0.263
1.2	0	0	0.418	0.321
1.0	0	0	0.427	0.326
0.7	0	0	0.436	0.330
0.5	0	0	0.434	0.337
0.2	0	0	0.434	0.348
0	0	0	0.431	0.353
-0.3	0	180	0.431	0.357
-0.5	0	180	0.427	0.362
-0.8	0	180	0.425	0.364
-1.3	0	180	0.427	0.378
-1.7	0	180	0.438	0.382
0	2.2	90	0.290	0.236
0	1.6	90	0.297	0.236
0	1.2	90	0.328	0.272
0	0.8	90	0.362	0.299
0	0.6	90	0.391	0.315
0	0.3	90	0.413	0.335
0	0.2	90	0.422	0.360
0	0.1	90	0.429	0.342
0	-0.2	270	0.425	0.344
0	-0.4	270	0.413	0.333
0	-1.4	270	0.291	0.218
0	-1.9	270	0.283	0.227

TABLE 3.–Continued

(h) $M_\infty = 1.30$; $U_\infty/\nu_\infty \cong 9.8 \times 10^6$ per m (3.0×10^6 per ft); source, NASA Ames 11- by 11-Foot Transonic Wind Tunnel

α, deg	β, deg	ϕ, deg	X_T/L	X_t/L
2.0	0	0	0.337	0.247
1.5	0	0	0.353	0.261
1.0	0	0	0.387	0.288
0.75	0	0	0.404	0.315
0.5	0	0	0.404	0.317
0.2	0	0	0.404	0.321
0	0	0	0.404	0.324
-0.3	0	180	0.404	0.326
-0.5	0	180	0.404	0.326
-0.75	0	180	0.411	0.346
-1.0	0	180	0.416	0.355
-1.5	0	180	0.431	0.371
-2.0	0	180	0.449	0.382
0	1.9	90	0.261	0.216
0	1.4	90	0.258	0.206
0	0.9	90	0.306	0.231
0	0.7	90	0.360	0.258
0	0.4	90	0.378	0.281
0	0.2	90	0.398	0.317
0	-0.1	270	0.400	0.319
0	-0.3	270	0.387	0.294
0	-0.6	270	0.360	0.267
0	-0.8	270	0.301	0.231
0	-1.1	270	0.279	0.218
0	-1.6	270	0.252	0.200
0	-2.1	270	0.247	0.204

TABLE 3.-Continued

(i) M_∞ = 1.50; source, NASA Ames 9- by 7-Foot Supersonic Wind Tunnel

U_∞/ν_∞, per m (per ft)	α, deg	β, deg	ϕ, deg	X_T/L	X_t/L
8.2×10^6 (2.5×10^6)	1.0	-0.2	0	0.593	0.404
	0.8	-0.2	0	-----	0.474
	0.6	-0.2	0	0.724	0.564
	0.3	-0.2	0	-----	0.587
	0.1	-0.2	0	-----	0.609
	-0.2	-0.2	180	0.730	0.602
	-0.4	-0.2	180	0.719	0.596
	-0.7	-0.2	180	0.699	0.542
9.8×10^6 (3.0×10^6)	0.1	1.1	90	0.272	0.182
	0.1	0.8	90	0.373	0.209
	0.1	0.6	90	0.490	0.281
	0.1	0.2	90	0.591	0.436
	0.1	0.1	90	0.631	0.485
	0.1	-0.1	270	0.618	0.488
	0.1	-0.4	270	0.562	0.429
	0.1	-0.7	270	0.492	0.342
	0.1	-0.9	270	0.434	0.306

TABLE 3.-Continued

(j) $M_\infty = 1.60$; $U_\infty/\nu_\infty \cong 9.8 \times 10^6$ per m (3.0×10^6 per ft); source, NASA Langley Unitary Plan Wind Tunnel (low Mach number test section)

α, deg	β, deg	ϕ, deg	X_T/L	X_t/L
1.0	0	0	0.458	0.171
0.75	0	0	0.512	0.211
0.5	0	0	0.564	0.245
0.25	0	0	0.587	0.252
0	0	0	0.582	0.256
-0.25	0	180	0.555	0.276
-0.5	0	180	0.571	0.254
-0.75	0	180	0.551	0.261
-1.0	0	180	0.548	0.283
0	1.0	90	0.438	0.187
0	0.75	90	0.490	0.209
0	0.5	90	0.539	0.261
0	0.25	90	0.578	0.288
0	0	90	0.582	0.285
0	-0.25	270	0.566	0.274
0	-0.5	270	0.508	0.227
0	-0.75	270	0.438	0.202
0	-1.0	270	0.342	0.191

TABLE 3.-Continued

(k) $M_\infty = 1.60$; $U_\infty/\nu_\infty \cong 9.8 \times 10^6$ per m (3.0×10^6 per ft); source, NASA Ames 9- by 7-Foot Supersonic Wind Tunnel

α, deg	β, deg	ϕ, deg	X_T/L	X_t/L
0	1.0	90	0.315	0.227
0	0.75	90	0.384	0.274
0	0.5	90	0.526	0.378
0	0.25	90	0.598	0.436
0	0	90	0.620	0.503
0	-0.25	270	0.589	0.418
0	-0.5	270	0.501	0.373
0	-0.75	270	0.422	0.301
0	-1.0	270	0.371	0.274

(l) $M_\infty = 1.70$; $U_\infty/\nu_\infty \cong 9.8 \times 10^6$ per m (3.0×10^6 per ft); source, NASA Ames 9- by 7-Foot Supersonic Wind Tunnel

α, deg	β, deg	ϕ, deg	X_T/L	X_t/L
0.2	0.9	90	0.324	0.227
0.2	0.6	90	0.402	0.263
0.2	0.4	90	0.542	0.362
0.2	0.1	90	0.598	0.458
0.2	-0.1	270	0.587	0.476
0.2	-0.4	270	0.537	0.407
0.2	-0.6	270	0.449	0.346
0.2	-0.9	270	0.407	0.315
0.2	-1.1	270	0.360	0.263

TABLE 3.-Continued

(m) $M_\infty = 1.80$; $U_\infty/\nu_\infty \cong 9.8 \times 10^6$ per m (3.0×10^6 per ft); source, NASA Ames 9- by 7-Foot Supersonic Wind Tunnel

α, deg	β, deg	ϕ, deg	X_T/L	X_t/L
0	0.9	90	0.369	0.283
0	0.65	90	0.422	0.328
0	0.4	90	0.530	0.413
0	0.15	90	0.604	0.492
0	-0.1	270	0.602	0.481
0	-0.35	270	0.537	0.416
0	-0.6	270	0.434	0.344
0	-0.85	270	0.389	0.301
0	-1.1	270	0.355	0.272

(n) $M_\infty = 2.00$; $U_\infty/\nu_\infty = 9.8 \times 10^6$ per m (3.0×10^6 per ft); source, NASA Langley Unitary Plan Wind Tunnel (low Mach number test section)

α, deg	β, deg	ϕ, deg	X_T/L	X_t/L
1.0	0	0	0.366	0.162
0.75	0	0	0.440	0.193
0.5	0	0	0.515	0.256
0.25	0	0	0.535	0.290
0	0	0	0.544	0.303
-0.25	0	180	0.557	0.404
-0.5	0	180	0.564	0.407
-0.75	0	180	0.562	0.413
-1.0	0	180	0.564	0.422

TABLE 3.–Continued

(o) $M_\infty = 2.00$; $U_\infty/\nu_\infty = 9.8 \times 10^6$ per m (3.0×10^6 per ft); source, NASA Ames 9- by 7-Foot Supersonic Wind Tunnel

α, deg	β, deg	ϕ, deg	X_T/L	X_t/L
1.5	-0.1	0	0.234	0.162
1.2	-0.1	0	0.243	0.180
1.0	-0.1	0	0.267	0.191
0.7	-0.1	0	0.337	0.227
0.5	-0.1	0	0.449	0.272
0.2	-0.1	0	0.535	0.382
0	-0.1	0	0.566	0.461
-0.3	-0.1	180	0.587	0.485
-0.5	-0.1	180	0.598	0.501
0.1	1.0	90	0.317	0.247
0.1	0.75	90	0.373	0.288
0.1	0.5	90	0.452	0.333
0.1	0.25	90	0.544	0.409
0.1	0	90	0.578	0.454
0.1	-0.25	270	0.546	0.398
0.1	-0.5	270	0.445	0.339
0.1	-0.75	270	0.384	0.274
0.1	-1.0	270	0.328	0.225

TABLE 3.—Continued

(p) $M_\infty = 2.00$; $U_\infty/\nu_\infty = 9.8 \times 10^6$ per m $(3.0 \times 10^6$ per ft); source, NASA Langley 4- by 4-Foot Supersonic Pressure Tunnel

α, deg	β, deg	ϕ, deg	X_T/L	X_t/L
-0.25	0.75	90	0.387	0.267
-0.25	0.5	90	0.483	0.316
-0.25	0.25	90	0.580	0.443
-0.25	0	90	0.631	0.488
-0.25	-0.25	270	0.616	0.458
-0.25	-0.5	270	0.528	0.321
-0.25	-0.75	270	0.407	0.270
-0.25	-1.0	270	0.355	0.254
-0.25	-1.25	270	0.310	0.227

(q) $M_\infty = 2.20$; $U_\infty/\nu_\infty = 9.8 \times 10^6$ per m $(3.0 \times 10^6$ per ft); source, NASA Ames 9- by 7-Foot Supersonic Wind Tunnel

α, deg	β, deg	ϕ, deg	X_T/L	X_t/L
1.0	0.05	0	0.252	0.180
0.75	0.05	0	0.288	0.207
0.6	0.05	0	0.413	0.272
0.25	0.05	0	0.555	0.425
0	0.05	0	0.587	0.488
-0.25	0.05	180	0.600	0.508
-0.75	0.05	180	0.616	0.519
0	1.0	90	0.270	0.196
0	0.75	90	0.333	0.256
0	0.5	90	0.416	0.317
0	0.25	90	0.499	0.396
0	0	90	0.542	0.449
0	-0.25	270	0.503	0.373
0	-0.50	270	0.402	0.299
0	-0.75	270	0.337	0.234
0	-1.0	270	0.299	0.213

TABLE 3.–Continued

(r) $M_\infty = 2.50$; $U_\infty/\nu_\infty \cong 9.8 \times 10^6$ per m (3.0×10^6 per ft); source, NASA Ames 9- by 7-Foot Supersonic Wind Tunnel

α, deg	β, deg	ϕ, deg	X_T/L	X_t/L
1.1	0.15	0	0.222	0.137
0.9	0.15	0	0.252	0.191
0.6	0.15	0	0.351	0.252
0.4	0.15	0	0.485	0.357
0.1	0.15	0	0.534	0.438
-0.1	0.15	180	0.564	0.461
-0.4	0.15	180	0.589	0.485
-0.6	0.15	180	0.591	0.494
-0.9	0.15	180	0.591	0.490
-1.2	0.15	180	0.569	0.485
-0.1	0.9	90	0.310	0.220
-0.1	0.6	90	0.342	0.254
-0.1	0.4	90	0.427	0.324
-0.1	0.1	90	0.506	0.402
-0.1	-0.1	270	0.490	0.393
-0.1	-0.4	270	0.431	0.328
-0.1	-0.6	270	0.355	0.265
-0.1	-0.9	270	0.299	0.229
-0.1	-1.1	270	0.274	0.207

TABLE 3.–Continued

(s) $M_\infty = 2.86$; $U_\infty/\nu_\infty \cong 8.2 \times 10^6$ per m (2.5×10^6 per ft); source, NASA Langley Unitary Plan Wind Tunnel (high Mach number test section)

α, deg	β, deg	ϕ, deg	X_T/L	X_t/L
0.75	0	0	0.294	0.196
0.5	0	0	0.402	0.270
0.25	0	0	0.479	0.339
-0.25	0	180	0.544	0.387
-0.5	0	180	0.578	0.440
-0.75	0	180	0.598	0.485
0	1.25	90	0.339	0.245
0	1.0	90	0.353	0.256
0	0.75	90	0.389	0.290
0	0.5	90	0.431	0.317
0	0	90	0.515	0.404
0	-0.25	270	0.503	0.373
0	-0.5	270	0.440	0.321

(t) $M_\infty = 3.51$; $U_\infty/\nu_\infty \cong 9.8 \times 10^6$ per m (3.0×10^6 per ft); source, NASA Langley Unitary Plan Wind Tunnel (high Mach number section)

α, deg	β, deg	ϕ, deg	X_T/L	X_t/L
1.0	0	0	0.222	0.139
0.75	0	0	0.267	0.178
0.5	0	0	0.335	0.234
0.25	0	0	0.418	0.315
-0.25	0	180	0.494	0.418
-0.5	0	180	0.584	0.436
-0.75	0	180	0.566	0.456
-1.0	0	180	0.598	0.490
0	0.75	90	0.353	0.263
0	0.5	90	0.375	0.297
0	0.25	90	0.411	0.330
0	0	90	0.465	0.389
0	-0.5	270	0.400	0.308
0	-0.75	270	0.369	0.274
0	-1.0	270	0.317	0.216
0	-1.25	270	0.301	0.166

TABLE 3.–Concluded

(u) M_∞ = 4.60; $U_\infty/\nu_\infty \cong 9.8 \times 10^6$ per m (3.0×10^6 per ft); source, NASA Langley Unitary Plan Wind Tunnel (high Mach number test section)

α, deg	β, deg	ϕ, deg	X_T/L	X_t/L
0.9	-0.1	0	0.301	0.211
0.65	-0.1	0	0.371	0.265
0.4	-0.1	0	0.429	0.324
0.15	-0.1	0	0.483	0.364
-0.1	-0.1	180	0.566	0.373
-0.35	-0.1	180	0.548	0.438
-0.6	-0.1	180	0.602	0.470
-0.85	-0.1	180	0.634	0.501
-1.1	-0.1	180	0.654	0.515
-0.1	1.1	90	0.452	0.326
-0.1	0.85	90	0.456	0.353
-0.1	0.6	90	0.470	0.362
-0.1	0.35	90	0.492	0.380
-0.1	0.1	90	0.519	0.409
-0.1	-0.15	270	0.524	0.407
-0.1	-0.4	270	0.503	0.384
-0.1	-0.65	270	0.479	0.373
-0.1	-0.9	270	0.452	0.335

TABLE 4.-ATMOSPHERIC CONDITIONS FROM RADIOSONDE BALLOON AT EDWARDS, CALIFORNIA

H,		p,		RHO,		T,		D,		RH,	V,		THETA,	Z,	
m	ft	mb	lb/ft^2	gm/m^3	lb/ft^3	°C	°F	°C	°F	percent	m/sec	knots	deg	m	ft
MONTH 8 DAY 14 YEAR 78 HOUR OF RELEASE 900Z															
727.	2385.	928.9	1940.0	1105.9	.069039	18.3	64.9	7.6	45.7	49.7	6.7	13.0	235.0	724.	2375.
911.	2989.	908.5	1897.4	1081.6	.067522	18.3	64.9	7.3	45.1	48.6	6.7	13.0	249.0	914.	3000.
1203.	3948.	876.8	1831.2	1043.8	.065162	18.3	64.9	6.8	44.2	46.8	6.7	13.0	270.0	1219.	4000.
1494.	4901.	846.2	1767.3	1008.1	.062934	18.1	64.6	6.0	42.7	44.8	12.3	24.0	274.0	1524.	5000.
1734.	5653.	816.5	1705.3	977.8	.061042	16.7	62.1	3.5	38.4	41.4	18.0	35.0	273.0	1829.	6000.
2073.	6800.	787.8	1645.4	948.4	.059207	15.4	59.7	1.0	33.8	37.6	15.9	31.0	281.0	2134.	7000.
2362.	7748.	759.9	1587.1	919.6	.057409	14.0	57.2	-1.6	29.1	34.0	8.2	16.0	293.0	2438.	8000.
2650.	8693.	732.9	1530.7	891.6	.055661	12.6	54.7	-4.3	24.2	30.4	6.2	12.0	315.0	2743.	9000.
2937.	9637.	706.7	1476.0	864.3	.053956	11.2	52.2	-7.2	19.0	26.7	8.7	17.0	351.0	3048.	10000.
3224.	10579.	681.3	1422.9	840.0	.052439	8.9	48.0	-8.3	17.1	28.7	9.3	18.0	4.0	3353.	11000.
3513.	11527.	656.5	1371.1	817.3	.051022	6.2	43.2	-8.9	15.9	32.9	6.7	13.0	341.0	3658.	12000.
3802.	12473.	632.5	1321.0	795.0	.049630	3.6	38.5	-9.8	14.3	36.8	9.8	19.0	281.0	3962.	13000.
4090.	13419.	609.2	1272.3	769.3	.048026	2.3	36.1	-11.6	11.2	35.0	10.8	21.0	262.0	4267.	14000.
4378.	14365.	586.6	1225.1	744.2	.046459	1.1	34.0	-13.4	7.9	33.0	9.3	18.0	267.0	4572.	15000.
4665.	15306.	564.8	1179.6	719.9	.044942	-.1	31.8	-15.2	4.6	30.9	8.2	16.0	273.0	4877.	16000.
4952.	16245.	543.7	1135.5	696.3	.043469	-1.3	29.7	-17.1	1.2	28.8	8.2	16.0	292.0	5182.	17000.
5237.	17182.	523.3	1092.9	673.3	.042033	-2.5	27.5	-19.1	-2.3	26.8	9.3	18.0	303.0	5486.	18000.
5523.	18120.	503.5	1051.6	651.0	.040641	-3.8	25.2	-21.0	-5.9	24.9	9.8	19.0	299.0	5791.	19000.
5807.	19053.	484.4	1011.7	631.4	.039417	-5.9	21.4	-22.7	-8.9	25.1	9.8	19.0	300.0	6096.	20000.
6093.	19991.	465.8	972.8	612.7	.038250	-8.3	17.1	-24.4	-12.0	26.0	9.8	19.0	298.0	6401.	21000.
6377.	20923.	447.9	935.5	594.5	.037113	-10.7	12.7	-26.1	-15.1	26.9	10.8	21.0	296.0	6706.	22000.
6664.	21864.	430.4	898.9	576.7	.036002	-13.1	8.4	-27.9	-18.2	27.7	10.8	21.0	288.0	7010.	23000.
6950.	22802.	413.5	863.6	559.3	.034916	-15.6	3.9	-29.7	-21.5	28.8	10.8	21.0	281.0	7315.	24000.
7237.	23743.	397.1	829.4	542.3	.033855	-18.1	-.6	-31.6	-24.9	29.6	10.8	21.0	279.0	7620.	25000.
7526.	24691.	381.1	795.9	526.0	.032837	-20.7	-5.3	-33.9	-29.1	29.6	11.3	22.0	278.0	7925.	26000.
7814.	25635.	365.7	763.8	510.1	.031845	-23.3	-9.9	-36.3	-33.3	29.5	10.8	21.0	278.0	8230.	27000.
8101.	26580.	350.8	732.7	494.6	.030877	-26.0	-14.8	-38.6	-37.5	29.7	10.8	21.0	278.0	8534.	28000.
8391.	27530.	336.3	702.4	479.4	.029928	-28.7	-19.7	-41.0	-41.8	29.8	11.3	22.0	283.0	8839.	29000.
8683.	28487.	322.2	672.9	464.6	.029004	-31.5	-24.7	-43.4	-46.1	30.0	11.3	22.0	287.0	9144.	30000.
8974.	29443.	308.6	644.5	450.1	.028099	-34.2	-29.6	-45.9	-50.5	29.9	11.3	22.0	288.0	9449.	31000.
9267.	30404.	295.4	617.0	435.5	.027187	-36.8	-34.2	-48.1	-54.6	30.2	11.8	23.0	288.0	9754.	32000.
9561.	31369.	282.6	590.2	420.5	.026251	-38.9	-38.0	-50.0	-57.9	30.3	12.3	24.0	285.0	10058.	33000.
9855.	32331.	270.3	564.5	406.2	.025358	-41.2	-42.2	-54.1	-65.3	23.9	12.9	25.0	282.0	10363.	34000.
10149.	33296.	258.4	539.7	392.4	.024497	-43.6	-46.5	-59.6	-75.2	15.7	13.9	27.0	277.0	10668.	35000.
10441.	34255.	247.0	515.9	378.8	.023648	-45.9	-50.6	-65.3	-85.6	9.6	15.4	30.0	271.0	10973.	36000.
10736.	35223.	235.9	492.7	365.0	.022786	-47.9	-54.2	-66.9	-88.4	9.7	17.0	33.0	266.0	11278.	37000.
11031.	36192.	225.2	470.3	351.6	.021950	-49.8	-57.6	-68.5	-91.3	9.6	20.1	39.0	262.0	11582.	38000.
11325.	37157.	215.0	449.0	338.6	.021138	-51.8	-61.2	-70.1	-94.2	9.7	23.1	45.0	259.0	11887.	39000.
11624.	38138.	205.1	428.4	326.0	.020352	-53.9	-65.0	-71.8	-97.2	9.8	25.7	50.0	257.0	12192.	40000.
11925.	39124.	195.6	408.5	313.4	.019565	-55.6	-68.1	-73.2	-99.8	9.8	28.3	55.0	257.0	12497.	41000.
12231.	40127.	186.4	389.3	300.8	.018778	-57.1	-70.8	-74.4	-102.0	9.8	30.9	60.0	256.0	12802.	42000.
12534.	41121.	177.7	371.1	288.7	.018023	-58.6	-73.5	-75.7	-104.2	9.8	31.4	61.0	257.0	13106.	43000.
12841.	42129.	169.3	353.6	277.0	.017293	-60.1	-76.2	-76.9	-106.4	9.8	31.4	61.0	257.0	13411.	44000.
13152.	43149.	161.2	336.7	265.7	.016587	-61.7	-79.1	-78.2	-108.7	10.0	0.0	0.0	0.0	13716.	45000.
13462.	44167.	153.5	320.6	254.8	.015907	-63.2	-81.8	-79.4	-111.0	10.0	0.0	0.0	0.0	14021.	46000.
13783.	45209.	146.0	304.9	243.2	.015162	-63.8	-82.6	-80.0	-111.9	9.9	0.0	0.0	0.0	14326.	47000.
14091.	46231.	139.0	290.3	231.3	.014440	-63.7	-82.7	-79.9	-111.8	9.9	0.0	0.0	0.0	14630.	48000.
14405.	47259.	132.3	276.3	220.1	.013740	-63.6	-82.5	-79.8	-111.6	9.9	0.0	0.0	0.0	14935.	49000.
14719.	48291.	125.9	262.9	209.4	.013072	-63.5	-82.3	-79.7	-111.5	9.9	0.0	0.0	0.0	15240.	50000.

TABLE 4.–Continued

MONTH 8 DAY 16 YEAR 78 HOUR OF RELEASE 900Z

H,		p,		RHO,		T,		D,		RH,	V,		THETA,	Z,	
m	ft	mb	lb/ft^2	gm/m^3	lb/ft^3	°C	°F	°C	°F	percent	m/sec	knots	deg	m	ft
720.	2362.	929.7	1941.7	1097.8	.068533	21.4	70.5	-3.6	25.4	18.3	4.6	9.0	225.0	724.	2375.
902.	2959.	909.5	1899.5	1072.4	.066948	21.4	70.5	3.2	37.8	30.1	7.2	14.0	243.0	914.	3000.
1192.	3911.	878.0	1833.7	1039.7	.064906	19.9	67.8	5.8	42.4	39.6	10.3	20.0	270.0	1219.	4000.
1483.	4866.	847.3	1769.6	1012.7	.063221	17.3	63.1	3.8	38.9	40.7	7.7	15.0	278.0	1524.	5000.
1773.	5817.	817.6	1707.6	981.2	.061254	16.2	61.2	2.1	35.8	38.6	9.3	18.0	270.0	1829.	6000.
2063.	6767.	788.8	1647.4	950.5	.059338	15.1	59.2	.3	32.6	36.4	11.3	22.0	260.0	2134.	7000.
2352.	7717.	760.8	1589.0	920.7	.057477	14.0	57.2	-1.5	29.4	34.3	13.9	27.0	260.0	2438.	8000.
2640.	8661.	733.8	1532.6	891.7	.055667	12.9	55.2	-3.3	26.0	32.1	14.9	29.0	261.0	2743.	9000.
2927.	9604.	707.6	1477.9	863.6	.053913	11.7	53.1	-5.2	22.6	30.2	14.4	28.0	266.0	3048.	10000.
3214.	10545.	682.2	1424.8	836.4	.052215	10.5	50.9	-7.7	18.2	27.1	13.4	26.0	272.0	3353.	11000.
3499.	11481.	657.7	1373.6	810.1	.050573	9.3	48.7	-10.5	13.1	23.5	11.8	23.0	275.0	3658.	12000.
3785.	12417.	633.9	1323.9	786.3	.049087	7.3	45.1	-12.7	9.1	22.5	11.3	22.0	276.0	3962.	13000.
4070.	13353.	610.8	1275.7	763.2	.047645	5.3	41.5	-14.9	5.2	21.7	11.3	22.0	276.0	4267.	14000.
4355.	14289.	588.4	1228.9	740.7	.046240	3.3	37.9	-17.1	1.3	20.8	10.8	21.0	275.0	4572.	15000.
4641.	15227.	566.6	1183.4	718.8	.044873	1.3	34.3	-19.3	-2.7	19.9	10.8	21.0	272.0	4877.	16000.
4927.	16164.	545.5	1139.3	697.3	.043531	-.7	30.7	-21.5	-6.7	19.0	11.3	22.0	272.0	5182.	17000.
5213.	17103.	525.0	1096.5	676.4	.042226	-2.8	27.0	-23.7	-10.7	18.2	12.3	24.0	270.0	5486.	18000.
5498.	18038.	505.2	1055.1	655.9	.040947	-4.9	23.2	-26.0	-14.8	17.4	13.4	26.0	267.0	5791.	19000.
5785.	18979.	485.9	1014.8	636.6	.039742	-7.2	19.0	-27.9	-18.3	17.4	14.4	28.0	268.0	6096.	20000.
6072.	19920.	467.2	975.8	617.9	.038574	-9.7	14.5	-29.8	-21.6	17.8	15.4	30.0	268.0	6401.	21000.
6360.	20865.	449.0	937.8	599.7	.037438	-12.3	9.9	-31.6	-24.9	18.3	18.0	35.0	268.0	6706.	22000.
6647.	21809.	431.4	901.0	581.9	.036327	-14.8	5.4	-33.5	-28.3	18.7	21.6	42.0	269.0	7010.	23000.
6936.	22757.	414.3	865.3	564.5	.035241	-17.4	.7	-35.5	-31.8	19.2	22.1	43.0	266.0	7315.	24000.
7224.	23702.	397.8	830.8	547.3	.034167	-19.9	-3.8	-37.4	-35.3	19.6	22.6	44.0	264.0	7620.	25000.
7515.	24655.	381.7	797.2	529.5	.033056	-21.9	-7.4	-38.9	-38.1	19.9	23.1	45.0	262.0	7925.	26000.
7804.	25604.	366.2	764.8	512.1	.031969	-24.0	-11.2	-40.5	-40.9	20.4	23.7	46.0	261.0	8230.	27000.
8094.	26554.	351.2	733.5	495.3	.030921	-26.0	-14.8	-42.1	-43.8	20.7	23.1	45.0	262.0	8534.	28000.
8383.	27504.	336.7	703.2	478.9	.029897	-28.1	-18.6	-43.7	-46.7	21.1	21.6	42.0	264.0	8839.	29000.
8672.	28453.	322.7	674.0	462.9	.028898	-30.2	-22.4	-45.4	-49.7	21.4	23.1	45.0	263.0	9144.	30000.
8963.	29407.	309.1	645.6	447.4	.027930	-32.3	-26.1	-47.1	-52.7	21.8	27.8	54.0	260.0	9449.	31000.
9254.	30360.	296.0	618.2	432.4	.026994	-34.6	-30.3	-48.8	-55.8	22.4	31.9	62.0	258.0	9754.	32000.
9545.	31316.	283.3	591.7	418.4	.026120	-37.1	-34.8	-50.7	-59.2	23.2	35.0	68.0	258.0	10058.	33000.
9835.	32268.	271.1	566.2	404.6	.025258	-39.6	-39.3	-52.8	-63.1	23.4	38.1	74.0	258.0	10363.	34000.
10126.	33222.	259.3	541.6	390.3	.024366	-41.6	-42.9	-57.8	-72.1	15.8	40.6	79.0	258.0	10668.	35000.
10417.	34178.	247.9	517.7	376.5	.023504	-43.7	-46.7	-63.5	-82.4	9.6	43.2	84.0	258.0	10973.	36000.
10712.	35143.	236.8	494.6	363.3	.022680	-45.9	-50.6	-65.4	-85.6	9.6	41.7	81.0	259.0	11278.	37000.
11003.	36100.	226.2	472.4	350.5	.021881	-48.2	-54.8	-67.2	-88.9	9.6	40.1	78.0	260.0	11582.	38000.
11295.	37060.	216.0	451.1	338.1	.021107	-50.5	-58.9	-69.0	-92.3	9.7	39.6	77.0	261.0	11887.	39000.
11593.	38036.	206.1	430.4	326.0	.020352	-52.8	-63.0	-70.9	-95.7	9.7	40.1	78.0	261.0	12192.	40000.
11893.	39018.	196.6	410.6	314.0	.019602	-54.9	-66.8	-72.7	-98.8	9.7	41.2	80.0	261.0	12497.	41000.
12197.	40015.	187.4	391.4	301.8	.018841	-56.7	-70.1	-74.1	-101.4	9.8	42.7	83.0	261.0	12802.	42000.
12502.	41016.	178.6	373.0	290.1	.018110	-58.5	-73.3	-75.6	-104.1	9.8	44.8	87.0	260.0	13106.	43000.
12807.	42018.	170.2	355.5	278.7	.017399	-60.3	-76.5	-77.1	-106.7	9.8	46.8	91.0	259.0	13411.	44000.
13120.	43046.	162.0	338.3	267.7	.016712	-62.2	-80.0	-78.6	-109.4	10.0	0.0	0.0	0.0	13716.	45000.
13433.	44072.	154.2	322.1	257.1	.016050	-64.0	-83.2	-80.1	-112.2	10.0	0.0	0.0	0.0	14021.	46000.
13749.	45110.	146.7	306.4	246.4	.015382	-65.6	-86.1	-81.4	-114.5	10.1	0.0	0.0	0.0	14326.	47000.
14064.	46142.	139.6	291.6	235.6	.014708	-66.7	-88.1	-82.3	-116.1	10.1	0.0	0.0	0.0	14630.	48000.
14385.	47196.	132.7	277.1	225.1	.014053	-67.6	-89.7	-83.1	-117.5	10.1	0.0	0.0	0.0	14935.	49000.
14704.	48241.	126.2	263.6	214.6	.013397	-68.2	-90.8	-83.6	-118.4	10.1	0.0	0.0	0.0	15240.	50000.

TABLE 4.–Continued

H, m	H, ft	p, mb	p, lb/ft^2	RHO, gm/m^3	RHO, lb/ft^3	T, °C	T, °F	D, °C	D, °F	RH, percent	V, m/sec	V, knots	THETA, deg	Z, m	Z, ft
MONTH 8 DAY 16 YEAR 76 HOUR OF RELEASE 1630Z															
717.	2353.	930.0	1942.3	1082.0	.067547	25.4	77.7	3.0	37.4	23.4	10.3	20.0	230.0	724.	2375.
897.	2944.	910.0	1900.6	1063.7	.066405	24.0	75.2	3.2	37.6	25.6	10.3	20.0	244.0	914.	3000.
1186.	3890.	878.7	1835.2	1034.9	.064607	21.7	71.1	3.3	37.9	29.8	10.8	21.0	263.0	1219.	4000.
1475.	4838.	848.2	1771.5	1006.6	.062840	19.4	66.9	2.9	37.3	33.5	10.8	21.0	269.0	1524.	5000.
1763.	5785.	818.6	1709.7	976.2	.060942	18.2	64.6	.5	32.9	30.3	12.3	24.0	269.0	1829.	6000.
2051.	6730.	789.9	1649.7	946.5	.059088	16.9	62.4	-2.0	28.4	27.4	13.9	27.0	271.0	2134.	7000.
2339.	7672.	762.1	1591.7	917.5	.057278	15.6	60.1	-4.7	23.6	24.3	14.9	29.0	273.0	2438.	8000.
2626.	8615.	735.1	1535.3	889.4	.055523	14.3	57.7	-7.5	18.4	21.3	14.4	28.0	271.0	2743.	9000.
2912.	9553.	709.0	1480.8	861.9	.053807	13.1	55.6	-10.6	12.9	18.1	14.4	28.0	268.0	3048.	10000.
3197.	10489.	683.7	1427.9	836.2	.052202	11.3	52.3	-12.8	8.9	17.1	14.4	28.0	267.0	3353.	11000.
3483.	11426.	659.1	1376.6	811.8	.050679	9.4	48.9	-14.5	6.0	16.9	14.4	28.0	266.0	3658.	12000.
3769.	12365.	635.2	1326.6	788.0	.049193	7.4	45.3	-16.1	3.0	16.9	13.9	27.0	265.0	3962.	13000.
4054.	13299.	612.1	1278.4	764.7	.047739	5.5	41.9	-17.8	-.1	16.7	13.9	27.0	264.0	4267.	14000.
4340.	14238.	589.6	1231.4	742.0	.046322	3.5	38.3	-19.5	-3.1	16.7	13.9	27.0	265.0	4572.	15000.
4625.	15175.	567.8	1185.9	719.9	.044942	1.5	34.7	-21.2	-6.2	16.6	14.4	28.0	267.0	4877.	16000.
4910.	16110.	546.7	1141.8	698.3	.043593	-.4	31.3	-22.9	-9.3	16.4	15.4	30.0	269.0	5182.	17000.
5196.	17047.	526.2	1099.0	677.2	.042276	-2.5	27.5	-24.7	-12.4	16.4	15.9	31.0	268.0	5486.	18000.
5482.	17985.	506.3	1057.4	656.6	.040990	-4.5	23.9	-26.4	-15.5	16.2	17.0	33.0	266.0	5791.	19000.
5768.	18924.	487.0	1017.1	636.8	.039754	-6.7	19.9	-28.4	-19.0	16.0	15.9	31.0	266.0	6096.	20000.
6054.	19863.	468.3	978.1	617.6	.038556	-9.0	15.8	-30.4	-22.8	15.8	17.0	33.0	268.0	6401.	21000.
6340.	20802.	450.2	940.3	598.8	.037382	-11.2	11.8	-32.5	-26.5	15.4	17.5	34.0	268.0	6706.	22000.
6628.	21744.	432.6	903.5	580.6	.036246	-13.5	7.7	-34.6	-30.3	15.1	18.0	35.0	267.0	7010.	23000.
6914.	22684.	415.6	868.0	562.7	.035128	-15.8	3.6	-36.7	-34.1	14.8	19.5	38.0	265.0	7315.	24000.
7203.	23632.	399.0	833.3	545.3	.034042	-18.1	-.6	-38.8	-37.9	14.5	21.1	41.0	264.0	7620.	25000.
7491.	24577.	383.0	799.9	528.2	.032974	-20.4	-4.7	-40.6	-41.0	14.7	22.1	43.0	262.0	7925.	26000.
7779.	25523.	367.5	767.5	511.5	.031932	-22.7	-8.9	-42.4	-44.2	15.0	23.1	45.0	259.0	8230.	27000.
8066.	26464.	352.6	736.4	495.2	.030914	-25.1	-13.2	-44.2	-47.5	15.3	23.7	46.0	259.0	8534.	28000.
8357.	27417.	338.0	705.9	479.4	.029928	-27.4	-17.3	-46.0	-50.7	15.5	24.7	48.0	259.0	8839.	29000.
8645.	28363.	324.0	676.7	464.0	.028967	-29.8	-21.6	-47.8	-54.1	15.8	0.0	0.0	0.0	9144.	30000.
8935.	29315.	310.4	648.3	448.9	.028024	-32.1	-25.8	-49.7	-57.5	15.9	0.0	0.0	0.0	9449.	31000.

TABLE 4.-Continued

MONTH 8 DAY 16 YEAR 78 HOUR OF RELEASE 1500Z

H, m	H, ft	p, mb	p, lb/ft^2	RHO, gm/m^3	RHO, lb/ft^3	T, °C	T, °F	D, °C	D, °F	RH, percent	V, m/sec	V, knots	THETA, deg	Z, m	Z, ft
695.	2283.	932.4	1947.4	1125.0	.070231	15.0	59.0	-1.7	29.0	31.6	0.0	0.0	0.0	724.	2375.
882.	2893.	911.7	1904.1	1098.1	.068552	15.5	59.9	-2.7	27.1	28.4	3.1	6.0	20.0	914.	3000.
1178.	3865.	879.5	1836.9	1056.4	.065949	16.4	61.5	-4.7	23.5	23.1	8.2	16.0	51.0	1219.	4000.
1471.	4825.	848.6	1772.3	1016.9	.063483	17.1	62.8	-7.3	18.9	18.2	12.3	24.0	55.0	1524.	5000.
1763.	5785.	818.6	1709.7	988.0	.061679	15.1	59.2	-7.5	18.5	20.3	13.9	27.0	60.0	1829.	6000.
2054.	6740.	789.6	1649.1	959.7	.059912	13.0	55.4	-7.9	17.7	22.5	14.9	29.0	64.0	2134.	7000.
2346.	7696.	761.4	1590.2	932.2	.058195	11.0	51.8	-8.5	16.7	24.5	14.9	29.0	74.0	2438.	8000.
2639.	8657.	733.9	1532.8	905.3	.056516	8.9	48.0	-9.2	15.5	26.8	13.9	27.0	81.0	2743.	9000.
2931.	9615.	707.3	1477.2	879.0	.054874	6.8	44.2	-10.0	14.0	29.0	8.2	16.0	70.0	3048.	10000.
3222.	10571.	681.5	1423.3	849.0	.053001	6.2	43.2	-13.4	7.9	23.0	4.1	8.0	149.0	3353.	11000.
3512.	11523.	656.6	1371.3	818.4	.051091	6.2	43.2	-19.5	-3.1	13.8	6.7	13.0	232.0	3658.	12000.
3800.	12469.	632.6	1321.2	793.0	.049505	4.6	40.3	-22.4	-8.4	12.0	10.8	21.0	224.0	3962.	13000.
4089.	13415.	609.3	1272.5	769.2	.048020	2.7	36.9	-24.1	-11.4	11.8	11.3	22.0	261.0	4267.	14000.
4377.	14361.	586.7	1225.3	745.9	.046565	.8	33.4	-25.8	-14.5	11.6	11.8	23.0	273.0	4572.	15000.
4665.	15306.	564.8	1179.6	723.3	.045154	-1.1	30.0	-27.5	-17.6	11.4	11.8	23.0	271.0	4877.	16000.
4953.	16250.	543.6	1135.3	701.2	.043774	-3.0	26.6	-29.3	-20.7	11.1	11.8	23.0	271.0	5182.	17000.
5241.	17196.	523.0	1092.3	679.6	.042426	-5.0	23.0	-31.0	-23.8	11.0	12.9	25.0	268.0	5486.	18000.
5529.	18139.	503.1	1050.7	658.6	.041115	-7.0	19.4	-32.8	-27.0	10.8	13.4	26.0	273.0	5791.	19000.
5818.	19088.	483.7	1010.2	637.8	.039817	-8.9	16.0	-33.9	-29.0	11.3	13.9	27.0	273.0	6096.	20000.
6106.	20032.	465.0	971.2	617.4	.038543	-10.7	12.7	-34.9	-30.8	11.7	14.4	28.0	274.0	6401.	21000.
6394.	20976.	446.9	933.4	597.6	.037307	-12.6	9.3	-35.9	-32.7	12.3	18.0	35.0	271.0	6706.	22000.
6681.	21918.	429.4	896.8	578.4	.036108	-14.5	5.9	-37.0	-34.7	12.9	20.1	39.0	268.0	7010.	23000.
6969.	22864.	412.4	861.3	559.6	.034935	-16.3	2.7	-38.2	-36.7	13.3	21.6	42.0	267.0	7315.	24000.
7256.	23807.	396.0	827.1	541.5	.033805	-18.3	-.9	-39.4	-39.0	13.9	23.1	45.0	266.0	7620.	25000.
7544.	24752.	380.1	793.9	524.5	.032743	-20.6	-5.1	-41.0	-41.8	14.4	25.2	49.0	267.0	7925.	26000.
7833.	25698.	364.7	761.7	507.8	.031701	-22.8	-9.0	-42.6	-44.7	14.7	27.3	53.0	269.0	8230.	27000.
8119.	26638.	349.9	730.8	491.6	.030690	-25.1	-13.2	-44.2	-47.6	15.2	29.3	57.0	269.0	8534.	28000.
8408.	27584.	335.5	700.7	475.8	.029703	-27.4	-17.3	-45.9	-50.6	15.6	31.4	61.0	269.0	8839.	29000.
8698.	28536.	321.5	671.5	460.4	.028742	-29.7	-21.5	-47.6	-53.7	16.0	33.4	65.0	268.0	9144.	30000.
8987.	29486.	308.0	643.3	445.4	.027805	-32.1	-25.8	-49.3	-56.8	16.6	35.0	68.0	266.0	9449.	31000.
9276.	30434.	295.0	616.1	430.4	.026869	-34.3	-29.7	-51.0	-59.8	16.9	36.5	71.0	264.0	9754.	32000.
9566.	31385.	282.4	589.8	415.4	.025933	-36.2	-33.2	-52.6	-62.7	17.0	36.5	71.0	262.0	10058.	33000.
9857.	32339.	270.2	564.3	400.9	.025027	-38.2	-36.8	-55.5	-67.9	14.7	36.5	71.0	260.0	10363.	34000.
10146.	33288.	258.5	539.9	386.8	.024147	-40.2	-40.4	-59.0	-74.2	11.8	36.5	71.0	259.0	10668.	35000.
10435.	34237.	247.2	516.3	373.3	.023304	-42.3	-44.1	-62.4	-80.4	9.5	36.5	71.0	258.0	10973.	36000.
10725.	35188.	236.3	493.5	360.7	.022518	-44.8	-48.6	-64.4	-84.0	9.6	36.5	71.0	257.0	11278.	37000.
11017.	36146.	225.7	471.4	348.4	.021750	-47.3	-53.1	-66.5	-87.6	9.6	36.0	70.0	257.0	11582.	38000.
11311.	37108.	215.5	450.1	336.5	.021007	-49.9	-57.8	-68.5	-91.3	9.7	37.0	72.0	257.0	11887.	39000.
11606.	38077.	205.7	429.6	324.8	.020277	-52.4	-62.3	-70.6	-95.1	9.7	38.6	75.0	257.0	12192.	40000.
11905.	39061.	196.2	409.8	312.9	.019534	-54.5	-66.1	-72.3	-98.2	9.7	38.6	75.0	257.0	12497.	41000.
12207.	40049.	187.1	390.8	300.3	.018747	-56.0	-68.8	-73.5	-100.3	9.8	38.1	74.0	257.0	12802.	42000.
12512.	41051.	178.3	372.4	288.2	.017992	-57.4	-71.3	-74.7	-102.4	9.8	37.6	73.0	258.0	13106.	43000.
12818.	42055.	169.9	354.8	276.5	.017261	-58.9	-74.0	-75.9	-104.6	9.9	36.5	71.0	259.0	13411.	44000.
13124.	43058.	161.9	338.1	265.2	.016556	-60.3	-76.5	-77.1	-106.7	9.9	35.5	69.0	259.0	13716.	45000.
13433.	44072.	154.2	322.1	254.3	.015875	-61.8	-79.2	-78.3	-108.9	9.9	34.0	66.0	260.0	14021.	46000.
13745.	45096.	146.8	306.6	243.3	.015189	-62.9	-81.2	-79.2	-110.6	9.9	31.4	61.0	260.0	14326.	47000.
14059.	46127.	139.7	291.8	232.3	.014502	-63.6	-82.5	-79.7	-111.5	10.0	29.3	57.0	261.0	14630.	48000.
14376.	47165.	132.9	277.6	221.8	.013847	-64.2	-83.6	-80.3	-112.5	10.0	26.8	52.0	263.0	14935.	49000.
14689.	48192.	126.5	264.2	211.7	.013216	-64.9	-84.8	-80.8	-113.4	10.1	23.7	46.0	266.0	15240.	50000.

TABLE 4.–Continued

H, m	H, ft	p, mb	p, lb/ft²	RHO, gm/m³	RHO, lb/ft³	T, °C	T, °F	D, °C	D, °F	RH, percent	V, m/sec	V, knots	THETA, deg	Z, m	Z, ft

MONTH 8 DAY 18 YEAR 78 HOUR OF RELEASE 2200Z

H, m	H, ft	p, mb	p, lb/ft²	RHO, gm/m³	RHO, lb/ft³	T, °C	T, °F	D, °C	D, °F	RH, percent	V, m/sec	V, knots	THETA, deg	Z, m	Z, ft
711.	2333.	930.7	1943.8	1062.4	.066323	31.3	88.3	1.2	34.1	14.6	5.1	10.0	60.0	724.	2375.
885.	2905.	911.3	1903.3	1019.5	.063645	36.6	97.9	11.2	52.2	21.7	5.1	10.0	77.0	914.	3000.
1154.	3786.	892.1	1842.3	953.5	.059525	44.9	112.6	24.7	76.5	32.6	4.6	9.0	105.0	1219.	4000.
1412.	4633.	854.7	1785.1	888.6	.055473	52.8	127.0	36.6	97.9	43.4	5.7	11.0	106.0	1524.	5000.
1664.	5459.	828.7	1730.8	855.5	.053407	53.7	128.7	38.6	101.9	46.9	7.2	14.0	114.0	1829.	6000.
1913.	6275.	803.6	1678.4	830.0	.051815	53.1	127.6	39.0	102.2	48.7	7.7	15.0	99.0	2134.	7000.
2161.	7089.	779.2	1627.4	805.3	.050273	52.5	126.5	39.1	102.5	50.5	8.7	17.0	89.0	2438.	8000.
2409.	7900.	755.5	1577.9	781.3	.048775	51.8	125.2	39.3	102.7	52.6	8.7	17.0	82.0	2743.	9000.
2653.	8703.	732.6	1530.1	758.0	.047320	51.2	124.2	39.4	102.8	54.4	7.7	15.0	76.0	3048.	10000.
2897.	9505.	710.3	1483.5	735.4	.045910	50.6	123.1	39.4	103.0	56.3	4.1	8.0	101.0	3353.	11000.
3139.	10298.	688.8	1438.6	698.4	.043600	54.0	129.2	43.2	109.7	58.2	4.1	8.0	217.0	3658.	12000.
3370.	11057.	668.7	1396.6	650.8	.040628	60.4	140.7	49.6	121.3	59.6	7.2	14.0	240.0	3962.	13000.
3595.	11796.	649.6	1356.7	630.5	.039361	60.3	140.5	49.8	121.6	60.5	7.7	15.0	244.0	4267.	14000.
3819.	12529.	631.1	1318.1	610.9	.038137	60.2	140.4	50.0	122.0	61.4	7.7	15.0	246.0	4572.	15000.
4040.	13254.	613.2	1280.7	591.9	.036951	60.1	140.2	50.2	122.3	62.3	7.7	15.0	252.0	4877.	16000.
4259.	13972.	595.9	1244.6	573.5	.035802	60.0	140.0	50.4	122.7	63.1	8.2	16.0	257.0	5182.	17000.
4476.	14686.	579.1	1209.5	555.6	.034685	59.9	139.8	50.6	123.0	64.0	8.7	17.0	260.0	5486.	18000.
4692.	15394.	562.8	1175.4	538.3	.033605	59.8	139.6	50.7	123.3	64.9	9.8	19.0	263.0	5791.	19000.
4906.	16097.	547.0	1142.4	521.5	.032556	59.8	139.6	50.9	123.6	65.4	10.3	20.0	266.0	6096.	20000.
5117.	16788.	531.8	1110.7	505.2	.031539	59.7	139.5	51.1	124.0	66.3	11.3	22.0	267.0	6401.	21000.
5327.	17477.	517.0	1079.8	489.4	.030552	59.6	139.3	51.3	124.3	67.1	59.2	115.0	263.0	6706.	22000.
5535.	18163.	502.6	1049.7	474.1	.029597	59.5	139.1	51.4	124.6	68.0	214.0	416.0	248.0	7010.	23000.
5743.	18841.	488.7	1020.7	458.6	.028629	59.6	139.3	51.7	125.1	68.6	145.6	283.0	254.0	7315.	24000.
5948.	19513.	475.2	992.5	443.6	.027693	59.7	139.5	52.0	125.6	69.3	15.4	30.0	265.0	7620.	25000.
6149.	20171.	462.3	965.5	429.1	.026788	59.8	139.6	52.3	126.1	70.0	17.5	34.0	262.0	7925.	26000.
6349.	20828.	449.7	939.2	415.0	.025908	59.9	139.8	52.6	126.7	70.7	53.0	103.0	311.0	8230.	27000.
6545.	21473.	437.6	913.9	401.4	.025059	60.0	140.0	52.9	127.2	71.4	102.4	199.0	22.0	8534.	28000.
6739.	22111.	425.9	889.5	388.2	.024235	60.1	140.2	53.2	127.7	72.1	111.1	216.0	33.0	8839.	29000.
6933.	22746.	414.5	865.7	375.4	.023435	60.2	140.4	53.5	128.2	72.8	78.2	152.0	341.0	9144.	30000.
7124.	23372.	403.5	842.7	363.0	.022661	60.4	140.7	53.8	128.8	73.1	45.3	88.0	288.0	9449.	31000.
7312.	23989.	392.9	820.6	351.9	.021968	60.2	140.4	53.8	128.8	73.9	28.3	55.0	261.0	9754.	32000.
7500.	24607.	382.5	798.9	341.8	.021338	59.9	139.8	53.7	128.6	74.5	30.4	59.0	261.0	10058.	33000.
7695.	25215.	372.5	778.0	331.9	.020720	59.6	139.3	53.6	128.4	75.2	31.9	62.0	262.0	10363.	34000.
7869.	25817.	362.8	757.7	322.3	.020121	59.3	138.7	53.5	128.2	75.8	0.0	0.0	0.0	10668.	35000.
8051.	26413.	353.4	738.1	312.9	.019534	59.0	138.2	53.4	128.0	76.5	0.0	0.0	0.0	10973.	36000.
8232.	27008.	344.2	718.9	303.9	.018972	58.7	137.7	53.2	127.8	77.1	0.0	0.0	0.0	11278.	37000.
8412.	27597.	335.3	700.3	295.1	.018422	58.5	137.3	53.1	127.6	77.5	0.0	0.0	0.0	11582.	38000.
8591.	28185.	326.6	682.1	286.6	.017892	58.2	136.8	53.0	127.4	78.1	0.0	0.0	0.0	11887.	39000.
8768.	28765.	318.2	664.6	278.3	.017374	57.9	136.2	52.9	127.2	78.8	0.0	0.0	0.0	12192.	40000.

TABLE 4.–Continued

MONTH 8 DAY 23 YEAR 78 HOUR OF RELEASE 900Z

H, m	H, ft	p, mb	p, lb/ft^2	RHO, gm/m^3	RHO, lb/ft^3	T, °C	T, °F	D, °C	D, °F	RH, percent	V, m/sec	V, knots	THETA, deg	Z, m	Z, ft
730.	2394.	928.6	1939.4	1114.1	.069551	15.9	60.6	9.2	48.5	64.3	7.2	14.0	240.0	724.	2375.
915.	3000.	908.1	1896.6	1082.8	.067597	17.6	63.7	9.4	48.8	58.4	8.7	17.0	244.0	914.	3000.
1206.	3957.	876.5	1830.6	1043.4	.065137	18.2	64.8	7.4	45.3	49.3	11.3	22.0	250.0	1219.	4000.
1499.	4917.	845.7	1766.3	1016.8	.063477	15.7	60.3	2.1	35.8	39.9	12.3	24.0	254.0	1524.	5000.
1790.	5873.	815.9	1704.0	976.8	.060980	17.3	63.1	-4.3	24.2	22.5	13.4	26.0	258.0	1829.	6000.
2079.	6820.	787.2	1644.1	948.6	.059219	15.4	59.7	-5.6	21.9	23.0	13.9	27.0	257.0	2134.	7000.
2368.	7769.	759.3	1585.8	921.0	.057496	13.6	56.5	-6.9	19.5	23.3	13.9	27.0	254.0	2438.	8000.
2657.	8717.	732.2	1529.2	894.1	.055817	11.7	53.1	-8.3	17.1	23.8	13.4	26.0	252.0	2743.	9000.
2946.	9666.	705.9	1474.3	867.8	.054175	9.8	49.6	-9.7	14.6	24.3	13.4	26.0	250.0	3048.	10000.
3235.	10613.	680.4	1421.0	842.7	.052608	7.8	46.0	-11.0	12.2	25.0	13.9	27.0	249.0	3353.	11000.
3524.	11562.	655.6	1369.2	818.3	.051085	5.6	42.1	-12.4	9.7	26.0	13.9	27.0	246.0	3658.	12000.
3813.	12509.	631.6	1319.1	794.5	.049599	3.5	38.3	-13.8	7.1	26.6	14.4	28.0	242.0	3962.	13000.
4103.	13460.	608.2	1270.3	771.2	.048144	1.3	34.3	-15.3	4.5	27.8	13.9	27.0	236.0	4267.	14000.
4391.	14408.	585.6	1223.1	748.5	.046727	-.8	30.6	-16.8	1.8	28.6	13.4	26.0	234.0	4572.	15000.
4681.	15359.	563.6	1177.1	726.4	.045348	-3.0	26.6	-18.3	-1.0	29.5	13.4	26.0	234.0	4877.	16000.
4971.	16309.	542.3	1132.6	704.7	.043993	-5.2	22.6	-19.9	-3.8	30.4	14.4	28.0	235.0	5182.	17000.
5261.	17261.	521.6	1089.4	683.6	.042676	-7.4	18.7	-21.5	-6.8	31.3	15.4	30.0	235.0	5486.	18000.
5552.	18216.	501.5	1047.4	663.0	.041390	-9.7	14.5	-23.2	-9.7	32.4	16.5	32.0	229.0	5791.	19000.
5844.	19173.	482.0	1006.7	642.2	.040091	-11.7	10.9	-24.9	-12.9	32.5	17.0	33.0	226.0	6096.	20000.
6135.	20130.	463.1	967.2	622.0	.038830	-13.8	7.2	-26.7	-16.0	32.9	17.5	34.0	230.0	6401.	21000.
6426.	21082.	444.9	929.2	602.4	.037607	-15.8	3.6	-28.4	-19.2	32.9	18.0	35.0	246.0	6706.	22000.
6719.	22039.	427.2	892.2	583.2	.036408	-17.9	-.2	-30.2	-22.4	33.2	19.0	37.0	263.0	7010.	23000.
7009.	22995.	410.1	856.5	564.5	.035241	-20.0	-4.0	-32.0	-25.7	33.4	19.5	38.0	251.0	7315.	24000.
7299.	23948.	393.6	822.1	546.4	.034111	-22.2	-8.0	-34.0	-29.1	33.6	23.7	46.0	259.0	7620.	25000.
7590.	24903.	377.6	788.6	528.8	.033012	-24.4	-11.9	-36.1	-33.0	33.1	26.2	51.0	260.0	7925.	26000.
7882.	25860.	362.1	756.3	511.7	.031944	-26.6	-15.9	-38.2	-36.8	32.6	26.8	56.0	255.0	8230.	27000.
8174.	26819.	347.1	724.9	495.1	.030908	-28.8	-19.8	-40.4	-40.7	32.0	30.4	59.0	255.0	8534.	28000.
8467.	27778.	332.6	694.6	478.9	.029897	-31.1	-24.0	-42.5	-44.6	31.7	31.9	62.0	258.0	8839.	29000.
8761.	28744.	318.5	665.2	463.1	.028910	-33.4	-28.1	-44.7	-48.5	31.3	33.4	65.0	259.0	9144.	30000.
9053.	29702.	305.0	637.0	447.7	.027949	-35.7	-32.3	-46.9	-52.5	30.8	34.0	66.0	256.0	9449.	31000.
9347.	30665.	291.9	609.6	432.6	.027006	-38.0	-36.4	-50.0	-58.0	27.5	34.0	66.0	254.0	9754.	32000.
9641.	31632.	279.2	583.1	418.0	.026095	-40.4	-40.7	-53.9	-64.9	22.5	34.5	67.0	251.0	10058.	33000.
9935.	32595.	267.0	557.6	403.8	.025208	-42.7	-44.9	-58.1	-72.5	17.2	34.5	67.0	248.0	10363.	34000.
10232.	33570.	255.1	532.8	390.0	.024347	-45.1	-49.2	-63.0	-81.3	12.0	34.5	67.0	245.0	10668.	35000.
10527.	34539.	243.7	509.0	376.2	.023485	-47.3	-53.1	-66.5	-87.6	9.6	34.0	66.0	244.0	10973.	36000.
10823.	35509.	232.7	486.0	362.6	.022636	-49.4	-56.9	-68.2	-90.7	9.7	34.0	66.0	242.0	11278.	37000.
11116.	36471.	222.2	464.1	349.4	.021812	-51.5	-60.7	-69.9	-93.7	9.7	34.0	66.0	241.0	11582.	38000.
11414.	37449.	212.0	442.8	336.5	.021007	-53.6	-64.5	-71.6	-96.8	9.7	34.0	66.0	239.0	11887.	39000.
11719.	38444.	202.1	422.1	324.1	.020233	-55.8	-68.4	-73.3	-100.0	9.6	34.5	67.0	238.0	12192.	40000.
12020.	39435.	192.7	402.5	311.6	.019453	-57.6	-71.7	-74.8	-102.7	9.8	33.4	65.0	240.0	12497.	41000.
12327.	40442.	183.6	383.5	299.3	.018685	-59.4	-74.9	-76.3	-105.3	9.9	32.4	63.0	242.0	12802.	42000.
12634.	41452.	174.9	365.3	287.5	.017948	-61.2	-78.2	-77.8	-108.0	10.0	31.4	61.0	244.0	13106.	43000.
12947.	42476.	166.5	347.7	275.1	.017174	-62.2	-80.0	-78.6	-109.5	9.9	30.9	60.0	246.0	13411.	44000.
13259.	43500.	158.5	331.0	261.2	.016306	-61.6	-78.9	-78.1	-108.6	9.9	29.8	58.0	247.0	13716.	45000.
13570.	44522.	150.9	315.2	248.0	.015482	-61.0	-77.8	-77.6	-107.7	9.9	29.3	57.0	249.0	14021.	46000.
13880.	45540.	143.7	300.1	236.4	.014758	-61.2	-78.2	-77.8	-108.0	10.0	27.8	54.0	249.0	14326.	47000.
14193.	46548.	136.9	285.9	225.4	.014071	-61.4	-78.5	-78.0	-108.4	9.9	25.7	50.0	250.0	14630.	48000.
14501.	47576.	130.3	272.1	214.9	.013416	-61.7	-79.1	-78.2	-108.8	9.9	24.2	47.0	250.0	14935.	49000.
14810.	48591.	124.1	259.2	204.8	.012785	-62.0	-79.6	-78.4	-109.2	10.0	22.1	43.0	249.0	15240.	50000.

TABLE 4.–Continued

H, m	H, ft	p, mb	p, lb/ft^2	RHO, gm/m^3	RHO, lb/ft^3	T, °C	T, °F	D, °C	D, °F	RH, percent	V, m/sec	V, knots	THETA, deg	Z, m	Z, ft
							MONTH 6 DAY 24 YEAR 76 HOUR OF RELEASE 900Z								
709.	2324.	931.0	1944.4	1122.4	.070069	15.1	59.2	.0	32.0	35.6	4.1	8.0	205.0	724.	2375.
894.	2932.	910.4	1901.4	1086.4	.067822	17.8	64.0	3.9	38.9	39.5	7.2	14.0	229.0	914.	3000.
1186.	3893.	878.6	1835.0	1048.4	.065449	17.9	64.2	2.8	37.0	36.4	11.3	22.0	257.0	1219.	4000.
1478.	4850.	847.8	1770.7	1016.6	.063464	16.6	61.9	-.5	31.1	31.1	11.3	22.0	246.0	1524.	5000.
1770.	5808.	817.9	1708.2	986.4	.061579	15.1	59.2	-2.7	27.2	29.2	11.3	22.0	243.0	1829.	6000.
2061.	6763.	789.9	1647.7	956.8	.059731	13.5	56.3	-4.9	23.2	27.4	10.3	20.0	249.0	2134.	7000.
2352.	7717.	760.8	1589.0	928.1	.057939	12.0	53.6	-7.2	19.1	25.5	8.7	17.0	258.0	2438.	8000.
2643.	8671.	733.5	1531.9	900.0	.056185	10.4	50.7	-9.5	15.0	23.7	8.2	16.0	260.0	2743.	9000.
2933.	9622.	707.1	1476.8	872.6	.054475	8.8	47.8	-11.8	10.7	21.8	7.7	15.0	254.0	3048.	10000.
3223.	10575.	681.4	1423.1	845.8	.052802	7.2	45.0	-13.5	7.7	21.3	7.7	15.0	244.0	3353.	11000.
3512.	11523.	656.6	1371.3	819.6	.051166	5.7	42.3	-14.9	5.2	21.1	7.7	15.0	236.0	3658.	12000.
3802.	12473.	632.5	1321.0	791.6	.049418	4.9	40.8	-15.9	3.4	20.5	7.7	15.0	233.0	3962.	13000.
4089.	13415.	609.3	1272.5	766.3	.047839	3.6	38.5	-17.1	1.2	20.3	7.2	14.0	232.0	4267.	14000.
4376.	14357.	586.8	1225.6	745.3	.046528	.9	33.6	-18.9	-2.0	21.1	6.7	13.0	230.0	4572.	15000.
4664.	15302.	564.9	1179.8	724.7	.045242	-1.7	28.9	-20.7	-5.3	21.8	6.7	13.0	227.0	4877.	16000.
4953.	16250.	543.6	1135.3	704.5	.043980	-4.4	24.1	-22.7	-8.8	22.6	6.7	13.0	229.0	5182.	17000.
5243.	17201.	522.9	1092.1	684.8	.042751	-7.2	19.0	-24.6	-12.3	23.5	7.7	15.0	236.0	5486.	18000.
5535.	18158.	502.7	1049.9	665.5	.041546	-10.0	14.0	-26.6	-15.9	24.3	9.3	18.0	243.0	5791.	19000.
5826.	19113.	483.2	1009.2	644.5	.040235	-12.0	10.4	-28.4	-19.2	24.1	11.3	22.0	248.0	6096.	20000.
6117.	20068.	464.3	969.7	623.8	.038943	-13.8	7.2	-30.2	-22.4	23.6	11.3	22.0	250.0	6401.	21000.
6408.	21024.	446.0	931.5	603.6	.037682	-15.7	3.7	-32.0	-25.7	23.3	10.8	21.0	252.0	6706.	22000.
6699.	21979.	428.3	894.5	583.9	.036452	-17.6	.3	-33.8	-28.9	22.9	11.3	22.0	254.0	7010.	23000.
6990.	22932.	411.2	858.8	564.8	.035259	-19.5	-3.1	-35.7	-32.2	22.5	11.8	23.0	256.0	7315.	24000.
7281.	23889.	394.6	824.1	546.6	.034123	-21.6	-6.9	-37.6	-35.6	22.3	12.9	25.0	257.0	7620.	25000.
7572.	24842.	378.6	790.7	529.7	.033068	-24.1	-11.4	-39.7	-39.4	22.5	13.9	27.0	257.0	7925.	26000.
7865.	25804.	363.0	758.1	513.3	.032044	-26.7	-16.1	-41.8	-43.2	22.8	15.4	30.0	258.0	8230.	27000.
8157.	26761.	348.0	726.6	497.2	.031039	-29.2	-20.6	-43.9	-47.0	22.9	16.5	32.0	258.0	8534.	28000.
8450.	27725.	333.4	696.3	481.6	.030065	-31.9	-25.4	-46.1	-50.9	23.4	18.0	35.0	258.0	8839.	29000.
8744.	28688.	319.3	666.9	466.3	.029110	-34.5	-30.1	-48.3	-54.9	23.6	19.0	37.0	258.0	9144.	30000.
9040.	29659.	305.6	638.3	451.4	.028180	-37.2	-35.0	-50.5	-58.9	24.0	20.6	40.0	257.0	9449.	31000.
9335.	30627.	292.4	610.7	436.5	.027250	-39.7	-39.5	-53.4	-64.1	22.1	21.6	42.0	257.0	9754.	32000.
9632.	31601.	279.6	584.0	421.7	.026326	-42.1	-43.8	-56.9	-70.4	18.6	22.6	44.0	256.0	10058.	33000.
9928.	32571.	267.3	558.3	407.4	.025433	-44.5	-48.1	-60.7	-77.2	15.1	23.1	45.0	255.0	10363.	34000.
10224.	33545.	255.4	533.4	393.4	.024559	-46.9	-52.4	-64.9	-84.8	11.3	24.2	47.0	254.0	10668.	35000.
10522.	34521.	243.9	509.4	378.9	.023654	-48.8	-55.8	-67.7	-89.8	9.6	24.7	48.0	254.0	10973.	36000.
10820.	35500.	232.8	486.2	364.1	.022730	-50.2	-58.4	-68.8	-91.9	9.6	25.7	50.0	254.0	11278.	37000.
11116.	36471.	222.2	464.1	349.7	.021831	-51.7	-61.1	-70.0	-94.1	9.7	26.8	52.0	254.0	11582.	38000.
11414.	37449.	212.0	442.8	335.9	.020970	-53.2	-63.8	-71.2	-96.2	9.8	27.8	54.0	254.0	11887.	39000.
11715.	38434.	202.2	422.3	322.6	.020139	-54.6	-66.3	-72.4	-98.4	9.7	28.8	56.0	255.0	12192.	40000.
12017.	39424.	192.8	402.7	308.9	.019284	-55.6	-68.1	-73.2	-99.8	9.8	29.8	58.0	257.0	12497.	41000.
12320.	40419.	183.8	383.9	295.6	.018454	-56.4	-69.5	-73.9	-101.0	9.7	30.4	59.0	259.0	12802.	42000.
12624.	41416.	175.2	365.9	282.9	.017661	-57.3	-71.1	-74.6	-102.2	9.9	31.4	61.0	260.0	13106.	43000.
12928.	42413.	167.0	348.8	270.6	.016893	-58.1	-72.6	-75.2	-103.4	9.8	31.4	61.0	260.0	13411.	44000.
13235.	43421.	159.1	332.3	258.9	.016163	-58.9	-74.0	-75.9	-104.6	9.8	31.4	61.0	260.0	13716.	45000.
13541.	44426.	151.6	316.6	247.6	.015457	-59.8	-75.6	-76.6	-105.9	9.9	30.9	60.0	260.0	14021.	46000.
13850.	45438.	144.4	301.6	236.2	.014745	-60.1	-76.2	-76.9	-106.4	9.9	29.8	58.0	258.0	14326.	47000.
14160.	46457.	137.5	287.2	225.2	.014059	-60.3	-76.5	-77.1	-106.7	9.9	29.3	57.0	257.0	14630.	48000.
14467.	47465.	131.0	273.6	214.7	.013403	-60.5	-76.9	-77.2	-107.0	9.9	27.8	54.0	256.0	14935.	49000.
14780.	48490.	124.7	260.4	205.1	.012804	-61.2	-78.2	-77.8	-108.0	9.9	26.8	52.0	256.0	15240.	50000.

TABLE 4.-Continued

H, m	H, ft	p, mb	p, lb/ft^2	RHO, gm/m^3	RHO, lb/ft^3	T, °C	T, °F	D, °C	D, °F	RH, percent	V, m/sec	V, knots	THETA, deg	Z, m	Z, ft
MONTH 8 DAY 25 YEAR 78 HOUR OF RELEASE 9007															
707.	2318.	931.2	1944.9	1111.8	.069407	17.4	63.3	7.4	45.4	51.9	5.1	10.0	285.0	724.	2375.
891.	2923.	910.7	1902.0	1088.1	.067928	17.4	63.3	5.1	41.1	44.0	7.2	14.0	282.0	914.	3000.
1186.	3890.	878.7	1835.2	1051.2	.065624	17.3	63.1	.4	32.7	31.8	10.3	20.0	278.0	1219.	4000.
1477.	4847.	847.9	1770.9	1015.9	.063421	17.1	62.8	-5.8	21.5	20.3	10.3	20.0	266.0	1524.	5000.
1769.	5804.	818.0	1708.4	984.9	.061485	15.8	60.4	-7.3	18.8	19.6	8.7	17.0	266.0	1829.	6000.
2059.	6757.	789.1	1648.1	954.8	.059606	14.4	57.9	-8.9	16.0	19.1	7.7	15.0	265.0	2134.	7000.
2350.	7710.	761.0	1589.4	925.4	.057771	13.0	55.4	-10.4	13.2	18.5	6.7	13.0	275.0	2438.	8000.
2639.	8657.	733.9	1532.8	896.8	.055985	11.6	52.9	-12.0	10.5	17.9	5.7	11.0	281.0	2743.	9000.
2928.	9607.	707.5	1477.6	869.0	.054250	10.2	50.4	-13.5	7.6	17.3	5.1	10.0	287.0	3048.	10000.
3216.	10553.	682.0	1424.4	843.2	.052639	8.4	47.1	-15.3	4.5	16.9	4.6	9.0	293.0	3353.	11000.
3505.	11500.	657.2	1372.6	818.6	.051104	6.3	43.3	-17.1	1.2	16.8	4.1	8.0	293.0	3658.	12000.
3794.	12449.	633.1	1322.3	794.5	.049599	4.3	39.7	-18.9	-2.1	16.6	3.6	7.0	288.0	3962.	13000.
4083.	13394.	609.8	1273.6	771.1	.048138	2.2	36.0	-20.8	-5.4	16.4	3.6	7.0	280.0	4267.	14000.
4372.	14344.	587.1	1226.2	748.1	.046702	.1	32.2	-22.6	-8.7	16.2	4.1	8.0	278.0	4572.	15000.
4660.	15289.	565.2	1180.4	725.8	.045310	-1.9	28.6	-24.5	-12.1	15.9	4.1	8.0	283.0	4877.	16000.
4950.	16241.	543.8	1135.7	704.0	.043949	-4.0	24.8	-26.4	-15.5	15.7	4.6	9.0	286.0	5182.	17000.
5239.	17187.	523.2	1092.7	682.7	.042620	-6.1	21.0	-28.3	-18.9	15.4	6.2	12.0	287.0	5486.	18000.
5529.	18139.	503.1	1050.7	661.9	.041321	-8.3	17.1	-30.2	-22.3	15.3	8.2	16.0	285.0	5791.	19000.
5820.	19093.	483.6	1010.0	641.7	.040060	-10.5	13.1	-32.0	-25.5	15.3	10.8	21.0	279.0	6096.	20000.
6109.	20043.	464.8	970.8	622.1	.038836	-12.8	9.0	-33.8	-28.8	15.5	12.3	24.0	275.0	6401.	21000.
6398.	20992.	446.6	932.7	603.0	.037644	-15.1	4.8	-35.6	-32.0	15.7	13.4	26.0	271.0	6706.	22000.
6689.	21946.	428.9	895.8	584.4	.036483	-17.4	.7	-37.4	-35.3	15.8	14.4	28.0	271.0	7010.	23000.
6981.	22904.	411.7	859.9	566.2	.035347	-19.7	-3.5	-39.2	-38.6	15.9	15.9	31.0	272.0	7315.	24000.
7272.	23860.	395.1	825.2	548.4	.034235	-22.1	-7.8	-41.1	-42.0	16.2	17.5	34.0	273.0	7620.	25000.
7565.	24818.	379.0	791.6	531.0	.033149	-24.4	-11.9	-42.9	-45.2	16.5	18.0	35.0	273.0	7925.	26000.
7855.	25773.	363.5	759.2	514.0	.032088	-26.7	-16.1	-44.7	-48.4	16.7	18.5	36.0	273.0	8230.	27000.
8149.	26735.	348.4	727.6	497.5	.031058	-29.1	-20.4	-46.5	-51.8	17.1	18.5	36.0	272.0	8534.	28000.
8442.	27698.	333.6	697.2	481.4	.030053	-31.4	-24.5	-48.4	-55.1	17.2	19.0	37.0	273.0	8839.	29000.
8735.	28661.	319.7	667.7	465.7	.029073	-33.8	-28.8	-50.3	-58.5	17.5	19.5	38.0	273.0	9144.	30000.
9029.	29623.	306.1	639.3	450.4	.028118	-36.3	-33.3	-52.2	-62.0	17.9	19.5	38.0	273.0	9449.	31000.
9324.	30590.	292.9	611.7	435.4	.027181	-38.7	-37.7	-54.8	-66.6	16.9	20.1	39.0	274.0	9754.	32000.
9620.	31562.	280.1	585.0	420.9	.026276	-41.2	-42.2	-57.9	-72.3	14.9	21.1	41.0	276.0	10058.	33000.
9915.	32531.	267.8	559.3	406.8	.025396	-43.7	-46.7	-61.2	-78.2	12.9	22.1	43.0	279.0	10363.	34000.
10212.	33503.	255.9	534.5	393.0	.024534	-46.2	-51.2	-64.7	-84.5	10.7	23.7	46.0	281.0	10668.	35000.
10509.	34478.	244.4	510.4	378.9	.023654	-48.3	-54.9	-67.3	-89.1	9.6	25.2	49.0	282.0	10973.	36000.
10807.	35455.	233.3	487.3	364.6	.022761	-50.1	-58.2	-68.7	-91.7	9.7	26.2	51.0	284.0	11278.	37000.
11102.	36425.	222.7	465.1	350.8	.021900	-51.8	-61.2	-70.1	-94.2	9.7	26.8	52.0	285.0	11582.	38000.
11400.	37400.	212.5	443.8	337.3	.021057	-53.6	-64.5	-71.6	-96.8	9.7	27.3	53.0	286.0	11887.	39000.
11702.	38393.	202.6	423.1	324.4	.020252	-55.4	-67.7	-73.0	-99.5	9.8	27.3	53.0	286.0	12192.	40000.
12003.	39381.	193.2	403.5	310.5	.019384	-56.3	-69.3	-73.8	-100.8	9.8	27.3	53.0	285.0	12497.	41000.
12309.	40385.	184.1	384.5	296.7	.018522	-56.8	-70.2	-74.2	-101.6	9.8	26.2	51.0	283.0	12802.	42000.
12613.	41380.	175.5	366.5	283.6	.017705	-57.4	-71.3	-74.7	-102.4	9.8	25.2	49.0	281.0	13106.	43000.
12916.	42376.	167.3	349.4	271.0	.016918	-58.0	-72.4	-75.1	-103.2	9.9	23.7	46.0	279.0	13411.	44000.
13223.	43382.	159.4	332.9	258.9	.016163	-58.5	-73.3	-75.6	-104.1	9.8	22.6	44.0	276.0	13716.	45000.
13529.	44385.	151.9	317.2	247.3	.015438	-59.1	-74.4	-76.1	-104.9	9.9	21.1	41.0	273.0	14021.	46000.
13835.	45395.	144.7	302.2	236.6	.014770	-60.0	-76.0	-76.8	-106.3	9.8	19.0	37.0	267.0	14326.	47000.
14146.	46412.	137.8	287.8	226.6	.014146	-61.2	-78.2	-77.8	-108.0	10.0	15.9	31.0	260.0	14630.	48000.
14459.	47433.	131.2	274.0	216.9	.013541	-62.3	-80.1	-78.7	-109.6	10.0	13.4	26.0	252.0	14935.	49000.
14779.	48457.	124.9	260.9	207.5	.012954	-63.4	-82.1	-79.6	-111.2	10.0	14.4	28.0	253.0	15240.	50000.

TABLE 4.–Continued

H, m	H, ft	P, mb	P, lb/ft^2	RHO, gm/m^3	RHO, lb/ft^3	T, °C	T, °F	D, °C	D, °F	RH, percent	V, m/sec	V, knots	THETA, deg	Z, m	Z, ft
MONTH 9 DAY 1 YEAR 78 HOUR OF RELEASE 900Z															
743.	2438.	927.1	1936.3	1105.0	.068983	18.1	64.6	6.2	43.2	45.7	3.1	6.0	235.0	724.	2375.
925.	3036.	906.9	1894.1	1065.0	.066486	22.3	72.1	7.2	44.9	37.6	4.6	9.0	241.0	914.	3000.
1214.	3982.	875.7	1828.9	1024.5	.063957	23.6	74.5	4.2	39.5	28.2	6.7	13.0	249.0	1219.	4000.
1500.	4920.	845.6	1766.1	992.5	.061960	22.9	73.2	-.3	31.4	21.3	5.1	10.0	223.0	1524.	5000.
1785.	5856.	816.4	1705.1	965.7	.060287	20.7	69.3	-1.3	29.7	22.8	7.2	14.0	203.0	1829.	6000.
2071.	6794.	788.0	1645.8	939.4	.058645	18.4	65.1	-2.3	27.8	24.3	10.3	20.0	208.0	2134.	7000.
2356.	7731.	760.4	1588.1	913.7	.057040	16.1	61.0	-3.4	25.8	25.9	12.9	25.0	214.0	2438.	8000.
2643.	8671.	733.5	1531.9	888.6	.055473	13.8	56.8	-4.6	23.6	27.4	14.4	28.0	211.0	2743.	9000.
2931.	9615.	707.3	1477.2	864.0	.053938	11.5	52.7	-5.9	21.3	29.0	15.9	31.0	205.0	3048.	10000.
3218.	10556.	681.9	1424.2	838.7	.052358	9.6	49.3	-8.0	17.7	28.1	15.4	30.0	200.0	3353.	11000.
3504.	11496.	657.3	1372.8	813.5	.050785	7.9	46.2	-10.3	13.4	26.2	13.4	26.0	197.0	3658.	12000.
3791.	12437.	633.4	1322.9	788.9	.049249	6.2	43.2	-12.7	9.1	24.3	9.8	19.0	196.0	3962.	13000.
4077.	13378.	610.2	1274.4	764.9	.047751	4.5	40.1	-15.2	4.6	22.3	7.2	14.0	199.0	4267.	14000.
4364.	14318.	587.7	1227.4	741.5	.046290	2.7	36.9	-17.8	.0	20.4	4.6	9.0	202.0	4572.	15000.
4651.	15258.	565.9	1181.9	719.5	.044917	.7	33.3	-20.0	-3.9	19.6	2.6	5.0	201.0	4877.	16000.
4936.	16196.	544.8	1137.8	698.8	.043625	-1.6	29.1	-21.7	-7.1	19.9	2.6	5.0	204.0	5182.	17000.
5223.	17135.	524.3	1095.0	678.6	.042364	-4.1	24.6	-23.5	-10.3	20.5	3.1	6.0	207.0	5486.	18000.
5511.	18081.	504.3	1053.3	658.9	.041134	-6.5	20.3	-25.3	-13.5	20.9	3.1	6.0	212.0	5791.	19000.
5798.	19023.	485.0	1012.9	639.6	.039929	-9.0	15.8	-27.2	-17.0	21.3	3.1	6.0	217.0	6096.	20000.
6087.	19971.	466.2	973.7	620.7	.038749	-11.5	11.3	-29.2	-20.5	21.7	1.5	3.0	241.0	6401.	21000.
6376.	20918.	448.0	935.7	602.3	.037600	-14.0	6.8	-31.2	-24.1	22.0	1.5	3.0	289.0	6706.	22000.
6666.	21869.	430.3	898.7	584.3	.036477	-16.6	2.1	-33.2	-27.7	22.4	2.6	5.0	327.0	7010.	23000.
6957.	22825.	413.1	862.8	566.7	.035378	-19.1	-2.4	-35.2	-31.4	22.7	2.6	5.0	334.0	7315.	24000.
7247.	23778.	396.5	828.1	549.5	.034304	-21.7	-7.1	-37.3	-35.2	23.0	3.1	6.0	341.0	7620.	25000.
7539.	24733.	380.4	794.5	532.4	.033237	-24.2	-11.6	-39.4	-39.0	23.2	4.1	8.0	347.0	7925.	26000.
7831.	25691.	364.8	761.9	515.8	.032200	-26.7	-16.1	-41.6	-42.8	23.3	4.1	8.0	353.0	8230.	27000.
8125.	25657.	349.6	730.2	499.5	.031183	-29.2	-20.6	-43.7	-46.7	23.4	4.1	8.0	358.0	8534.	28000.
8419.	27617.	335.0	699.7	483.7	.030196	-31.8	-25.2	-45.9	-50.6	23.6	4.1	8.0	2.0	8839.	29000.
8712.	28584.	320.8	670.0	468.3	.029235	-34.4	-29.9	-48.1	-54.6	23.7	4.6	9.0	6.0	9144.	30000.
9007.	29551.	307.1	641.4	453.2	.028292	-37.0	-34.6	-50.4	-58.7	23.8	4.1	8.0	7.0	9449.	31000.
9303.	30523.	293.8	613.6	437.8	.027331	-39.3	-38.7	-53.0	-63.3	22.3	3.1	6.0	3.0	9754.	32000.
9597.	31493.	281.0	586.9	422.2	.026357	-41.1	-42.0	-56.0	-68.8	18.7	3.1	6.0	347.0	10058.	33000.
9893.	32459.	268.7	561.2	407.0	.025408	-43.0	-45.4	-59.3	-74.8	15.2	2.6	5.0	316.0	10363.	34000.
10189.	33428.	256.8	536.3	392.2	.024484	-45.0	-49.0	-63.0	-81.4	11.8	3.6	7.0	293.0	10668.	35000.
10485.	34401.	245.3	512.3	377.5	.023567	-46.6	-51.9	-65.9	-86.6	9.6	5.1	10.0	277.0	10973.	36000.
10779.	35366.	234.3	489.3	362.6	.022636	-47.9	-54.2	-66.9	-88.5	9.6	6.2	12.0	269.0	11278.	37000.
11074.	36331.	223.7	467.2	348.2	.021737	-49.2	-56.6	-68.0	-90.3	9.7	7.7	15.0	270.0	11582.	38000.
11367.	37293.	213.6	446.1	334.3	.020870	-50.5	-58.9	-69.0	-92.2	9.7	0.0	0.0	0.0	11887.	39000.
11665.	38270.	203.8	425.6	320.9	.020033	-51.8	-61.2	-70.1	-94.1	9.7	0.0	0.0	0.0	12192.	40000.
11961.	39242.	194.5	406.2	307.9	.019222	-53.0	-63.4	-71.1	-96.0	9.7	0.0	0.0	0.0	12497.	41000.

TABLE 4.–Continued

H, m	H, ft	p, mb	p, lb/ft^2	RHO, gm/m^3	RHO, lb/ft^3	T, °C	T, °F	D, °C	D, °F	RH, percent	V, m/sec	V, knots	THETA, deg	Z, m	Z, ft
							MONTH 9 DAY 6 YEAR 78 HOUR OF RELEASE 900Z								
757.	2485.	925.5	1932.9	1096.7	.068465	18.7	65.7	15.9	60.5	83.5	1.5	3.0	210.0	724.	2375.
941.	3087.	905.2	1890.5	1075.9	.067166	17.9	64.2	15.3	59.6	84.8	4.1	8.0	227.0	914.	3000.
1233.	4046.	873.6	1824.6	1045.2	.065250	16.1	61.0	13.8	56.9	86.4	6.2	12.0	244.0	1219.	4000.
1527.	5009.	842.8	1760.2	1015.6	.063402	14.1	57.4	12.1	53.8	87.6	4.1	8.0	241.0	1524.	5000.
1819.	5967.	813.0	1698.0	985.6	.061529	12.5	54.5	10.5	51.0	87.8	3.1	6.0	232.0	1829.	6000.
2112.	6928.	784.0	1637.4	956.3	.059700	10.9	51.6	8.9	48.1	87.7	3.6	7.0	218.0	2134.	7000.
2404.	7886.	755.9	1578.7	927.6	.057908	9.3	46.7	7.4	45.2	87.6	5.7	11.0	221.0	2438.	8000.
2696.	8846.	728.6	1521.7	899.7	.056166	7.7	45.9	5.7	42.3	87.4	7.2	14.0	235.0	2743.	9000.
2987.	9801.	702.2	1466.6	872.5	.054468	6.0	42.8	4.1	39.4	87.8	8.2	16.0	241.0	3048.	10000.
3279.	10757.	676.6	1413.1	843.1	.052633	5.9	42.6	-6.8	19.8	39.7	8.2	16.0	239.0	3353.	11000.
3569.	11710.	651.8	1361.3	816.8	.050991	4.7	40.5	-20.8	-5.4	13.7	9.8	19.0	237.0	3658.	12000.
3859.	12661.	627.8	1311.2	792.6	.049480	2.7	36.9	-25.3	-13.6	10.6	11.8	23.0	235.0	3962.	13000.
4147.	13605.	604.7	1262.9	757.7	.047302	4.8	40.6	-23.9	-11.0	10.4	13.4	26.0	227.0	4267.	14000.
4432.	14540.	582.5	1216.6	734.2	.045835	3.1	37.6	-25.1	-13.1	10.5	13.9	27.0	217.0	4572.	15000.
4718.	15478.	560.9	1171.5	712.7	.044492	.9	33.6	-26.6	-15.8	10.7	12.9	25.0	210.0	4877.	16000.
5003.	16413.	540.0	1127.8	691.6	.043175	-1.2	29.8	-28.1	-18.6	10.8	12.9	25.0	212.0	5182.	17000.
5290.	17355.	519.6	1085.2	671.1	.041895	-3.4	25.9	-29.7	-21.5	11.0	13.4	26.0	215.0	5486.	18000.
5576.	18294.	499.9	1044.1	651.0	.040641	-5.6	21.9	-31.3	-24.4	11.2	14.4	28.0	217.0	5791.	19000.
5862.	19232.	480.8	1004.2	631.8	.039442	-8.0	17.6	-33.0	-27.5	11.4	14.4	28.0	215.0	6096.	20000.
6148.	20171.	462.3	965.5	613.0	.038268	-10.4	13.3	-34.8	-30.6	11.6	14.9	29.0	212.0	6401.	21000.
6436.	21114.	444.3	927.9	594.6	.037120	-12.8	9.0	-36.6	-33.8	11.8	15.9	31.0	211.0	6706.	22000.
6724.	22061.	426.8	891.4	576.7	.036002	-15.2	4.6	-38.4	-37.1	11.9	17.0	33.0	210.0	7010.	23000.
7012.	23006.	409.9	856.1	559.2	.034910	-17.7	.1	-40.2	-40.4	12.2	18.5	36.0	211.0	7315.	24000.
7301.	23953.	393.5	821.8	541.5	.033805	-19.9	-3.8	-41.9	-43.3	12.4	20.1	39.0	211.0	7620.	25000.
7590.	24903.	377.6	788.6	523.3	.032669	-21.7	-7.1	-43.2	-45.7	12.6	20.6	40.0	212.0	7925.	26000.
7879.	25848.	362.3	756.7	505.6	.031564	-23.4	-10.1	-44.5	-48.1	12.6	21.6	42.0	212.0	8230.	27000.
8167.	26793.	347.5	725.8	488.4	.030490	-25.2	-13.4	-45.9	-50.5	12.8	22.6	44.0	211.0	8534.	28000.
8455.	27738.	333.2	695.9	471.7	.029447	-27.0	-16.6	-47.2	-53.0	13.0	23.1	45.0	211.0	8839.	29000.
8742.	28681.	319.4	667.1	455.5	.028436	-28.8	-19.8	-48.6	-55.5	13.2	23.7	46.0	210.0	9144.	30000.
9029.	29623.	306.1	639.3	439.8	.027456	-30.6	-23.1	-50.0	-58.0	13.3	24.2	47.0	209.0	9449.	31000.
9317.	30567.	293.2	612.4	424.9	.026526	-32.7	-26.9	-51.6	-60.9	13.5	25.2	49.0	209.0	9754.	32000.
9606.	31516.	280.7	586.3	410.9	.025652	-35.0	-31.0	-53.4	-64.2	13.7	26.2	51.0	208.0	10058.	33000.
9893.	32459.	268.7	561.2	397.2	.024796	-37.4	-35.3	-55.3	-67.5	14.0	26.2	51.0	208.0	10363.	34000.
10181.	33404.	257.1	537.0	383.9	.023966	-39.7	-39.5	-57.1	-70.9	14.1	26.8	52.0	208.0	10668.	35000.
10472.	34358.	245.8	513.4	370.4	.023123	-41.8	-43.2	-62.0	-79.7	9.5	27.3	53.0	207.0	10973.	36000.
10760.	35303.	235.0	490.8	357.7	.022330	-44.1	-47.4	-63.9	-83.0	9.5	26.8	52.0	207.0	11278.	37000.
11049.	36248.	224.6	469.1	345.3	.021556	-46.5	-51.7	-65.8	-86.4	9.6	26.8	52.0	206.0	11582.	38000.
11340.	37205.	214.5	448.0	333.3	.020807	-48.9	-56.0	-67.7	-89.9	9.7	26.8	52.0	205.0	11887.	39000.
11637.	38178.	204.7	427.5	321.6	.020077	-51.2	-60.2	-69.7	-93.4	9.6	26.8	52.0	204.0	12192.	40000.
11935.	39156.	195.3	407.9	309.8	.019340	-53.4	-64.1	-71.4	-96.5	9.8	25.7	50.0	202.0	12497.	41000.
12234.	40138.	186.3	389.1	297.9	.018597	-55.2	-67.4	-72.9	-99.2	9.8	23.7	46.0	211.0	12802.	42000.
12537.	41133.	177.6	370.9	286.4	.017879	-57.0	-70.6	-74.4	-101.9	9.8	19.0	37.0	233.0	13106.	43000.
12845.	42141.	169.2	353.4	275.3	.017186	-58.9	-74.0	-75.9	-104.6	9.9	19.0	37.0	232.0	13411.	44000.
13152.	43149.	161.2	336.7	264.6	.016518	-60.8	-77.4	-77.4	-107.4	9.9	23.1	45.0	210.0	13716.	45000.
13462.	44167.	153.5	320.6	254.2	.015869	-62.7	-80.9	-79.0	-110.2	10.0	24.7	48.0	202.0	14021.	46000.
13775.	45195.	146.1	305.1	243.8	.015220	-64.3	-83.7	-80.4	-112.6	10.0	24.2	47.0	202.0	14326.	47000.
14091.	46231.	139.0	290.3	233.6	.014583	-65.8	-86.4	-81.5	-114.8	10.1	27.8	54.0	197.0	14630.	48000.
14409.	47275.	132.2	276.1	223.7	.013965	-67.2	-89.0	-82.7	-116.9	10.1	33.4	65.0	187.0	14935.	49000.
14729.	48324.	125.7	262.5	214.2	.013372	-68.6	-91.5	-83.9	-119.1	10.1	30.9	60.0	189.0	15240.	50000.

TABLE 4.–Continued

H, m	H, ft	p, mb	p, lb/ft^2	RHO, gm/m^3	RHO, lb/ft^3	T, °C	T, °F	D, °C	D, °F	RH, percent	V, m/sec	V, knots	THETA, deg	Z, m	Z, ft

MONTH 9 DAY 8 YEAR 78 HOUR OF RELEASE 900Z

742.	2435.	927.2	1936.5	1123.6	.070144	13.1	55.6	7.5	45.4	68.6	.5	1.0	195.0	724.	2375.
929.	3048.	906.5	1893.3	1093.7	.068277	14.5	58.1	6.3	43.3	57.8	1.0	2.0	130.0	914.	3000.
1225.	4019.	874.5	1826.4	1057.1	.065993	14.1	57.4	3.7	38.7	49.6	1.5	3.0	35.0	1219.	4000.
1521.	4990.	843.4	1761.5	1023.4	.063889	13.1	55.6	1.3	34.3	44.5	3.1	6.0	39.0	1524.	5000.
1815.	5954.	813.4	1698.8	986.1	.061560	13.5	56.3	-.5	31.1	38.1	6.2	12.0	52.0	1829.	6000.
2107.	6914.	784.4	1638.3	956.9	.059737	11.8	53.2	-4.2	24.5	32.4	8.7	17.0	62.0	2134.	7000.
2400.	7872.	756.3	1579.6	928.4	.057958	10.2	50.4	-8.2	17.2	26.5	9.8	19.0	67.0	2438.	8000.
2692.	8831.	729.0	1522.5	900.6	.056223	8.6	47.5	-12.8	9.0	20.5	7.7	15.0	72.0	2743.	9000.
2983.	9787.	702.6	1467.4	873.4	.054525	6.9	44.4	-18.2	-.8	14.7	4.1	8.0	87.0	3048.	10000.
3275.	10745.	676.9	1413.7	842.8	.052614	6.5	43.7	-18.3	-.9	15.0	2.1	4.0	204.0	3353.	11000.
3564.	11694.	652.2	1362.1	812.9	.050748	6.2	43.2	-17.7	.1	16.1	4.1	8.0	265.0	3658.	12000.
3852.	12637.	628.4	1312.4	784.0	.048944	5.9	42.6	-17.2	1.0	17.1	6.2	12.0	267.0	3962.	13000.
4138.	13576.	605.4	1264.4	762.0	.047570	3.4	38.1	-18.6	-1.5	18.1	7.2	14.0	257.0	4267.	14000.
4425.	14518.	583.0	1217.6	740.6	.046234	.9	33.6	-20.1	-4.2	19.1	8.7	17.0	247.0	4572.	15000.
4714.	15464.	561.2	1172.1	719.7	.044929	-1.6	29.1	-21.7	-7.0	20.0	9.3	18.0	238.0	4877.	16000.
5003.	16413.	540.0	1127.8	699.2	.043650	-4.1	24.6	-23.3	-9.9	20.9	10.8	21.0	243.0	5182.	17000.
5291.	17360.	519.5	1085.0	679.2	.042401	-6.7	19.9	-25.0	-12.9	21.9	13.9	27.0	240.0	5486.	18000.
5582.	18313.	499.5	1043.2	659.6	.041177	-9.3	15.3	-26.7	-16.1	22.8	17.0	33.0	239.0	5791.	19000.
5871.	19262.	480.2	1002.9	639.2	.039904	-11.4	11.5	-29.1	-20.3	21.7	17.5	34.0	235.0	6096.	20000.
6162.	20218.	461.4	963.7	619.3	.038662	-13.6	7.5	-31.4	-24.5	20.8	15.9	31.0	237.0	6401.	21000.
6453.	21173.	443.2	925.6	599.9	.037451	-15.7	3.7	-33.8	-28.9	19.6	15.9	31.0	241.0	6706.	22000.
6744.	22127.	425.6	888.9	581.0	.036271	-17.9	-.2	-36.3	-33.3	18.5	16.5	32.0	243.0	7010.	23000.
7035.	23080.	408.6	853.4	562.6	.035122	-20.0	-4.0	-38.7	-37.7	17.3	17.5	34.0	245.0	7315.	24000.
7326.	24036.	392.1	818.9	544.7	.034005	-22.3	-8.1	-40.9	-41.6	16.9	18.0	35.0	247.0	7620.	25000.
7618.	24994.	376.1	785.5	527.4	.032925	-24.6	-12.3	-42.7	-44.8	17.2	19.0	37.0	249.0	7925.	26000.
7909.	25949.	360.7	753.3	510.6	.031876	-27.0	-16.6	-44.5	-48.1	17.6	20.1	39.0	250.0	8230.	27000.
8202.	26910.	345.7	722.0	494.2	.030852	-29.3	-20.7	-46.3	-51.4	17.8	21.6	42.0	250.0	8534.	28000.
8496.	27873.	331.2	691.7	478.2	.029853	-31.7	-25.1	-48.2	-54.8	18.1	23.1	45.0	250.0	8839.	29000.
8789.	28835.	317.2	662.5	462.6	.028879	-34.1	-29.4	-50.1	-58.2	18.4	24.7	48.0	249.0	9144.	30000.
9082.	29796.	303.7	634.3	447.4	.027930	-36.6	-33.9	-52.1	-61.7	18.8	26.2	51.0	248.0	9449.	31000.
9376.	30762.	290.6	606.9	432.4	.026994	-38.9	-38.0	-54.8	-66.7	17.2	27.8	54.0	247.0	9754.	32000.
9672.	31733.	277.9	580.4	417.8	.026082	-41.3	-42.3	-58.0	-72.3	15.0	29.3	57.0	246.0	10058.	33000.
9967.	32700.	265.7	554.9	403.5	.025190	-43.7	-46.7	-61.3	-78.3	12.8	30.9	60.0	244.0	10363.	34000.
10263.	33670.	253.9	530.3	389.7	.024328	-46.1	-51.0	-64.8	-84.7	10.4	31.9	62.0	244.0	10668.	35000.
10559.	34643.	242.5	506.5	375.4	.023435	-48.0	-54.4	-67.0	-88.7	9.6	32.4	63.0	242.0	10973.	36000.
10856.	35617.	231.5	483.5	361.2	.022549	-49.7	-57.5	-68.4	-91.2	9.6	32.9	64.0	239.0	11278.	37000.
11151.	36584.	221.0	461.6	347.5	.021694	-51.5	-60.7	-69.6	-93.7	9.7	32.9	64.0	237.0	11582.	38000.
11450.	37567.	210.8	440.3	334.2	.020863	-53.2	-63.8	-71.3	-96.3	9.7	33.4	65.0	235.0	11887.	39000.
11749.	38547.	201.1	420.0	321.3	.020058	-55.0	-67.0	-72.7	-98.8	9.8	34.0	66.0	234.0	12192.	40000.
12053.	39543.	191.7	400.4	307.7	.019209	-55.9	-68.6	-73.5	-100.2	9.8	33.4	65.0	233.0	12497.	41000.
12354.	40532.	182.8	381.8	294.5	.018385	-56.8	-70.2	-74.2	-101.5	9.8	32.4	63.0	232.0	12802.	42000.
12660.	41535.	174.2	363.8	281.8	.017592	-57.6	-71.7	-74.9	-102.8	9.8	31.9	62.0	233.0	13106.	43000.
12966.	42538.	166.0	346.7	269.6	.016831	-58.5	-73.3	-75.6	-104.0	9.8	30.9	60.0	234.0	13411.	44000.
13271.	43539.	158.2	330.4	257.9	.016100	-59.4	-74.9	-76.3	-105.3	9.9	28.8	56.0	235.0	13716.	45000.
13579.	44550.	150.7	314.7	246.7	.015401	-60.2	-76.4	-77.0	-106.6	9.9	26.8	52.0	235.0	14021.	46000.
13889.	45569.	143.5	299.7	235.9	.014727	-61.2	-78.2	-77.8	-108.0	9.9	24.7	48.0	235.0	14326.	47000.
14202.	46594.	136.6	285.3	225.7	.014090	-62.1	-79.8	-78.6	-109.4	9.9	22.6	44.0	233.0	14630.	48000.
14511.	47608.	130.1	271.7	215.8	.013472	-63.1	-81.6	-79.4	-110.8	10.0	21.1	41.0	230.0	14935.	49000.
14826.	48641.	123.8	258.6	206.4	.012885	-64.1	-83.4	-80.1	-112.3	10.0	19.5	38.0	227.0	15240.	50000.

MONTH 9 DAY 13 YEAR 78 HOUR OF RELEASE 1100Z

H, m	H, ft	p, mb	p, lb/ft^2	RHO, gm/m^3	RHO, lb/ft^3	T, °C	T, °F	D, °C	D, °F	RH, percent	V, m/sec	V, knots	THETA, deg	Z, m	Z, ft
744.	2441.	927.0	1936.1	1119.4	.069882	14.2	57.6	7.1	44.8	62.3	1.5	3.0	295.0	724.	2375.
929.	3048.	906.5	1893.3	1077.8	.067285	18.9	66.0	4.2	39.5	37.7	2.1	4.0	344.0	914.	3000.
1229.	4003.	875.0	1827.5	1037.0	.064738	20.1	68.2	-.6	30.9	24.8	3.1	6.0	54.0	1219.	4000.
1509.	4952.	844.6	1764.0	1005.0	.062740	19.0	66.2	-3.5	25.7	21.5	4.6	9.0	64.0	1524.	5000.
1800.	5905.	814.9	1702.0	979.3	.061136	16.2	61.2	-3.6	25.6	25.5	5.1	10.0	76.0	1829.	6000.
2093.	6857.	786.1	1641.8	954.2	.059569	13.3	55.9	-4.0	24.8	29.7	5.1	10.0	97.0	2134.	7000.
2382.	7814.	758.0	1583.1	929.6	.058033	10.4	50.7	-4.8	23.3	33.9	4.6	9.0	112.0	2438.	8000.
2674.	8774.	730.6	1525.9	905.6	.056535	7.3	45.1	-5.1	22.8	40.8	3.6	7.0	123.0	2743.	9000.
2968.	9739.	703.9	1470.1	882.7	.055105	4.0	39.2	-4.3	24.2	54.5	2.6	5.0	164.0	3048.	10000.
3264.	10707.	677.9	1415.8	857.9	.053557	1.4	34.5	-2.3	27.9	76.5	3.6	7.0	228.0	3353.	11000.
3557.	11671.	652.8	1363.4	825.4	.051528	2.2	36.0	-17.0	1.4	22.6	5.7	11.0	277.0	3658.	12000.
3849.	12629.	628.6	1312.9	796.3	.049711	1.7	35.1	-18.5	-1.3	20.7	9.8	19.0	303.0	3962.	13000.
4139.	13580.	605.3	1264.2	768.1	.047951	1.2	34.2	-20.0	-4.0	18.8	13.9	27.0	314.0	4267.	14000.
4428.	14527.	582.8	1217.2	740.8	.046247	.8	33.4	-21.7	-7.0	16.8	15.4	30.0	313.0	4572.	15000.
4715.	15469.	561.1	1171.9	714.5	.044605	.3	32.5	-23.5	-10.2	14.8	14.4	28.0	312.0	4877.	16000.
5001.	16409.	540.1	1128.0	692.8	.043250	-1.6	29.1	-24.3	-11.8	15.8	13.4	26.0	316.0	5182.	17000.
5287.	17346.	519.8	1085.6	672.0	.041952	-3.7	25.3	-25.2	-13.4	17.0	13.9	27.0	321.0	5486.	18000.
5573.	18284.	500.1	1044.5	651.7	.040684	-5.8	21.6	-26.2	-15.1	18.3	14.9	29.0	322.0	5791.	19000.
5861.	19227.	480.9	1004.4	631.8	.039442	-8.0	17.6	-28.2	-18.8	17.9	16.5	32.0	321.0	6096.	20000.
6147.	20166.	462.4	965.7	612.4	.038231	-10.1	13.8	-30.3	-22.5	17.4	18.0	35.0	321.0	6401.	21000.
6434.	21109.	444.4	928.1	593.5	.037051	-12.2	10.0	-32.4	-26.3	16.9	18.5	36.0	322.0	6706.	22000.
6721.	22050.	427.0	891.8	575.0	.035896	-14.4	6.1	-34.5	-30.1	16.5	19.5	38.0	323.0	7010.	23000.
7007.	22989.	410.2	856.7	557.0	.034772	-16.6	2.1	-36.6	-33.9	16.0	19.5	38.0	322.0	7315.	24000.
7296.	23936.	393.8	822.5	539.9	.033705	-19.0	-2.2	-38.6	-37.4	16.1	19.5	38.0	321.0	7620.	25000.
7583.	24879.	378.0	789.5	523.9	.032706	-21.7	-7.1	-40.3	-40.5	17.0	20.1	39.0	320.0	7925.	26000.
7873.	25829.	362.6	757.3	508.2	.031726	-24.5	-12.1	-42.1	-43.7	18.1	20.1	39.0	319.0	8230.	27000.
8163.	26780.	347.7	726.2	492.9	.030771	-27.3	-17.1	-44.0	-47.1	19.1	20.6	40.0	319.0	8534.	28000.
8455.	27738.	333.2	695.9	477.9	.029834	-30.2	-22.4	-45.9	-50.6	20.3	20.6	40.0	319.0	8839.	29000.
8746.	28695.	319.2	666.7	463.3	.028923	-33.0	-27.4	-47.9	-54.3	21.2	20.6	40.0	319.0	9144.	30000.
9040.	29659.	305.6	638.3	449.1	.028036	-35.9	-32.6	-50.0	-58.0	22.2	21.1	41.0	320.0	9449.	31000.
9335.	30627.	292.4	610.7	434.5	.027125	-38.6	-37.5	-52.8	-63.1	21.1	21.1	41.0	320.0	9754.	32000.
9630.	31593.	279.7	584.2	419.9	.026214	-40.9	-41.6	-56.3	-69.3	17.7	20.1	39.0	318.0	10058.	33000.
9925.	32563.	267.4	558.5	405.6	.025321	-43.3	-45.9	-60.0	-75.9	14.5	19.0	37.0	317.0	10363.	34000.
10219.	33528.	255.6	533.8	391.8	.024459	-45.8	-50.4	-64.0	-83.2	11.3	21.1	41.0	315.0	10668.	35000.
10517.	34504.	244.1	509.8	378.1	.023604	-48.1	-54.6	-67.1	-88.8	9.6	22.6	44.0	313.0	10973.	36000.
10812.	35473.	233.1	486.8	364.8	.022774	-50.5	-58.9	-69.0	-92.3	9.7	23.1	45.0	310.0	11278.	37000.
11111.	36453.	222.4	464.5	351.9	.021968	-52.8	-63.0	-71.0	-95.7	9.7	23.1	45.0	307.0	11582.	38000.
11412.	37439.	212.1	443.0	337.7	.021082	-54.2	-65.6	-72.1	-97.7	9.7	23.1	45.0	303.0	11887.	39000.
11711.	38424.	202.3	422.5	322.5	.020133	-54.5	-66.1	-72.3	-98.1	9.8	23.1	45.0	299.0	12192.	40000.
12013.	39413.	192.9	402.9	307.2	.019176	-54.2	-65.6	-72.1	-97.6	9.7	23.1	45.0	294.0	12497.	41000.
12313.	40396.	184.0	384.3	292.4	.018254	-53.8	-64.8	-71.7	-97.1	9.7	22.1	43.0	290.0	12802.	42000.
12613.	41380.	175.5	366.5	280.6	.017517	-55.1	-67.2	-72.8	-99.0	9.8	20.6	40.0	286.0	13106.	43000.
12916.	42376.	167.3	349.4	269.4	.016818	-56.6	-69.9	-74.0	-101.3	9.8	19.5	38.0	282.0	13411.	44000.
13219.	43369.	159.5	333.1	258.6	.016144	-58.2	-72.8	-75.3	-103.5	9.9	19.0	37.0	277.0	13716.	45000.
13529.	44385.	151.9	317.2	248.2	.015495	-59.7	-75.5	-76.6	-105.8	9.8	18.0	35.0	272.0	14021.	46000.
13836.	45395.	144.7	302.2	237.6	.014833	-60.8	-77.4	-77.5	-107.5	9.9	15.4	30.0	227.0	14326.	47000.
14145.	46412.	137.8	287.8	227.2	.014184	-61.8	-79.2	-78.2	-108.8	10.0	11.3	22.0	337.0	14630.	48000.
14459.	47433.	131.2	274.0	217.3	.013566	-62.7	-80.9	-79.0	-110.2	10.0	7.2	14.0	19.0	14935.	49000.
14779.	48457.	124.9	260.9	207.8	.012973	-63.6	-82.5	-79.8	-111.6	9.9	6.2	12.0	24.0	15240.	50000.

TABLE 4.–Continued

H, m	H, ft	p, mb	p, lb/ft^2	RHO, gm/m^3	RHO, lb/ft^3	T, °C	T, °F	D, °C	D, °F	RH, percent	V, m/sec	V, knots	THETA, deg	Z, m	Z, ft
MONTH 9 DAY 25 YEAR 78 HOUR OF RELEASE 9007															
699.	2295.	932.0	1946.5	1120.3	.069938	16.0	60.8	.8	33.5	35.7	2.1	4.0	275.0	724.	2375.
884.	2899.	911.5	1903.7	1077.0	.067235	20.9	69.6	1.3	34.3	27.1	2.6	5.0	334.0	914.	3000.
1171.	3841.	880.3	1838.5	1023.3	.063883	25.8	78.4	-.1	31.9	18.3	2.6	5.0	57.0	1219.	4000.
1455.	4775.	850.2	1775.7	990.1	.061810	25.3	77.5	-.5	31.1	18.3	2.6	5.0	61.0	1524.	5000.
1740.	5707.	821.0	1714.7	964.9	.060237	22.6	72.7	-1.8	28.7	19.5	3.1	6.0	61.0	1829.	6000.
2024.	6640.	792.6	1655.4	940.2	.058695	19.9	67.8	-3.2	26.2	20.7	3.1	6.0	71.0	2134.	7000.
2309.	7576.	764.9	1597.5	916.0	.057184	17.2	63.0	-4.7	23.5	21.9	4.6	9.0	86.0	2438.	8000.
2596.	8516.	737.9	1541.1	892.3	.055704	14.4	57.9	-6.3	20.6	23.2	6.2	12.0	83.0	2743.	9000.
2882.	9454.	711.7	1486.4	869.1	.054256	11.7	53.1	-8.0	17.6	24.3	7.7	15.0	79.0	3048.	10000.
3171.	10402.	686.0	1432.7	846.4	.052839	8.8	47.6	-9.6	14.4	25.7	9.3	18.0	74.0	3353.	11000.
3459.	11349.	661.1	1380.7	824.2	.051453	5.9	42.6	-11.6	11.1	27.1	9.8	19.0	75.0	3658.	12000.
3748.	12297.	636.9	1330.2	802.5	.050098	3.0	37.4	-13.5	7.6	28.4	9.3	18.0	71.0	3962.	13000.
4040.	13254.	613.2	1280.7	781.0	.048756	.1	32.2	-15.6	3.9	29.6	8.7	17.0	61.0	4267.	14000.
4329.	14204.	590.4	1233.1	753.1	.047014	-.2	31.6	-19.5	-3.1	21.7	8.2	16.0	44.0	4572.	15000.
4619.	15153.	568.3	1186.9	726.2	.045335	-.5	31.1	-24.8	-12.7	13.9	8.2	16.0	23.0	4877.	16000.
4906.	16097.	547.0	1142.4	704.9	.044005	-2.8	27.0	-26.9	-16.4	13.7	9.8	19.0	9.0	5182.	17000.
5195.	17042.	526.3	1099.2	684.4	.042726	-5.2	22.6	-28.7	-19.7	13.8	10.8	21.0	2.0	5486.	18000.
5483.	17990.	506.2	1057.2	664.3	.041471	-7.7	18.1	-30.6	-23.1	14.0	10.3	20.0	359.0	5791.	19000.
5773.	18939.	486.7	1016.5	644.2	.040216	-9.9	14.2	-32.3	-26.2	14.1	9.3	18.0	358.0	6096.	20000.
6062.	19889.	467.8	977.0	624.3	.038974	-12.1	10.2	-34.0	-29.3	14.3	7.7	15.0	360.0	6401.	21000.
6353.	20844.	449.4	938.6	604.9	.037763	-14.2	6.4	-35.8	-32.4	14.3	7.2	14.0	360.0	6706.	22000.
6642.	21793.	431.7	901.6	586.0	.036583	-16.4	2.5	-37.5	-35.5	14.4	7.2	14.0	356.0	7010.	23000.
6933.	22746.	414.5	865.7	567.5	.035428	-18.6	-1.5	-39.3	-38.7	14.5	7.7	15.0	349.0	7315.	24000.
7223.	23696.	397.9	831.0	549.6	.034310	-20.9	-5.6	-41.1	-41.9	14.6	8.2	16.0	345.0	7620.	25000.
7515.	24655.	381.7	797.2	532.7	.033255	-23.4	-10.1	-43.0	-45.4	14.9	8.7	17.0	341.0	7925.	26000.
7806.	25610.	366.1	764.6	516.1	.032219	-25.9	-14.6	-45.0	-48.9	15.1	9.8	19.0	338.0	8230.	27000.
8098.	26567.	351.0	733.1	500.0	.031214	-28.5	-19.3	-47.0	-52.5	15.4	10.8	21.0	336.0	8534.	28000.
8391.	27530.	336.3	702.4	484.2	.030228	-31.1	-24.0	-49.0	-56.2	15.6	12.3	24.0	336.0	8839.	29000.
8685.	28494.	322.1	672.7	468.9	.029272	-33.7	-28.7	-51.1	-59.9	15.9	13.4	26.0	335.0	9144.	30000.
8979.	29457.	308.4	644.1	453.9	.028336	-36.3	-33.3	-53.2	-63.7	16.1	14.4	28.0	335.0	9449.	31000.
9274.	30426.	295.1	616.3	439.2	.027418	-39.0	-38.2	-55.6	-68.2	15.7	14.9	29.0	334.0	9754.	32000.
9571.	31400.	282.2	589.4	424.8	.026519	-41.6	-42.9	-58.7	-73.7	14.1	14.9	29.0	333.0	10058.	33000.
9867.	32371.	269.8	563.5	410.7	.025639	-44.2	-47.6	-61.9	-79.5	12.4	14.9	29.0	331.0	10363.	34000.
10164.	33346.	257.8	538.4	397.1	.024790	-46.9	-52.4	-65.2	-85.4	10.8	14.4	28.0	328.0	10668.	35000.
10464.	34332.	246.1	514.0	382.9	.023904	-49.1	-56.4	-67.9	-90.2	9.7	13.9	27.0	326.0	10973.	36000.
10760.	35303.	235.0	490.6	367.7	.022955	-50.4	-58.7	-69.0	-92.1	9.7	13.4	26.0	323.0	11278.	37000.
11057.	36276.	224.3	468.5	353.0	.022037	-51.7	-61.1	-70.0	-94.0	9.7	12.9	25.0	319.0	11582.	38000.
11355.	37254.	214.0	446.9	338.8	.021151	-53.0	-63.4	-71.1	-95.9	9.7	12.3	24.0	313.0	11887.	39000.
11655.	38239.	204.1	426.3	325.1	.020295	-54.3	-65.7	-72.2	-97.9	9.7	11.8	23.0	305.0	12192.	40000.
11958.	39231.	194.6	406.4	311.5	.019446	-55.4	-67.7	-73.0	-99.4	9.8	11.3	22.0	296.0	12497.	41000.
12258.	40216.	185.6	387.6	298.2	.018616	-56.2	-69.2	-73.7	-100.7	9.8	11.3	22.0	287.0	12802.	42000.
12562.	41215.	176.9	369.5	285.4	.017817	-57.1	-70.8	-74.4	-102.0	9.8	11.8	23.0	278.0	13106.	43000.
12867.	42215.	168.6	352.1	273.1	.017049	-58.0	-72.4	-75.1	-103.2	9.9	12.9	25.0	269.0	13411.	44000.
13175.	43226.	160.6	335.4	261.2	.016306	-58.8	-73.8	-75.8	-104.5	9.8	13.9	27.0	262.0	13716.	45000.
13483.	44235.	153.0	319.5	249.9	.015601	-59.7	-75.5	-76.5	-105.8	9.9	13.9	27.0	261.0	14021.	46000.
13788.	45238.	145.8	304.5	239.6	.014958	-61.1	-78.0	-77.7	-107.9	9.9	13.9	27.0	261.0	14326.	47000.
14100.	46261.	138.8	289.9	229.5	.014327	-62.4	-80.3	-78.8	-109.8	10.0	13.9	27.0	261.0	14630.	48000.
14414.	47291.	132.1	275.9	219.3	.013690	-63.2	-81.8	-79.4	-111.0	10.0	13.4	26.0	261.0	14935.	49000.
14729.	48324.	125.7	262.5	209.6	.013085	-64.0	-83.2	-80.1	-112.2	9.9	12.9	25.0	261.0	15240.	50000.

TABLE 4.—Continued

MONTH 9 DAY 27 YEAR 78 HOUR OF RELEASE 900Z

H, m	H, ft	P, mb	P, lb/ft^2	RHO, gm/m^3	RHO, lb/ft^3	T, °C	T, °F	D, °C	D, °F	RH, percent	V, m/sec	V, knots	THETA, deg	Z, m	Z, ft
695.	2280.	932.5	1947.6	1107.1	.069114	18.9	66.0	9.3	48.8	53.7	.5	1.0	210.0	724.	2375.
877.	2878.	912.2	1905.2	1070.7	.066842	22.5	72.5	6.8	44.3	36.3	.5	1.0	268.0	914.	3000.
1164.	3819.	881.0	1840.0	1026.2	.064064	25.2	77.4	.4	32.7	19.6	.5	1.0	334.0	1219.	4000.
1450.	4756.	850.8	1776.9	994.3	.062072	24.4	75.9	-3.3	26.1	15.7	1.0	2.0	292.0	1524.	5000.
1735.	5691.	821.5	1715.7	968.5	.060461	21.7	71.1	-3.5	25.8	18.2	1.5	3.0	259.0	1829.	6000.
2020.	6627.	793.0	1656.2	943.5	.058901	19.1	66.4	-3.9	25.0	20.7	2.1	4.0	204.0	2134.	7000.
2306.	7566.	765.2	1598.2	919.0	.057371	16.3	61.3	-4.5	23.8	23.5	2.6	5.0	160.0	2438.	8000.
2593.	8509.	738.1	1541.6	895.0	.055873	13.6	56.5	-5.4	22.2	26.2	3.1	6.0	133.0	2743.	9000.
2881.	9451.	711.8	1486.6	871.5	.054406	10.8	51.4	-6.5	20.3	29.0	3.6	7.0	129.0	3048.	10000.
3170.	10399.	686.1	1432.9	848.9	.052995	7.9	46.2	-7.0	19.5	34.1	3.6	7.0	130.0	3353.	11000.
3459.	11349.	661.1	1380.7	827.2	.051640	4.7	40.5	-7.3	19.0	41.5	3.1	6.0	143.0	3658.	12000.
3749.	12301.	636.8	1330.0	797.5	.049786	4.8	40.6	-15.6	3.9	21.1	2.6	5.0	183.0	3962.	13000.
4036.	13242.	613.5	1281.3	769.7	.048051	4.5	40.1	-30.0	-22.0	6.1	3.1	6.0	228.0	4267.	14000.
4323.	14183.	590.9	1234.1	746.6	.046609	2.5	36.5	-27.7	-17.9	8.6	4.1	8.0	238.0	4572.	15000.
4611.	15127.	568.9	1188.2	724.1	.045204	.5	32.9	-26.5	-15.6	11.1	4.6	9.0	240.0	4877.	16000.
4897.	16065.	547.7	1143.9	703.5	.043918	-1.9	28.6	-28.2	-18.7	11.4	4.6	9.0	244.0	5182.	17000.
5185.	17010.	527.0	1100.7	683.4	.042663	-4.5	23.9	-30.1	-22.1	11.6	4.6	9.0	255.0	5486.	18000.
5473.	17957.	506.9	1058.7	663.8	.041440	-7.1	19.2	-31.9	-25.5	11.8	5.1	10.0	263.0	5791.	19000.
5762.	18905.	487.4	1018.0	644.2	.040216	-9.5	14.9	-33.8	-28.8	11.9	6.2	12.0	262.0	6096.	20000.
6051.	19853.	468.5	978.5	624.7	.038999	-11.8	10.8	-35.6	-32.0	12.0	7.7	15.0	260.0	6401.	21000.
6340.	20802.	450.2	940.3	605.8	.037819	-14.2	6.4	-37.4	-35.3	12.1	9.8	19.0	259.0	6706.	22000.
6631.	21755.	432.4	903.1	587.3	.036664	-16.6	2.1	-39.2	-38.6	12.3	10.3	20.0	259.0	7010.	23000.
6921.	22706.	415.2	867.2	569.3	.035540	-19.0	-2.2	-41.1	-42.0	12.4	11.3	22.0	260.0	7315.	24000.
7214.	23667.	398.4	832.1	551.6	.034435	-21.4	-6.5	-43.0	-45.4	12.5	12.3	24.0	261.0	7620.	25000.
7504.	24619.	382.3	798.5	534.0	.033337	-23.7	-10.7	-44.6	-48.2	12.9	13.9	27.0	261.0	7925.	26000.
7797.	25579.	366.6	765.7	516.8	.032263	-25.9	-14.6	-46.2	-51.1	13.2	14.9	29.0	261.0	8230.	27000.
8088.	26535.	351.5	734.1	500.1	.031220	-28.2	-18.8	-47.8	-54.1	13.6	16.5	32.0	260.0	8534.	28000.
8381.	27497.	336.8	703.4	483.8	.030203	-30.5	-22.9	-49.5	-57.1	14.0	17.5	34.0	259.0	8839.	29000.
8672.	28453.	322.7	674.0	467.9	.029210	-32.8	-27.0	-51.2	-60.2	14.3	18.5	36.0	257.0	9144.	30000.
8966.	29415.	309.0	645.4	452.5	.028249	-35.2	-31.4	-53.0	-63.3	14.8	19.0	37.0	257.0	9449.	31000.
9260.	30382.	295.7	617.6	437.4	.027306	-37.6	-35.7	-55.1	-67.1	14.6	20.1	39.0	256.0	9754.	32000.
9554.	31346.	282.9	590.8	422.9	.026401	-40.0	-40.0	-57.9	-72.2	13.2	20.6	40.0	256.0	10058.	33000.
9850.	32315.	270.5	565.0	408.8	.025521	-42.5	-44.5	-60.8	-77.5	11.9	21.6	42.0	256.0	10363.	34000.
10146.	33288.	258.5	539.9	395.0	.024659	-45.0	-49.0	-63.8	-82.9	10.6	23.1	45.0	258.0	10668.	35000.
10441.	34255.	247.0	515.9	381.5	.023816	-47.5	-53.5	-66.6	-87.9	9.6	24.2	47.0	259.0	10973.	36000.
10739.	35232.	235.8	492.5	367.9	.022967	-49.7	-57.5	-68.4	-91.2	9.6	26.2	51.0	261.0	11278.	37000.
11034.	36202.	225.1	470.1	354.8	.022149	-52.0	-61.6	-70.3	-94.5	9.7	28.3	55.0	262.0	11582.	38000.
11334.	37186.	214.7	448.4	342.0	.021350	-54.3	-65.7	-72.2	-97.9	9.7	29.8	58.0	263.0	11887.	39000.
11637.	38178.	204.7	427.5	329.6	.020576	-56.7	-70.1	-74.1	-101.3	9.9	30.4	59.0	264.0	12192.	40000.
11941.	39178.	195.1	407.5	317.8	.019840	-59.2	-74.6	-76.1	-105.0	9.9	30.4	59.0	264.0	12497.	41000.
12251.	40194.	185.8	388.1	306.5	.019134	-61.9	-79.4	-78.3	-109.0	10.0	28.8	56.0	263.0	12802.	42000.
12562.	41215.	176.9	369.5	293.4	.018316	-63.0	-81.4	-79.3	-110.7	9.9	27.3	53.0	262.0	13106.	43000.
12879.	42252.	168.3	351.5	279.9	.017474	-63.5	-82.3	-79.7	-111.4	10.0	24.7	48.0	260.0	13411.	44000.
13191.	43278.	160.2	334.6	267.0	.016668	-63.9	-83.0	-80.0	-112.1	9.9	22.6	44.0	259.0	13716.	45000.
13504.	44303.	152.5	318.5	254.6	.015894	-64.4	-83.9	-80.4	-112.8	10.0	21.6	42.0	260.0	14021.	46000.
13819.	45338.	145.1	303.0	243.0	.015170	-65.0	-85.0	-80.9	-113.7	10.0	20.6	40.0	260.0	14326.	47000.
14137.	46382.	138.0	288.2	231.9	.014477	-65.7	-86.3	-81.5	-114.7	10.0	20.1	39.0	261.0	14630.	48000.
14453.	47417.	131.3	274.2	221.3	.013815	-66.4	-87.5	-82.1	-115.7	10.1	19.0	37.0	261.0	14935.	49000.
14775.	48474.	124.8	260.7	211.2	.013185	-67.1	-88.8	-82.6	-116.7	10.1	18.5	36.0	262.0	15240.	50000.

TABLE 4.–Continued

H, m	H, ft	p, mb	p, lb/ft^2	RHO, gm/m^3	RHO, lb/ft^3	T, °C	T, °F	D, °C	D, °F	RH, percent	V, m/sec	V, knots	THETA, deg	Z, m	Z, ft
MONTH 9 DAY 27 YEAR 78 HOUR OF RELEASE 1730Z															
688.	2257.	933.3	1949.2	1092.0	.068171	23.5	74.3	5.8	42.4	31.7	2.1	4.0	30.0	724.	2375.
868.	2849.	913.2	1907.3	1066.8	.066598	23.9	75.0	6.1	43.0	31.7	2.1	4.0	33.0	914.	3000.
1156.	3792.	881.9	1841.9	1027.9	.064170	24.5	76.1	6.7	44.0	31.8	2.1	4.0	42.0	1219.	4000.
1440.	4725.	851.8	1779.0	990.5	.061835	25.1	77.2	7.3	45.1	32.0	3.1	6.0	65.0	1524.	5000.
1724.	5655.	822.6	1718.0	965.4	.060268	22.5	72.5	5.8	42.4	33.7	4.1	8.0	76.0	1829.	6000.
2009.	6590.	794.1	1658.5	941.4	.058770	19.6	67.3	4.0	39.3	35.7	4.6	9.0	79.0	2134.	7000.
2294.	7525.	766.4	1600.7	918.0	.057309	16.7	62.1	2.2	36.0	37.7	4.6	9.0	84.0	2438.	8000.
2579.	8463.	739.4	1544.3	894.9	.055867	13.8	56.8	.3	32.6	39.6	4.1	8.0	90.0	2743.	9000.
2867.	9407.	713.0	1489.1	872.3	.054456	10.8	51.4	-1.7	29.0	41.7	4.6	9.0	97.0	3048.	10000.
3156.	10354.	687.3	1435.5	848.4	.052964	8.4	47.1	-3.9	25.0	41.5	4.6	9.0	100.0	3353.	11000.
3444.	11299.	662.4	1383.5	823.4	.051403	6.5	43.7	-6.3	20.6	39.3	4.1	8.0	104.0	3658.	12000.
3732.	12245.	638.2	1332.9	798.9	.049874	4.7	40.5	-8.8	16.2	36.8	3.1	6.0	115.0	3962.	13000.
4021.	13193.	614.7	1283.8	775.0	.048382	2.8	37.0	-11.3	11.6	34.5	2.6	5.0	151.0	4267.	14000.
4309.	14136.	592.0	1236.4	751.7	.046927	.8	33.4	-13.9	7.1	32.4	3.1	6.0	195.0	4572.	15000.
4597.	15083.	569.9	1190.3	729.0	.045510	-1.0	30.2	-16.5	2.4	29.8	4.6	9.0	210.0	4877.	16000.
4886.	16029.	548.5	1145.6	706.8	.044124	-2.9	26.8	-19.1	-2.4	27.4	5.1	10.0	214.0	5182.	17000.
5175.	16978.	527.7	1102.1	685.1	.042769	-4.9	23.2	-21.9	-7.3	25.1	4.1	8.0	208.0	5486.	18000.
5463.	17923.	507.6	1060.1	664.0	.041452	-6.8	19.8	-24.7	-12.4	22.6	5.1	10.0	207.0	5791.	19000.
5752.	18870.	488.1	1019.4	643.9	.040197	-9.1	15.6	-27.2	-17.0	21.5	5.1	10.0	207.0	6096.	20000.
6040.	19818.	469.2	979.9	624.7	.038999	-11.5	11.3	-29.5	-21.1	21.0	6.2	12.0	205.0	6401.	21000.
6331.	20770.	450.8	941.5	606.0	.037831	-13.9	7.0	-31.8	-25.3	20.5	6.7	13.0	203.0	6706.	22000.
6619.	21717.	433.1	904.5	587.7	.036689	-16.4	2.5	-34.2	-29.5	20.1	8.2	16.0	199.0	7010.	23000.
6911.	22673.	415.8	868.4	569.8	.035571	-18.9	-2.0	-36.5	-33.7	19.6	9.3	18.0	196.0	7315.	24000.
7201.	23626.	399.1	833.5	552.4	.034485	-21.4	-6.5	-38.8	-37.9	19.2	9.8	19.0	196.0	7620.	25000.
7493.	24583.	382.9	799.7	535.4	.033424	-24.0	-11.2	-40.3	-40.6	20.7	10.8	21.0	194.0	7925.	26000.
7785.	25542.	367.2	766.9	518.9	.032394	-26.5	-15.7	-41.9	-43.5	22.0	11.8	23.0	192.0	8230.	27000.
8078.	26502.	352.0	735.2	502.8	.031389	-29.2	-20.6	-43.6	-46.5	23.6	12.9	25.0	189.0	8534.	28000.
8373.	27470.	337.2	704.3	487.0	.030402	-31.8	-25.2	-45.4	-49.7	25.0	13.9	27.0	186.0	8839.	29000.
8666.	28432.	323.0	674.6	471.6	.029441	-34.5	-30.1	-47.2	-53.0	26.5	0.0	0.0	0.0	9144.	30000.
8963.	29407.	309.1	645.6	456.7	.028511	-37.2	-35.0	-49.1	-56.4	28.0	0.0	0.0	0.0	9449.	31000.
9260.	30382.	295.7	617.6	441.5	.027562	-39.7	-39.5	-52.5	-62.5	24.6	0.0	0.0	0.0	9754.	32000.
9557.	31354.	282.8	590.6	425.9	.026588	-41.7	-43.1	-61.2	-78.1	10.5	0.0	0.0	0.0	10058.	33000.

TABLE 4.–Continued

H, m	H, ft	P, mb	P, lb/ft^2	RHO, gm/m^3	RHO, lb/ft^3	T, °C	T, °F	D, °C	D, °F	RH, percent	V, m/sec	V, knots	THETA, deg	Z, m	Z, ft
							MONTH 10 DAY 2 YEAR 78 HOUR OF RELEASE 900Z								
717.	2353.	930.0	1942.3	1115.7	.069651	17.1	62.8	-16.0	3.2	9.0	1.5	3.0	205.0	724.	2375.
990.	2953.	909.7	1899.9	1065.9	.066542	23.9	75.0	-10.9	12.4	9.0	1.5	3.0	207.0	914.	3000.
1188.	3899.	878.4	1834.6	1028.1	.064182	24.2	75.6	-10.6	12.9	9.0	1.5	3.0	214.0	1219.	4000.
1474.	4835.	848.3	1771.7	995.2	.062128	23.5	74.3	-11.2	11.9	9.0	1.0	2.0	263.0	1524.	5000.
1759.	5772.	819.0	1710.5	967.4	.060393	21.5	70.7	-12.6	9.2	9.0	2.1	4.0	328.0	1829.	6000.
2045.	6710.	790.5	1651.0	940.2	.058695	19.5	67.1	-14.2	6.5	9.0	3.1	6.0	325.0	2134.	7000.
2331.	7648.	762.8	1593.1	913.6	.057034	17.5	63.5	-15.7	3.8	9.0	1.5	3.0	311.0	2438.	8000.
2616.	8583.	736.0	1537.2	887.7	.055417	15.5	59.9	-17.2	1.1	9.0	.5	1.0	228.0	2743.	9000.
2902.	9520.	709.9	1482.7	862.3	.053832	13.5	56.3	-18.7	-1.7	9.0	2.1	4.0	104.0	3048.	10000.
3189.	10459.	684.5	1429.6	837.9	.052308	11.3	52.3	-20.4	-4.7	9.1	1.5	3.0	44.0	3353.	11000.
3475.	11399.	659.8	1378.0	814.2	.050829	9.0	48.2	-22.1	-7.8	9.1	2.6	5.0	283.0	3658.	12000.
3760.	12337.	635.9	1328.1	791.1	.049387	6.8	44.2	-23.8	-10.9	9.1	5.1	10.0	283.0	3962.	13000.
4047.	13279.	612.6	1279.4	768.5	.047976	4.5	40.1	-25.6	-14.1	9.1	5.1	10.0	288.0	4267.	14000.
4333.	14217.	590.1	1232.4	746.5	.046602	2.1	35.6	-27.4	-17.3	9.1	3.6	7.0	304.0	4572.	15000.
4621.	15162.	568.1	1186.5	724.9	.045254	-.1	31.8	-29.2	-20.5	9.1	3.1	6.0	318.0	4877.	16000.
4909.	16106.	546.8	1142.0	703.8	.043937	-2.4	27.7	-31.0	-23.8	9.0	3.6	7.0	322.0	5182.	17000.
5196.	17047.	526.2	1099.0	683.3	.042657	-4.8	23.4	-32.8	-27.1	9.1	5.1	10.0	334.0	5486.	18000.
5485.	17995.	506.1	1057.0	663.1	.041396	-7.2	19.0	-34.7	-30.4	9.1	6.2	12.0	335.0	5791.	19000.
5776.	18949.	486.5	1016.1	643.4	.040166	-9.6	14.7	-36.6	-33.8	9.1	6.2	12.0	342.0	6096.	20000.
6064.	19894.	467.7	976.8	624.3	.038974	-12.1	10.2	-38.5	-37.2	9.2	6.2	12.0	335.0	6401.	21000.
6355.	20849.	449.3	938.4	605.5	.037800	-14.5	5.9	-40.4	-40.7	9.1	7.2	14.0	336.0	6706.	22000.
6644.	21798.	431.6	901.4	587.2	.036658	-17.0	1.4	-42.3	-44.2	9.2	8.2	16.0	336.0	7010.	23000.
6936.	22757.	414.3	865.3	569.4	.035546	-19.5	-3.1	-44.3	-47.8	9.2	9.3	18.0	335.0	7315.	24000.
7228.	23714.	397.6	830.4	551.9	.034454	-22.1	-7.8	-46.3	-51.4	9.3	9.8	19.0	334.0	7620.	25000.
7520.	24673.	381.4	796.6	534.9	.033393	-24.6	-12.3	-48.3	-55.0	9.3	10.3	20.0	332.0	7925.	26000.
7814.	25635.	365.7	763.8	518.2	.032350	-27.2	-17.0	-50.3	-58.6	9.3	10.3	20.0	329.0	8230.	27000.
8107.	26599.	350.5	732.0	502.0	.031339	-29.7	-21.5	-52.4	-62.3	9.3	10.6	21.0	326.0	8534.	28000.
8401.	27564.	335.8	701.3	486.1	.030346	-32.4	-26.3	-54.5	-66.0	9.4	11.3	22.0	323.0	8839.	29000.
8696.	28529.	321.6	671.7	470.6	.029379	-35.0	-31.0	-56.6	-69.8	9.4	11.3	22.0	321.0	9144.	30000.
8992.	29500.	307.8	642.9	455.6	.028442	-37.7	-35.9	-58.7	-73.6	9.5	11.3	22.0	320.0	9449.	31000.
9290.	30478.	294.4	614.9	440.7	.027512	-40.3	-40.5	-60.8	-77.4	9.5	11.3	22.0	318.0	9754.	32000.
9587.	31454.	281.5	587.9	425.9	.026588	-42.8	-45.0	-62.8	-81.0	9.6	11.3	22.0	317.0	10058.	33000.
9884.	32427.	269.1	562.0	411.6	.025695	-45.3	-49.5	-64.8	-84.7	9.6	11.3	22.0	315.0	10363.	34000.
10184.	33412.	257.0	536.8	397.6	.024821	-47.8	-54.0	-66.9	-88.4	9.6	11.8	23.0	313.0	10668.	35000.
10483.	34392.	245.4	512.5	383.9	.023966	-50.3	-58.5	-68.9	-92.0	9.6	11.8	23.0	311.0	10973.	36000.
10782.	35375.	234.2	489.1	370.3	.023117	-52.7	-62.9	-70.8	-95.5	9.7	12.3	24.0	309.0	11278.	37000.
11085.	36369.	223.3	466.4	357.1	.022293	-55.1	-67.2	-72.8	-99.0	9.8	11.8	23.0	309.0	11582.	38000.
11388.	37361.	212.9	444.7	344.2	.021488	-57.5	-71.5	-74.8	-102.6	9.8	11.3	22.0	310.0	11887.	39000.
11693.	38362.	202.9	423.8	331.8	.020714	-60.0	-76.0	-76.8	-106.2	9.9	10.3	20.0	312.0	12192.	40000.
12003.	39381.	193.2	403.5	317.1	.019796	-60.8	-77.4	-77.4	-107.4	9.9	8.7	17.0	324.0	12497.	41000.
12313.	40396.	184.0	384.3	302.1	.018859	-60.8	-77.4	-77.5	-107.5	9.9	7.7	15.0	337.0	12802.	42000.
12624.	41416.	175.2	365.9	287.7	.017961	-60.9	-77.6	-77.5	-107.6	9.9	6.7	13.0	350.0	13106.	43000.
12931.	42426.	166.9	348.6	274.1	.017112	-60.9	-77.6	-77.6	-107.6	9.8	6.7	13.0	4.0	13411.	44000.
13243.	43448.	158.9	331.9	261.1	.016300	-61.0	-77.8	-77.6	-107.7	9.9	7.2	14.0	18.0	13716.	45000.
13554.	44467.	151.3	316.0	248.7	.015526	-61.1	-78.0	-77.7	-107.8	9.9	7.2	14.0	30.0	14021.	46000.
13863.	45482.	144.1	301.0	237.4	.014820	-61.6	-78.9	-78.1	-108.6	9.9	8.2	16.0	36.0	14326.	47000.
14174.	46503.	137.2	286.5	226.8	.014159	-62.3	-80.1	-78.7	-109.6	10.0	8.7	17.0	41.0	14630.	48000.
14487.	47528.	130.6	272.8	216.5	.013516	-62.9	-81.2	-79.2	-110.5	9.9	8.7	17.0	39.0	14935.	49000.
14800.	48557.	124.3	259.6	206.8	.012910	-63.6	-82.5	-79.7	-111.5	10.0	6.7	13.0	11.0	15240.	50000.

TABLE 4.–Continued

H, m	H, ft	p, mb	p, lb/ft^2	RHO, gm/m^3	RHO, lb/ft^3	T, °C	T, °F	D, °C	D, °F	RH, percent	V, m/sec	V, knots	THETA, deg	Z, m	Z, ft
MONTH 10 DAY 2 YEAR 78 HOUR OF RELEASE 1800Z															
699.	2295.	932.0	1946.5	1072.3	.066942	28.3	82.9	8.7	47.6	29.1	2.1	4.0	115.0	724.	2375.
878.	2881.	912.1	1905.0	1055.7	.065905	26.7	80.1	6.5	43.7	27.6	2.1	4.0	79.0	914.	3000.
1164.	3819.	881.0	1840.0	1029.5	.064270	24.1	75.4	2.9	37.2	25.1	1.5	3.0	27.0	1219.	4000.
1451.	4759.	850.7	1776.7	1003.6	.062653	21.4	70.5	-.8	30.6	22.7	2.1	4.0	356.0	1524.	5000.
1739.	5704.	821.1	1714.9	975.8	.060917	19.4	66.9	-2.7	27.1	22.2	2.6	5.0	339.0	1829.	6000.
2026.	6647.	792.4	1655.0	948.6	.059219	17.3	63.1	-4.7	23.6	21.9	1.0	2.0	347.0	2134.	7000.
2313.	7590.	764.5	1596.7	922.0	.057559	15.2	59.4	-6.6	20.1	21.6	1.0	2.0	87.0	2438.	8000.
2601.	8533.	737.4	1540.1	896.0	.055935	13.1	55.6	-8.6	16.6	21.3	1.5	3.0	133.0	2743.	9000.
2888.	9476.	711.1	1485.2	870.5	.054344	11.0	51.8	-10.5	13.0	20.9	2.6	5.0	134.0	3048.	10000.
3178.	10425.	685.4	1431.5	845.6	.052789	8.9	48.0	-12.3	9.9	20.9	3.1	6.0	114.0	3353.	11000.
3465.	11368.	660.6	1379.7	821.3	.051272	6.7	44.1	-13.9	7.1	21.4	3.6	7.0	95.0	3658.	12000.
3754.	12317.	636.4	1329.1	797.6	.049793	4.6	40.3	-15.4	4.2	21.7	2.6	5.0	100.0	3962.	13000.
4042.	13263.	613.0	1280.3	774.4	.048344	2.4	36.3	-17.1	1.3	22.2	7.2	14.0	351.0	4267.	14000.
4332.	14212.	590.2	1232.7	751.8	.046933	.1	32.2	-18.7	-1.7	22.7	10.3	20.0	313.0	4572.	15000.
4621.	15162.	568.1	1186.5	729.7	.045554	-2.0	28.4	-20.4	-4.7	23.0	6.2	12.0	294.0	4877.	16000.
4910.	16110.	546.7	1141.8	708.1	.044205	-4.2	24.4	-22.1	-7.8	23.3	4.6	9.0	294.0	5182.	17000.
5200.	17061.	525.9	1098.4	687.0	.042888	-6.5	20.3	-23.8	-10.9	23.8	7.2	14.0	309.0	5486.	18000.
5489.	18009.	505.8	1056.4	666.4	.041602	-8.8	16.2	-25.6	-14.1	24.3	7.7	15.0	303.0	5791.	19000.
5782.	18969.	486.1	1015.2	646.0	.040328	-11.0	12.2	-27.6	-17.7	24.1	6.7	13.0	299.0	6096.	20000.
6072.	19920.	467.2	975.8	626.1	.039086	-13.2	8.2	-29.7	-21.4	23.7	6.7	13.0	298.0	6401.	21000.
6363.	20876.	448.8	937.3	606.7	.037875	-15.4	4.3	-31.8	-25.2	23.2	7.2	14.0	299.0	6706.	22000.
6654.	21831.	431.0	900.2	587.8	.036695	-17.6	.3	-33.9	-29.0	22.6	7.7	15.0	299.0	7010.	23000.
6945.	22785.	413.8	864.2	569.3	.035540	-19.9	-3.8	-36.0	-32.8	22.5	7.7	15.0	300.0	7315.	24000.
7239.	23749.	397.0	829.2	551.3	.034417	-22.2	-8.0	-38.2	-36.7	22.1	8.7	17.0	301.0	7620.	25000.
7530.	24703.	380.9	795.5	534.1	.033343	-24.6	-12.3	-40.4	-40.8	21.7	9.3	18.0	302.0	7925.	26000.
7823.	25666.	365.2	762.7	517.4	.032300	-27.1	-16.8	-42.7	-44.9	21.4	10.3	20.0	305.0	8230.	27000.
8115.	26625.	350.1	731.2	501.0	.031276	-29.6	-21.3	-45.0	-49.0	21.1	10.8	21.0	306.0	8534.	28000.
8410.	27591.	335.4	700.5	485.0	.030278	-32.2	-26.0	-47.3	-53.2	20.9	10.3	20.0	308.0	8839.	29000.
8704.	28557.	321.2	670.8	469.5	.029310	-34.7	-30.5	-49.7	-57.4	20.5	10.3	20.0	308.0	9144.	30000.
9000.	29529.	307.4	642.0	454.3	.028361	-37.3	-35.1	-52.0	-61.7	20.3	11.3	22.0	309.0	9449.	31000.
9297.	30500.	294.1	614.2	439.4	.027431	-39.9	-39.8	-54.8	-66.7	19.0	10.8	21.0	310.0	9754.	32000.
9594.	31477.	281.2	587.3	424.9	.026526	-42.5	-44.5	-58.2	-72.8	16.5	0.0	0.0	0.0	10058.	33000.
9891.	32451.	268.8	561.4	410.7	.025639	-45.0	-49.0	-61.8	-79.2	13.8	0.0	0.0	0.0	10363.	34000.
10189.	33428.	256.8	536.3	396.9	.024778	-47.7	-53.9	-65.6	-86.1	11.3	0.0	0.0	0.0	10668.	35000.

TABLE 4.—Continued

H, m	H, ft	p, mb	p, lb/ft^2	RHO, gm/m^3	RHO, lb/ft^3	T, °C	T, °F	D, °C	D, °F	RH, percent	V, m/sec	V, knots	THETA, deg	Z, m	Z, ft
MONTH 10 DAY 4 YEAR 78 HOUR OF RELEASE 900Z															
715.	2347.	930.2	1942.8	1105.4	.069008	19.0	66.2	5.1	41.1	39.8	2.1	4.0	215.0	724.	2375.
897.	2944.	910.0	1900.6	1060.7	.066217	24.5	76.1	6.9	44.5	32.4	3.6	7.0	241.0	914.	3000.
1193.	3880.	879.0	1835.8	1021.5	.063770	25.4	77.7	6.2	43.2	29.3	6.2	12.0	282.0	1219.	4000.
1467.	4813.	849.0	1773.2	990.1	.061810	24.4	75.9	4.9	40.8	28.3	5.7	11.0	289.0	1524.	5000.
1751.	5746.	819.8	1712.2	964.7	.060224	21.9	71.4	3.4	38.1	29.7	6.2	12.0	283.0	1829.	6000.
2036.	6680.	791.4	1652.9	939.9	.058676	19.2	66.6	1.9	35.3	31.4	5.7	11.0	274.0	2134.	7000.
2322.	7617.	763.7	1595.0	915.5	.057153	16.6	61.9	.2	32.4	32.9	5.1	10.0	269.0	2438.	8000.
2608.	8558.	736.7	1538.6	891.6	.055661	13.9	57.0	-1.5	29.4	34.6	4.1	8.0	245.0	2743.	9000.
2895.	9498.	710.5	1483.9	868.2	.054200	11.3	52.3	-3.2	26.2	36.0	2.6	5.0	220.0	3048.	10000.
3183.	10444.	684.9	1430.4	844.3	.052708	8.9	48.0	-5.5	22.1	35.6	2.1	4.0	184.0	3353.	11000.
3471.	11388.	660.1	1378.6	820.3	.051210	6.7	44.1	-8.1	17.4	33.8	2.1	4.0	120.0	3658.	12000.
3759.	12333.	636.0	1328.3	796.9	.049749	4.5	40.1	-10.8	12.6	32.0	3.6	7.0	97.0	3962.	13000.
4047.	13279.	612.6	1279.4	773.9	.048313	2.3	36.1	-13.4	7.8	30.2	4.6	9.0	98.0	4267.	14000.
4337.	14229.	589.8	1231.8	751.5	.046915	0.0	32.0	-16.2	2.9	28.4	4.1	8.0	101.0	4572.	15000.
4625.	15175.	567.8	1185.9	729.5	.045541	-2.1	28.2	-18.9	-2.0	26.3	2.6	5.0	100.0	4877.	16000.
4916.	16128.	546.3	1141.0	708.1	.044205	-4.4	24.1	-21.7	-7.1	24.5	2.1	4.0	85.0	5182.	17000.
5204.	17075.	525.6	1097.7	687.1	.042894	-6.7	19.9	-24.6	-12.3	22.6	2.6	5.0	61.0	5486.	18000.
5495.	18029.	505.4	1055.5	666.6	.041614	-9.0	15.8	-27.5	-17.5	20.7	3.1	6.0	43.0	5791.	19000.
5788.	18989.	485.7	1014.4	646.1	.040335	-11.2	11.8	-29.6	-21.3	20.3	4.6	9.0	33.0	6096.	20000.
6078.	19940.	466.8	974.9	626.0	.039080	-13.3	8.1	-31.3	-24.4	20.4	6.2	12.0	27.0	6401.	21000.
6369.	20897.	448.4	936.5	606.3	.037850	-15.5	4.1	-33.1	-27.6	20.6	7.7	15.0	29.0	6706.	22000.
6661.	21853.	430.6	899.3	587.2	.036658	-17.6	.3	-34.9	-30.8	20.6	9.3	18.0	36.0	7010.	23000.
6952.	22808.	413.4	863.4	568.6	.035497	-19.8	-3.6	-36.7	-34.1	20.8	9.3	18.0	38.0	7315.	24000.
7244.	23766.	396.7	828.5	550.6	.034373	-22.1	-7.8	-38.6	-37.5	21.0	9.3	18.0	39.0	7620.	25000.
7535.	24721.	380.6	794.9	533.7	.033318	-24.7	-12.5	-40.7	-41.3	21.2	9.3	18.0	40.0	7925.	26000.
7829.	25685.	364.9	762.1	517.3	.032294	-27.3	-17.1	-42.9	-45.2	21.4	8.7	17.0	38.0	8230.	27000.
8121.	26644.	349.8	730.6	501.2	.031289	-29.9	-21.8	-45.1	-49.1	21.6	8.2	16.0	35.0	8534.	28000.
8416.	27611.	335.1	699.9	485.5	.030309	-32.6	-26.7	-47.3	-53.1	21.8	8.2	16.0	32.0	8839.	29000.
8712.	28584.	320.8	670.0	470.2	.029354	-35.3	-31.5	-49.6	-57.2	22.0	8.2	16.0	27.0	9144.	30000.
9007.	29551.	307.1	641.4	455.3	.028423	-38.1	-36.6	-51.9	-61.3	22.4	8.2	16.0	23.0	9449.	31000.
9306.	30530.	293.7	613.4	440.6	.027506	-40.8	-41.4	-54.8	-66.6	21.0	7.7	15.0	19.0	9754.	32000.
9604.	31508.	280.8	586.5	426.2	.026607	-43.5	-46.3	-58.4	-73.2	17.9	7.7	15.0	16.0	10058.	33000.
9903.	32491.	268.3	560.4	412.2	.025733	-46.2	-51.2	-62.3	-80.2	14.7	6.7	13.0	14.0	10363.	34000.
10202.	33470.	256.3	535.3	398.5	.024878	-49.0	-56.2	-66.6	-87.8	11.5	6.2	12.0	12.0	10668.	35000.
10504.	34461.	244.6	510.9	384.5	.024004	-51.4	-60.5	-69.8	-93.6	9.7	5.1	10.0	9.0	10973.	36000.
10804.	35446.	233.4	487.5	370.3	.023117	-53.5	-64.3	-71.5	-96.6	9.8	4.6	9.0	5.0	11278.	37000.
11105.	36434.	222.6	464.9	356.5	.022256	-55.5	-67.9	-73.1	-99.7	9.8	4.1	8.0	360.0	11582.	38000.
11409.	37430.	212.2	443.2	343.1	.021419	-57.6	-71.7	-74.9	-102.7	9.8	4.1	8.0	354.0	11887.	39000.
11718.	38444.	202.1	422.1	330.1	.020607	-59.7	-75.5	-76.6	-105.8	9.9	4.6	9.0	347.0	12192.	40000.
12026.	39457.	192.5	402.0	314.9	.019659	-60.0	-76.0	-76.8	-106.3	9.9	5.1	10.0	343.0	12497.	41000.
12333.	40464.	183.4	383.0	299.7	.018710	-59.8	-75.6	-76.7	-106.0	9.8	5.7	11.0	343.0	12802.	42000.
12642.	41475.	174.7	364.9	285.2	.017804	-59.6	-75.3	-76.5	-105.7	9.8	5.7	11.0	341.0	13106.	43000.
12950.	42488.	166.4	347.5	271.4	.016943	-59.4	-74.9	-76.3	-105.4	9.6	5.7	11.0	332.0	13411.	44000.
13259.	43500.	158.5	331.0	258.8	.016156	-59.6	-75.3	-76.5	-105.6	9.9	6.2	12.0	324.0	13716.	45000.
13565.	44509.	151.0	315.4	247.6	.015457	-60.5	-76.9	-77.3	-107.1	9.8	5.7	11.0	316.0	14021.	46000.
13876.	45525.	143.8	300.3	236.7	.014777	-61.3	-78.3	-77.9	-108.2	9.9	5.7	11.0	307.0	14326.	47000.
14189.	46548.	136.9	285.9	226.2	.014121	-62.1	-79.8	-78.5	-109.4	9.9	6.7	13.0	299.0	14630.	48000.
14496.	47560.	130.4	272.3	216.1	.013491	-62.9	-81.2	-79.2	-110.5	9.9	7.7	15.0	290.0	14935.	49000.
14810.	48591.	124.1	259.2	206.5	.012891	-63.7	-82.7	-79.8	-111.7	10.0	8.2	16.0	288.0	15240.	50000.

TABLE 4.-Continued

H, m	H, ft	p, mb	p, lb/ft^2	RHO, gm/m^3	RHO, lb/ft^3	T, °C	T, °F	D, °C	D, °F	RH, percent	V, m/sec	V, knots	THETA, deg	Z, m	Z, ft
							MONTH 10 DAY 5 YEAR 78 HOUR OF RELEASE 9007								
708.	2324.	931.0	1944.4	1103.3	.068877	20.0	68.0	3.0	37.3	32.3	1.5	3.0	225.0	724.	2375.
890.	2920.	910.8	1902.2	1062.4	.066323	24.5	76.1	4.8	40.7	28.0	2.1	4.0	209.0	914.	3000.
1175.	3856.	879.9	1837.5	1021.1	.063745	26.0	78.8	4.0	39.3	24.2	2.1	4.0	223.0	1219.	4000.
1459.	4787.	849.8	1774.8	991.7	.061910	24.5	76.1	1.6	34.8	22.2	2.6	5.0	306.0	1524.	5000.
1744.	5723.	820.5	1713.6	967.4	.060393	21.5	70.7	.7	33.3	25.1	4.1	8.0	310.0	1829.	6000.
2030.	6660.	792.0	1654.1	943.6	.058907	18.5	65.3	-.3	31.4	28.0	3.6	7.0	271.0	2134.	7000.
2317.	7600.	764.2	1596.1	920.3	.057452	15.4	59.7	-1.6	29.1	31.0	4.1	8.0	232.0	2438.	8000.
2604.	8544.	737.1	1539.5	897.4	.056023	12.3	54.1	-3.1	26.5	34.1	3.6	7.0	219.0	2743.	9000.
2894.	9494.	710.6	1484.1	875.0	.054624	9.2	48.6	-4.7	23.5	37.0	4.1	8.0	211.0	3048.	10000.
3184.	10447.	684.8	1430.2	852.1	.053195	6.2	43.2	-5.6	22.0	42.6	4.1	8.0	202.0	3353.	11000.
3475.	11399.	659.8	1376.0	829.2	.051765	3.5	38.3	-6.1	21.0	49.3	3.6	7.0	199.0	3658.	12000.
3766.	12357.	635.4	1327.1	804.0	.050192	1.8	35.2	-12.8	9.0	33.0	3.1	6.0	190.0	3962.	13000.
4057.	13312.	611.8	1277.6	778.9	.048625	.2	32.4	-15.3	4.5	30.1	3.1	6.0	190.0	4267.	14000.
4349.	14267.	588.9	1229.9	754.5	.047102	-1.4	29.5	-17.9	-.3	27.2	2.6	5.0	193.0	4572.	15000.
4639.	15219.	566.8	1183.8	730.8	.045622	-3.0	26.6	-20.6	-5.2	24.2	2.1	4.0	193.0	4877.	16000.
4928.	16169.	545.4	1139.1	707.6	.044174	-4.7	23.5	-23.5	-10.3	21.4	1.5	3.0	177.0	5182.	17000.
5219.	17121.	524.6	1095.6	685.0	.042763	-6.4	20.5	-26.5	-15.7	18.6	1.0	2.0	118.0	5486.	18000.
5508.	18072.	504.5	1053.7	663.1	.041396	-8.1	17.4	-29.7	-21.5	15.7	2.1	4.0	32.0	5791.	19000.
5798.	19023.	485.0	1012.9	643.3	.040160	-10.5	13.1	-32.0	-25.5	15.3	3.6	7.0	17.0	6096.	20000.
6089.	19976.	466.1	973.5	624.6	.038993	-13.1	8.4	-33.9	-29.0	15.7	4.1	8.0	11.0	6401.	21000.
6379.	20928.	447.8	935.2	606.2	.037844	-15.8	3.6	-35.9	-32.5	16.1	4.1	8.0	8.0	6706.	22000.
6671.	21886.	430.0	898.1	588.3	.036726	-18.4	-1.1	-37.9	-36.1	16.4	4.6	9.0	4.0	7010.	23000.
6964.	22847.	412.7	861.9	570.8	.035634	-21.2	-6.2	-39.9	-39.8	17.0	4.6	9.0	360.0	7315.	24000.
7258.	23813.	395.9	826.9	553.5	.034554	-23.9	-11.0	-42.0	-43.5	17.3	5.1	10.0	356.0	7620.	25000.
7552.	24776.	379.7	793.0	536.4	.033486	-26.4	-15.5	-44.0	-47.3	17.4	6.2	12.0	354.0	7925.	26000.
7846.	25741.	364.0	760.2	519.7	.032444	-29.0	-20.2	-46.1	-51.0	17.7	6.2	12.0	346.0	8230.	27000.
8141.	26709.	348.8	728.5	503.4	.031426	-31.7	-25.1	-48.3	-54.9	18.0	6.7	13.0	337.0	8534.	28000.
8438.	27684.	334.0	697.6	487.4	.030427	-34.3	-29.7	-50.4	-58.7	18.2	6.7	13.0	336.0	8839.	29000.
8736.	28661.	319.7	667.7	471.9	.029460	-37.0	-34.6	-52.6	-62.7	18.4	6.2	12.0	336.0	9144.	30000.
9033.	29637.	305.9	638.9	456.8	.028517	-39.7	-39.5	-54.9	-66.9	18.4	5.1	10.0	331.0	9449.	31000.
9333.	30620.	292.5	610.9	441.6	.027568	-42.3	-44.1	-62.4	-80.3	9.5	4.6	9.0	326.0	9754.	32000.
9632.	31601.	279.6	584.0	426.1	.026601	-44.5	-48.1	-64.2	-83.5	9.6	4.1	8.0	345.0	10058.	33000.
9933.	32587.	267.1	557.8	411.1	.025664	-46.6	-51.9	-65.9	-86.7	9.6	3.1	6.0	5.0	10363.	34000.
10232.	33570.	255.1	532.8	396.4	.024746	-48.9	-56.0	-67.7	-69.9	9.7	3.1	6.0	356.0	10668.	35000.
10533.	34556.	243.5	508.6	381.7	.023829	-50.8	-59.4	-69.3	-92.7	9.7	2.6	5.0	345.0	10973.	36000.
10831.	35536.	232.4	485.4	367.0	.022911	-52.4	-62.3	-70.6	-95.1	9.7	2.6	5.0	352.0	11278.	37000.
11131.	36519.	221.7	463.0	352.8	.022025	-54.1	-65.4	-72.0	-97.6	9.7	2.6	5.0	354.0	11582.	38000.
11432.	37508.	211.4	441.5	339.0	.021163	-55.8	-68.4	-73.4	-100.1	9.7	3.1	6.0	330.0	11887.	39000.
11737.	38506.	201.5	420.8	325.8	.020339	-57.5	-71.5	-74.8	-102.6	9.8	3.1	6.0	310.0	12192.	40000.
12043.	39511.	192.0	401.0	311.5	.019446	-58.3	-72.9	-75.4	-103.8	9.8	3.6	7.0	299.0	12497.	41000.
12351.	40521.	182.9	382.0	297.7	.018585	-58.9	-74.0	-75.9	-104.7	9.8	4.1	8.0	290.0	12802.	42000.
12656.	41523.	174.3	364.0	284.4	.017755	-59.6	-75.3	-76.4	-105.6	9.9	6.2	12.0	286.0	13106.	43000.
12966.	42538.	166.0	346.7	271.7	.016962	-60.2	-76.4	-76.9	-106.5	9.9	7.7	15.0	283.0	13411.	44000.
13275.	43553.	158.1	330.2	259.5	.016200	-60.8	-77.4	-77.4	-107.4	9.9	8.7	17.0	281.0	13716.	45000.
13583.	44564.	150.6	314.5	247.9	.015476	-61.4	-78.5	-78.0	-108.3	9.9	9.3	18.0	279.0	14021.	46000.
13894.	45583.	143.4	299.5	237.2	.014808	-62.5	-80.5	-78.9	-110.0	9.9	9.8	19.0	280.0	14326.	47000.
14206.	46609.	136.5	285.1	227.1	.014177	-63.7	-82.7	-79.8	-111.7	10.0	10.3	20.0	282.0	14630.	48000.
14525.	47656.	129.8	271.1	217.3	.013566	-64.9	-84.8	-80.6	-113.5	10.0	9.8	19.0	285.0	14935.	49000.
14841.	48691.	123.5	257.9	207.9	.012979	-66.1	-87.0	-81.8	-115.2	10.1	9.3	18.0	288.0	15240.	50000.

TABLE 4.–Continued

H, m	H, ft	p, mb	p, lb/ft^2	RHO, gm/m^3	RHO, lb/ft^3	T, °C	T, °F	D, °C	D, °F	RH, percent	V, m/sec	V, knots	THETA, deg	Z, m	Z, ft
MONTH 10 DAY 11 YEAR 78 HOUR OF RELEASE 900Z															
677.	2222.	934.5	1951.7	1133.2	.070743	13.3	55.9	2.5	36.6	48.0	1.0	2.0	355.0	724.	2375.
862.	2828.	913.9	1908.7	1081.3	.067503	20.4	68.7	3.5	38.4	32.8	1.0	2.0	321.0	914.	3000.
1153.	3783.	882.2	1842.5	1046.0	.065300	19.8	67.6	2.4	36.2	31.3	1.5	3.0	300.0	1219.	4000.
1443.	4734.	851.5	1778.4	1011.8	.063165	19.2	66.6	1.1	34.1	29.8	2.1	4.0	12.0	1524.	5000.
1733.	5684.	821.7	1716.2	984.8	.061479	16.8	62.2	-.8	30.6	30.2	3.6	7.0	84.0	1829.	6000.
2023.	6637.	792.7	1655.6	958.7	.059850	14.2	57.6	-2.8	27.0	30.8	4.1	8.0	70.0	2134.	7000.
2314.	7593.	764.4	1596.5	933.1	.058252	11.7	53.1	-4.8	23.4	31.2	4.6	9.0	44.0	2438.	8000.
2605.	8547.	737.0	1539.3	908.0	.056685	9.1	48.4	-6.8	19.7	31.7	4.6	9.0	13.0	2743.	9000.
2897.	9505.	710.3	1483.5	883.4	.055149	6.5	43.7	-8.9	16.0	32.2	4.6	9.0	15.0	3048.	10000.
3190.	10466.	684.3	1429.2	856.9	.053495	4.7	40.5	-11.0	12.1	30.9	3.1	6.0	29.0	3353.	11000.
3483.	11426.	659.1	1376.6	829.5	.051784	3.3	37.9	-13.2	8.2	28.5	3.6	7.0	26.0	3658.	12000.
3774.	12381.	634.8	1325.8	802.9	.050123	2.0	35.6	-15.5	4.1	26.0	4.1	8.0	41.0	3962.	13000.
4065.	13336.	611.2	1276.5	777.0	.048507	.7	33.3	-17.8	-.1	23.5	4.6	9.0	48.0	4267.	14000.
4355.	14289.	588.4	1228.9	753.0	.047008	-1.0	30.2	-19.8	-3.7	22.4	4.1	8.0	59.0	4572.	15000.
4645.	15240.	566.3	1182.7	730.3	.045591	-3.1	26.4	-21.5	-6.6	22.7	2.6	5.0	46.0	4877.	16000.
4936.	16196.	544.8	1137.8	707.7	.044180	-5.0	23.0	-23.2	-9.8	22.5	2.1	4.0	3.0	5182.	17000.
5226.	17145.	524.1	1094.6	685.7	.042807	-6.9	19.6	-25.0	-12.9	22.2	4.1	8.0	353.0	5486.	18000.
5516.	18096.	504.0	1052.6	664.2	.041465	-8.8	16.2	-26.7	-16.1	21.9	5.1	10.0	356.0	5791.	19000.
5807.	19053.	484.4	1011.7	644.1	.040210	-11.1	12.0	-28.5	-19.3	22.3	6.7	13.0	3.0	6096.	20000.
6098.	20007.	465.5	972.2	624.8	.039005	-13.5	7.7	-30.3	-22.6	22.8	6.7	13.0	2.0	6401.	21000.
6389.	20960.	447.2	934.0	605.9	.037825	-16.0	3.2	-32.2	-26.0	23.4	6.7	13.0	353.0	6706.	22000.
6681.	21918.	429.4	896.8	587.4	.036670	-18.4	-1.1	-34.1	-29.4	23.9	6.7	13.0	339.0	7010.	23000.
6972.	22875.	412.2	860.9	569.4	.035546	-20.9	-5.6	-36.0	-32.9	24.4	6.2	12.0	322.0	7315.	24000.
7265.	23836.	395.5	826.0	551.6	.034435	-23.3	-9.9	-38.0	-36.4	24.8	7.2	14.0	315.0	7620.	25000.
7559.	24800.	379.3	792.2	533.6	.033312	-25.4	-13.7	-39.9	-39.7	24.7	8.2	16.0	310.0	7925.	26000.
7852.	25760.	363.7	759.6	516.0	.032213	-27.5	-17.5	-41.8	-43.2	24.6	10.3	20.0	306.0	8230.	27000.
8145.	26722.	348.6	728.1	498.9	.031145	-29.7	-21.5	-43.7	-46.6	24.6	12.3	24.0	302.0	8534.	28000.
8438.	27684.	334.0	697.6	482.3	.030109	-31.8	-25.2	-45.6	-50.1	24.4	15.4	30.0	300.0	8839.	29000.
8734.	28654.	319.8	667.9	466.1	.029098	-34.0	-29.2	-47.5	-53.6	24.4	20.1	39.0	299.0	9144.	30000.
9027.	29615.	306.2	639.5	450.4	.028118	-36.2	-33.2	-49.5	-57.1	24.3	24.2	47.0	299.0	9449.	31000.
9322.	30582.	293.0	611.9	434.7	.027137	-38.3	-36.9	-52.0	-61.6	22.5	25.7	50.0	299.0	9754.	32000.
9615.	31547.	280.3	585.4	419.3	.026176	-40.2	-40.4	-55.1	-67.3	18.9	26.8	52.0	300.0	10058.	33000.
9911.	32515.	268.0	559.7	404.3	.025240	-42.1	-43.8	-58.5	-73.3	15.3	28.3	55.0	297.0	10363.	34000.
10204.	33478.	256.2	535.1	389.7	.024328	-44.0	-47.2	-62.3	-80.2	11.6	29.3	57.0	295.0	10668.	35000.
10498.	34444.	244.8	511.3	375.7	.023454	-46.0	-50.8	-65.4	-85.8	9.6	29.8	58.0	293.0	10973.	36000.
10793.	35410.	233.8	488.3	362.2	.022611	-48.1	-54.6	-67.1	-88.8	9.6	29.8	58.0	291.0	11278.	37000.
11088.	36378.	223.2	466.2	349.1	.021794	-50.3	-58.5	-68.9	-91.9	9.7	29.8	58.0	290.0	11582.	38000.
11335.	37351.	213.0	444.9	336.4	.021001	-52.4	-62.3	-70.6	-95.1	9.7	29.8	58.0	289.0	11887.	39000.
11683.	38331.	203.2	424.4	324.1	.020233	-54.6	-66.3	-72.4	-98.3	9.8	29.8	58.0	288.0	12192.	40000.
11984.	39317.	193.8	404.8	311.6	.019453	-56.4	-69.5	-73.9	-100.9	9.8	28.3	55.0	291.0	12497.	41000.
12289.	40317.	184.7	385.8	299.2	.018678	-58.0	-72.4	-75.2	-103.4	9.6	25.7	50.0	293.0	12802.	42000.
12599.	41333.	175.9	367.4	287.3	.017936	-59.7	-75.5	-76.5	-105.8	9.9	23.1	45.0	295.0	13106.	43000.
12905.	42339.	167.6	350.0	275.8	.017218	-61.3	-78.3	-77.9	-108.2	9.9	19.5	38.0	298.0	13411.	44000.
13219.	43369.	159.5	333.1	264.7	.016525	-63.0	-81.4	-79.3	-110.7	9.9	15.4	30.0	300.0	13716.	45000.
13533.	44399.	151.8	317.0	253.9	.015850	-64.7	-84.5	-80.7	-113.2	10.0	13.9	27.0	301.0	14021.	46000.
13850.	45438.	144.4	301.6	242.6	.015145	-65.6	-86.1	-81.4	-114.5	10.1	12.3	24.0	303.0	14326.	47000.
14165.	46472.	137.4	287.0	231.4	.014446	-66.2	-87.2	-81.9	-115.4	10.0	10.8	21.0	304.0	14630.	48000.
14482.	47512.	130.7	273.0	220.8	.013784	-66.8	-88.2	-82.4	-116.4	10.0	9.8	19.0	302.0	14935.	49000.
14801.	48557.	124.3	259.6	210.6	.013147	-67.4	-89.3	-82.9	-117.3	10.0	9.3	18.0	299.0	15240.	50000.

TABLE 4.–Continued

H, m	H, ft	p, mb	p, lb/ft^2	RHO, gm/m^3	RHO, lb/ft^3	T, °C	T, °F	D, °C	D, °F	RH, percent	V, m/sec	V, knots	THETA, deg	Z, m	Z, ft

MONTH 10 DAY 12 YEAR 78 HOUR OF RELEASE 9007

713.	2339.	930.5	1943.4	1121.5	.070013	15.2	59.4	.8	33.4	37.4	1.0	2.0	350.0	724.	2375.
897.	2944.	910.0	1900.6	1072.4	.066946	21.3	70.3	6.5	43.7	38.2	1.5	3.0	3.0	914.	3000.
1186.	3893.	879.6	1835.0	1032.4	.064451	22.1	71.8	6.5	43.8	36.5	2.6	5.0	15.0	1219.	4000.
1473.	4832.	848.4	1771.9	994.5	.062065	22.8	73.0	6.4	43.6	34.7	4.6	9.0	15.0	1524.	5000.
1758.	5769.	819.1	1710.7	968.0	.060430	20.5	68.9	4.6	40.3	35.2	5.7	11.0	50.0	1829.	6000.
2044.	6707.	790.6	1651.2	942.0	.058807	18.2	64.8	2.8	37.0	35.7	7.7	15.0	58.0	2134.	7000.
2331.	7645.	762.9	1593.3	916.6	.057221	15.9	60.6	.9	33.6	36.1	8.2	16.0	67.0	2438.	8000.
2617.	8586.	735.9	1537.0	891.6	.055661	13.6	56.5	-1.0	30.2	36.5	7.7	15.0	76.0	2743.	9000.
2904.	9527.	709.7	1482.2	667.2	.054138	11.2	52.2	-2.9	26.8	37.1	6.7	13.0	92.0	3048.	10000.
3192.	10474.	684.1	1428.8	842.5	.052596	9.1	48.4	-4.9	23.2	36.7	7.2	14.0	107.0	3353.	11000.
3479.	11415.	659.4	1377.2	817.9	.051060	7.1	44.8	-7.0	19.5	36.0	7.2	14.0	108.0	3658.	12000.
3769.	12361.	635.3	1326.9	793.9	.049562	5.2	41.4	-9.0	15.6	35.0	7.2	14.0	97.0	3962.	13000.
4055.	13304.	612.0	1278.2	770.4	.048095	3.2	37.6	-11.1	12.1	34.2	7.2	14.0	87.0	4267.	14000.
4342.	14246.	589.4	1231.0	747.5	.046665	1.2	34.2	-13.1	8.4	33.4	6.2	12.0	75.0	4572.	15000.
4631.	15192.	567.4	1185.0	725.2	.045273	-.8	30.6	-15.2	4.6	32.6	4.6	9.0	55.0	4877.	16000.
4919.	16137.	546.1	1140.6	703.3	.043906	-2.8	27.0	-17.3	.6	31.7	3.6	7.0	43.0	5182.	17000.
5206.	17080.	525.5	1097.5	682.0	.042576	-4.8	23.4	-19.5	-3.0	30.7	4.1	8.0	36.0	5486.	18000.
5494.	18024.	505.5	1055.6	661.2	.041277	-6.9	19.6	-21.6	-6.9	30.0	4.1	8.0	26.0	5791.	19000.
5783.	18974.	486.0	1015.0	641.5	.040048	-9.3	15.3	-23.6	-10.5	30.2	3.6	7.0	19.0	6096.	20000.
6072.	19920.	467.2	975.8	622.5	.038861	-11.7	10.9	-25.6	-14.1	30.5	3.1	6.0	16.0	6401.	21000.
6361.	20870.	448.9	937.5	604.0	.037706	-14.2	6.4	-27.7	-17.6	31.0	2.6	5.0	12.0	6706.	22000.
6651.	21820.	431.2	900.6	585.9	.036577	-16.8	1.8	-29.8	-21.6	31.7	2.1	4.0	4.0	7010.	23000.
6941.	22774.	414.0	864.7	568.2	.035472	-19.3	-2.7	-31.9	-25.3	32.1	1.5	3.0	4.0	7315.	24000.
7233.	23731.	397.3	829.8	550.8	.034385	-21.8	-7.2	-34.0	-29.2	32.4	1.5	3.0	14.0	7620.	25000.
7526.	24691.	381.1	795.9	533.7	.033318	-24.3	-11.7	-36.2	-33.1	32.6	1.5	3.0	17.0	7925.	26000.
7817.	25648.	365.5	763.4	517.0	.032275	-26.8	-16.2	-38.4	-37.0	32.7	1.5	3.0	19.0	8230.	27000.
8111.	26612.	350.3	731.6	500.8	.031264	-29.3	-20.7	-40.6	-41.1	32.8	1.5	3.0	347.0	8534.	28000.
8405.	27577.	335.6	700.9	484.9	.030271	-31.9	-25.4	-42.8	-45.1	33.1	2.1	4.0	318.0	8839.	29000.
8700.	28543.	321.4	671.3	469.4	.029304	-34.5	-30.1	-45.1	-49.2	33.4	4.1	8.0	305.0	9144.	30000.
8994.	29508.	307.7	642.6	454.3	.028361	-37.1	-34.8	-47.4	-53.4	33.5	7.2	14.0	297.0	9449.	31000.
9290.	30478.	294.4	614.9	438.7	.027387	-39.3	-38.7	-50.1	-58.1	31.2	10.3	20.0	296.0	9754.	32000.
9587.	31454.	281.5	587.9	422.5	.026376	-40.9	-41.6	-53.3	-63.9	25.3	14.4	28.0	296.0	10058.	33000.
9881.	32419.	269.2	562.2	406.8	.025396	-42.5	-44.5	-56.9	-70.5	19.4	18.0	35.0	296.0	10363.	34000.
10176.	33387.	257.3	537.4	391.7	.024453	-44.1	-47.4	-61.3	-78.3	13.4	22.1	43.0	296.0	10668.	35000.
10470.	34349.	245.9	513.6	377.1	.023542	-45.9	-50.6	-65.3	-85.5	9.6	26.2	51.0	295.0	10973.	36000.
10763.	35312.	234.9	490.6	363.2	.022674	-47.8	-54.0	-66.8	-88.3	9.7	29.3	57.0	295.0	11278.	37000.
11057.	36276.	224.3	468.5	349.8	.021837	-49.7	-57.5	-68.4	-91.1	9.7	31.9	62.0	295.0	11582.	38000.
11355.	37254.	214.0	446.9	336.8	.021026	-51.6	-60.9	-70.0	-93.9	9.7	31.9	62.0	296.0	11887.	39000.
11652.	38229.	204.2	426.5	324.1	.020233	-53.5	-64.3	-71.5	-96.8	9.7	31.9	62.0	296.0	12192.	40000.
11954.	39220.	194.7	406.6	311.7	.019459	-55.4	-67.7	-73.0	-99.5	9.8	29.8	58.0	298.0	12497.	41000.
12254.	40205.	185.7	387.8	299.6	.018703	-57.2	-71.0	-74.5	-102.0	9.9	27.3	53.0	299.0	12802.	42000.
12562.	41215.	176.9	369.5	287.9	.017973	-58.9	-74.0	-75.9	-104.7	9.8	24.7	48.0	301.0	13106.	43000.
12871.	42227.	168.5	351.9	276.5	.017261	-60.7	-77.3	-77.4	-107.3	9.9	22.1	43.0	303.0	13411.	44000.
13179.	43239.	160.5	335.2	265.6	.016581	-62.5	-80.5	-78.9	-110.0	9.9	21.6	42.0	302.0	13716.	45000.
13495.	44276.	152.7	318.9	255.0	.015919	-64.4	-83.9	-80.4	-112.7	10.0	20.6	40.0	302.0	14021.	46000.
13810.	45309.	145.3	303.5	244.7	.015276	-66.2	-87.2	-81.9	-115.4	10.1	20.1	39.0	304.0	14326.	47000.
14129.	46352.	138.2	288.6	234.7	.014652	-67.9	-90.2	-83.3	-118.0	10.1	19.5	38.0	305.0	14630.	48000.
14453.	47417.	131.3	274.2	225.0	.014046	-69.7	-93.5	-84.8	-120.7	10.1	17.5	34.0	305.0	14935.	49000.
14775.	48474.	124.8	260.7	214.8	.013410	-70.7	-95.3	-85.6	-122.1	10.2	16.5	32.0	306.0	15240.	50000.

TABLE 4.-Continued

H, m	H, ft	p, mb	p, lb/ft^2	RHO, gm/m^3	RHO, lb/ft^3	T, °C	T, °F	D, °C	D, °F	RH, percent	V, m/sec	V, knots	THETA, deg	Z, m	Z, ft
MONTH 10 DAY 13 YEAR 78 HOUR OF RELEASE 900Z															
691.	2265.	933.0	1948.6	1126.0	.070294	15.0	59.0	-4.9	23.1	24.9	2.1	4.0	285.0	724.	2375.
876.	2875.	912.3	1905.4	1092.5	.068203	17.2	63.0	-3.4	25.8	24.1	3.6	7.0	338.0	914.	3000.
1159.	3834.	880.5	1839.0	1041.6	.065025	20.7	69.3	-1.1	29.9	23.0	6.2	12.0	49.0	1219.	4000.
1456.	4778.	850.1	1775.5	993.6	.062028	24.1	75.4	1.1	33.9	21.9	8.2	16.0	59.0	1524.	5000.
1741.	5714.	820.8	1714.3	968.7	.060474	21.3	70.3	-.5	31.0	23.2	9.8	19.0	65.0	1829.	6000.
2027.	6650.	792.3	1654.8	944.4	.058957	18.4	65.1	-2.2	28.0	24.5	10.3	20.0	67.0	2134.	7000.
2314.	7593.	764.4	1596.5	920.5	.057465	15.5	59.9	-4.0	24.8	25.8	10.3	20.0	69.0	2438.	8000.
2602.	8537.	737.3	1539.9	897.1	.056004	12.6	54.7	-5.8	21.5	27.1	9.3	18.0	73.0	2743.	9000.
2891.	9483.	710.9	1484.7	874.1	.054568	9.7	49.5	-7.8	18.1	28.4	8.7	17.0	80.0	3048.	10000.
3180.	10432.	685.2	1431.1	848.2	.052951	7.8	46.0	-9.5	14.9	28.2	7.7	15.0	86.0	3353.	11000.
3469.	11380.	660.3	1379.1	820.7	.051235	6.8	44.2	-11.1	12.1	26.6	6.7	13.0	94.0	3658.	12000.
3757.	12325.	636.2	1328.7	793.9	.049562	5.7	42.3	-12.7	9.2	25.2	5.7	11.0	97.0	3962.	13000.
4044.	13267.	612.9	1280.1	768.7	.047988	4.3	39.7	-14.6	5.8	23.9	5.1	10.0	105.0	4267.	14000.
4331.	14208.	590.3	1232.9	749.0	.046759	1.2	34.2	-18.0	-.4	22.3	2.6	5.0	188.0	4572.	15000.
4620.	15157.	568.2	1186.7	728.1	.045454	-1.3	29.7	-20.4	-4.8	21.7	1.5	3.0	256.0	4877.	16000.
4909.	16106.	546.8	1142.0	706.8	.044124	-3.7	25.3	-22.3	-8.1	22.1	3.1	6.0	286.0	5182.	17000.
5197.	17052.	526.1	1098.8	686.0	.042826	-6.0	21.2	-24.2	-11.5	22.3	3.6	7.0	321.0	5486.	18000.
5488.	18005.	505.9	1056.6	665.7	.041558	-8.4	16.9	-26.0	-14.9	22.6	3.1	6.0	357.0	5791.	19000.
5777.	18954.	486.4	1015.9	646.4	.040353	-11.0	12.2	-28.1	-18.6	23.0	3.1	6.0	345.0	6096.	20000.
6068.	19909.	467.4	976.2	627.7	.039186	-13.7	7.3	-30.3	-22.5	23.3	3.1	6.0	320.0	6401.	21000.
6360.	20865.	449.0	937.8	609.4	.038044	-16.5	2.3	-32.5	-26.5	23.8	3.6	7.0	309.0	6706.	22000.
6653.	21826.	431.1	900.4	591.6	.036932	-19.2	-2.6	-34.7	-30.5	24.1	5.1	10.0	297.0	7010.	23000.
6947.	22791.	413.7	864.0	574.1	.035840	-22.1	-7.8	-37.0	-34.6	24.7	6.7	13.0	298.0	7315.	24000.
7242.	23760.	396.8	828.7	556.8	.034760	-24.8	-12.6	-39.1	-38.3	25.4	8.2	16.0	299.0	7620.	25000.
7537.	24727.	380.5	794.7	536.8	.033636	-27.1	-16.8	-40.3	-40.5	27.7	10.3	20.0	302.0	7925.	26000.
7833.	25698.	364.7	761.7	521.3	.032544	-29.3	-20.7	-41.6	-42.8	29.6	12.3	24.0	303.0	8230.	27000.
8129.	26670.	349.4	729.7	504.5	.031495	-31.8	-25.2	-41.9	-43.4	36.4	14.9	29.0	303.0	8534.	28000.
8426.	27644.	334.6	698.8	488.9	.030521	-34.6	-30.3	-39.4	-38.9	61.8	17.5	34.0	303.0	8839.	29000.
8721.	28612.	320.4	669.2	470.4	.029366	-35.8	-32.4	-43.5	-46.3	45.1	19.5	38.0	303.0	9144.	30000.
9018.	29587.	306.6	640.3	453.8	.028330	-37.7	-35.9	-44.4	-48.0	49.5	21.1	41.0	304.0	9449.	31000.
9315.	30560.	293.3	612.6	437.7	.027325	-39.6	-39.3	-46.8	-52.2	46.5	22.1	43.0	304.0	9754.	32000.
9611.	31531.	280.5	585.8	422.2	.026357	-41.6	-42.9	-50.8	-59.4	36.5	22.6	44.0	303.0	10058.	33000.
9906.	32499.	268.2	560.1	407.1	.025414	-43.6	-46.5	-55.4	-67.8	26.1	22.6	44.0	303.0	10363.	34000.
10202.	33470.	256.3	535.3	392.5	.024503	-45.6	-50.1	-61.4	-78.5	15.5	22.1	43.0	303.0	10668.	35000.
10498.	34444.	244.8	511.3	378.3	.023616	-47.6	-53.7	-66.7	-88.0	9.6	21.6	42.0	302.0	10973.	36000.
10793.	35410.	233.8	488.3	364.5	.022755	-49.6	-57.3	-68.3	-91.0	9.7	21.1	41.0	302.0	11278.	37000.
11091.	36387.	223.1	466.0	351.0	.021912	-51.6	-60.9	-70.0	-93.9	9.7	21.1	41.0	301.0	11582.	38000.
11388.	37361.	212.9	444.7	338.0	.021101	-53.7	-64.7	-71.6	-96.9	9.8	20.6	40.0	301.0	11887.	39000.
11690.	38352.	203.0	424.0	325.4	.020314	-55.7	-68.3	-73.3	-99.9	9.8	20.1	39.0	300.0	12192.	40000.
11994.	39349.	193.5	404.1	312.9	.019534	-57.6	-71.7	-74.9	-102.7	9.8	20.1	39.0	300.0	12497.	41000.
12299.	40351.	184.4	385.1	300.7	.018772	-59.4	-74.9	-76.3	-105.4	9.6	19.5	38.0	302.0	12802.	42000.
12609.	41368.	175.6	366.7	288.9	.018035	-61.3	-78.3	-77.6	-108.1	10.0	18.5	36.0	303.0	13106.	43000.
12920.	42388.	167.2	349.2	277.4	.017318	-63.1	-81.6	-79.4	-110.8	9.9	17.5	34.0	305.0	13411.	44000.
13235.	43421.	159.1	332.3	266.4	.016631	-65.0	-85.0	-80.9	-113.6	10.0	16.5	32.0	306.0	13716.	45000.
13554.	44467.	151.3	316.0	255.7	.015963	-66.9	-88.4	-82.4	-116.4	10.1	15.4	30.0	308.0	14021.	46000.
13872.	45511.	143.9	300.5	245.0	.015295	-68.5	-91.3	-83.8	-118.8	10.2	14.4	28.0	311.0	14326.	47000.
14197.	46579.	136.7	285.5	234.6	.014646	-70.0	-94.0	-85.1	-121.1	10.1	13.9	27.0	314.0	14630.	48000.
14521.	47640.	129.9	271.3	224.6	.014021	-71.6	-96.9	-86.3	-123.4	10.3	12.9	25.0	316.0	14935.	49000.
14845.	48703.	123.4	257.7	214.9	.013416	-73.0	-99.4	-87.5	-125.5	10.3	11.8	23.0	319.0	15240.	50000.

TABLE 4.-Continued

H,		p,		RHO,		T,		D,		RH,	V,		THETA,	Z,	
m	ft	mb	lb/ft^2	gm/m^3	lb/ft^3	°C	°F	°C	°F	percent	m/sec	knots	deg	m	ft
						MONTH 10 DAY 24 YEAR 78 HOUR OF RELEASE 9007									
717.	2353.	930.0	1942.3	1141.2	.071243	10.3	50.5	-4.2	24.5	35.9	2.1	4.0	225.0	724.	2375.
905.	2971.	909.1	1898.7	1096.6	.068459	15.1	59.2	-1.6	29.1	31.6	3.6	7.0	302.0	914.	3000.
1200.	3936.	877.2	1832.1	1048.6	.065462	17.6	63.7	-.3	31.4	29.6	6.2	12.0	44.0	1219.	4000.
1492.	4895.	846.4	1767.7	1019.0	.063614	15.5	59.9	-1.0	30.3	32.3	8.7	17.0	54.0	1524.	5000.
1785.	5856.	816.4	1705.1	992.2	.061941	12.8	55.0	-1.2	29.6	37.9	9.3	18.0	60.0	1829.	6000.
2079.	6820.	787.2	1644.1	966.1	.060312	10.0	50.0	-1.8	28.7	43.6	9.8	19.0	61.0	2134.	7000.
2374.	7790.	758.7	1584.6	940.5	.058713	7.2	45.0	-2.7	27.1	49.3	9.3	18.0	59.0	2438.	8000.
2670.	8760.	731.0	1526.7	915.2	.057134	4.4	39.9	-2.9	26.9	59.2	9.8	19.0	56.0	2743.	9000.
2965.	9732.	704.1	1470.5	890.4	.055586	1.7	35.1	-3.4	25.9	69.0	9.8	19.0	52.0	3048.	10000.
3264.	10707.	677.9	1415.8	865.0	.054000	-.7	30.7	-3.9	24.9	78.7	9.6	19.0	49.0	3353.	11000.
3561.	11683.	652.5	1362.8	838.5	.052346	-2.5	27.5	-6.3	20.7	75.3	10.3	20.0	47.0	3658.	12000.
3858.	12657.	627.9	1311.4	810.7	.050610	-3.6	25.5	-10.9	12.5	57.1	11.3	22.0	47.0	3962.	13000.
4154.	13630.	604.1	1261.7	783.8	.048931	-4.8	23.4	-15.1	4.7	44.2	12.3	24.0	47.0	4267.	14000.
4450.	14600.	581.1	1213.7	757.7	.047302	-6.0	21.2	-20.4	-4.6	31.1	13.9	27.0	46.0	4572.	15000.
4744.	15566.	558.9	1167.3	733.6	.045797	-7.8	18.0	-22.4	-8.4	29.8	13.9	27.0	43.0	4877.	16000.
5039.	16532.	537.4	1122.4	710.4	.044349	-9.7	14.5	-23.7	-10.6	31.0	13.4	26.0	39.0	5182.	17000.
5334.	17501.	516.5	1078.7	687.8	.042938	-11.6	11.1	-24.9	-12.9	32.2	12.9	25.0	34.0	5486.	18000.
5629.	18468.	496.3	1036.5	666.0	.041577	-13.6	7.5	-26.4	-15.5	33.2	12.9	25.0	32.0	5791.	19000.
5923.	19433.	476.8	995.8	645.9	.040322	-16.0	3.2	-28.5	-19.3	33.4	13.4	26.0	34.0	6096.	20000.
6219.	20404.	457.8	956.1	626.2	.039092	-18.4	-1.1	-30.6	-23.1	33.5	14.4	28.0	37.0	6401.	21000.
6515.	21376.	439.4	917.7	607.0	.037894	-20.9	-5.6	-32.8	-27.0	33.8	16.5	32.0	40.0	6706.	22000.
6812.	22349.	421.6	880.5	588.3	.036726	-23.4	-10.1	-34.9	-30.9	34.0	18.0	35.0	37.0	7010.	23000.
7108.	23320.	404.4	844.6	570.0	.035584	-25.9	-14.6	-37.1	-34.8	34.2	19.5	38.0	34.0	7315.	24000.
7405.	24296.	387.7	809.7	551.5	.034429	-28.2	-18.8	-39.9	-39.9	31.7	21.6	42.0	32.0	7620.	25000.
7704.	25276.	371.5	775.9	533.4	.033299	-30.4	-22.7	-43.0	-45.4	28.2	24.7	48.0	30.0	7925.	26000.
8002.	26253.	355.9	743.3	515.7	.032194	-32.7	-26.9	-46.2	-51.2	24.8	28.8	56.0	28.0	8230.	27000.
8300.	27232.	340.8	711.8	495.0	.030902	-33.2	-27.8	-48.3	-55.0	20.6	32.9	64.0	27.0	8534.	28000.
8595.	28199.	326.4	681.7	477.1	.029784	-34.7	-30.5	-50.3	-58.6	19.0	37.0	72.0	28.0	8839.	29000.
8892.	29173.	312.4	652.5	461.2	.028792	-37.1	-34.8	-52.3	-62.1	19.3	39.6	77.0	28.0	9144.	30000.
9189.	30146.	298.9	624.3	445.7	.027824	-39.4	-38.9	-54.3	-65.8	19.2	41.7	81.0	29.0	9449.	31000.
9487.	31125.	285.8	596.9	430.1	.026850	-41.5	-42.7	-57.2	-71.0	16.8	42.7	83.0	28.0	9754.	32000.
9782.	32093.	273.3	570.8	415.0	.025908	-43.6	-46.5	-60.3	-76.5	14.4	42.7	83.0	28.0	10058.	33000.
10081.	33074.	261.1	545.3	400.3	.024990	-45.8	-50.4	-63.5	-82.3	12.0	43.2	84.0	27.0	10363.	34000.
10379.	34050.	249.4	520.9	386.0	.024097	-47.9	-54.2	-66.9	-88.5	9.6	42.7	83.0	27.0	10668.	35000.
10674.	35019.	238.2	497.5	371.4	.023186	-49.7	-57.5	-68.4	-91.1	9.7	42.2	82.0	28.0	10973.	36000.
10973.	35999.	227.3	474.7	356.4	.022249	-50.9	-59.6	-69.3	-92.8	9.7	40.1	78.0	27.0	11278.	37000.
11270.	36974.	216.9	453.0	340.3	.021244	-51.0	-59.8	-69.4	-93.0	9.7	38.1	74.0	26.0	11582.	38000.
11563.	37936.	207.1	432.5	325.0	.020269	-51.1	-60.0	-69.5	-93.1	9.7	36.0	70.0	27.0	11887.	39000.
11861.	38913.	197.6	412.7	310.5	.019384	-51.3	-60.3	-69.7	-93.5	9.7	33.4	65.0	28.0	12192.	40000.
12156.	39883.	188.6	393.9	297.3	.018560	-52.1	-61.8	-70.3	-94.6	9.8	29.8	58.0	29.0	12497.	41000.
12456.	40865.	179.9	375.7	284.6	.017767	-52.8	-63.0	-70.9	-95.6	9.7	25.7	50.0	30.0	12802.	42000.
12755.	41848.	171.6	358.4	272.4	.017005	-53.5	-64.3	-71.5	-96.7	9.7	21.6	42.0	34.0	13106.	43000.
13054.	42828.	163.7	341.9	260.7	.016275	-54.3	-65.7	-72.1	-97.8	9.8	18.5	36.0	40.0	13411.	44000.
13356.	43818.	156.1	326.0	249.5	.015576	-55.0	-67.0	-72.7	-98.9	9.7	15.4	30.0	46.0	13716.	45000.
13659.	44814.	148.8	310.8	238.8	.014908	-55.9	-68.6	-73.4	-100.2	9.8	11.8	23.0	51.0	14021.	46000.
13960.	45802.	141.9	296.4	229.0	.014296	-57.1	-70.8	-74.5	-102.0	9.8	8.2	16.0	57.0	14326.	47000.
14267.	46808.	135.2	282.4	219.5	.013703	-58.4	-73.1	-75.5	-103.9	9.8	6.7	13.0	50.0	14630.	48000.
14575.	47817.	128.8	269.0	210.4	.013135	-59.7	-75.5	-76.5	-105.8	9.9	5.1	10.0	43.0	14935.	49000.
14882.	48827.	122.7	256.3	201.6	.012585	-61.0	-77.8	-77.6	-107.7	9.9	4.1	8.0	27.0	15240.	50000.

TABLE 4.—Continued

H, m	H, ft	p, mb	p, lb/ft^2	RHO, gm/m^3	RHO, lb/ft^3	T, °C	T, °F	D, °C	D, °F	RH, percent	V, m/sec	V, knots	THETA, deg	Z, m	Z, ft
							MONTH 10 DAY 25 YEAR 76 HOUR OF RELEASE 900Z								
732.	2400.	928.4	1939.0	1117.2	.069745	15.1	59.2	7.7	45.9	61.4	4.1	8.0	225.0	724.	2375.
916.	3006.	907.9	1896.2	1085.0	.067734	17.6	63.7	1.3	34.4	33.4	5.7	11.0	243.0	914.	3000.
1210.	3969.	876.1	1829.8	1047.0	.065362	17.9	64.2	-7.3	18.9	17.3	7.2	14.0	273.0	1219.	4000.
1502.	4929.	845.3	1765.4	1015.4	.063389	16.5	61.7	-10.0	14.0	15.2	5.7	11.0	305.0	1524.	5000.
1794.	5886.	815.5	1703.2	985.2	.061504	14.9	58.8	-12.5	9.5	13.6	5.1	10.0	328.0	1829.	6000.
2086.	6844.	786.5	1642.6	955.8	.059669	13.3	55.9	-15.1	4.9	12.5	5.7	11.0	329.0	2134.	7000.
2377.	7800.	758.4	1584.0	924.0	.057683	12.6	54.7	-17.3	.8	10.8	4.6	9.0	331.0	2438.	8000.
2666.	8746.	731.4	1527.6	891.6	.055661	12.4	54.3	-17.5	.5	10.8	3.6	7.0	341.0	2743.	9000.
2955.	9695.	705.1	1472.6	868.2	.054200	9.6	49.3	-17.4	.7	13.1	3.1	6.0	343.0	3048.	10000.
3244.	10643.	679.6	1419.4	844.1	.052695	7.2	45.0	-18.5	-1.3	14.0	3.6	7.0	332.0	3353.	11000.
3534.	11593.	654.8	1367.6	820.2	.051203	4.8	40.6	-19.8	-3.7	14.8	6.2	12.0	327.0	3658.	12000.
3825.	12549.	630.6	1317.0	796.8	.049743	2.4	36.3	-21.3	-6.3	15.5	8.7	17.0	336.0	3962.	13000.
4115.	13501.	607.2	1268.2	773.9	.048313	.1	32.2	-22.7	-8.8	16.2	10.8	21.0	341.0	4267.	14000.
4406.	14454.	584.5	1220.8	751.0	.046883	-2.1	28.2	-22.6	-8.7	19.1	11.6	23.0	341.0	4572.	15000.
4697.	15411.	562.4	1174.6	728.6	.045485	-4.3	24.3	-22.9	-9.1	22.0	11.8	23.0	341.0	4877.	16000.
4989.	16368.	541.0	1129.9	706.8	.044124	-6.5	20.3	-23.4	-10.0	24.9	11.8	23.0	344.0	5182.	17000.
5280.	17322.	520.3	1086.7	685.5	.042794	-8.8	16.2	-24.1	-11.3	27.9	12.3	24.0	344.0	5486.	18000.
5573.	18284.	500.1	1044.5	664.8	.041502	-11.1	12.0	-24.9	-12.8	31.0	14.4	28.0	342.0	5791.	19000.
5865.	19242.	480.6	1003.8	645.1	.040272	-13.6	7.5	-26.1	-15.0	34.1	15.9	31.0	338.0	6096.	20000.
6158.	20202.	461.7	964.3	625.9	.039074	-16.2	2.8	-27.4	-17.3	37.4	18.0	35.0	338.0	6401.	21000.
6452.	21167.	443.3	925.9	607.0	.037894	-18.8	-1.8	-25.4	-13.7	56.2	19.0	37.0	340.0	6706.	22000.
6746.	22133.	425.5	888.7	588.6	.036745	-21.4	-6.5	-25.2	-13.4	71.4	19.0	37.0	339.0	7010.	23000.
7042.	23103.	408.2	852.5	570.5	.035615	-23.9	-11.0	-27.6	-17.6	71.6	19.0	37.0	337.0	7315.	24000.
7337.	24071.	391.5	817.7	552.4	.034485	-26.3	-15.3	-29.9	-21.8	71.6	19.5	38.0	335.0	7620.	25000.
7633.	25043.	375.3	783.8	534.5	.033368	-28.5	-19.3	-32.2	-25.9	70.5	19.5	38.0	333.0	7925.	26000.
7930.	26018.	359.6	751.0	517.0	.032275	-30.8	-23.4	-34.5	-30.1	70.0	19.5	38.0	329.0	8230.	27000.
8226.	26989.	344.5	719.5	500.0	.031214	-33.1	-27.6	-36.8	-34.3	69.3	19.5	38.0	325.0	8534.	28000.
8524.	27968.	329.8	688.8	483.5	.030184	-35.4	-31.7	-39.2	-38.5	68.4	20.6	40.0	324.0	8839.	29000.
8821.	28940.	315.7	659.4	467.3	.029173	-37.7	-35.9	-41.5	-42.7	67.5	22.1	43.0	322.0	9144.	30000.
9119.	29919.	302.0	630.7	451.9	.028211	-40.2	-40.4	-53.7	-64.7	22.4	22.6	44.0	321.0	9449.	31000.
9419.	30897.	288.8	603.2	436.3	.027237	-42.5	-44.5	-62.5	-80.6	9.6	23.1	45.0	320.0	9754.	32000.
9717.	31881.	276.0	576.4	420.9	.026276	-44.6	-48.3	-64.3	-83.7	9.6	24.2	47.0	320.0	10058.	33000.
10016.	32862.	263.7	550.7	406.0	.025346	-46.8	-52.2	-66.0	-86.8	9.7	25.7	50.0	320.0	10363.	34000.
10316.	33847.	251.8	525.9	391.5	.024441	-48.9	-56.0	-67.8	-90.0	9.6	25.2	49.0	320.0	10668.	35000.
10615.	34826.	240.4	502.1	377.7	.023579	-51.3	-60.3	-69.7	-93.5	9.7	24.2	47.0	319.0	10973.	36000.
10917.	35817.	229.3	478.9	363.8	.022711	-53.4	-64.1	-71.4	-96.6	9.7	23.7	46.0	320.0	11278.	37000.
11217.	36802.	218.7	456.8	347.4	.021687	-53.7	-64.7	-71.6	-97.0	9.8	24.2	47.0	322.0	11582.	38000.
11517.	37786.	208.6	435.7	331.8	.020714	-53.9	-65.0	-71.9	-97.3	9.7	23.1	45.0	326.0	11887.	39000.
11816.	38766.	199.0	415.6	316.9	.019783	-54.2	-65.6	-72.1	-97.8	9.7	20.6	40.0	331.0	12192.	40000.
12116.	39751.	189.8	396.4	303.1	.018922	-54.9	-66.8	-72.7	-98.8	9.7	18.0	35.0	337.0	12497.	41000.
12417.	40738.	181.0	378.0	289.9	.018098	-55.6	-68.1	-73.2	-99.8	9.6	17.0	33.0	342.0	12802.	42000.
12722.	41739.	172.5	360.3	277.3	.017311	-56.3	-69.3	-73.8	-100.6	9.6	15.9	31.0	347.0	13106.	43000.
13023.	42727.	164.5	343.6	265.2	.016556	-57.0	-70.6	-74.3	-101.8	9.8	14.9	29.0	352.0	13411.	44000.
13331.	43738.	156.7	327.3	253.5	.015825	-57.7	-71.9	-74.9	-102.8	9.9	13.4	26.0	355.0	13716.	45000.
13634.	44730.	149.4	312.0	242.4	.015133	-58.4	-73.1	-75.5	-103.8	9.9	11.8	23.0	358.0	14021.	46000.
13943.	45743.	142.3	297.2	232.0	.014483	-59.4	-74.9	-76.3	-105.3	9.9	10.3	20.0	354.0	14326.	47000.
14248.	46747.	135.6	283.2	222.1	.013865	-60.4	-76.7	-77.1	-106.8	10.0	9.3	18.0	350.0	14630.	48000.
14559.	47769.	129.1	269.6	212.5	.013266	-61.4	-78.5	-77.9	-108.2	10.0	8.2	16.0	346.0	14935.	49000.
14872.	48793.	122.9	256.7	203.3	.012692	-62.4	-80.3	-78.7	-109.7	10.0	7.7	15.0	341.0	15240.	50000.

H, m	H, ft	p, mb	p, lb/ft^2	RHO, gm/m^3	RHO, lb/ft^3	T, °C	T, °F	D, °C	D, °F	RH, percent	V, m/sec	V, knots	THETA, deg	Z, m	Z, ft

MONTH 10 DAY 25 YEAR 78 HOUR OF RELEASE 1900Z

709.	2327.	930.9	1944.2	1099.9	.068665	21.5	70.7	-13.7	7.4	8.3	1.5	3.0	125.0	724.	2375.
892.	2926.	910.6	1901.8	1078.8	.067347	20.7	69.3	-12.2	10.0	9.8	1.0	2.0	93.0	914.	3000.
1194.	3883.	878.9	1835.6	1045.6	.065275	19.4	66.9	-10.4	13.2	12.3	1.0	2.0	50.0	1219.	4000.
1476.	4841.	848.1	1771.3	1013.6	.063277	18.0	64.4	-9.3	15.3	14.7	1.5	3.0	49.0	1524.	5000.
1766.	5795.	818.3	1709.1	985.8	.061541	15.7	60.3	-10.2	13.6	15.8	4.1	8.0	57.0	1829.	6000.
2057.	6750.	789.3	1648.5	958.6	.059843	13.4	56.1	-11.3	11.7	16.8	6.2	12.0	49.0	2134.	7000.
2349.	7707.	761.1	1589.6	932.0	.058183	11.0	51.8	-12.4	9.7	18.0	7.2	14.0	43.0	2438.	8000.
2641.	8664.	733.7	1532.4	906.0	.056560	8.7	47.7	-13.6	7.5	19.1	6.2	12.0	32.0	2743.	9000.
2934.	9625.	707.0	1476.6	880.6	.054974	6.3	43.3	-14.9	5.2	20.2	5.7	11.0	24.0	3048.	10000.
3227.	10587.	681.1	1422.5	850.7	.053107	5.5	41.9	-15.6	3.9	20.1	5.7	11.0	35.0	3353.	11000.
3517.	11539.	656.2	1370.5	820.1	.051197	5.4	41.7	-16.2	2.9	19.4	6.7	13.0	34.0	3658.	12000.
3805.	12485.	632.2	1320.4	790.6	.049356	5.2	41.4	-16.7	1.9	18.7	8.2	16.0	24.0	3962.	13000.
4093.	13427.	609.0	1271.9	762.1	.047576	5.0	41.0	-17.3	.9	18.1	9.8	19.0	15.0	4267.	14000.
4377.	14361.	586.7	1225.3	734.7	.045866	4.8	40.6	-17.9	-.1	17.5	10.8	21.0	22.0	4572.	15000.
4660.	15289.	565.2	1180.4	708.2	.044211	4.7	40.5	-18.5	-1.2	16.8	10.3	20.0	34.0	4877.	16000.
4941.	16209.	544.5	1137.2	682.6	.042613	4.5	40.1	-19.1	-2.3	16.1	9.3	18.0	43.0	5182.	17000.
5220.	17126.	524.5	1095.4	658.0	.041078	4.3	39.7	-19.7	-3.4	15.5	9.8	19.0	43.0	5486.	18000.
5498.	18038.	505.2	1055.1	634.3	.039598	4.1	39.4	-20.3	-4.6	14.9	12.9	25.0	351.0	5791.	19000.
5776.	18949.	486.5	1016.1	619.1	.038649	.4	32.7	-20.5	-4.9	19.1	17.5	34.0	337.0	6096.	20000.
6056.	19869.	468.2	977.9	607.3	.037913	-4.6	23.7	-21.6	-7.0	25.0	19.0	37.0	331.0	6401.	21000.
6339.	20796.	450.3	940.5	595.7	.037188	-9.9	14.2	-23.7	-10.7	31.4	12.3	24.0	350.0	6706.	22000.
6625.	21738.	432.7	903.7	584.4	.036483	-15.2	4.6	-26.4	-15.6	37.7	12.3	24.0	15.0	7010.	23000.
6916.	22689.	415.5	867.8	573.3	.035790	-20.7	-5.3	-29.7	-21.5	44.4	12.3	24.0	23.0	7315.	24000.
7212.	23661.	398.5	832.3	561.8	.035072	-26.0	-14.8	-33.3	-28.0	50.3	12.9	25.0	5.0	7620.	25000.
7508.	24631.	382.1	798.0	543.5	.033930	-28.2	-18.6	-35.8	-32.4	48.2	13.4	26.0	353.0	7925.	26000.
7804.	25604.	366.2	764.8	525.7	.032818	-30.4	-22.7	-38.3	-36.9	46.1	14.4	28.0	352.0	8230.	27000.
8101.	26580.	350.8	732.7	508.3	.031732	-32.7	-26.9	-40.8	-41.5	44.3	15.4	30.0	348.0	8534.	28000.
8399.	27557.	335.9	701.5	491.4	.030677	-34.9	-30.8	-43.4	-46.1	41.9	17.5	34.0	341.0	8839.	29000.
8698.	28536.	321.5	671.5	474.9	.029647	-37.2	-35.0	-46.0	-50.7	39.8	18.5	36.0	337.0	9144.	30000.
8996.	29515.	307.6	642.4	458.9	.028648	-39.5	-39.1	-48.6	-55.4	37.7	17.0	33.0	349.0	9449.	31000.
9297.	30500.	294.1	614.2	443.0	.027656	-41.7	-43.1	-51.6	-60.9	33.6	15.4	30.0	360.0	9754.	32000.
9594.	31477.	281.2	587.3	427.4	.026682	-43.8	-46.8	-55.3	-67.6	27.0	14.4	28.0	9.0	10058.	33000.
9893.	32459.	268.7	561.2	412.2	.025733	-45.9	-50.6	-59.5	-75.1	20.4	13.4	26.0	18.0	10363.	34000.
10194.	33445.	256.6	535.9	397.4	.024809	-48.1	-54.6	-64.5	-84.1	13.7	14.4	28.0	30.0	10668.	35000.
10493.	34426.	245.0	511.7	382.4	.023872	-49.8	-57.6	-68.5	-91.3	9.7	14.9	29.0	42.0	10973.	36000.
10790.	35401.	233.9	488.5	367.1	.022917	-51.1	-60.0	-69.5	-93.1	9.7	14.9	29.0	46.0	11278.	37000.
11088.	36378.	223.2	466.2	352.3	.021993	-52.3	-62.1	-70.5	-94.9	9.7	14.9	29.0	50.0	11582.	38000.
11388.	37361.	212.9	444.7	338.0	.021101	-53.6	-64.5	-71.6	-96.8	9.8	15.4	30.0	49.0	11887.	39000.
11686.	38341.	203.1	424.2	324.2	.020239	-54.8	-66.6	-72.6	-98.6	9.7	16.5	32.0	45.0	12192.	40000.
11987.	39338.	193.6	404.3	308.9	.019284	-54.7	-66.5	-72.4	-98.4	9.8	15.4	30.0	41.0	12497.	41000.
12289.	40317.	184.7	385.8	293.5	.018323	-53.8	-64.8	-71.7	-97.1	9.7	14.4	28.0	36.0	12802.	42000.
12587.	41297.	176.2	368.0	278.8	.017405	-52.9	-63.2	-71.0	-95.9	9.7	13.4	26.0	32.0	13106.	43000.
12886.	42277.	168.1	351.1	265.0	.016543	-52.1	-61.8	-70.3	-94.6	9.7	12.9	25.0	28.0	13411.	44000.
13193.	43252.	160.4	335.0	254.2	.015869	-53.2	-63.8	-71.3	-96.3	9.7	11.8	23.0	27.0	13716.	45000.
13497.	44248.	152.9	319.3	245.1	.015301	-55.7	-68.3	-73.3	-99.9	9.8	10.8	21.0	26.0	14021.	46000.
13798.	45238.	145.8	304.5	235.8	.014721	-57.6	-71.7	-74.8	-102.7	9.8	10.3	20.0	25.0	14326.	47000.
14096.	46246.	138.9	290.1	226.3	.014127	-59.2	-74.6	-76.1	-105.0	9.9	10.8	21.0	24.0	14630.	48000.
14405.	47259.	132.3	276.3	217.2	.013559	-60.8	-77.4	-77.4	-107.4	10.0	11.3	22.0	22.0	14935.	49000.
14714.	48274.	126.0	263.2	208.4	.013010	-62.4	-80.3	-78.7	-109.7	10.0	11.8	23.0	23.0	15240.	50000.

TABLE 4.–Continued

H, m	H, ft	p, mb	p, lb/ft^2	RHO, gm/m^3	RHO, lb/ft^3	T, °C	T, °F	D, °C	D, °F	RH, percent	V, m/sec	V, knots	THETA, deg	Z, m	Z, ft
							MONTH 10 DAY 31 YEAR 76 HOUR OF RELEASE 1000Z								
690.	2263.	933.1	1948.8	1162.3	.072560	5.8	42.4	2.3	36.1	78.2	2.6	5.0	305.0	724.	2375.
883.	2896.	911.6	1903.9	1138.4	.071068	5.0	41.0	2.2	36.0	82.1	2.6	5.0	324.0	914.	3000.
1190.	3905.	878.2	1834.2	1101.2	.068746	3.9	39.0	2.0	35.6	87.5	2.6	5.0	323.0	1219.	4000.
1497.	4910.	845.9	1766.7	1065.5	.066517	2.6	36.7	1.6	34.8	92.8	4.1	8.0	248.0	1524.	5000.
1804.	5918.	814.5	1701.1	1033.9	.064544	.6	33.1	-.3	31.5	93.7	6.2	12.0	204.0	1829.	6000.
2110.	6921.	784.2	1637.8	1001.9	.062547	-.9	30.4	-6.3	20.6	66.6	7.2	14.0	187.0	2134.	7000.
2416.	7928.	754.7	1576.2	970.7	.060599	-2.4	27.7	-14.5	6.0	39.0	6.7	13.0	205.0	2438.	8000.
2722.	8931.	726.2	1516.7	939.0	.058620	-3.7	25.3	-22.6	-8.6	21.5	8.2	16.0	219.0	2743.	9000.
3027.	9930.	698.7	1459.3	907.7	.056666	-4.9	23.2	-31.3	-24.3	10.6	8.7	17.0	228.0	3048.	10000.
3332.	10931.	672.0	1403.5	880.2	.054949	-7.1	19.2	-31.8	-25.2	12.0	8.2	16.0	237.0	3353.	11000.
3636.	11929.	646.2	1349.6	853.3	.053270	-9.3	15.3	-32.4	-26.3	13.4	8.7	17.0	250.0	3658.	12000.
3942.	12932.	621.1	1297.2	827.1	.051634	-11.5	11.3	-33.2	-27.7	14.8	11.3	22.0	261.0	3962.	13000.
4247.	13934.	596.8	1246.4	799.5	.049911	-13.0	8.6	-34.1	-29.3	15.3	14.9	29.0	264.0	4267.	14000.
4551.	14931.	573.4	1197.6	769.4	.048032	-13.4	7.9	-35.0	-31.1	14.4	19.5	38.0	257.0	4572.	15000.
4853.	15922.	550.9	1150.6	740.5	.046228	-13.9	7.0	-36.0	-32.8	13.6	24.2	47.0	249.0	4877.	16000.
5152.	16904.	529.3	1105.5	712.6	.044486	-14.3	6.3	-37.1	-34.7	12.7	29.3	57.0	245.0	5182.	17000.
5451.	17885.	508.4	1061.8	685.7	.042807	-14.8	5.4	-38.1	-36.6	11.8	32.9	64.0	237.0	5486.	18000.
5749.	18860.	488.3	1019.8	662.3	.041346	-16.2	2.8	-39.3	-38.8	11.7	35.5	69.0	234.0	5791.	19000.
6045.	19833.	468.9	979.3	641.5	.040048	-18.4	-1.1	-40.7	-41.2	12.3	38.1	74.0	233.0	6096.	20000.
6342.	20807.	450.1	940.1	621.2	.038780	-20.6	-5.1	-42.0	-43.6	12.9	37.6	73.0	233.0	6401.	21000.
6639.	21782.	431.9	902.0	601.4	.037544	-22.9	-9.2	-43.4	-46.2	13.6	37.6	73.0	233.0	6706.	22000.
6938.	22763.	414.2	865.1	582.1	.036339	-25.1	-13.2	-44.9	-48.8	14.1	38.6	75.0	232.0	7010.	23000.
7235.	23737.	397.2	829.6	563.2	.035159	-27.4	-17.3	-46.5	-51.6	14.7	38.6	75.0	231.0	7315.	24000.
7535.	24721.	380.6	794.9	544.6	.033998	-29.6	-21.3	-48.2	-54.8	14.8	39.1	76.0	230.0	7620.	25000.
7833.	25698.	364.7	761.7	526.6	.032875	-31.8	-25.2	-50.0	-58.0	14.9	39.6	77.0	229.0	7925.	26000.
8131.	26677.	349.3	729.5	509.0	.031776	-34.0	-29.2	-51.8	-61.2	15.0	40.6	79.0	229.0	8230.	27000.
8430.	27658.	334.4	698.4	491.9	.030708	-36.2	-33.2	-53.6	-64.5	15.1	42.2	82.0	229.0	8534.	28000.
8729.	28640.	320.0	668.3	475.3	.029672	-38.5	-37.3	-55.5	-67.8	15.3	43.2	84.0	229.0	8839.	29000.
9031.	29630.	306.0	639.1	458.8	.028642	-40.6	-41.1	-59.2	-74.5	12.0	44.2	86.0	230.0	9144.	30000.
9331.	30612.	292.6	611.1	442.0	.027593	-42.4	-44.3	-62.5	-80.5	9.5	44.8	87.0	230.0	9449.	31000.
9630.	31593.	279.7	584.2	425.5	.026563	-44.0	-47.2	-63.8	-82.8	9.5	45.3	88.0	230.0	9754.	32000.
9928.	32571.	267.3	558.3	409.5	.025564	-45.6	-50.1	-65.1	-85.2	9.5	43.7	85.0	230.0	10058.	33000.
10227.	33553.	255.3	533.2	394.0	.024597	-47.3	-53.1	-66.4	-87.6	9.6	41.7	81.0	230.0	10363.	34000.
10525.	34530.	243.8	509.2	379.2	.023673	-49.0	-56.2	-67.8	-90.1	9.6	40.1	78.0	230.0	10668.	35000.
10823.	35509.	232.7	486.0	365.0	.022786	-50.9	-59.6	-69.3	-92.8	9.7	38.6	75.0	230.0	10973.	36000.
11119.	36481.	222.1	463.9	349.8	.021837	-51.9	-61.4	-70.2	-94.3	9.7	36.1	74.0	232.0	11278.	37000.
11414.	37449.	212.0	442.8	330.9	.020657	-49.8	-57.6	-68.5	-91.3	9.6	38.1	74.0	233.0	11582.	38000.
11711.	38424.	202.3	422.5	317.2	.019802	-50.8	-59.4	-69.3	-92.7	9.7	39.6	77.0	235.0	11887.	39000.
12007.	39392.	193.1	403.3	304.2	.018991	-51.9	-61.4	-70.2	-94.3	9.7	40.6	79.0	236.0	12192.	40000.
12306.	40374.	184.2	384.7	291.8	.018216	-53.1	-63.6	-71.1	-96.0	9.8	39.1	76.0	236.0	12497.	41000.
12605.	41357.	175.7	367.0	279.8	.017467	-54.2	-65.6	-72.1	-97.8	9.7	37.0	72.0	235.0	12802.	42000.
12905.	42339.	167.6	350.0	268.3	.016749	-55.4	-67.7	-73.1	-99.5	9.7	37.0	72.0	237.0	13106.	43000.
13207.	43330.	159.8	333.7	257.2	.016056	-56.6	-69.9	-74.0	-101.3	9.6	36.5	71.0	240.0	13411.	44000.
13512.	44330.	152.3	318.1	246.5	.015388	-57.8	-72.0	-75.0	-103.0	9.8	0.0	0.0	0.0	13716.	45000.
13819.	45338.	145.1	303.0	235.5	.014702	-58.4	-73.1	-75.5	-103.8	9.9	0.0	0.0	0.0	14021.	46000.
14123.	46337.	138.3	288.8	224.7	.014028	-58.6	-73.5	-75.7	-104.2	9.8	0.0	0.0	0.0	14326.	47000.

TABLE 4.—Continued

H, m	H, ft	p, mb	p, lb/ft^2	RHO, gm/m^3	RHO, lb/ft^3	T, °C	T, °F	D, °C	D, °F	RH, percent	V, m/sec	V, knots	THETA, deg	Z, m	Z, ft
							MONTH 10 DAY 31 YEAR 76 HOUR OF RELEASE 2230Z								
677.	2222.	934.5	1951.7	1127.4	.070381	14.7	58.5	3.2	37.7	45.8	1.5	3.0	295.0	724.	2375.
865.	2837.	913.6	1908.1	1107.6	.069145	13.4	56.1	2.6	36.7	47.9	1.5	3.0	312.0	914.	3000.
1163.	3816.	881.1	1840.2	1076.4	.067197	11.2	52.2	1.6	34.9	51.6	1.5	3.0	309.0	1219.	4000.
1463.	4800.	849.4	1774.0	1046.8	.065350	8.6	47.6	-.9	30.3	50.4	2.6	5.0	262.0	1524.	5000.
1763.	5785.	818.6	1709.7	1018.6	.063589	6.3	43.3	-5.2	22.7	43.6	3.6	7.0	228.0	1829.	6000.
2065.	6773.	788.6	1647.0	990.9	.061860	3.7	38.7	-9.6	14.7	37.0	4.1	8.0	203.0	2134.	7000.
2367.	7765.	759.4	1586.0	963.7	.060162	1.1	34.0	-14.4	6.0	30.3	5.1	10.0	182.0	2438.	8000.
2669.	8757.	731.1	1526.9	932.8	.058233	-.2	31.6	-17.9	-.2	24.9	5.1	10.0	182.0	2743.	9000.
2971.	9746.	703.7	1469.7	902.7	.056354	-1.6	29.1	-21.7	-7.0	19.9	5.7	11.0	199.0	3048.	10000.
3272.	10734.	677.2	1414.4	874.2	.054575	-3.3	26.1	-23.6	-10.4	19.1	7.2	14.0	224.0	3353.	11000.
3572.	11718.	651.6	1360.9	846.6	.052852	-5.0	23.0	-25.1	-13.2	18.9	9.3	18.0	245.0	3658.	12000.
3873.	12706.	626.7	1308.9	819.8	.051178	-6.8	19.8	-26.7	-16.0	18.8	10.8	21.0	253.0	3962.	13000.
4173.	13692.	602.6	1258.6	793.6	.049543	-8.6	16.5	-28.3	-18.9	16.7	12.9	25.0	246.0	4267.	14000.
4472.	14673.	579.4	1210.1	768.2	.047957	-10.4	13.3	-29.8	-21.7	18.6	14.4	28.0	232.0	4572.	15000.
4773.	15659.	556.8	1162.9	743.5	.046415	-12.2	10.0	-31.4	-24.6	18.5	16.5	32.0	228.0	4877.	16000.
5072.	16641.	535.0	1117.4	719.4	.044911	-14.0	6.8	-33.0	-27.5	18.3	18.5	36.0	227.0	5182.	17000.
5372.	17624.	513.9	1073.3	695.9	.043444	-15.8	3.6	-34.7	-30.4	18.2	19.5	38.0	226.0	5486.	18000.
5671.	18605.	493.5	1030.7	672.9	.042008	-17.6	.3	-36.2	-33.1	18.2	21.6	42.0	219.0	5791.	19000.
5971.	19589.	473.7	989.3	650.2	.040591	-19.2	-2.6	-37.5	-35.5	18.2	25.2	49.0	217.0	6096.	20000.
6269.	20566.	454.7	949.7	628.1	.039211	-20.9	-5.6	-38.9	-37.9	18.4	29.8	58.0	220.0	6401.	21000.
6566.	21543.	436.3	911.2	606.7	.037875	-22.5	-8.5	-40.2	-40.4	18.4	36.0	70.0	221.0	6706.	22000.
6864.	22521.	418.5	874.1	585.9	.036577	-24.2	-11.6	-41.6	-42.8	18.6	38.6	75.0	221.0	7010.	23000.
7161.	23493.	401.4	838.3	565.7	.035315	-25.9	-14.6	-42.9	-45.3	18.7	40.1	78.0	225.0	7315.	24000.
7458.	24469.	384.8	803.7	547.9	.034204	-28.4	-19.1	-44.8	-48.7	19.2	40.6	79.0	232.0	7620.	25000.
7757.	25449.	368.7	770.0	530.7	.033131	-31.0	-23.8	-46.8	-52.2	19.8	41.7	81.0	234.0	7925.	26000.
8056.	26432.	353.1	737.5	513.9	.032082	-33.7	-28.7	-48.8	-55.9	20.5	42.7	83.0	234.0	8230.	27000.
8355.	27411.	338.1	706.1	497.6	.031064	-36.3	-33.3	-50.9	-59.6	21.0	43.2	84.0	234.0	8534.	28000.
8656.	28398.	323.5	675.6	481.0	.030028	-38.7	-37.7	-54.5	-66.1	17.5	44.2	86.0	234.0	8839.	29000.
8957.	29386.	309.4	646.2	464.7	.029010	-41.1	-42.0	-59.1	-74.3	12.9	45.3	88.0	231.0	9144.	30000.
9258.	30374.	295.8	617.8	448.4	.027993	-43.2	-45.8	-63.2	-81.7	9.5	45.8	89.0	225.0	9449.	31000.
9559.	31362.	282.7	590.4	431.7	.026950	-44.9	-48.8	-64.5	-84.1	9.6	46.3	90.0	221.0	9754.	32000.
9859.	32347.	270.1	564.1	415.5	.025939	-46.5	-51.7	-65.8	-86.5	9.6	45.8	89.0	221.0	10058.	33000.
10159.	33329.	258.0	538.8	399.8	.024959	-48.2	-54.8	-67.2	-88.9	9.6	44.8	87.0	221.0	10363.	34000.
10459.	34315.	246.3	514.4	383.7	.023954	-49.4	-56.9	-68.2	-90.7	9.7	42.2	82.0	221.0	10668.	35000.
10758.	35294.	235.1	491.0	366.4	.022874	-49.5	-57.1	-68.2	-90.8	9.7	39.6	77.0	221.0	10973.	36000.
11051.	36257.	224.5	468.9	350.0	.021850	-49.6	-57.3	-68.3	-90.9	9.7	37.0	72.0	223.0	11278.	37000.
11346.	37225.	214.3	447.6	334.2	.020863	-49.7	-57.5	-68.4	-91.1	9.7	34.5	67.0	226.0	11582.	38000.
11643.	38188.	204.6	427.3	319.2	.019927	-49.8	-57.6	-68.4	-91.2	9.7	32.9	64.0	227.0	11887.	39000.
11935.	39156.	195.3	407.9	305.3	.019059	-50.2	-58.4	-68.8	-91.8	9.7	31.9	62.0	228.0	12192.	40000.
12231.	40127.	186.4	389.3	292.3	.018248	-50.8	-59.4	-69.3	-92.8	9.6	36.0	70.0	209.0	12497.	41000.
12527.	41098.	177.9	371.6	279.8	.017467	-51.5	-60.7	-69.9	-93.8	9.7	40.1	78.0	188.0	12802.	42000.
12822.	42067.	169.8	354.6	267.8	.016718	-52.2	-62.0	-70.5	-94.8	9.7	42.7	83.0	179.0	13106.	43000.
13120.	43046.	162.0	338.3	256.3	.016000	-52.9	-63.2	-71.0	-95.8	9.7	43.7	85.0	177.0	13411.	44000.
13421.	44032.	154.5	322.7	245.3	.015314	-53.6	-64.5	-71.6	-96.8	9.7	44.8	87.0	175.0	13716.	45000.
13719.	45011.	147.4	307.9	234.7	.014652	-54.3	-65.7	-72.1	-97.9	9.8	44.2	86.0	172.0	14021.	46000.
14023.	46008.	140.5	293.4	224.5	.014015	-55.0	-67.0	-72.7	-98.8	9.8	43.7	85.0	172.0	14326.	47000.
14324.	46994.	134.0	279.9	214.8	.013410	-55.7	-68.3	-73.2	-99.8	9.8	35.5	69.0	189.0	14630.	48000.
14624.	47979.	127.8	266.9	205.4	.012823	-56.3	-69.3	-73.8	-100.8	9.8	27.8	54.0	206.0	14935.	49000.
14922.	48980.	121.8	254.4	196.4	.012261	-57.0	-70.6	-74.4	-101.8	9.8	24.7	48.0	212.0	15240.	50000.

TABLE 4.—Concluded

H, m	H, ft	p, mb	p, lb/ft²	RHO, gm/m³	RHO, lb/ft³	T, °C	T, °F	D, °C	D, °F	RH, percent	V, m/sec	V, knots	THETA, deg	Z, m	Z, ft
MONTH 11 DAY 1 YEAR 78 HOUR OF RELEASE 1100Z															
673.	2207.	935.0	1952.8	1174.6	.073328	3.5	38.3	.1	32.2	78.5	2.1	4.0	245.0	724.	2375.
866.	2840.	913.5	1907.9	1135.6	.070893	6.2	43.2	2.8	37.0	78.6	1.0	2.0	267.0	914.	3000.
1171.	3841.	880.3	1838.5	1092.5	.068203	6.7	44.1	3.0	37.4	77.3	0.0	0.0	286.0	1219.	4000.
1475.	4838.	848.2	1771.5	1060.4	.066199	4.7	40.5	1.0	33.8	76.9	.5	1.0	244.0	1524.	5000.
1780.	5840.	816.9	1706.1	1031.5	.064394	2.0	35.6	-.3	31.4	84.6	1.5	3.0	219.0	1829.	6000.
2085.	6840.	786.6	1642.8	1003.1	.062621	-.6	30.9	-1.8	28.7	91.4	4.1	8.0	213.0	2134.	7000.
2391.	7845.	757.1	1581.2	966.4	.060330	-.4	31.3	-12.8	9.1	38.7	7.7	15.0	224.0	2438.	8000.
2694.	8839.	728.8	1522.1	934.4	.058333	-1.5	29.3	-17.8	.0	27.7	11.8	23.0	232.0	2743.	9000.
2996.	9831.	701.4	1464.9	905.0	.056497	-3.3	26.1	-17.5	.4	32.3	13.4	26.0	237.0	3048.	10000.
3299.	10825.	674.8	1409.3	877.1	.054756	-5.2	22.6	-18.4	-1.2	34.6	15.4	30.0	238.0	3353.	11000.
3603.	11820.	649.0	1355.5	849.9	.053058	-7.2	19.0	-19.4	-3.0	37.0	18.0	35.0	239.0	3658.	12000.
3905.	12810.	624.1	1303.5	818.4	.051091	-7.5	18.5	-22.2	-7.9	29.8	21.1	41.0	235.0	3962.	13000.
4204.	13792.	600.2	1253.5	790.1	.049324	-8.5	16.7	-24.7	-12.5	25.7	22.6	44.0	229.0	4267.	14000.
4505.	14780.	576.9	1204.9	767.8	.047932	-11.4	11.5	-25.5	-13.9	30.1	23.1	45.0	223.0	4572.	15000.
4805.	15765.	554.4	1157.9	745.9	.046565	-14.2	6.4	-26.5	-15.8	34.3	22.6	44.0	222.0	4877.	16000.
5109.	16761.	532.4	1111.9	724.6	.045235	-17.1	1.2	-27.9	-18.2	38.6	22.1	43.0	226.0	5182.	17000.
5411.	17752.	511.2	1067.7	703.7	.043931	-20.1	-4.2	-29.4	-20.9	43.3	21.1	41.0	234.0	5486.	18000.
5716.	18752.	490.5	1024.4	681.7	.042557	-22.5	-8.5	-31.5	-24.6	44.0	23.7	46.0	241.0	5791.	19000.
6020.	19751.	470.5	982.7	658.6	.041115	-24.2	-11.6	-34.0	-29.2	40.0	27.3	53.0	243.0	6096.	20000.
6324.	20749.	451.2	942.4	636.1	.039710	-26.0	-14.8	-36.6	-33.9	36.4	28.8	56.0	241.0	6401.	21000.
6628.	21744.	432.6	903.5	614.2	.038343	-27.7	-17.9	-39.3	-38.7	32.3	29.8	58.0	240.0	6706.	22000.
6931.	22740.	414.6	865.9	593.0	.037020	-29.5	-21.1	-42.1	-43.8	28.5	29.8	58.0	239.0	7010.	23000.
7235.	23737.	397.2	829.6	573.1	.035777	-31.6	-24.9	-45.0	-49.0	25.6	29.3	57.0	239.0	7315.	24000.
7539.	24733.	380.4	794.5	557.5	.034804	-35.3	-31.5	-47.6	-53.6	27.7	29.8	58.0	241.0	7620.	25000.
7846.	25741.	364.0	760.2	542.1	.033842	-39.1	-38.4	-50.3	-58.5	29.8	31.4	61.0	244.0	7925.	26000.
8155.	26754.	348.1	727.0	523.0	.032650	-41.2	-42.2	-53.3	-64.0	26.1	32.4	63.0	248.0	8230.	27000.
8463.	27765.	332.8	695.1	503.9	.031457	-42.9	-45.2	-56.6	-69.9	21.0	34.0	66.0	251.0	8534.	28000.
8770.	28772.	318.1	664.4	485.4	.030303	-44.7	-48.5	-60.4	-76.6	16.0	35.0	68.0	255.0	8839.	29000.
9077.	29781.	303.9	634.7	467.5	.029185	-46.6	-51.9	-64.8	-84.6	11.1	36.0	70.0	260.0	9144.	30000.
9385.	30792.	290.2	606.1	449.4	.028055	-48.0	-54.4	-67.0	-88.7	9.6	34.5	67.0	240.0	9449.	31000.
9691.	31795.	277.1	578.7	431.6	.026944	-49.3	-56.7	-68.1	-90.6	9.6	32.9	64.0	221.0	9754.	32000.
9997.	32797.	264.5	552.4	414.4	.025870	-50.6	-59.1	-69.2	-92.5	9.6	34.0	66.0	217.0	10058.	33000.
10299.	33788.	252.5	527.4	397.9	.024840	-52.0	-61.6	-70.2	-94.4	9.7	35.5	69.0	212.0	10363.	34000.
10602.	34782.	240.9	503.1	379.8	.023710	-52.1	-61.8	-70.3	-94.6	9.7	39.1	76.0	206.0	10668.	35000.
10903.	35771.	229.8	479.9	362.0	.022599	-51.8	-61.2	-70.1	-94.2	9.7	0.0	0.0	0.0	10973.	36000.
11203.	36745.	219.3	458.0	345.1	.021544	-51.6	-60.9	-69.9	-93.9	9.7	0.0	0.0	0.0	11278.	37000.
11496.	37716.	209.3	437.1	328.9	.020533	-51.4	-60.5	-69.8	-93.6	9.7	0.0	0.0	0.0	11582.	38000.

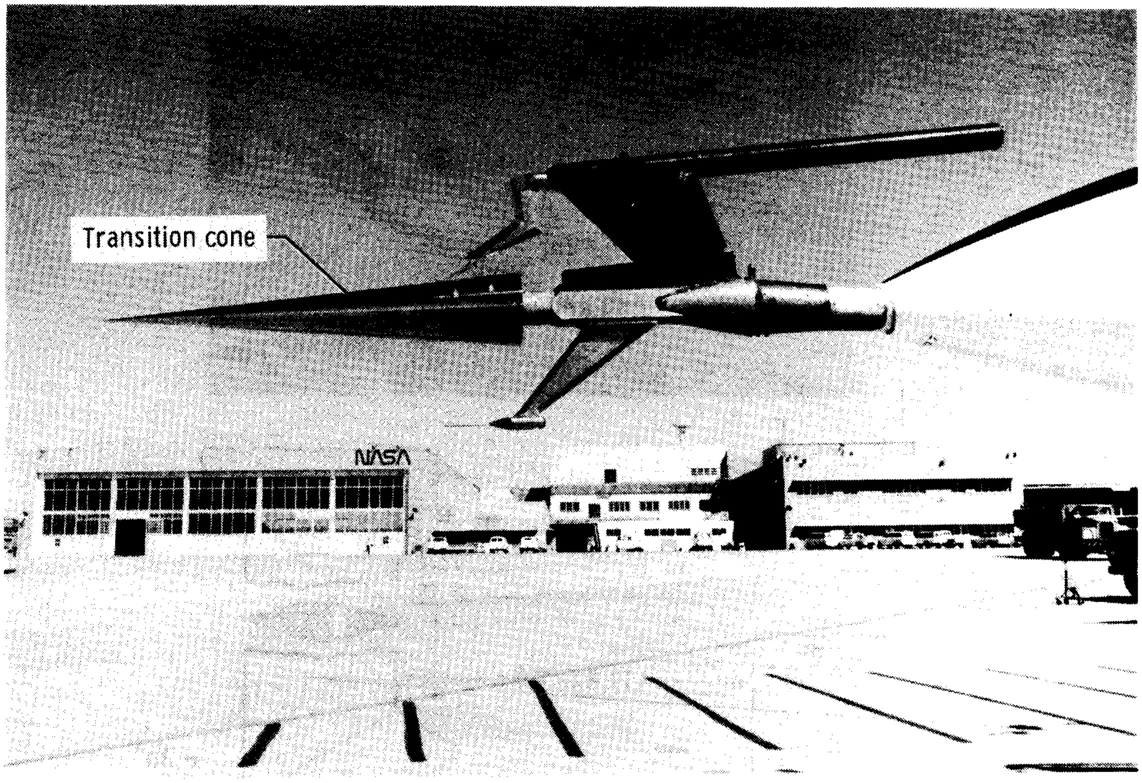

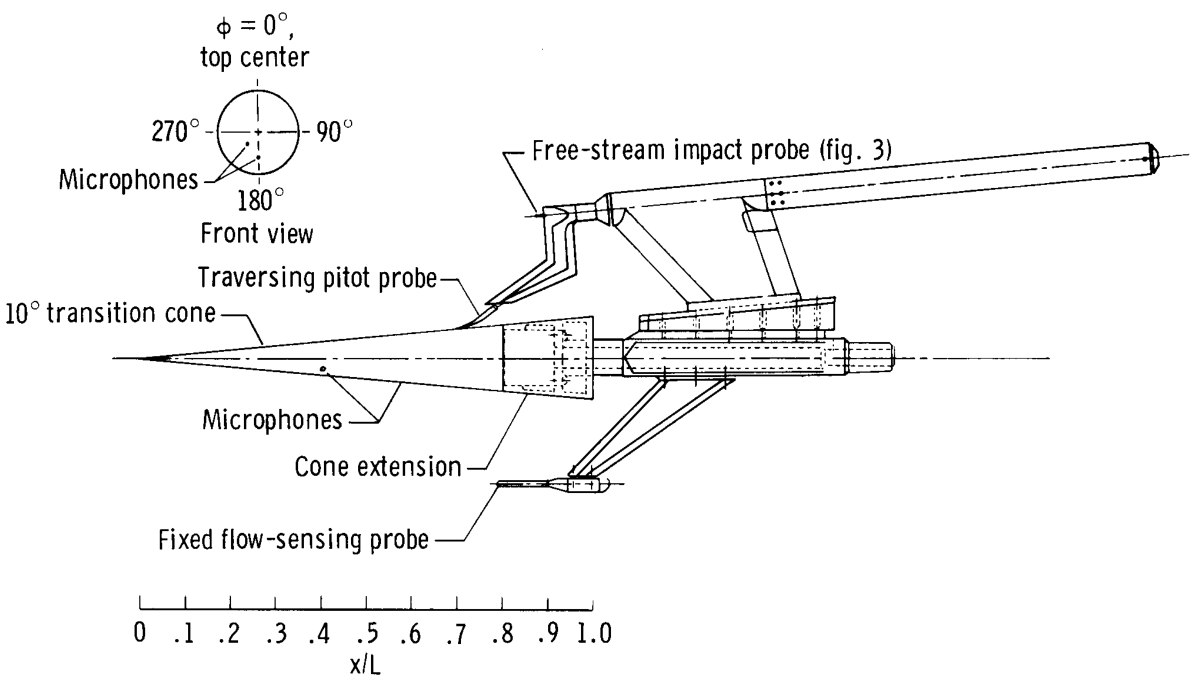

Figure 1. Transition cone and instrumentation.

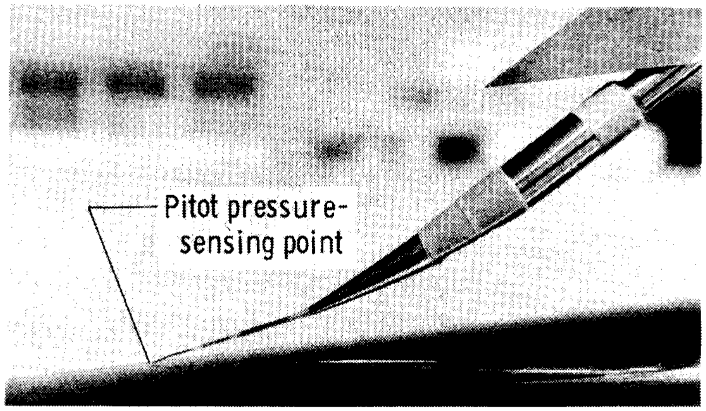

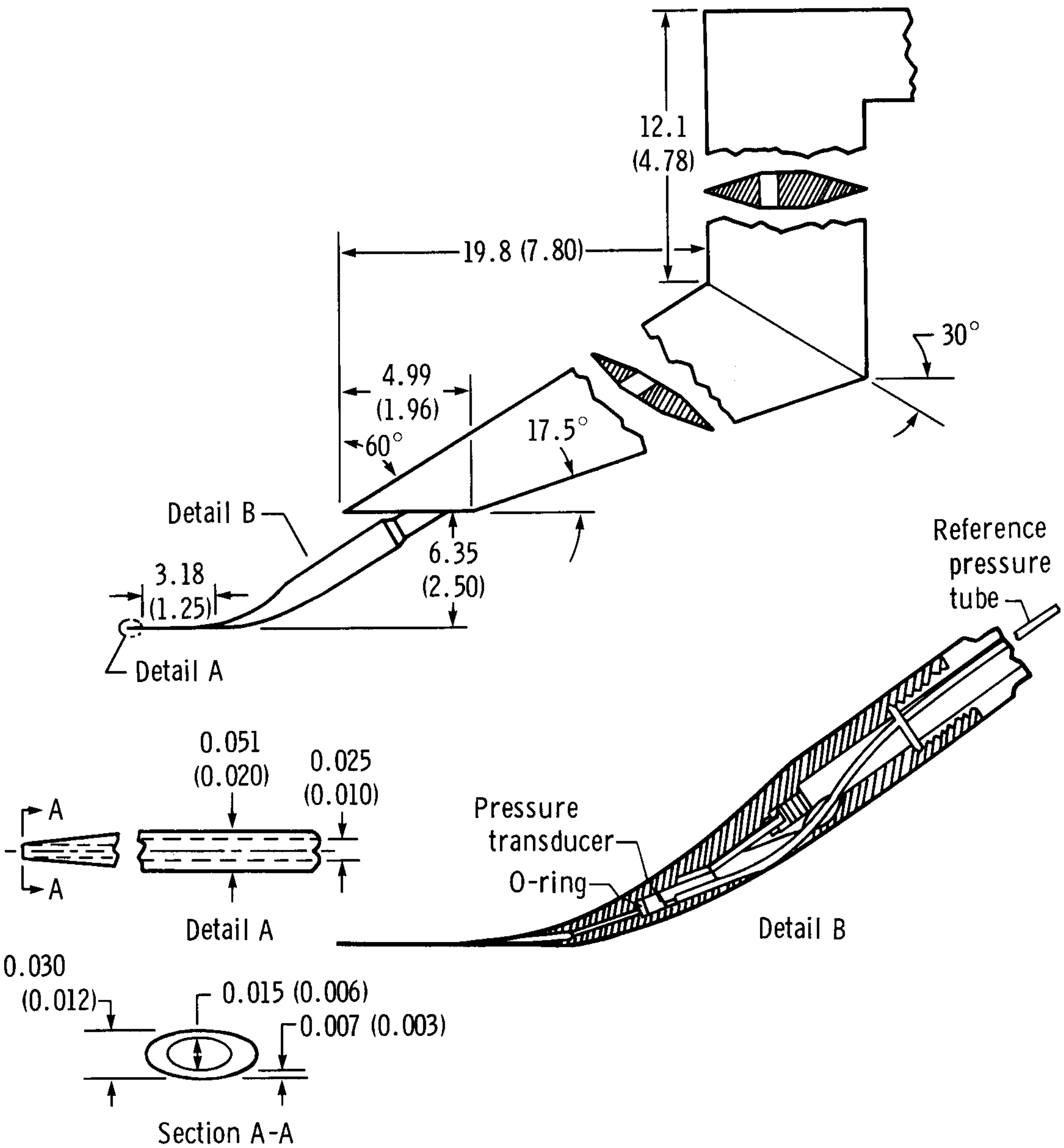

Figure 2. Pitot pressure probe. Dimensions are in centimeters (inches).

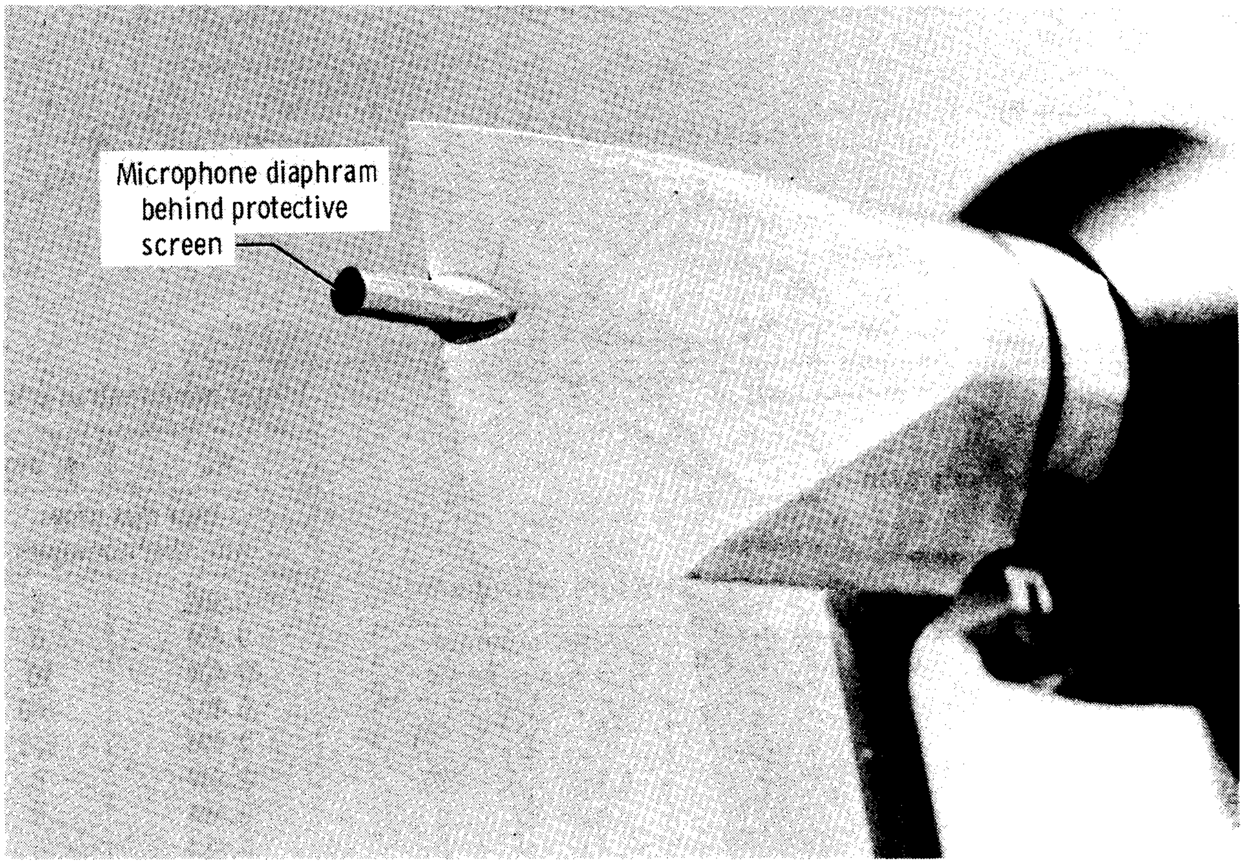

Figure 3. Probe for measurement of fluctuating free-stream impact pressure.

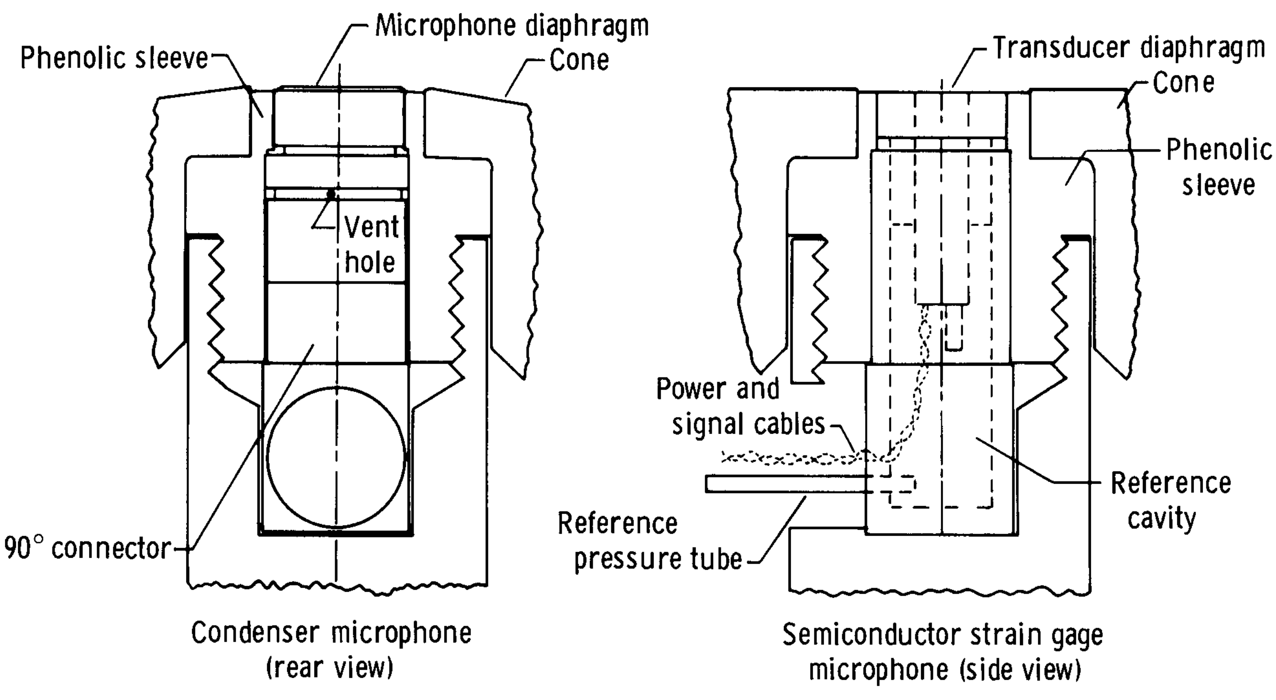

Figure 4. Microphone installations.

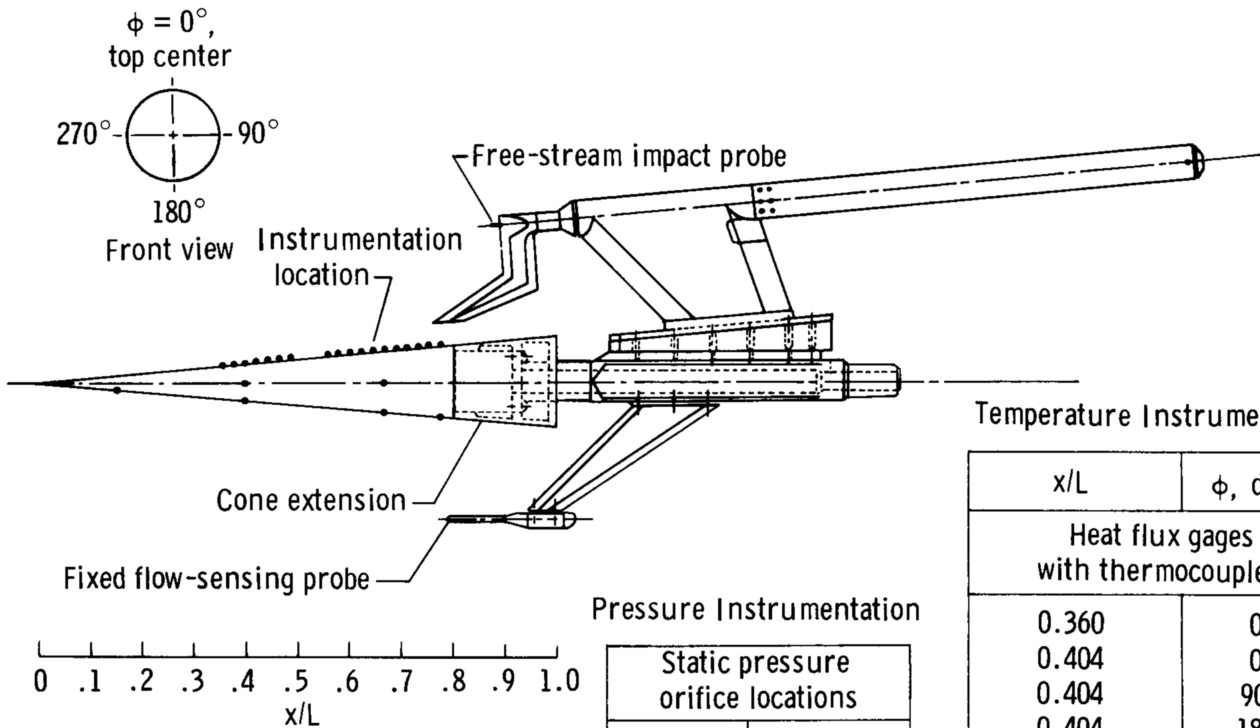

Pressure Instrumentation

Static pressure orifice locations	
x/L	ϕ, deg
0.157	180
0.360	0
0.382	0
0.404	90, 270*
0.427	0
0.449	0
0.472	0
0.494	0
0.562	0
0.584	0
0.607	0
0.629	0
0.652	0
0.674	0
0.674	90
0.674	180
0.674	270
0.697	0
0.719	0
0.742	0
0.764	0
0.787	0
0.787	180

*Differential pressure only

Temperature Instrumentation

x/L	ϕ, deg
Heat flux gages with thermocouples	
0.360	0
0.404	0
0.404	90
0.404	180
0.404	270
0.449	0
0.494	0
0.584	0
0.629	0
0.674	0
0.674	90
0.674	180
0.674	270
0.719	0
0.764	0
Thermocouples only	
0.157	180
0.382	0
0.427	0
0.472	0
0.562	0
0.607	0
0.652	0
0.697	0
0.742	0
0.787	0
0.787	180

Figure 5. Facsimile cone and instrumentation.

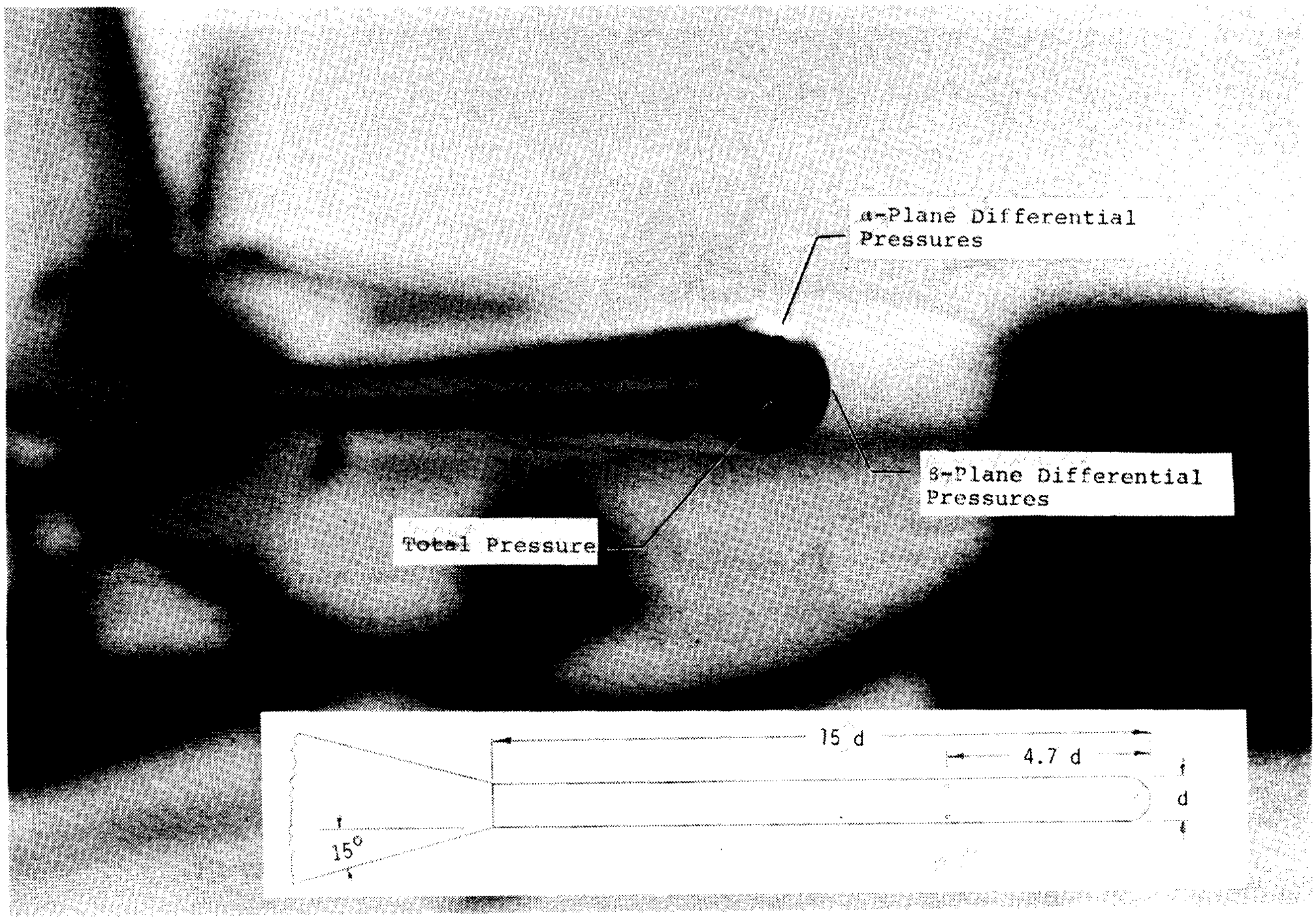

Figure 6. Fixed flow-sensing probe.

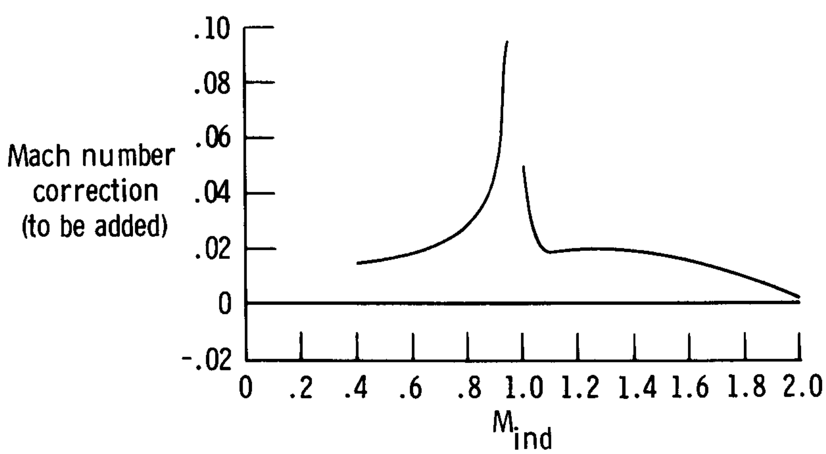

Figure 7. Fixed flow-sensing probe position error determined by in-flight calibration.

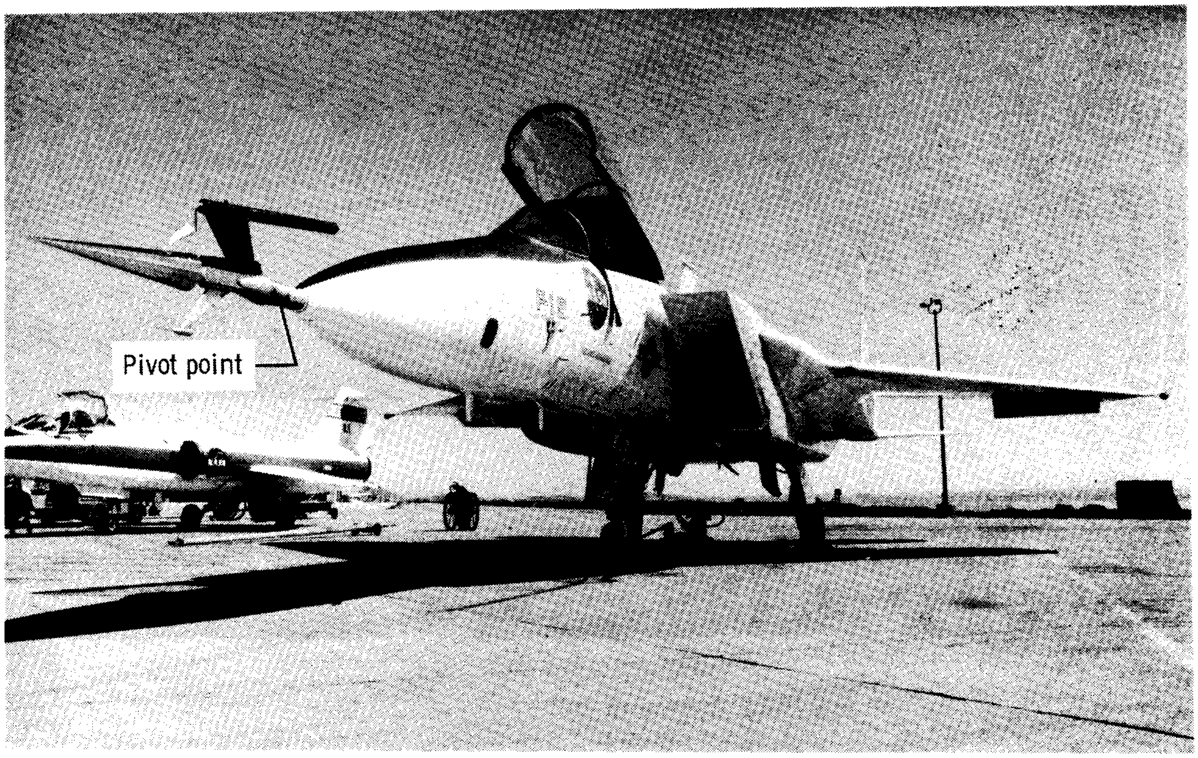

Figure 8. Transition cone mounted in front of testbed aircraft.

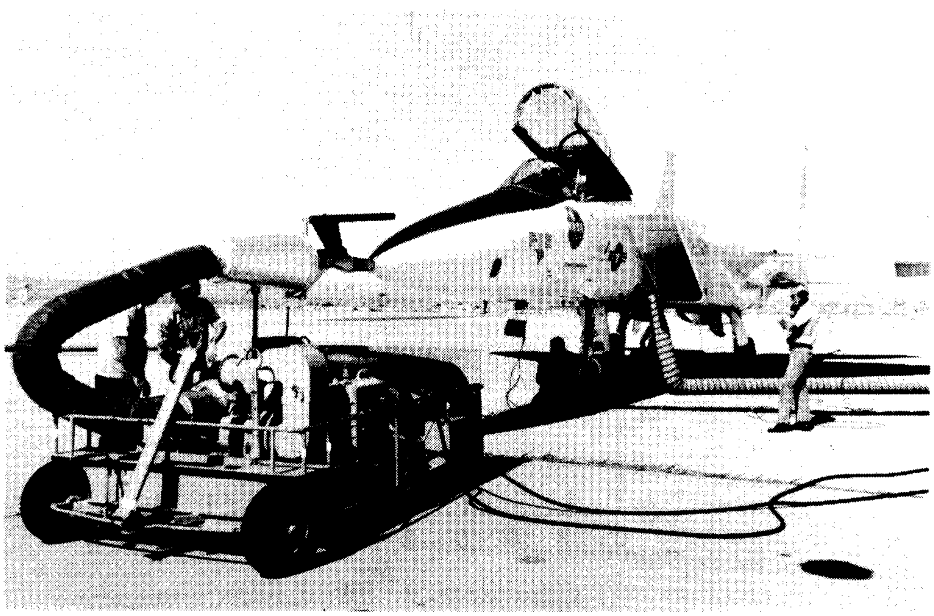

Figure 9. Transition cone being heated at end of runway before flight.

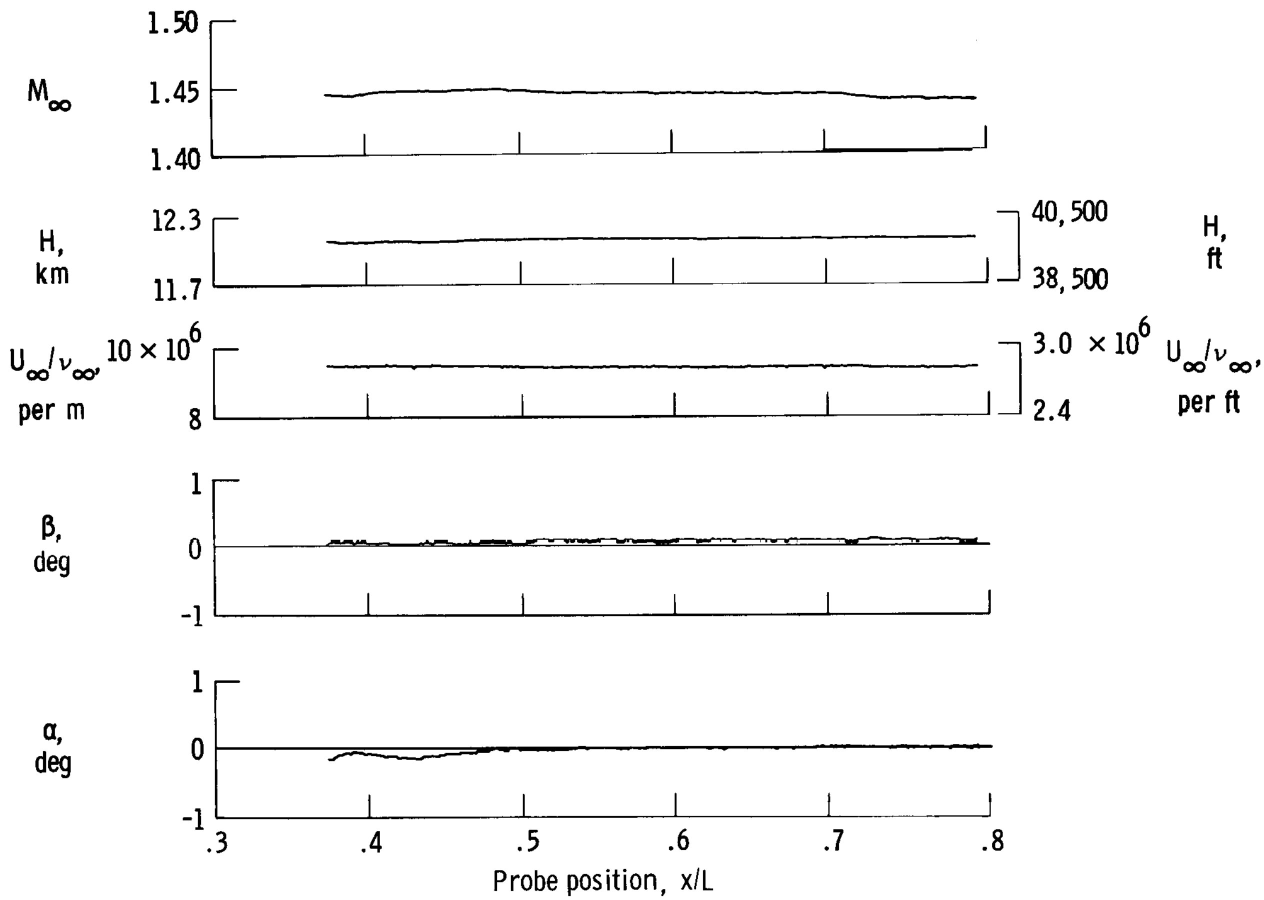

Figure 10. History of cone free-stream conditions during a typical pitot probe traverse.

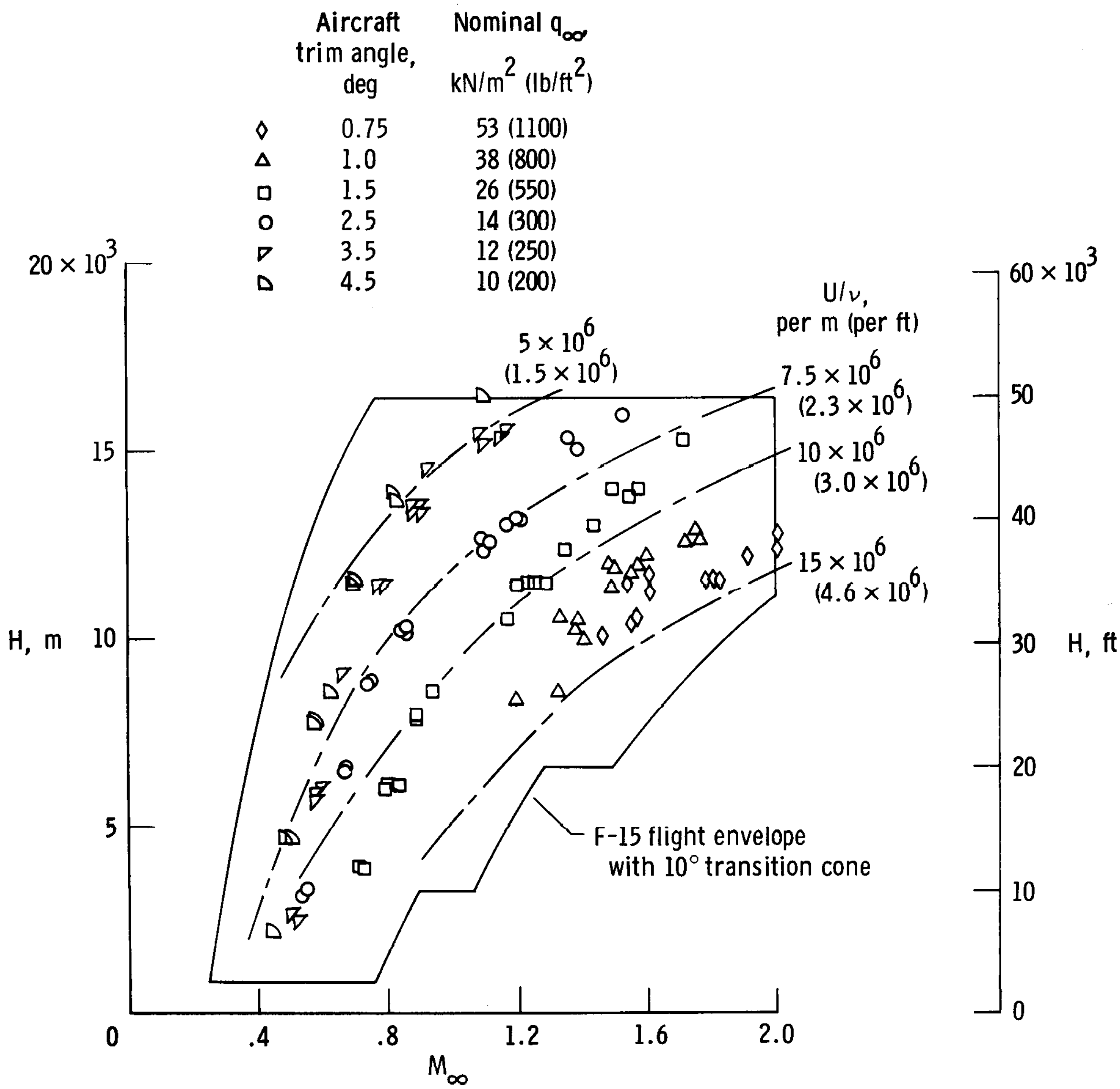

Figure 11. Transition cone flight test matrix.

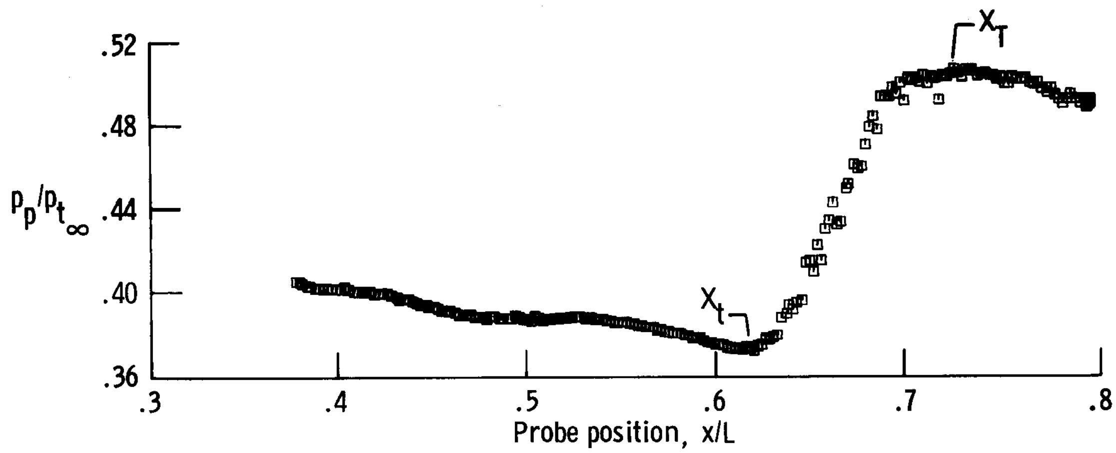

Figure 12. Typical pitot probe pressures as a function of probe location. At onset of transition (X_t), $M_\infty = 1.44$, $H = 13{,}074$ m (42,894 ft), $U_\infty/\nu_\infty = 9.45 \times 10^6$ per m (2.88×10^6 per ft), $\alpha = -0.30°$, and $\beta = 0.12°$; at end of transition (X_T), $M_\infty = 1.44$, $H = 13{,}071$ m (42,884 ft), $U_\infty/\nu_\infty = 9.42 \times 10^6$ per m (2.87×10^6 per ft), $\alpha = -0.28°$, and $\beta = 0.13°$.

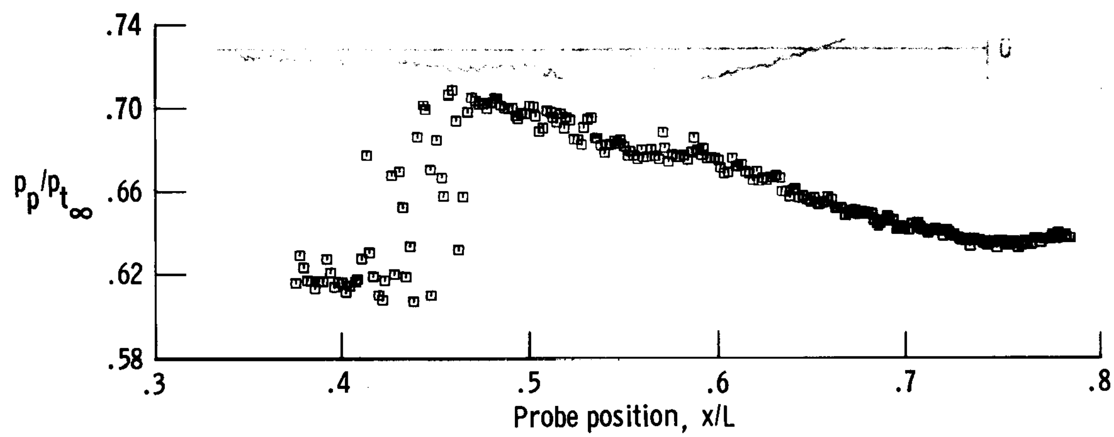

(a) Pitot probe pressures.

Figure 13. Data history during moderate turbulence.

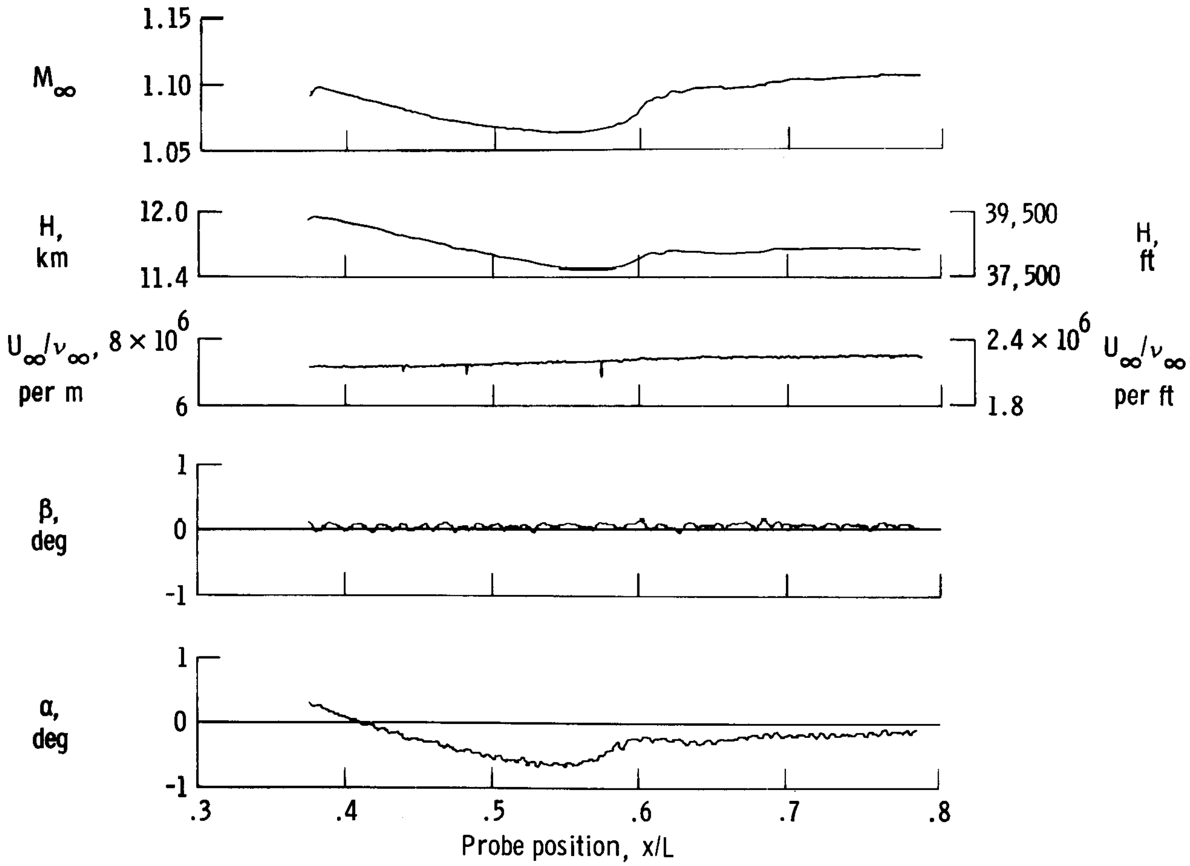

(b) Cone free-stream conditions.

Figure 13. Concluded.

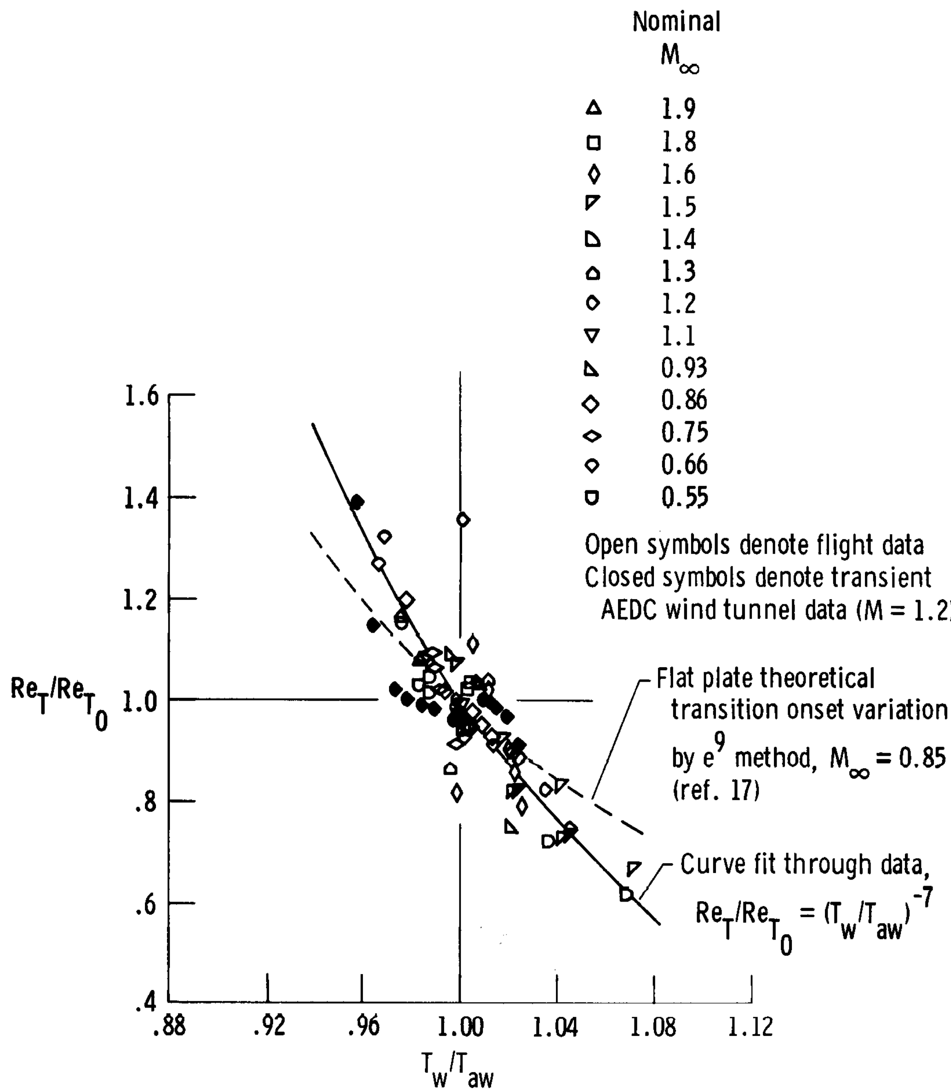

Figure 14. Variation in flight-determined transition Reynolds number with wall temperature and comparison with theoretical and wind tunnel results.

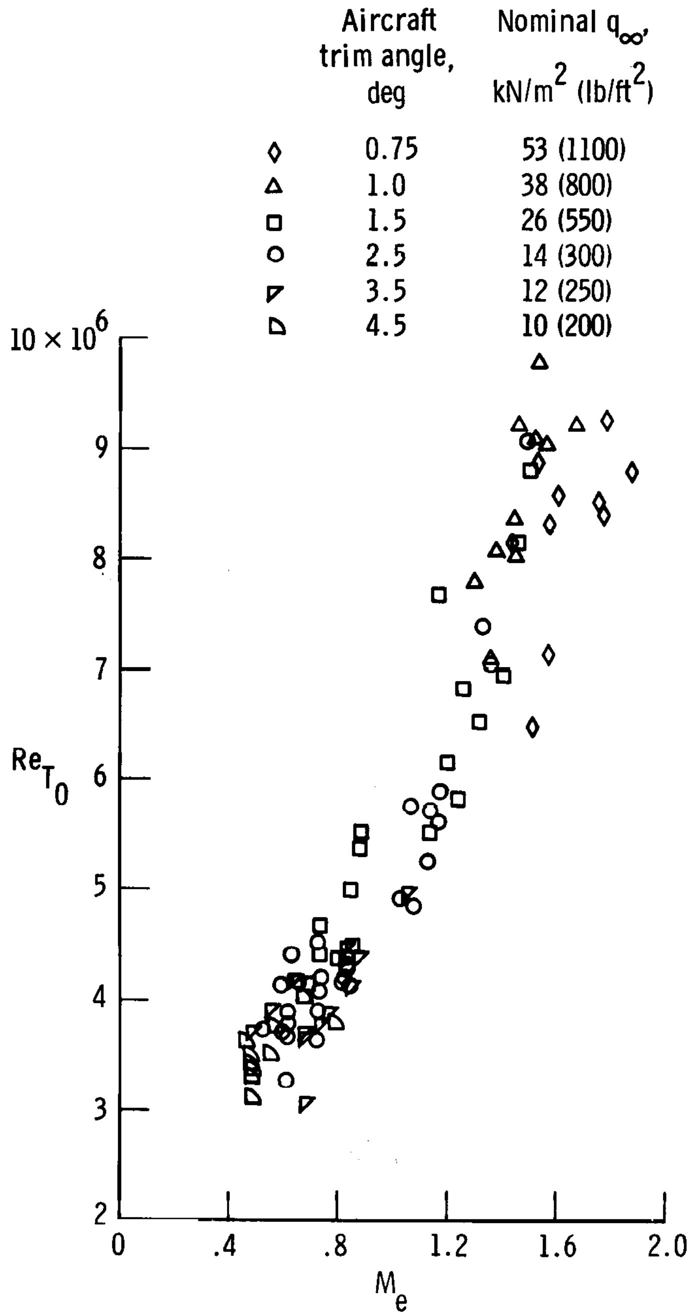

Figure 15. Transition Reynolds number as a function of Mach number.

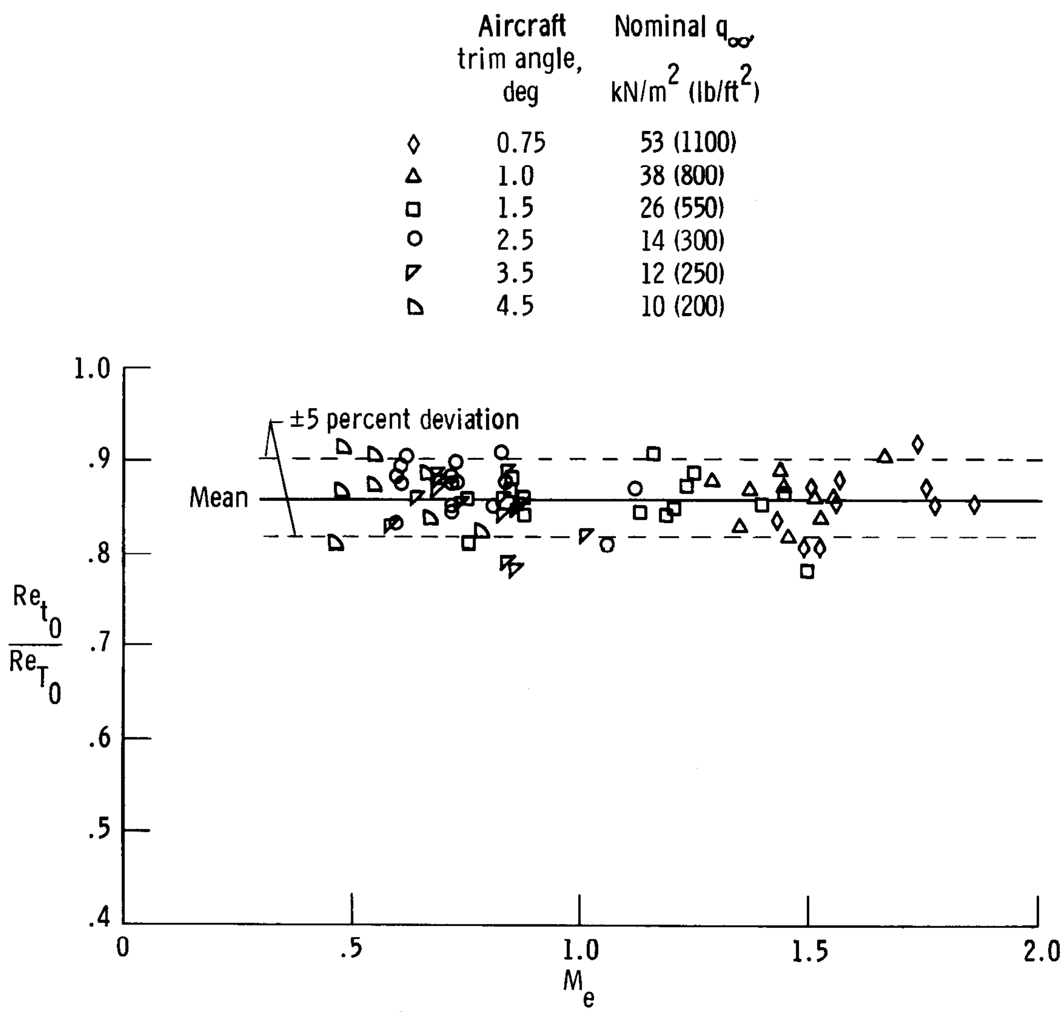

Figure 16. Ratio of onset of transition Reynolds number to end of transition Reynolds number as a function of Mach number.

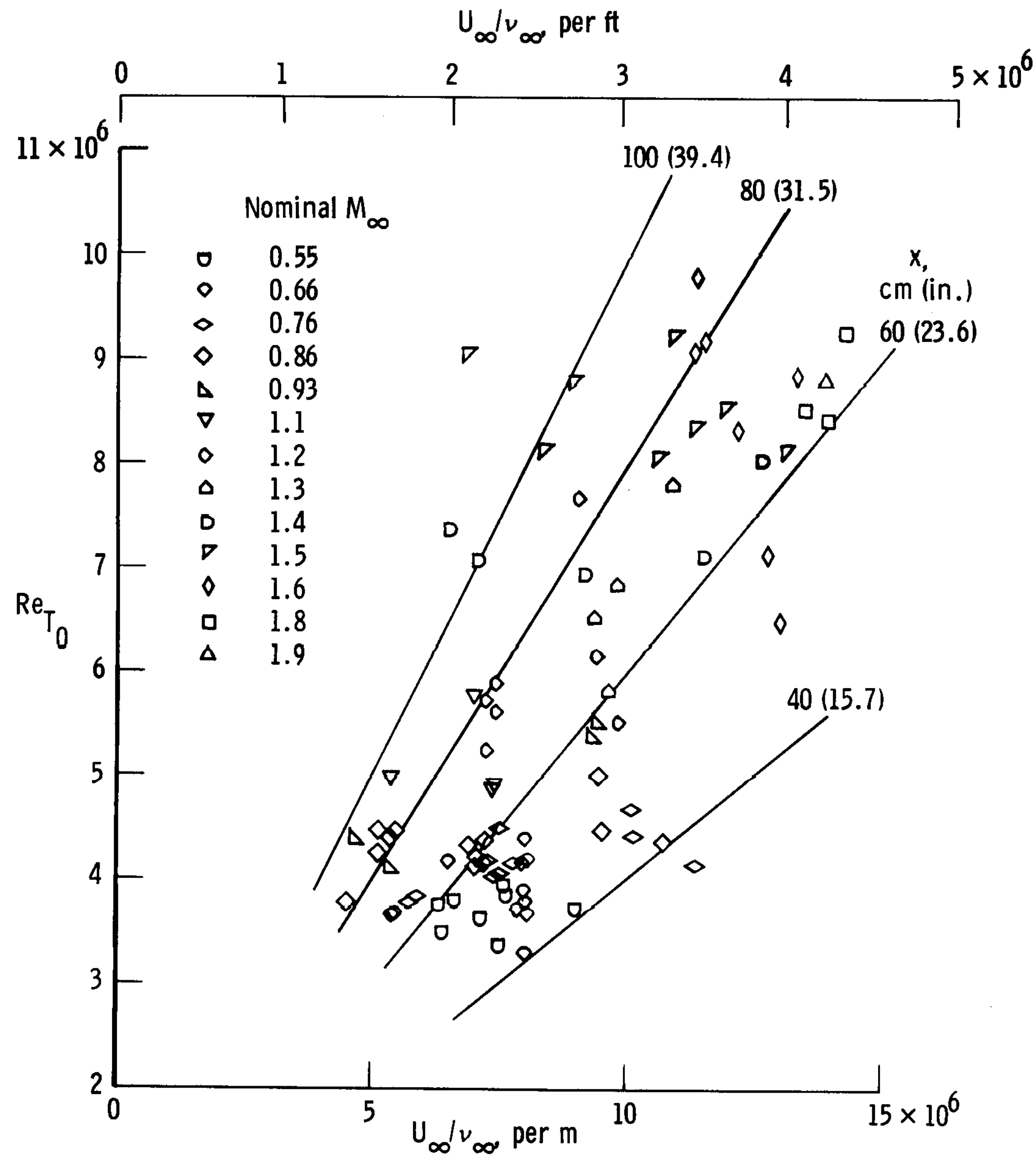

Figure 17. Transition Reynolds number as a function of unit Reynolds number.

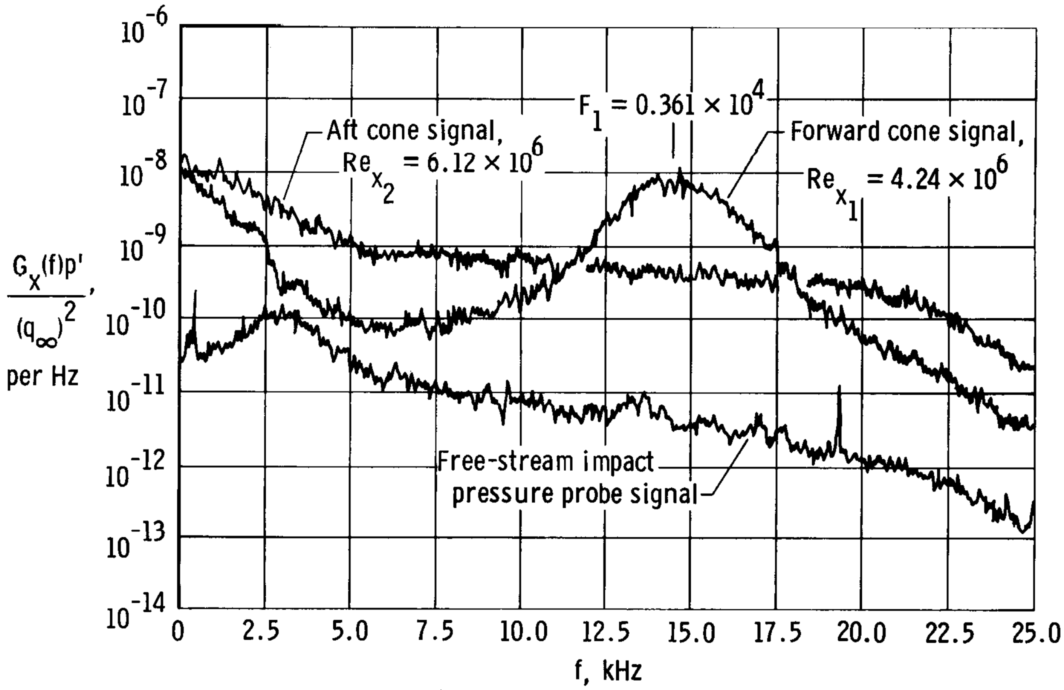

(a) $M_e = 0.84$.

Figure 18. Microphone power spectral density distribution.

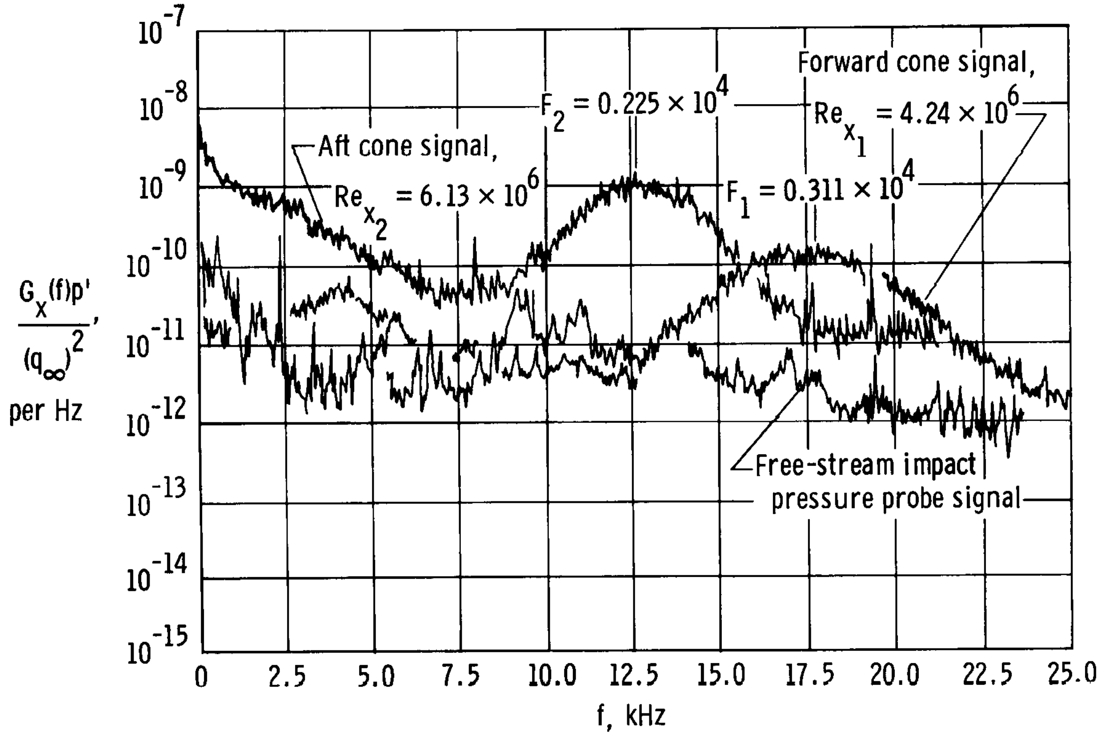

(b) $M_e = 1.31$.

Figure 18. Concluded.

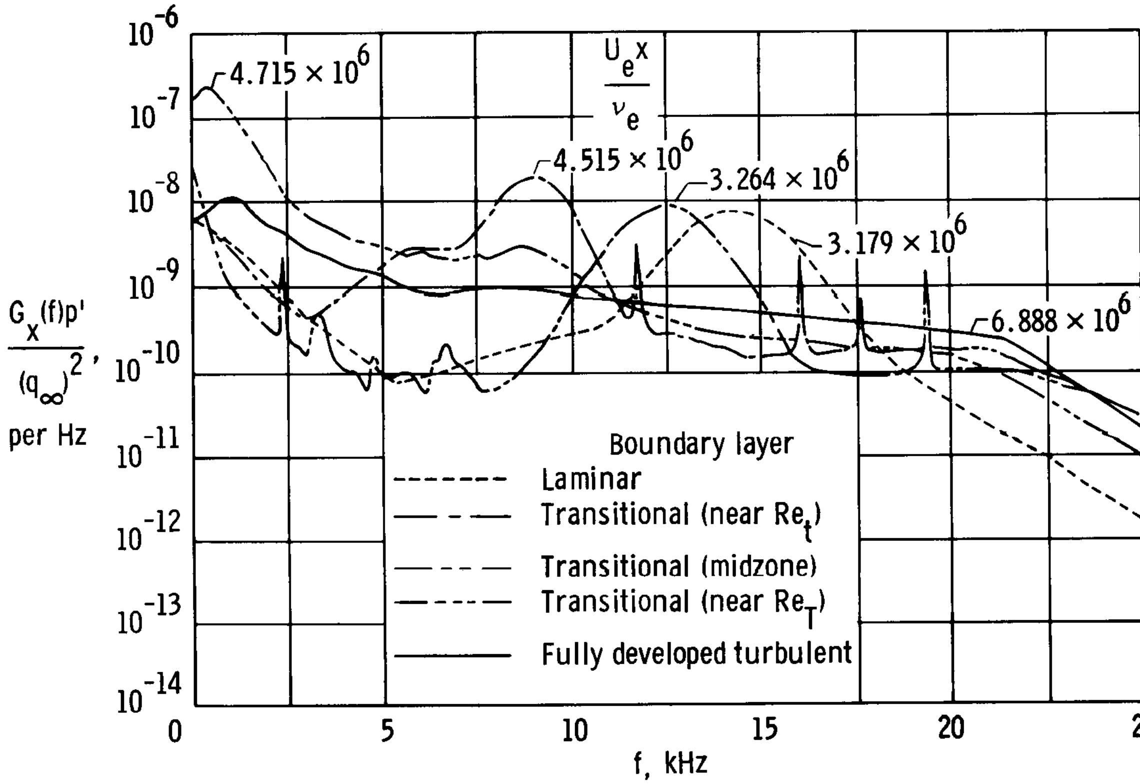

(a) $M_e \approx 0.8$.

Figure 19. Effect of Reynolds number on power spectral density distribution. Spectra are smoothed.

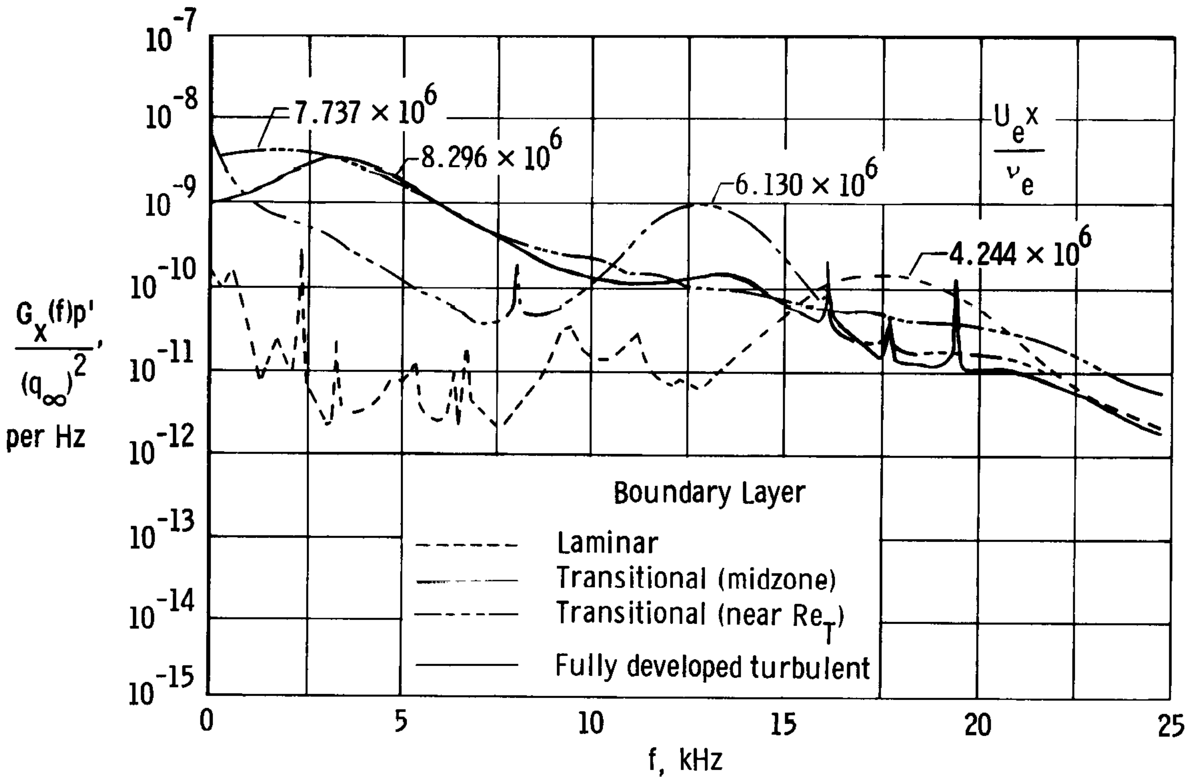

(b) $M_e \approx 1.35$.

Figure 19. Concluded.

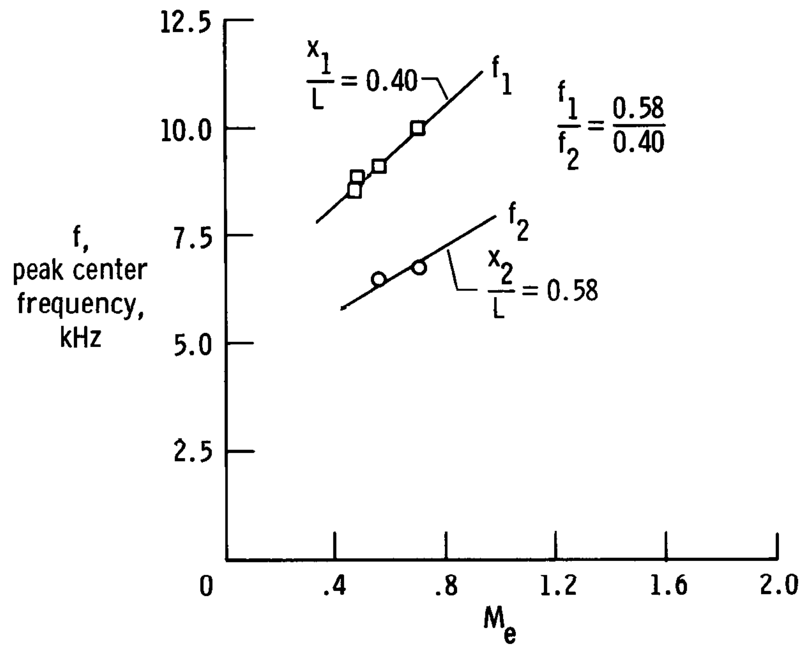

(a) $q = 9.6$ kN/m^2 (200 lb/ft^2).

Figure 20. Variation of laminar or transitional spectral peak with M_e.

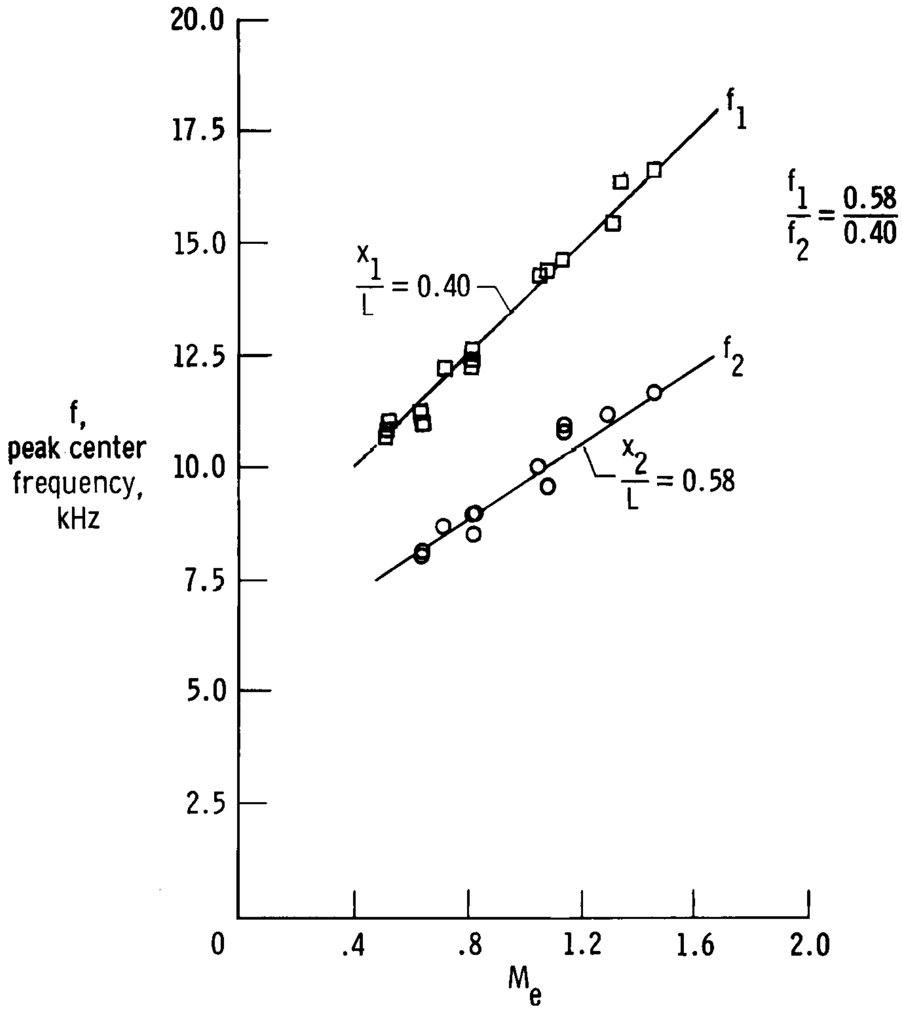

(b) $q = 14.4\ kN/m^2$ (300 lb/ft^2).

Figure 20. Continued.

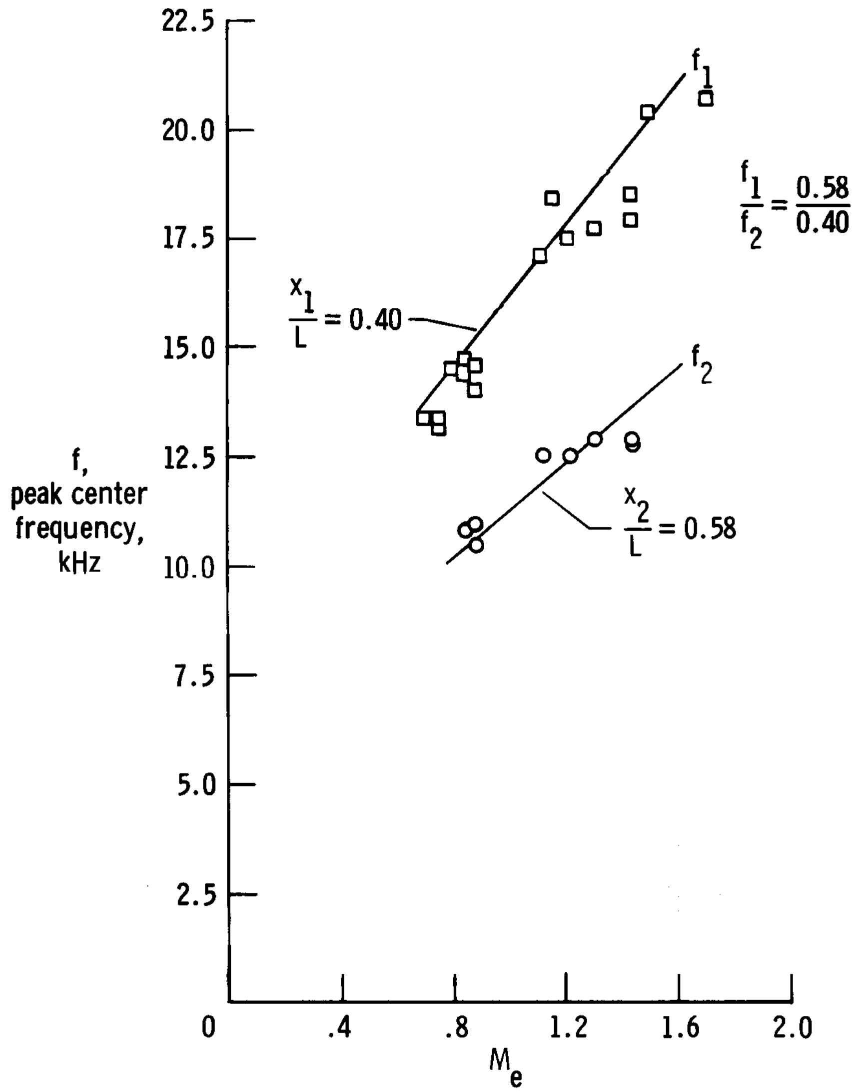

(c) $q = 26.3\ kN/m^2\ (550\ lb/ft^2)$.

Figure 20. Continued.

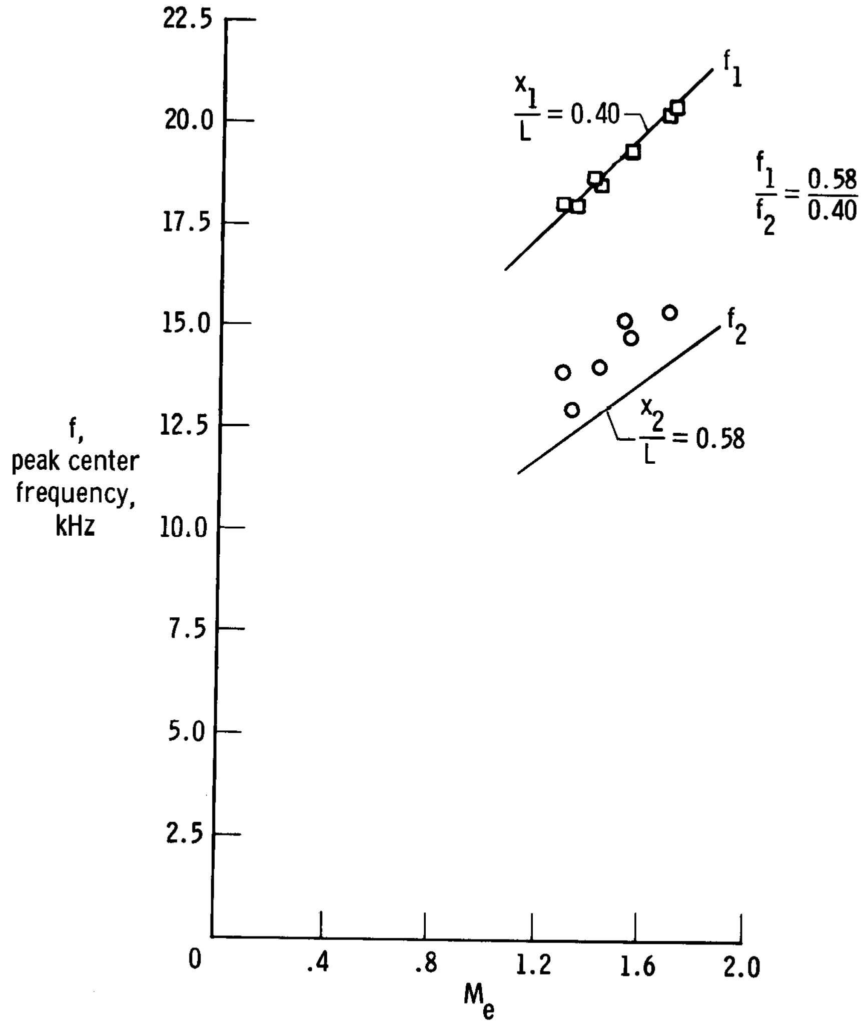

(d) $q = 38.2\ kN/m^2\ (800\ lb/ft^2)$.

Figure 20. Concluded.

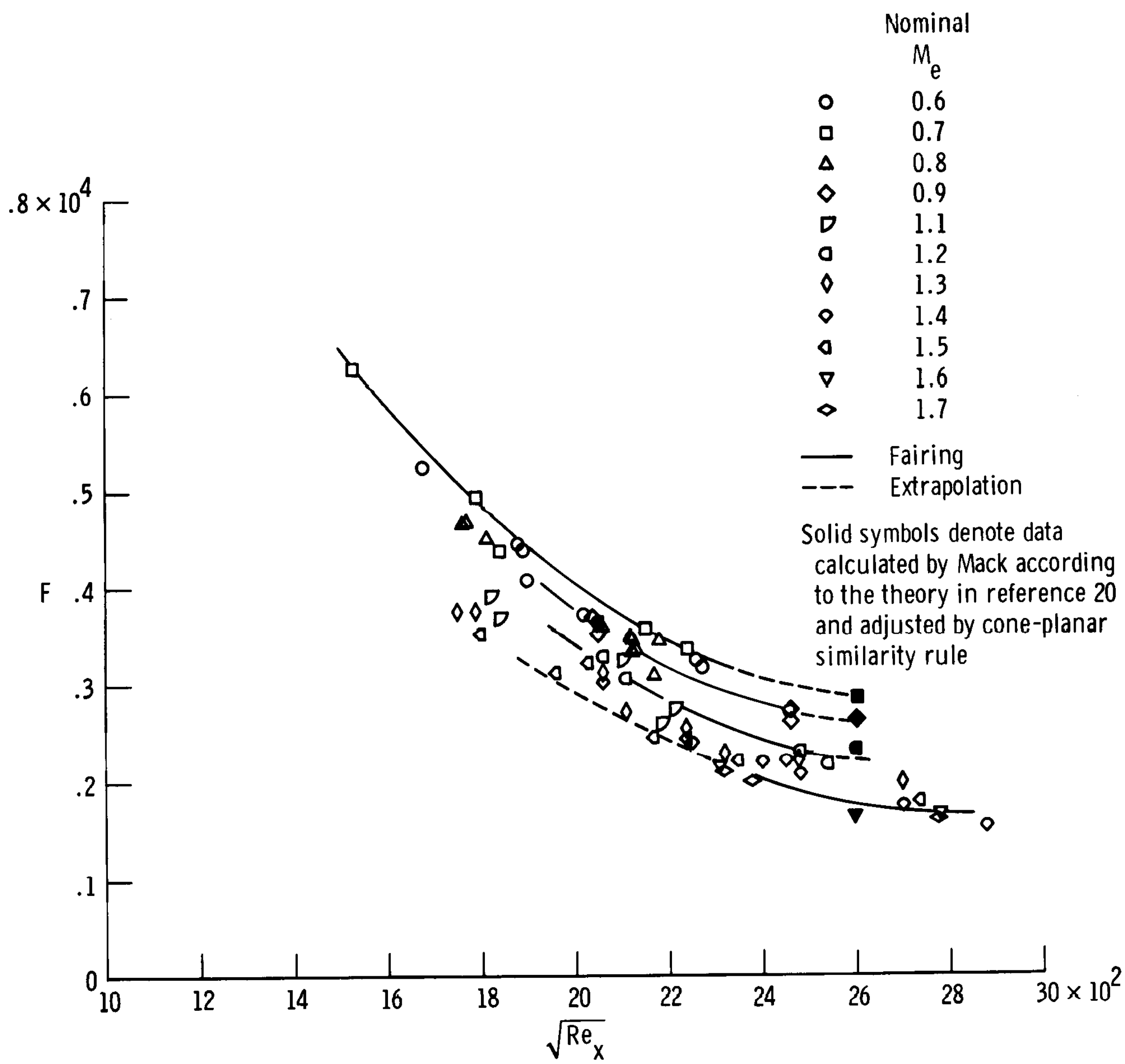

Figure 21. Variation of nondimensional frequency with Re_x.

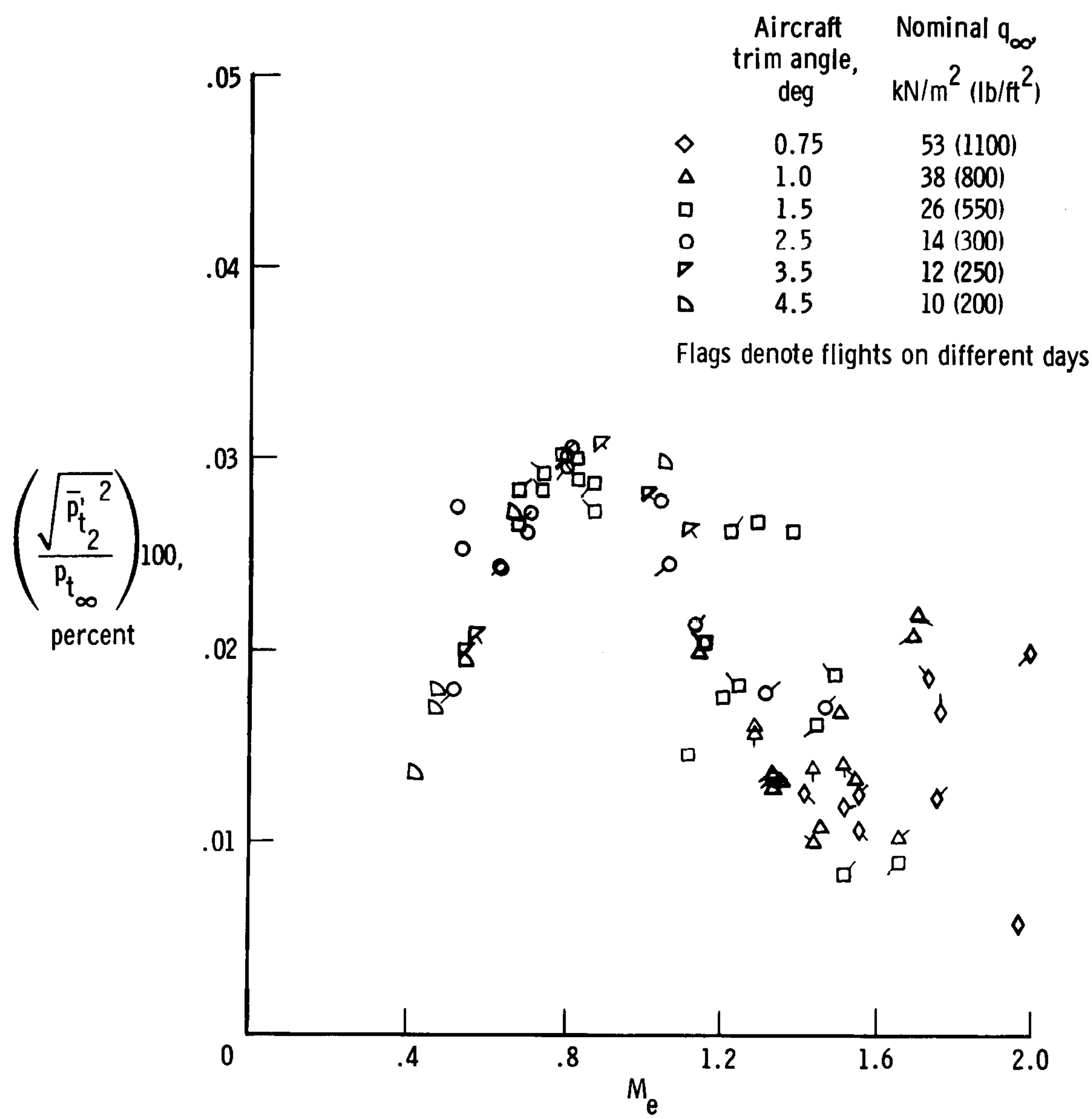

(a) Normalized with p_{t_∞}.

Figure 22. Fluctuating free-stream impact pressure as a function of Mach number at boundary layer edge.

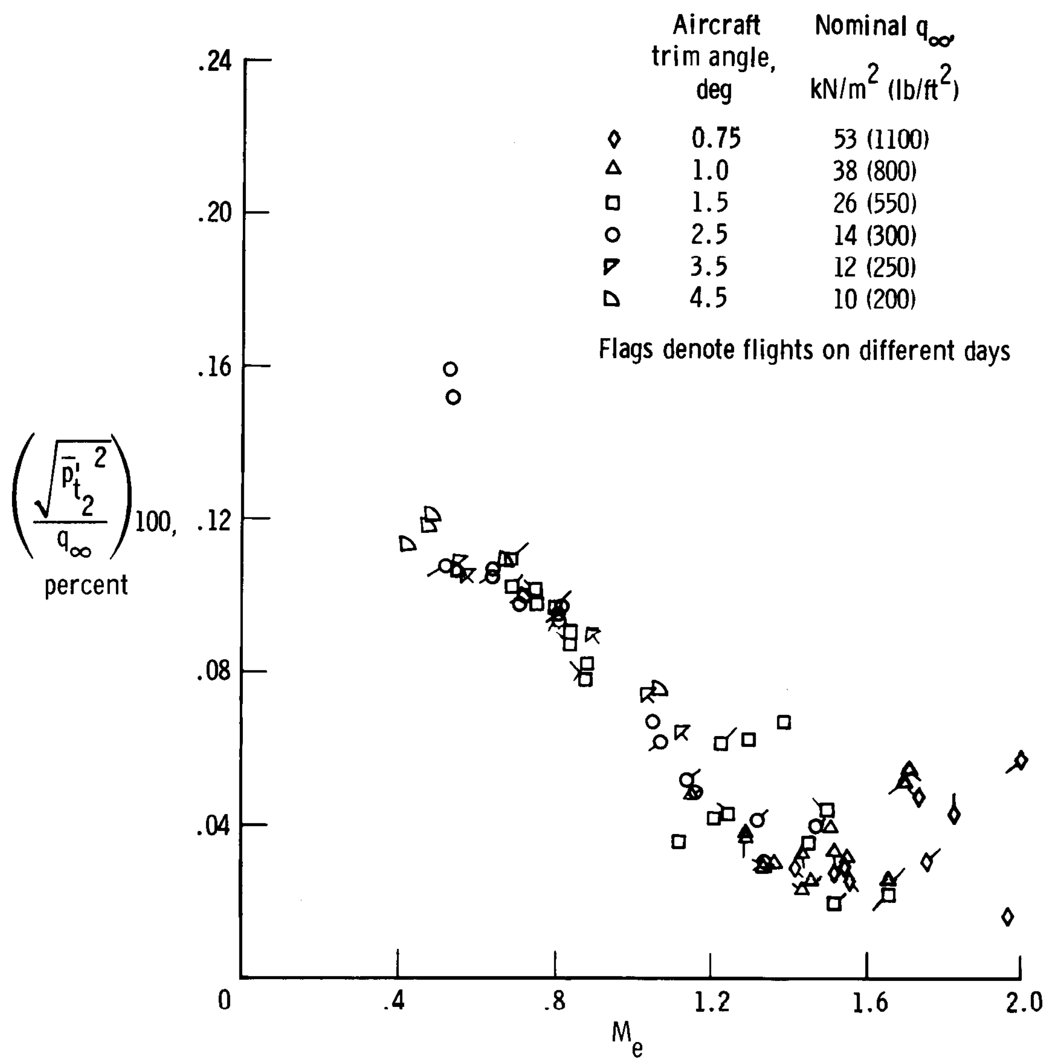

(b) Normalized with q_∞.

Figure 22. Concluded.

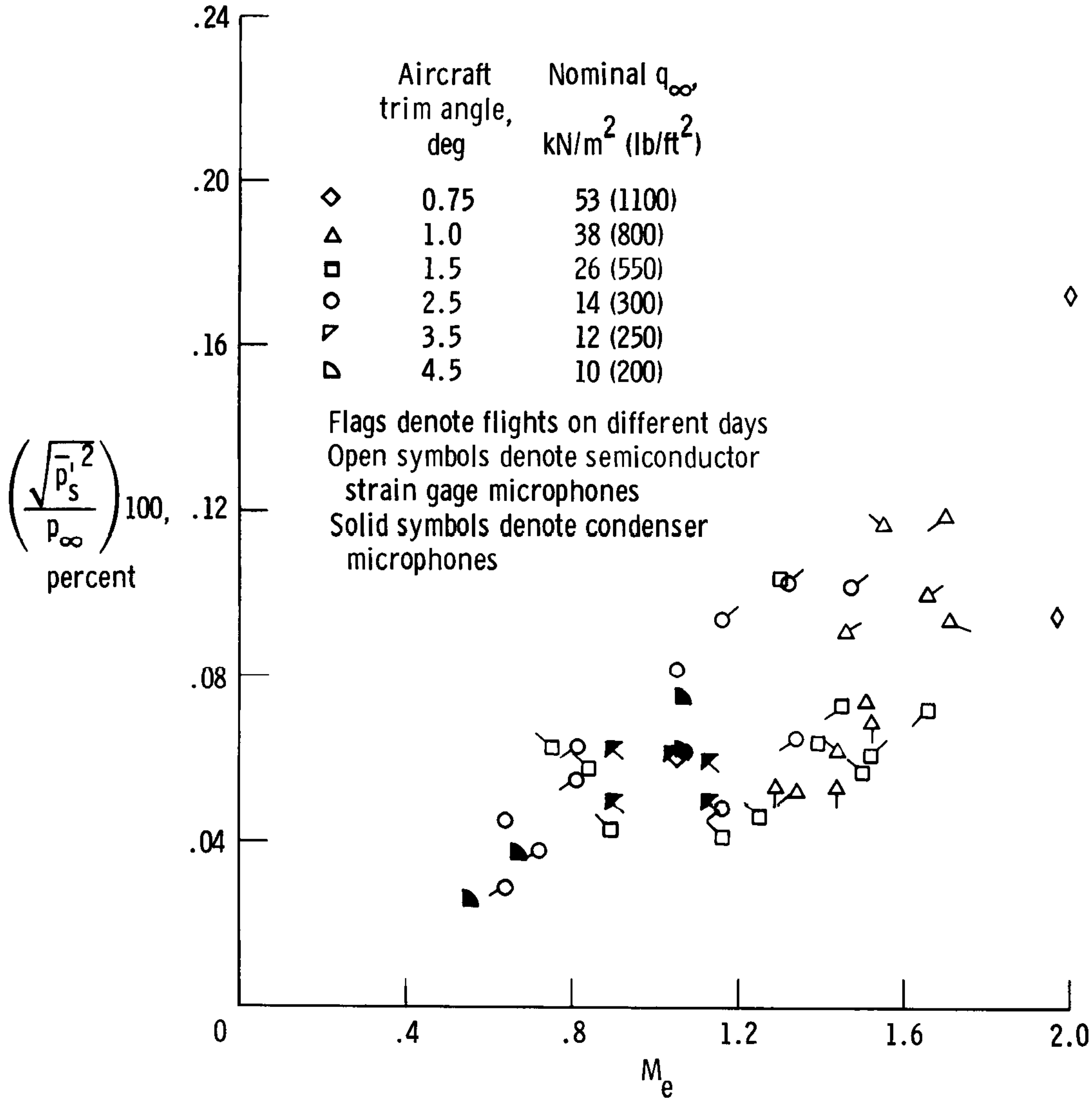

(a) Normalized with p_∞.

Figure 23. Fluctuating static pressure as a function of Mach number at boundary layer edge.

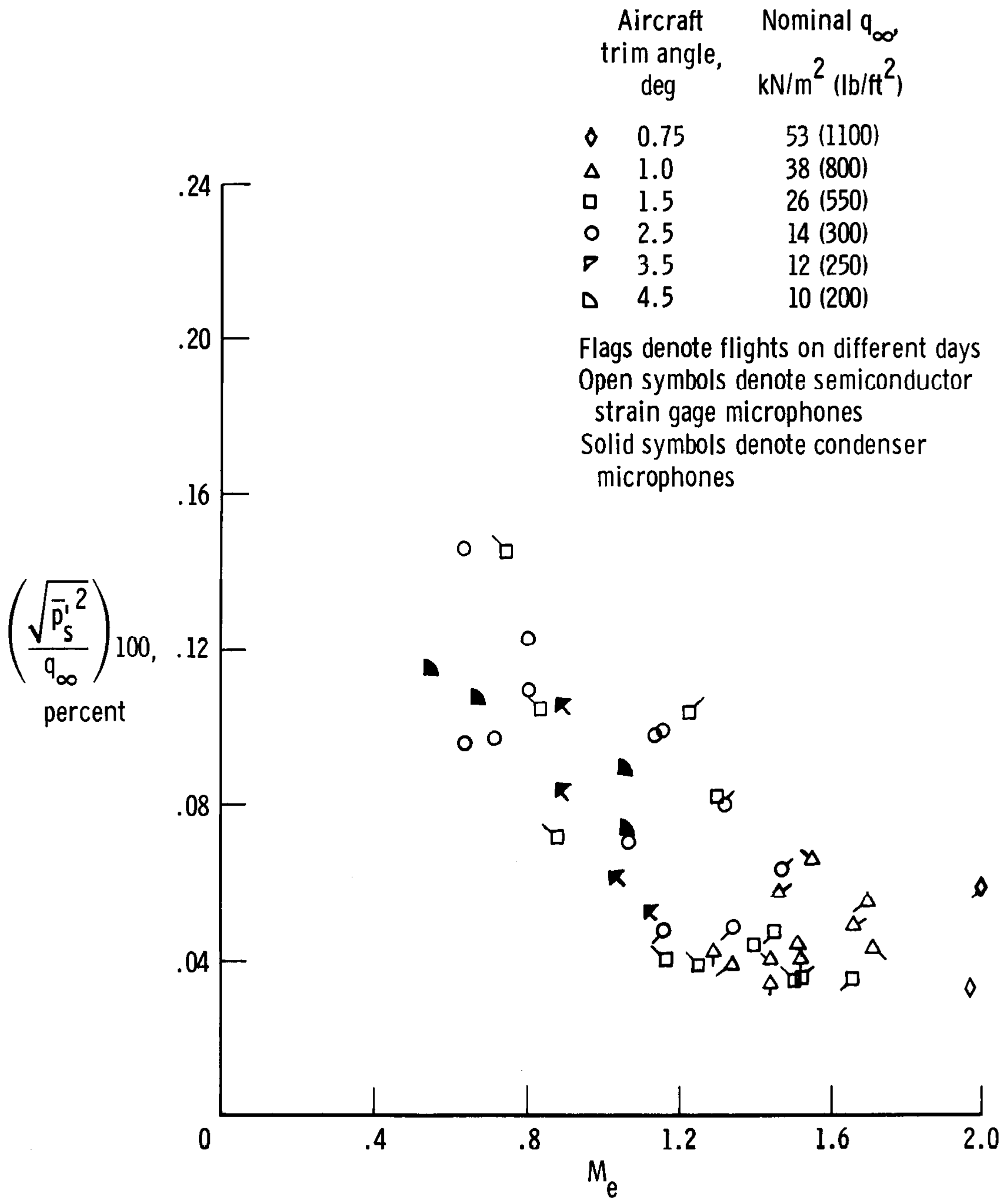

(b) Normalized with q_∞.

Figure 23. Concluded.

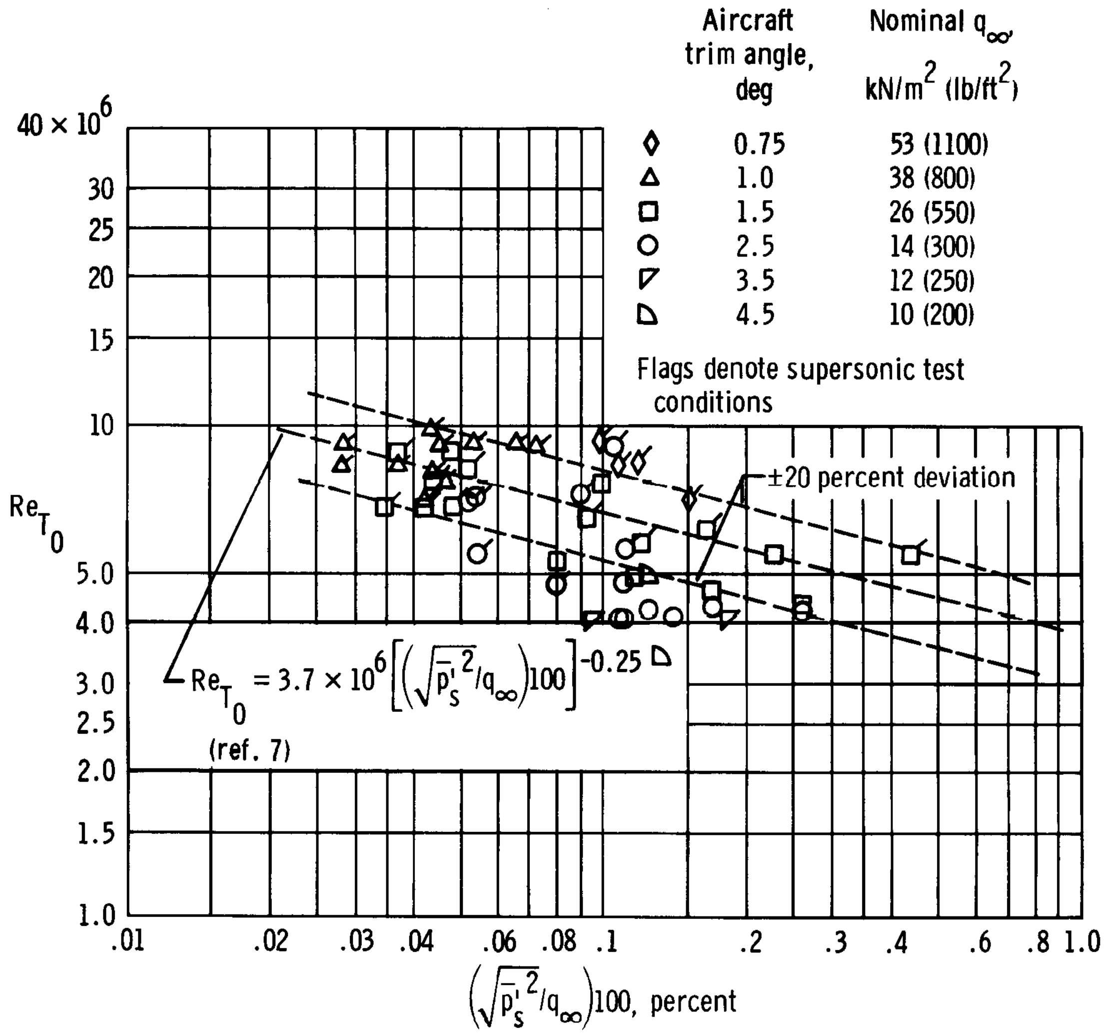

(a) Cone surface disturbance measurements.

Figure 24. Comparison between flight Re_{T_0} and flight disturbance measurements. Zero angles of incidence; adiabatic wall temperatures.

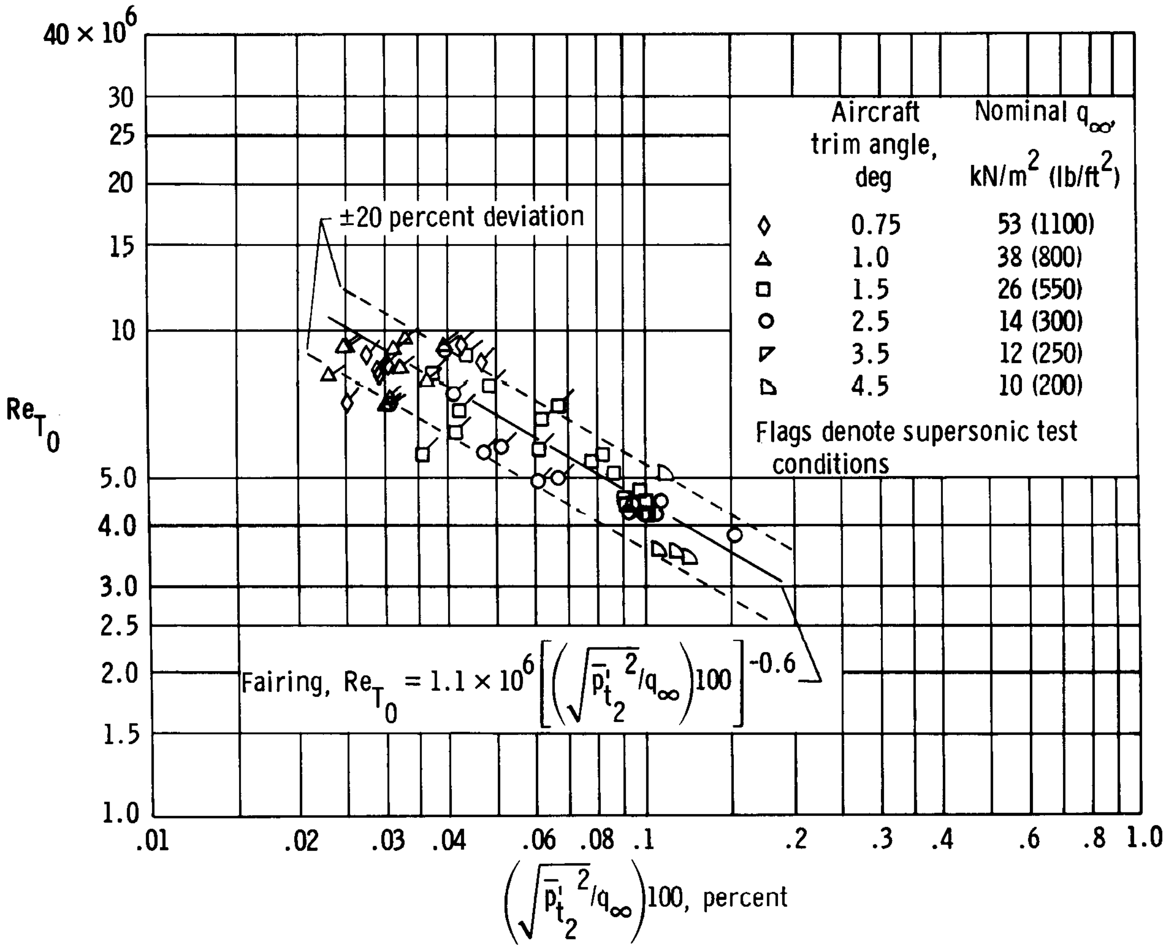

(b) Free-stream total disturbance measurements.

Figure 24. Concluded.

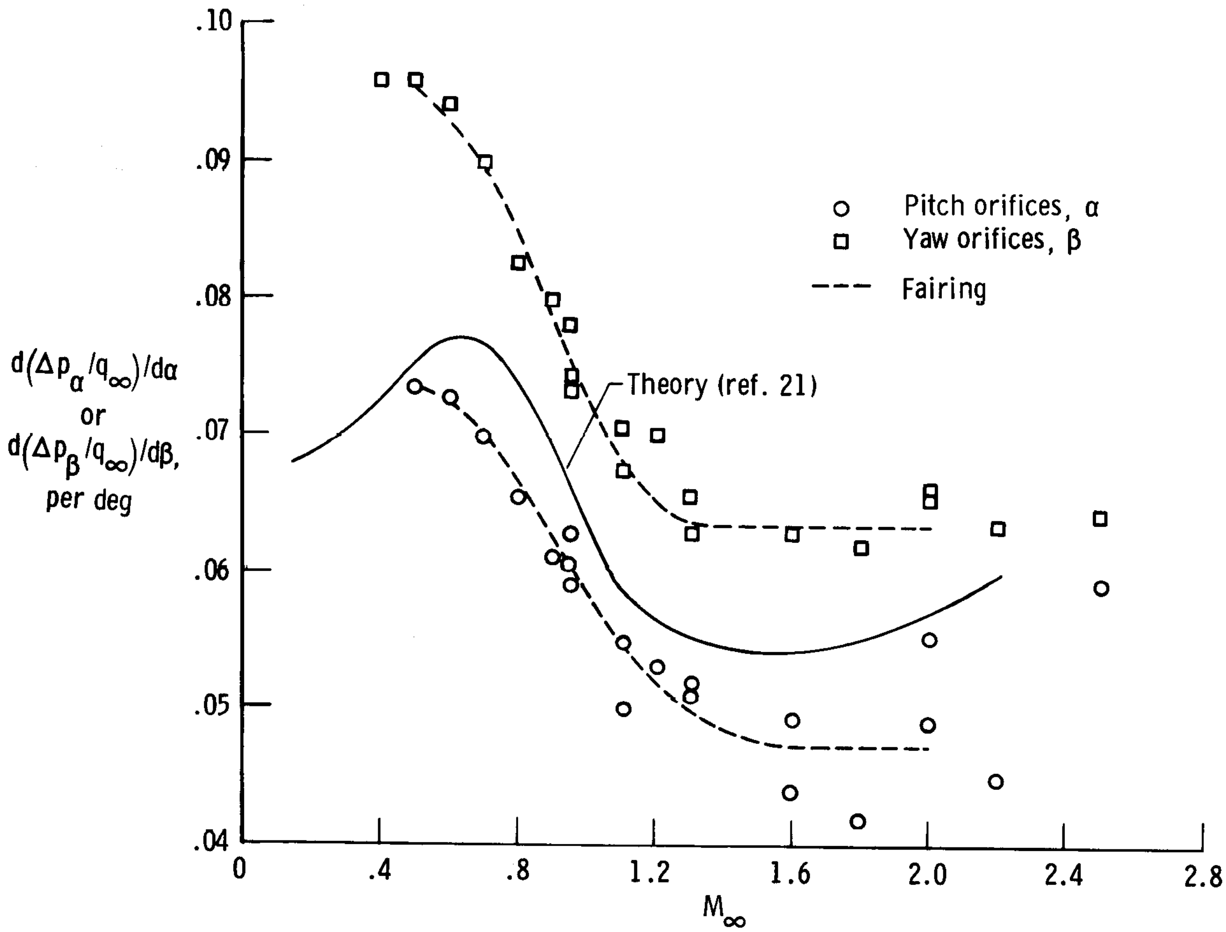

Figure 25. Fixed flow-sensing probe calibrations for sensitivity to flow angle.

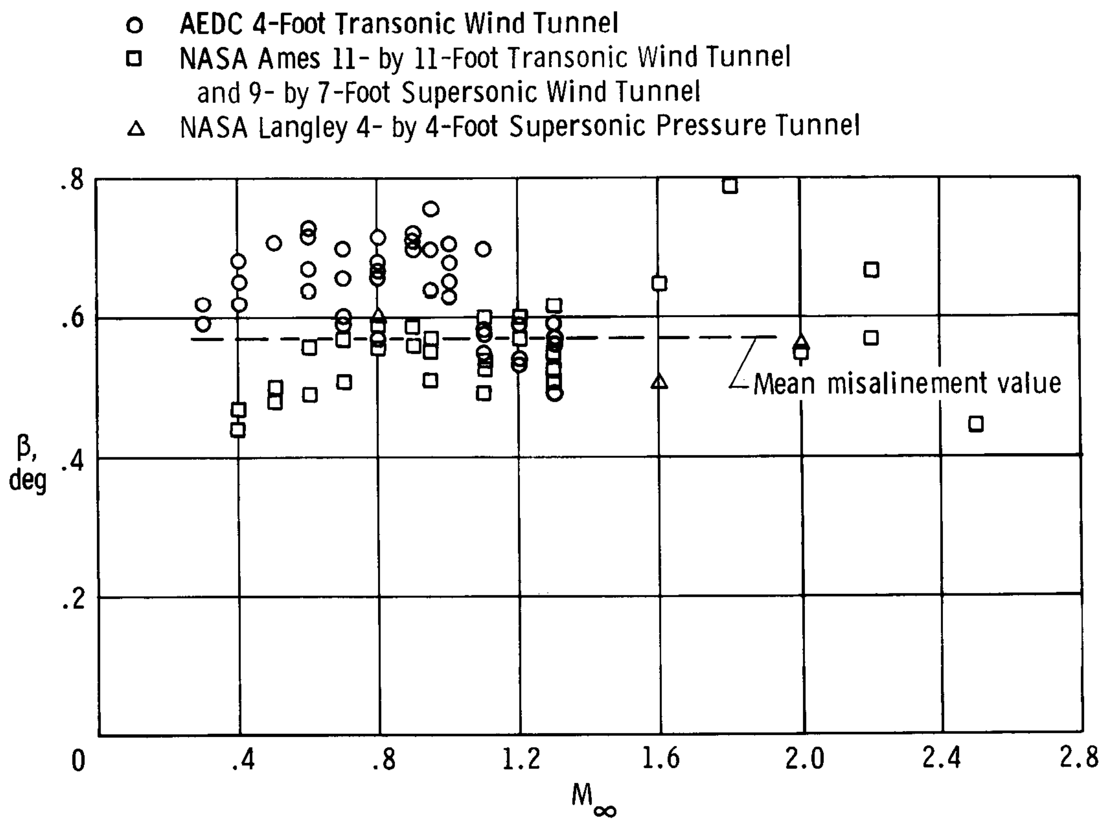

Figure 26. Fixed flow-sensing probe data on misalinement angle in sideslip plane.

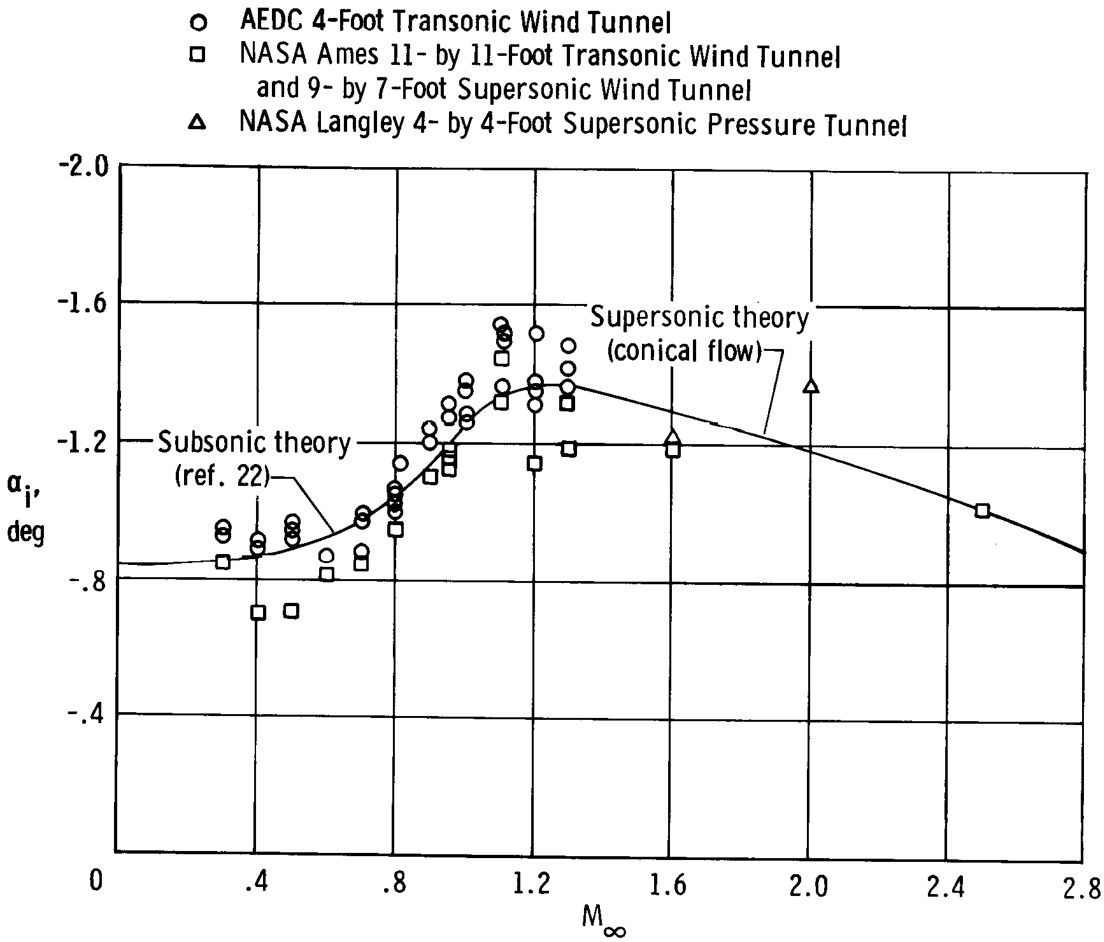

Figure 27. Fixed flow-sensing probe data for flow field affected by cone. Cone $\alpha = 0°$.

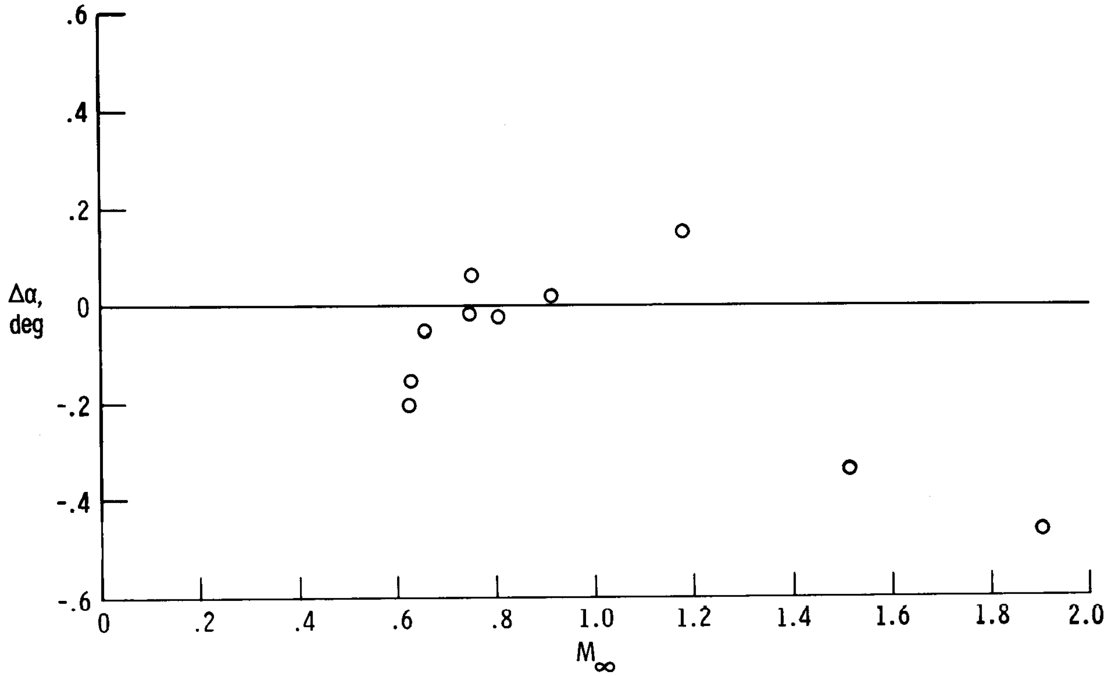

Figure 28. Comparison of angle of attack using the accelerometer method and wind tunnel calibration. Δα = aircraft angle of attack - aircraft trim angle.

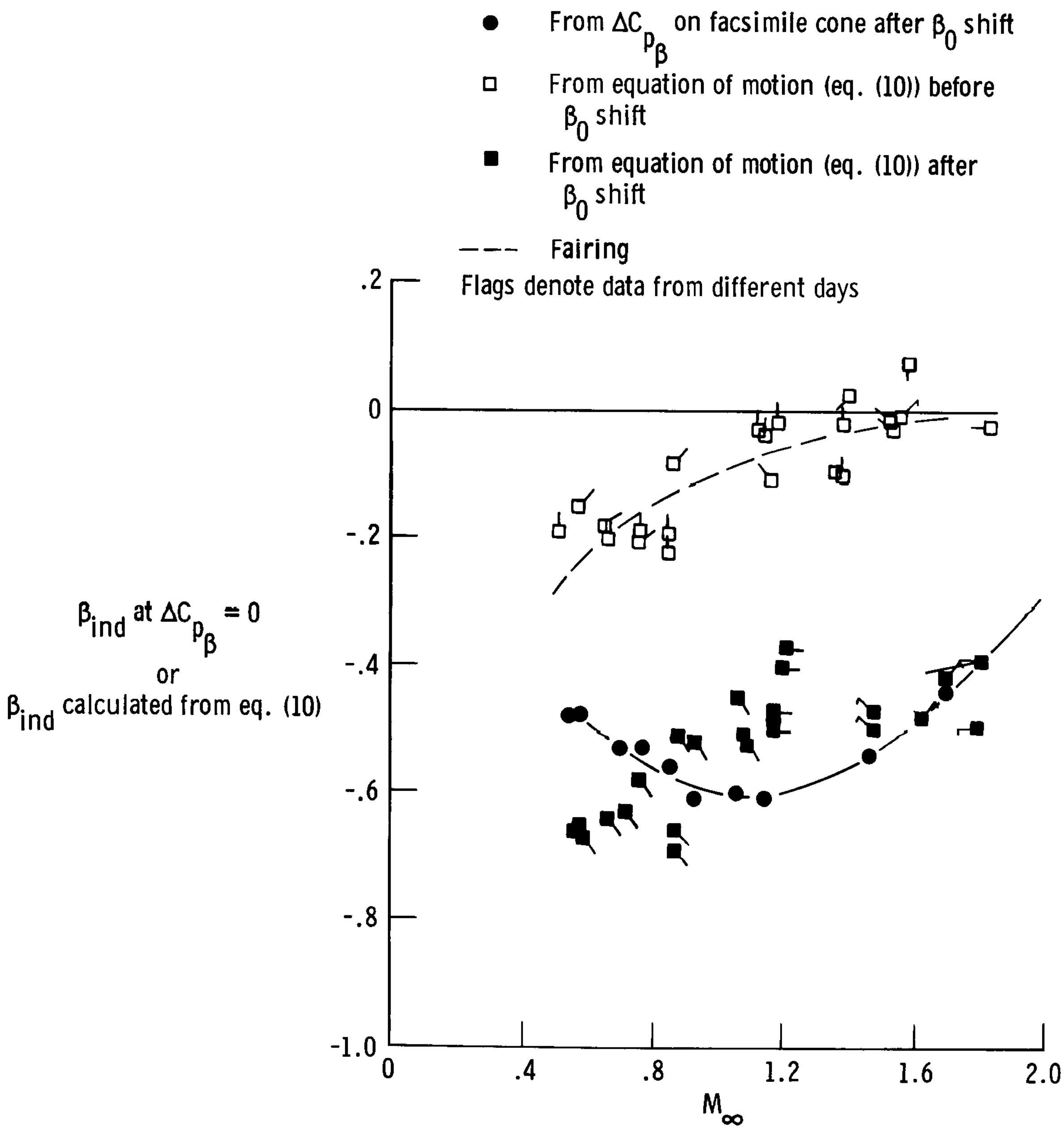

Figure 29. In-flight calibration of angle of sideslip.

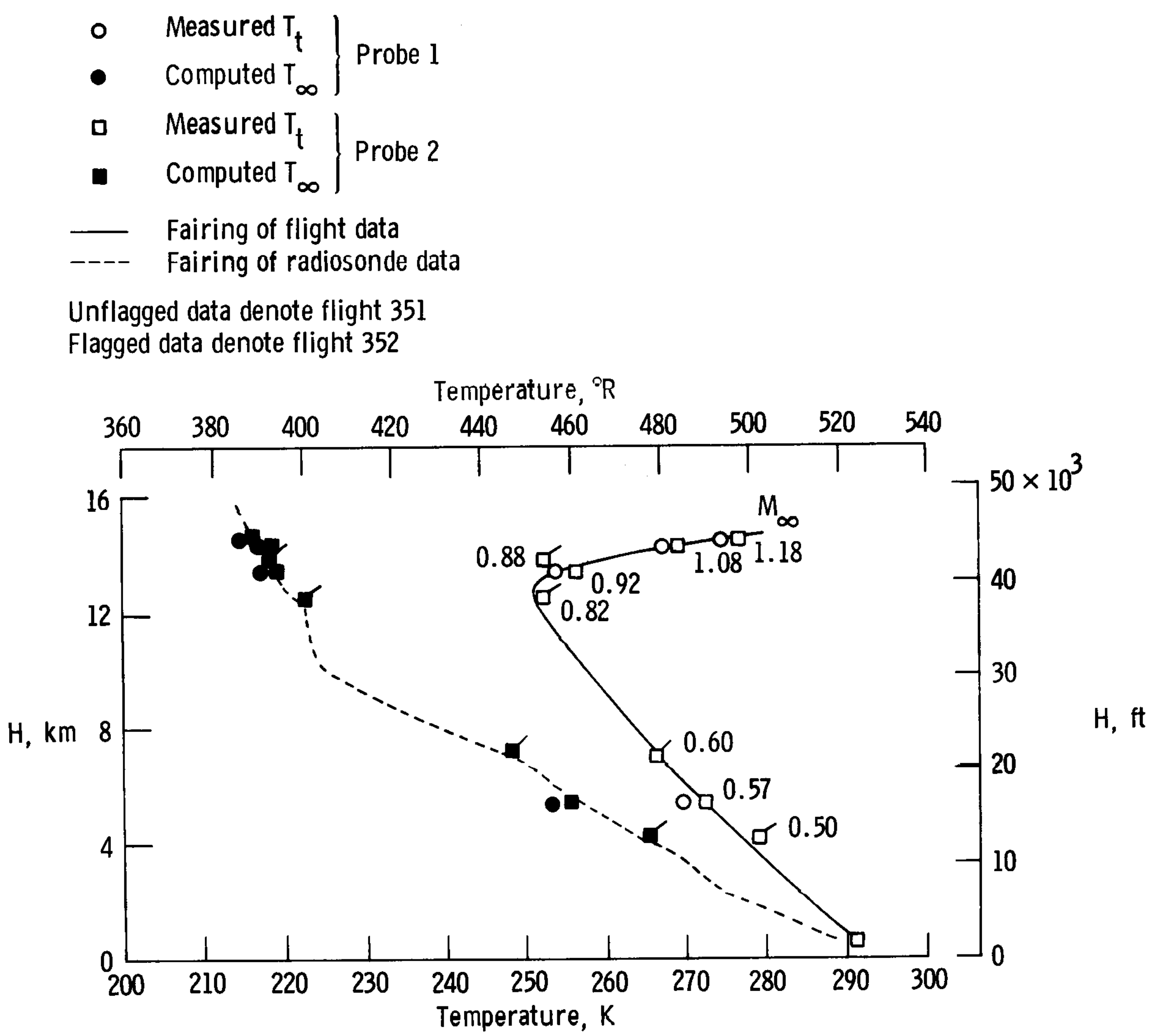

(a) Aircraft trim angle of attack = 3.5°. All data are for 10/31/78.

Figure 30. Comparison of in-flight temperatures with radiosonde data.

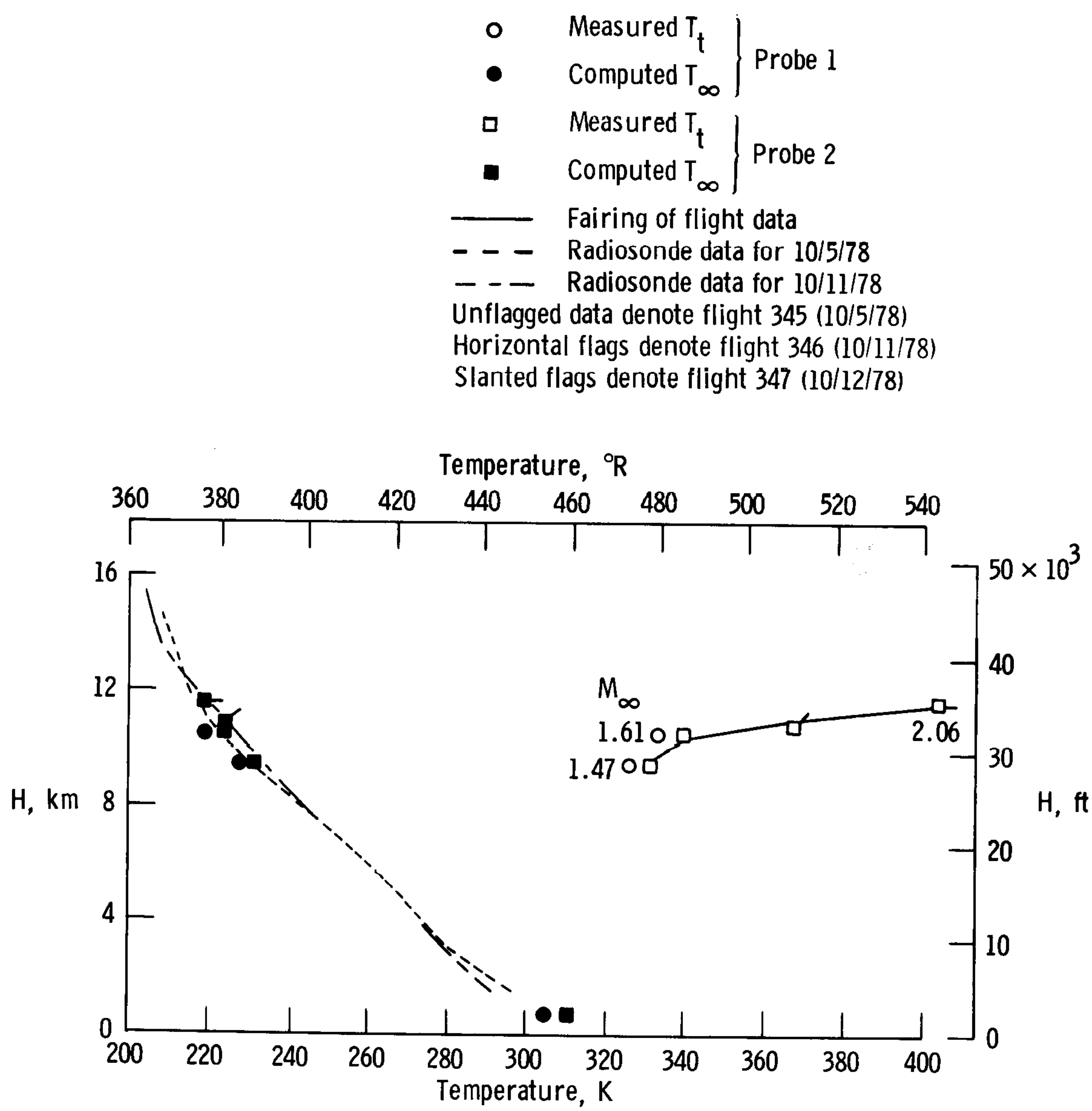

(b) Aircraft trim angle of attack = 1°.

Figure 30. Concluded.

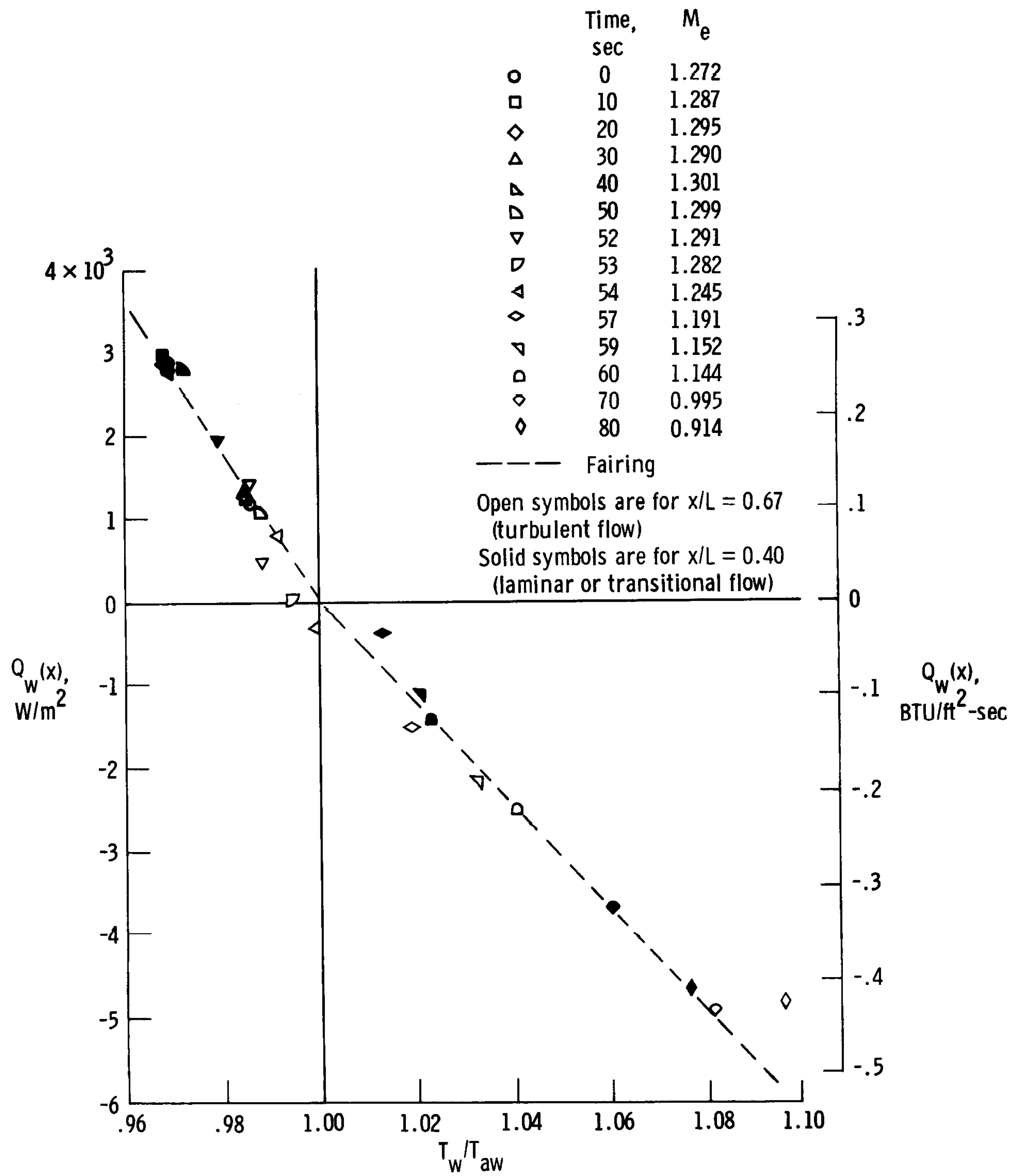

Figure 31. Heat transfer rate as a function of T_w/T_{aw} at selected locations on facsimile cone. $\phi = 135°$; $r_{laminar} = 0.84 \approx Pr^{1/2}$; $r_{turbulent} = 0.88 \approx Pr^{1/3}$.

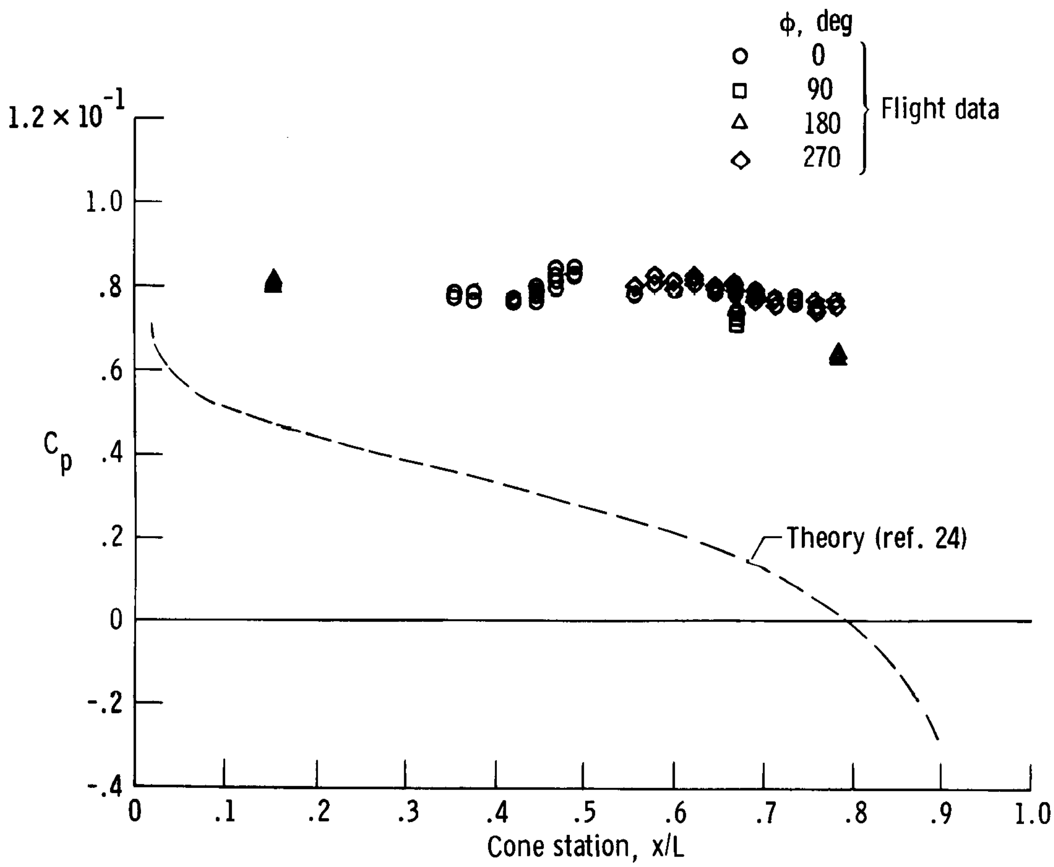

(a) $M_\infty = 0.55$.

Figure 32. Comparison of in-flight pressure distribution on facsimile cone with theory.

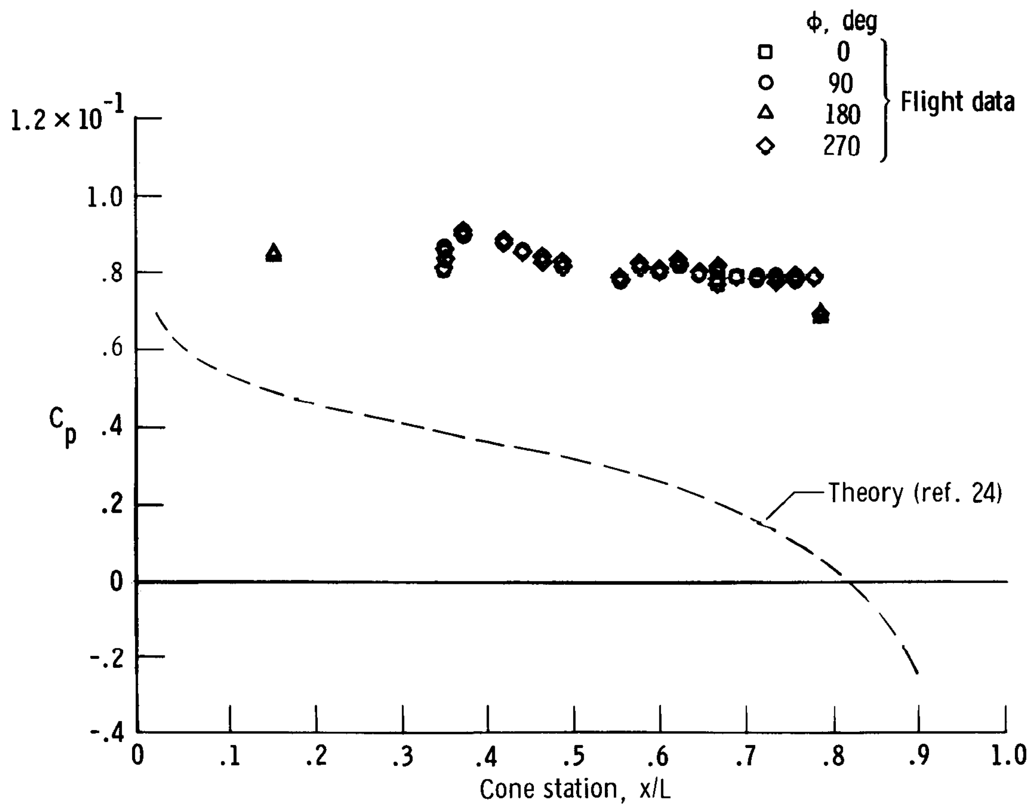

(b) $M_\infty = 0.69.$

Figure 32. Continued.

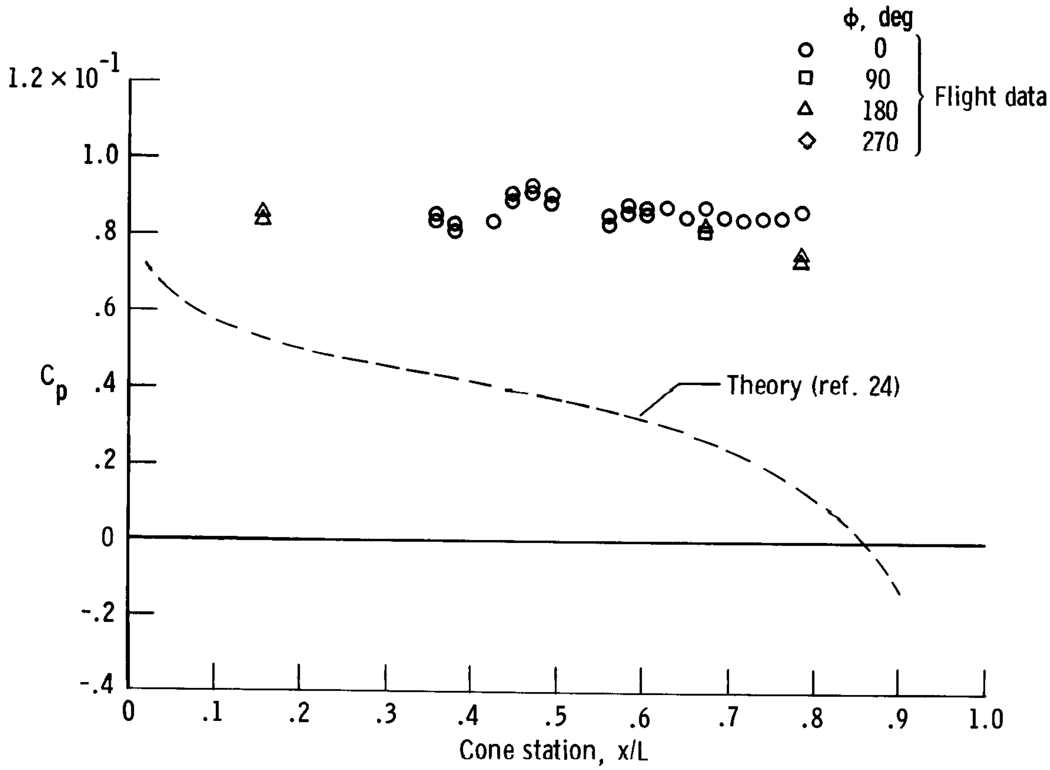

(c) $M_\infty = 0.86$.

Figure 32. Continued.

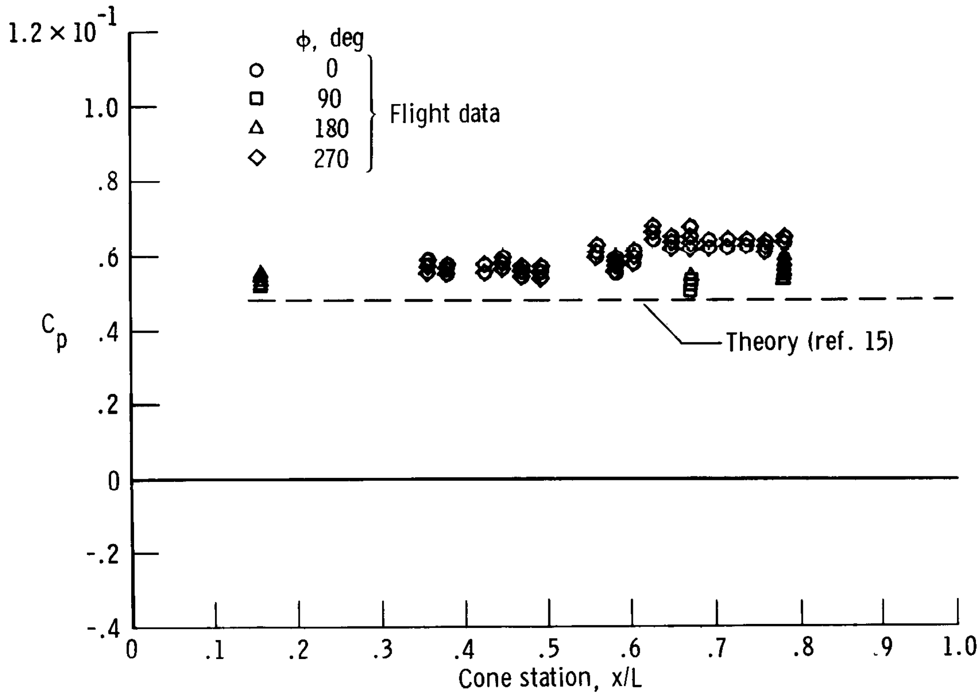

(d) $M_\infty = 1.17$.

Figure 32. Continued.

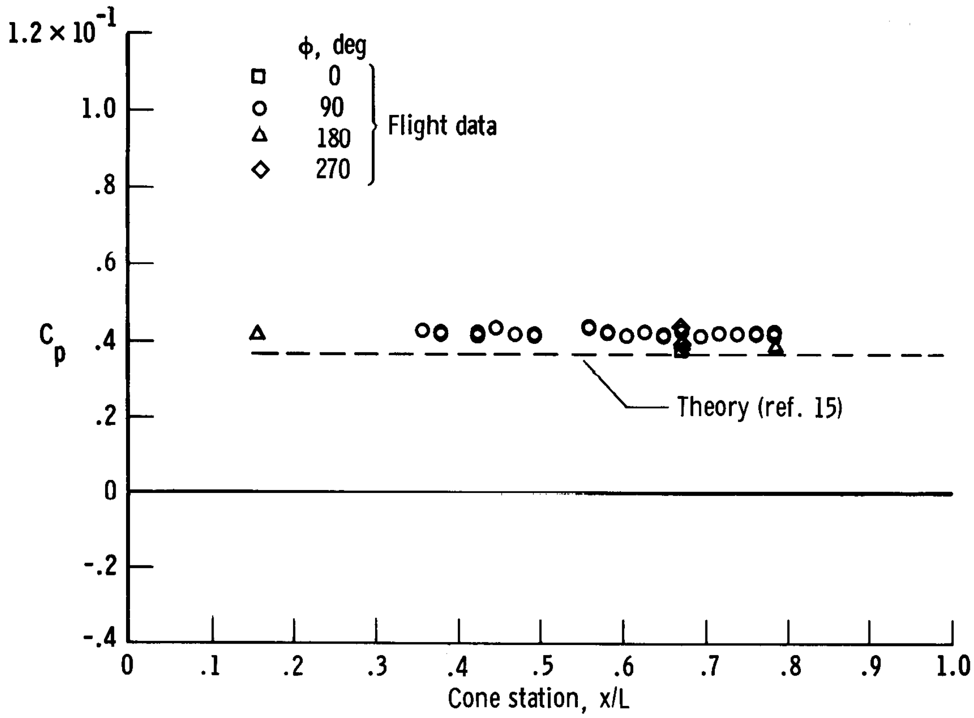

(e) $M_\infty = 1.68$.

Figure 32. Concluded.

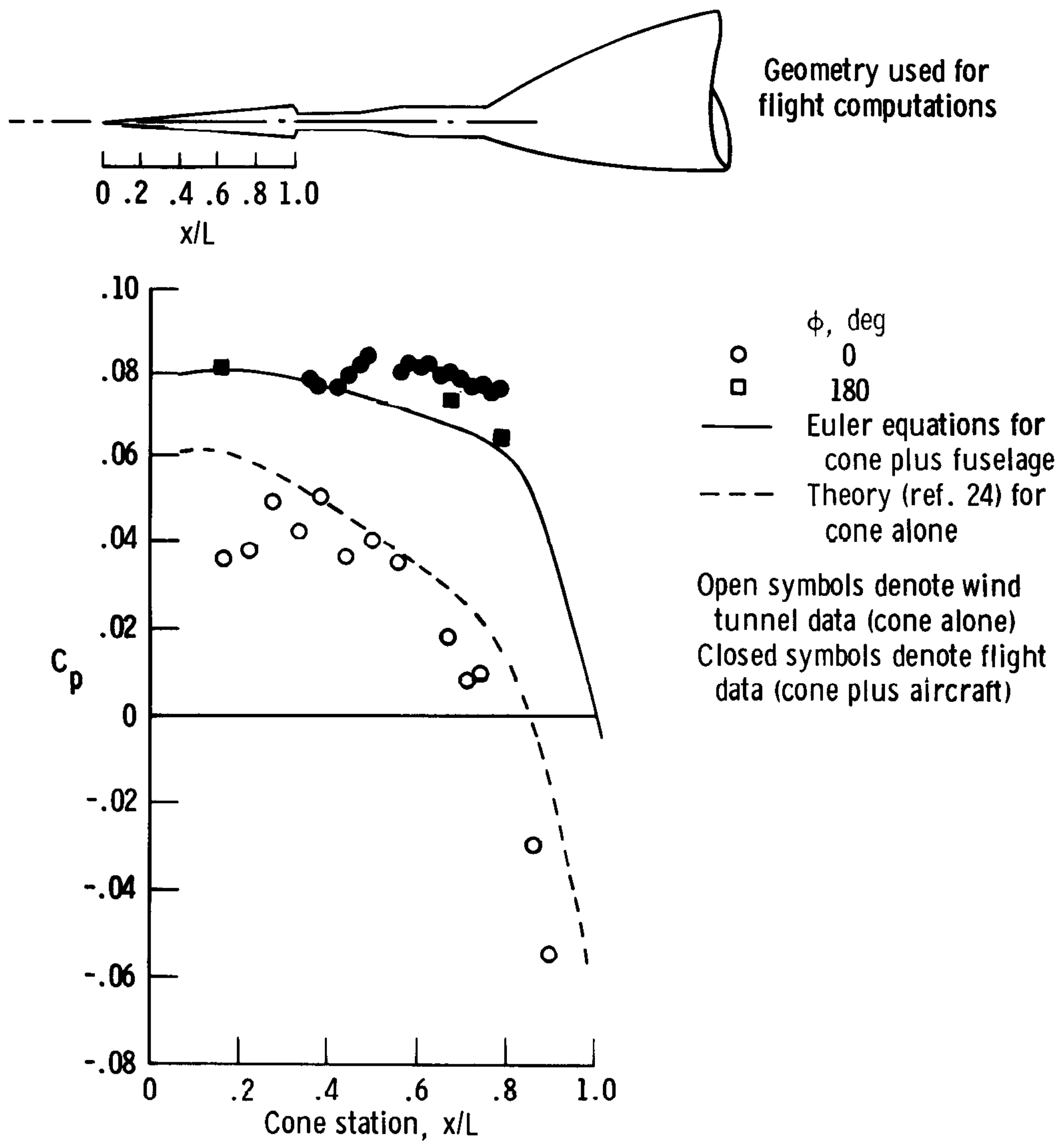

Figure 33. Comparison of cone pressure distribution from flight, wind tunnel, and theory. $M_\infty \approx 0.6$; zero incidence angle.

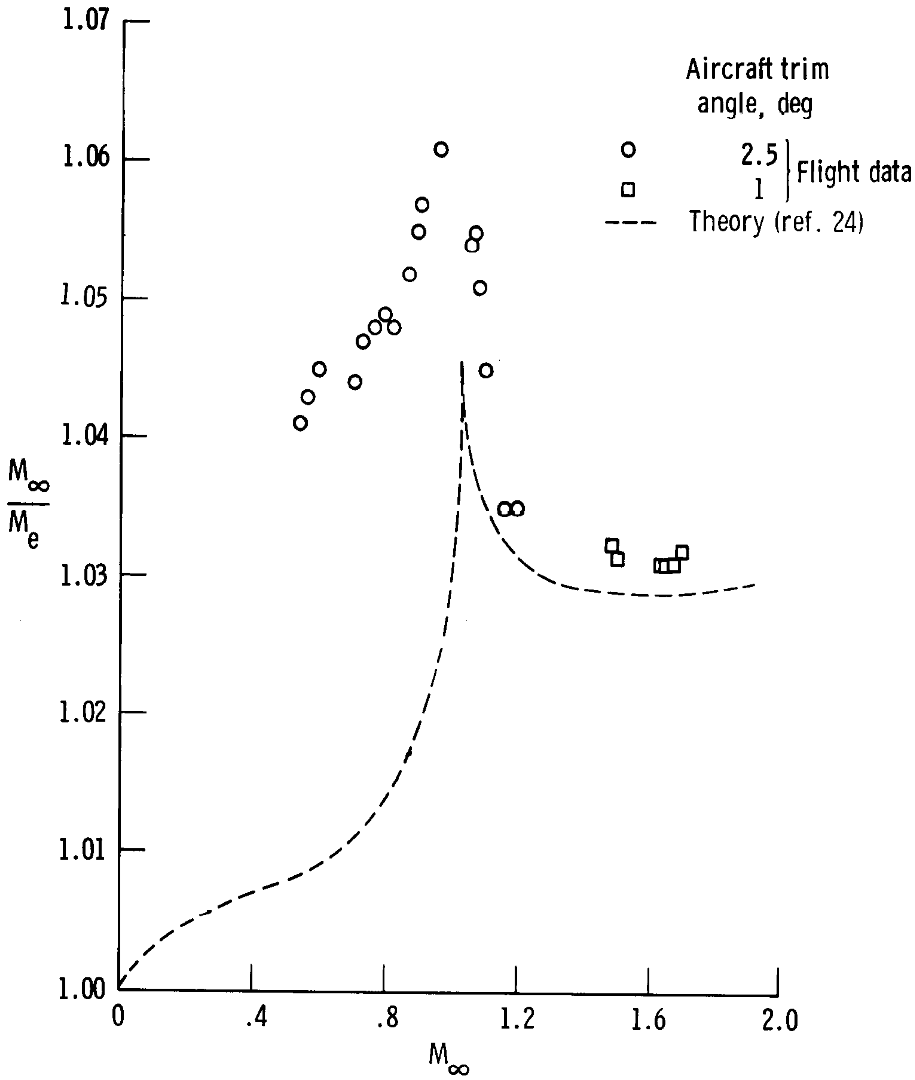

(a) Mach number at boundary layer edge.

Figure 34. Influence of aircraft forward flow field on cone at zero incidence. Theory and flight data are for x/L = 0.67.

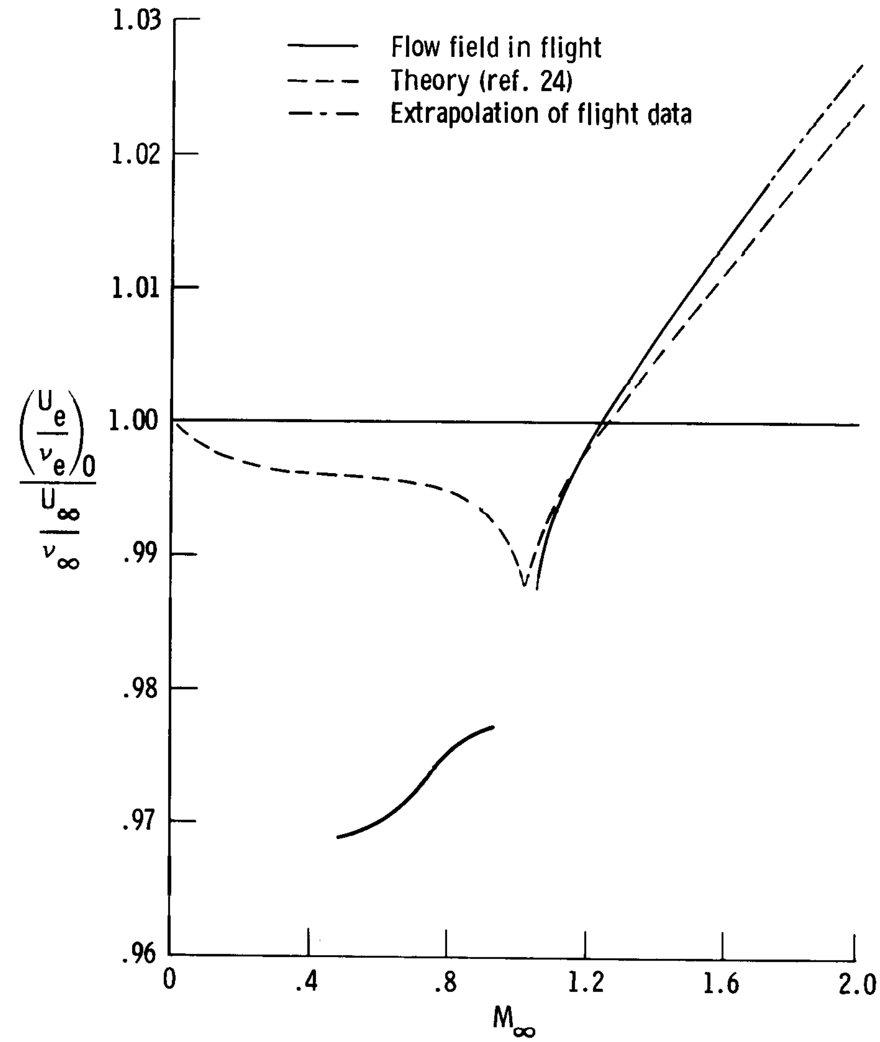

(b) Local unit Reynolds number. $U_\infty/\nu_\infty \approx 10^7$ *per m* (3.0×10^6 *per ft*).

Figure 34. Continued.

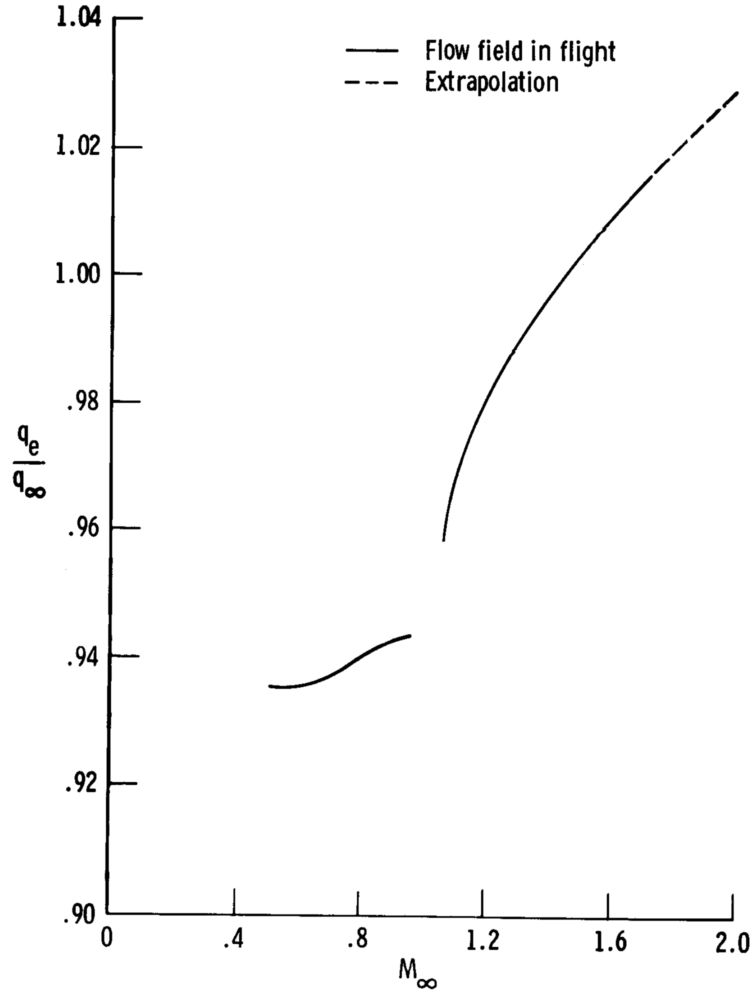

(c) Local dynamic pressure.

Figure 34. Concluded.

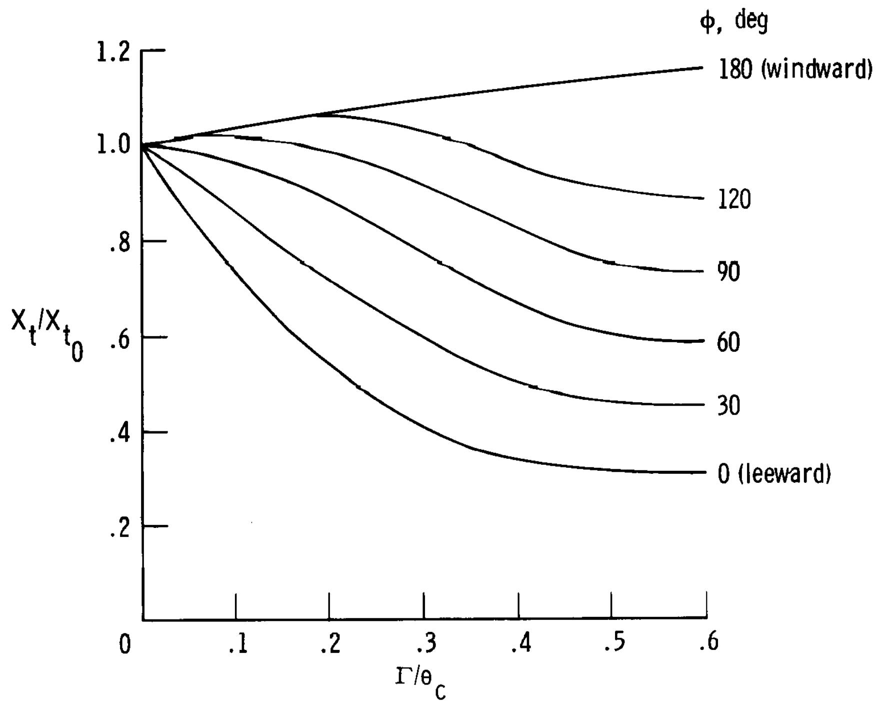

Figure 35. Location of transition onset as a function of total incidence angle, Γ, and meridian angle, ϕ, from reference 26.

	M_e	θ_c, deg	U_∞/ν_∞, per m (per ft)		Source
○	1.94	5	11.8×10^6	(3.6×10^6)	NASA Ames 9- by 7-Foot Supersonic Wind Tunnel
□	2.13	5	9.8	(3.0)	NASA Ames 9- by 7-Foot Supersonic Wind Tunnel
△	2.15	4	17.7	(5.4)	Reference 26
◇	2.03	10	18.7	(5.7)	Reference 26

——— Fairing of data for $\theta_c = 5°$

– – – Fairing of data for $\theta_c = 4°$

—·— Fairing of data for $\theta_c = 10°$

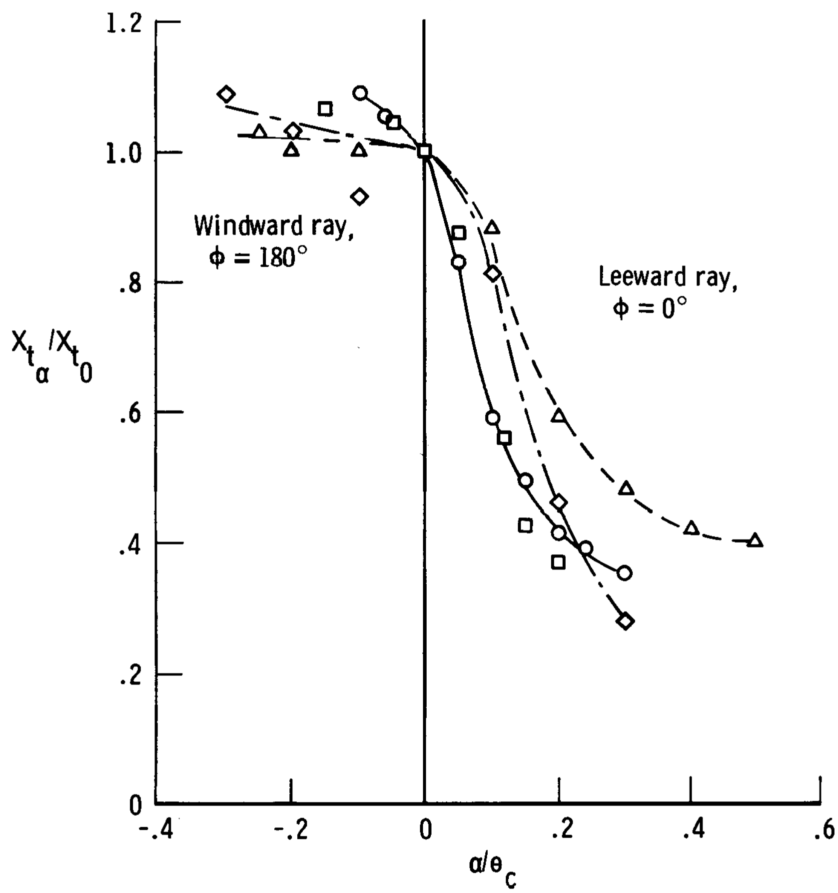

(a) $M_\infty \approx 2.00$.

Figure 36. Movement of data on cone windward-leeward transition with changing angle of attack. Wind tunnel data.

	M_e	θ_c, deg	U_∞/ν_∞, per m (per ft)		T_w/T_{aw}	Source
	4.36	5	9.8×10^6	(3.0×10^6)	1.0	NASA Langley Unitary Plan Wind Tunnel
	4.78	5	17.7	(5.4)	0.77	Reference 28
	5.15	8	81.7	(24.9)	0.59	Reference 29
	4.86	8	13.1	(4.0)	0.26	Reference 30

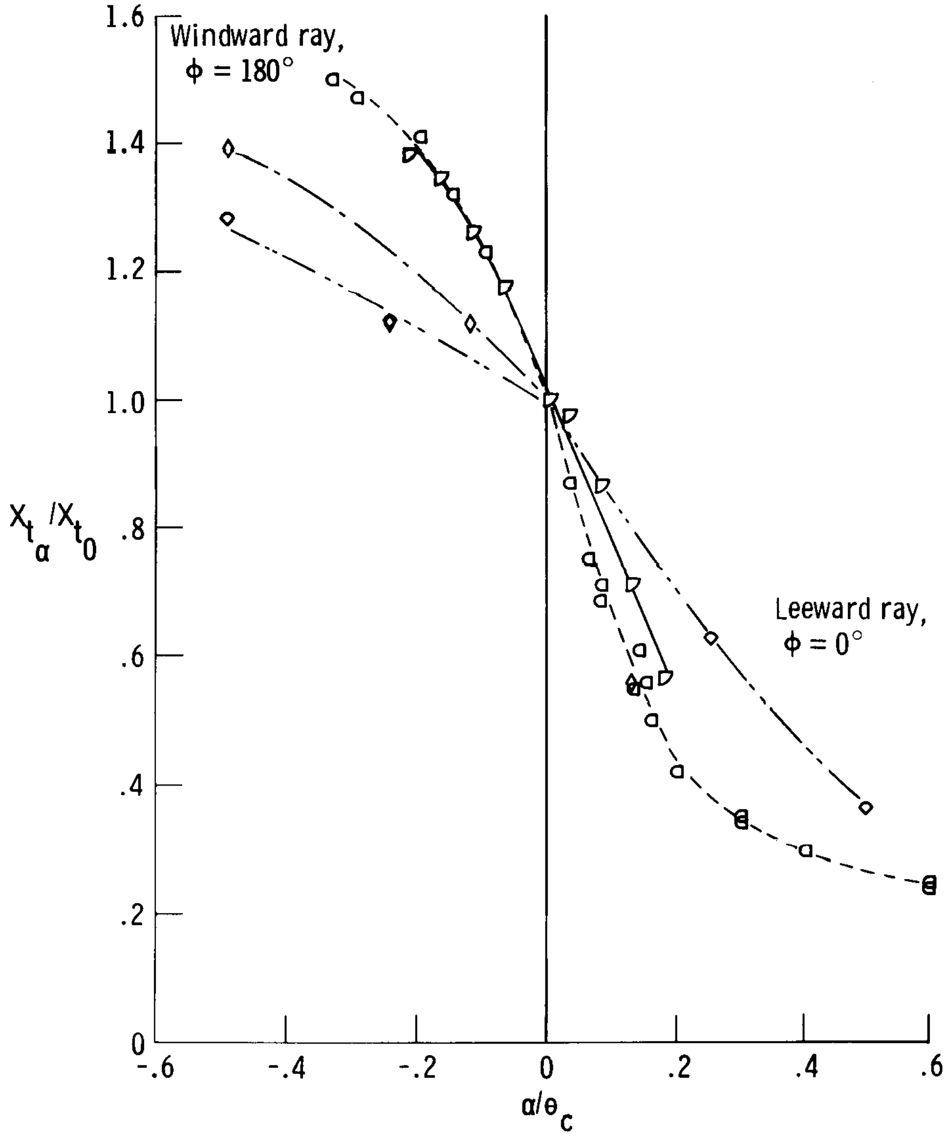

(b) $M_\infty \approx 4.36$ ≈ 5.15.

Figure 36. Concluded.

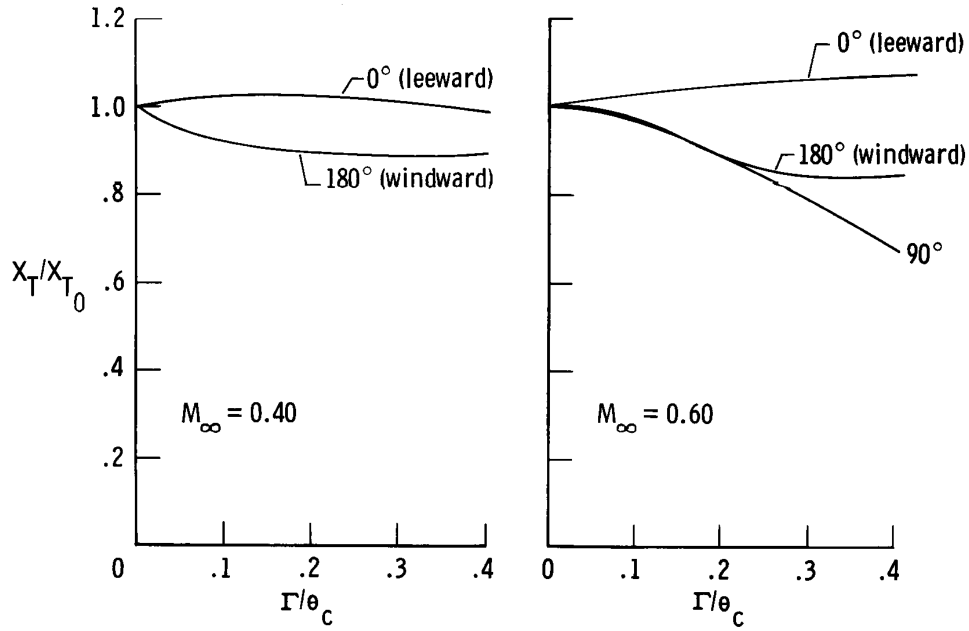

(a) $M_\infty = 0.40$ and $M_\infty = 0.60$.

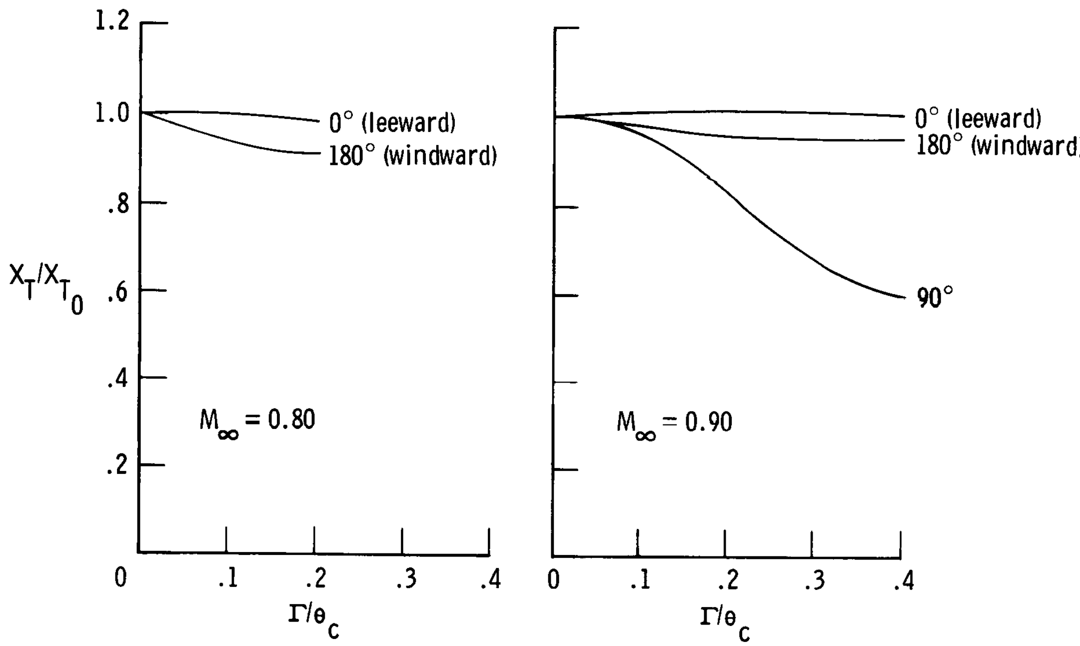

(b) $M_\infty = 0.80$ and $M_\infty = 0.90$.

Figure 37. Location of end of transition as a function of total incidence angle, Γ, and meridian angle, ϕ, from present wind tunnel tests (table 3).

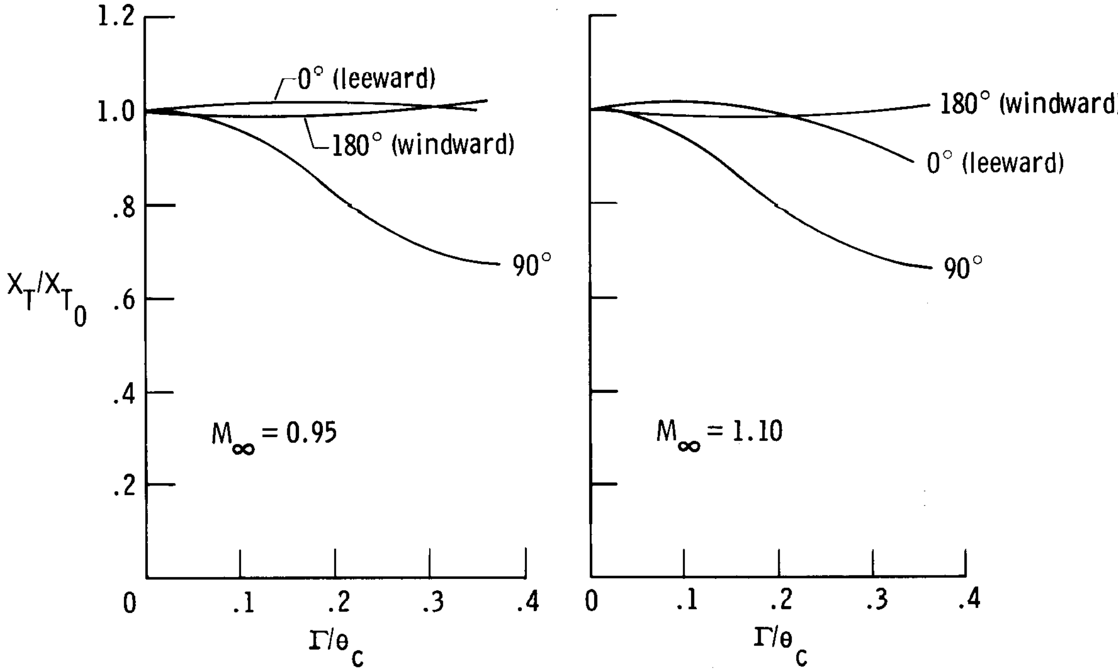

(c) $M_\infty = 0.95$ and $M_\infty = 1.10$.

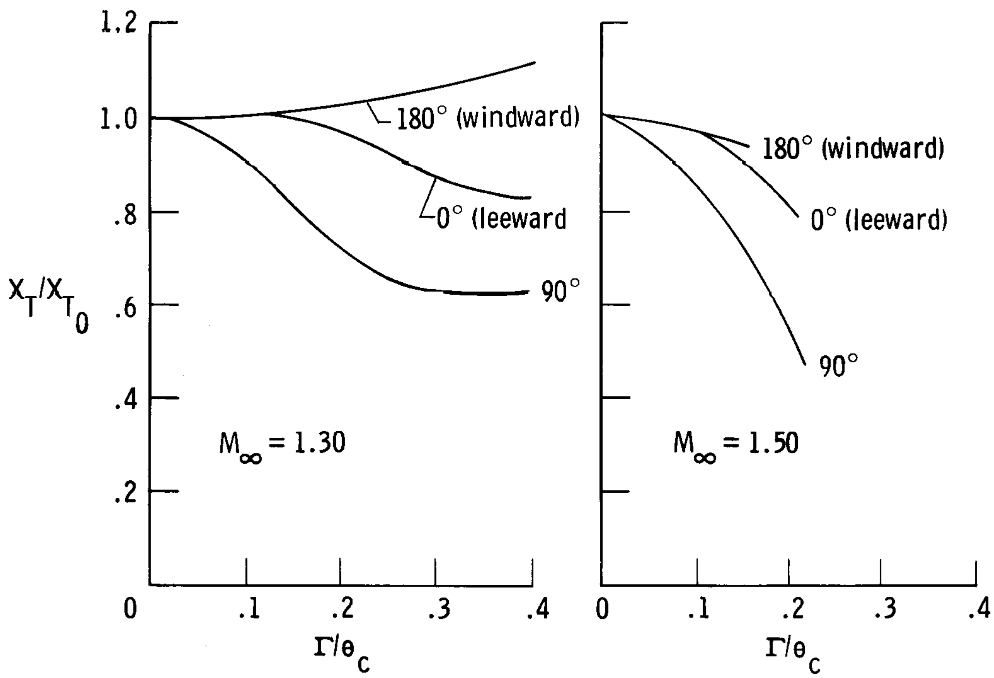

(d) $M_\infty = 1.30$ and $M_\infty = 1.50$.

Figure 37. Continued.

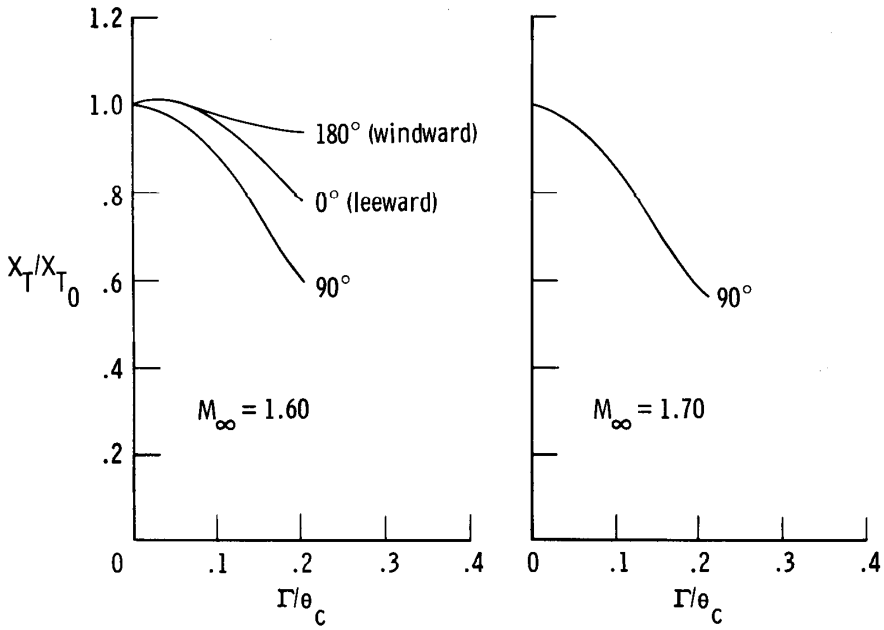

(e) $M_\infty = 1.60$ and $M_\infty = 1.70$.

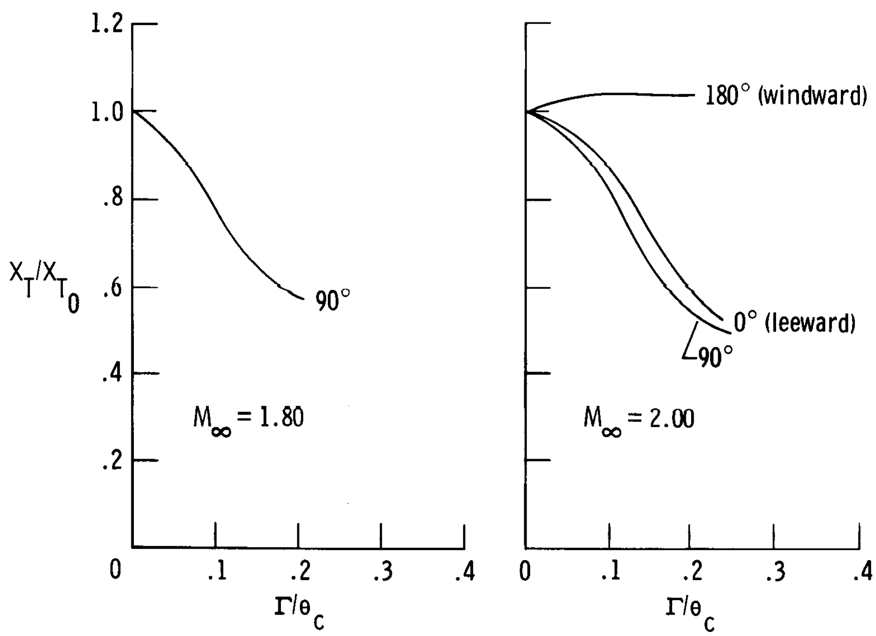

(f) $M_\infty = 1.80$ and $M_\infty = 2.00$.

Figure 37. Concluded.

1. Report No. NASA TP-1971	2. Government Accession No.	3. Recipient's Catalog No.
4. Title and Subtitle IN-FLIGHT TRANSITION MEASUREMENT ON A 10° CONE AT MACH NUMBERS FROM 0.5 TO 2.0		5. Report Date June 1982
		6. Performing Organization Code RTOP 505-31-44
7. Author(s) David F. Fisher and N. Sam Dougherty, Jr.		8. Performing Organization Report No. H-1117
9. Performing Organization Name and Address NASA Ames Research Center Dryden Flight Research Facility P.O. Box 273 Edwards, CA 93523		10. Work Unit No.
		11. Contract or Grant No.
12. Sponsoring Agency Name and Address National Aeronautics and Space Administration Washington, D.C. 20546		13. Type of Report and Period Covered Technical Paper
		14. Sponsoring Agency Code

15. Supplementary Notes

David F. Fisher: Ames Research Center.
N. Sam Dougherty, Jr.: Arnold Research Organization, Inc., Arnold Air Force Station, Tennessee.

16. Abstract

Boundary layer transition measurements were made in flight on a 10° transition cone tested previously in 23 wind tunnels.

The cone was mounted on the nose of an F-15 aircraft and flown at Mach numbers from 0.5 to 2.0 and altitudes from 1500 meters (5000 feet) to 15,000 meters (50,000 feet), overlapping the Mach number/Reynolds number envelope of the wind tunnel tests. Transition was detected using a traversing pitot probe in contact with the surface. Data were obtained near zero cone incidence and adiabatic wall temperature.

Transition Reynolds number was found to be a function of Mach number and of the ratio of wall temperature to adiabatic wall temperature. Microphones mounted flush with the cone surface measured free-stream disturbances imposed on the laminar boundary layer and identified Tollmien-Schlichting waves as the probable cause of transition. Transition Reynolds number also correlated with the disturbance levels as measured by the cone surface microphones under a laminar boundary layer as well as the free-stream impact microphone.

The experimental results and supporting data of this study are tabulated. The calibration data and the methods used to correct the data are provided in appendixes.

17. Key Words (Suggested by Author(s)) Transition Boundary layer Cones Tollmien-Schlichting waves		18. Distribution Statement Unclassified-Unlimited STAR Category: 02	
19. Security Classif. (of this report) Unclassified	20. Security Classif. (of this page) Unclassified	21. No. of Pages 143	22. Price* A07

*For sale by the National Technical Information Service, Springfield, Virginia 22161

NASA-Langley, 1982